What underlies the benefits of environmental enrichment on the brain? Investigation of a neurotrophin-stimulated kinase reveals its role in regulating sociability and experience-dependent changes in hippocampal gene expression.

Daniel David Cooper

A thesis submitted for the degree of Doctor of Philosophy

University of Warwick

School of Life Sciences

September 2019

Table of Contents

List of figures

List of tables

Acknowledgements

First and foremost I would like to express my deepest gratitude to Professor Bruno Frenguelli for his constant support and guidance. You were always there to offer advice and patient enough to let me figure out how things worked. You kept me engaged and focused even if it was with the promise of a pint and I could not have done this without you.

I would also like to thank my other supervisors Dr Daniel Hebenstreit for his endless patience with my frantic ramblings and for guiding me through my RNAseq analysis, Dr Mark Wall for his helping me find my feet with electrophysiology and for teaching me the correct chants to say in order to get my rig to behave and Dr Elliott Ludvig for his advice and input regarding my behavioural experiments.

To my panel members Professor Kevin Moffat and Dr Robert Huckstepp, thank you both deeply for your friendly mentorship, feedback and advice throughout the course of this work. I'd also like to thank my thesis committee Dr Robert Dallmann and Professor Zafir Bashir for their constructive criticism and comments on this thesis. You helped focus and organise the thoughts that I threw at you and I'm very grateful for your time and input.

I would like to thank Drs Gareth Barker and Lorenzo Moré for their time, support and advice regarding behavioural experiment conduct and protocol, as well as Drs Yuriy Pankratov and Paul Banks who provided invaluable advice for my electrophysiological investigations.

Thank you also to Sophie Pinder (MIBTP) for working out the kinks with the neurolucida analysis and for her diligent work establishing a workflow for neuronal reconstruction. Without you there would not have been time to finish them.

Thank you to Emma Condon (MIBTP) who joined at a very frantic time, and yet found her feet immediately and performed the neuronal reconstructions featured in this thesis. Somehow you managed to achieve several months' worth of work in a few weeks and I still don't understand how you possessed such determination and aptitude.

To Sam Dixon, Ian Bagley, Sarah Stanley and all the staff within the BSU. You were absolutely essential to helping me throughout my PhD, thank you so much for your friendly patience and support, and for helping me regain my footing when I felt overwhelmed.

To Ian Forsythe and his lab members: Amy, Deborah, Michelle and Sherylanne for teaching a helpless newbie what a rig is and what not to touch to stop it from breaking. Thank you for taking the time to teach me and make me feel welcome.

To past and present members of the Frenguelli lab and the labs C116 and C117 - Pippa, Em, Monicá, Martina, Gabri, Joe, Karen, Fakhra, Aditi, Saab, Jess, Greta, Rahul, Eric, Matei, Marianthi, Lorenzo and especially Lucy – you have been responsible for creating a working environment that was lively, fun and supportive and made working through the rougher patches of a PhD that much more doable. Thank you guys for making my time in the lab the best.

To my friends at Warwick outside of the lab, Anna, Rory, Edu, Natassa, Cathal, Carlotta, Alonso, Cantug, Rob, Liv, Julia, Chris, Magda, Jenna, Leng, and Victoria, and my friends away from the university, Alex, Matt, Jack, Hopkins and Shona: you're the funniest bunch of characters I could have hoped to find, and I've made some cherished lifelong memories with all of you and I'm very lucky to be surrounded by such amazing people/degenerates in my life.

There are also countless faculty members within the School of Life Sciences who have all helped me with various problems, provided me with guidance or been fantastic sources of conversation. Thank you all.

To my family, you're the best support anyone could ask for, and you've shaped me into who I am today. Not sure who to blame for that! To my brothers, Dom, James, Oli and Jon, you chaps are listed in age order and are pretty okay. Lotta love for you lads. You're the best mates anyone could ask for even if you've gotten used to glazing over at the merest mention of a neuron.

To my parents, you have always believed in me and are a constant source of strength and sanity for me. You've always nurtured and encouraged my interest in science and I certainly wouldn't have made it to this, or through this without you. Thank you so much for your endless love and support.

Finally, I would like to thank my funding body: the Biotechnology and Biological Sciences Research Council (BBSRC) for funding this research through their Midlands Integrative Biosciences Training Partnership (MIBTP) doctoral training programme and their additional award for *in vivo* skills training, without which this work would not have been possible.

Declaration

I hereby declare that all work in this thesis was carried out and written by myself, under the principle supervision of Professor Bruno Frenguelli with additional supervision provided by Dr. Daniel Hebenstreit, Dr Mark Wall and Dr Elliott Ludvig, with the exception of:

1) Some experimental data used in the immunofluorescence experiment detailed in Figure 3.2 was generated by Dr Lucia Privitera who prepared slices, stained and acquired confocal images for pCREB immunofluorescence after BDNF application.

2) Some experimental data used in the immunofluorescence experiment detailed in Figure 3.3. 4 of the 10 animals used for experiments were prepared slices, stained, acquired confocal images and quantified for pCREB immunofluorescence after DHF application by Siobhan Crilly at The University of Warwick as part of Professor Bruno Frenguelli's lab, which contributed to her final year undergraduate honours project dissertation.

3) RNA extraction and purification for the RNAseq experiments in Chapter 4 was carried out by Dr Lucia Privitera and Dr Lorenzo Moré.

4) Neurolucida 3D reconstruction of all CA1 apical dendrites shown in Figures 5.11 and 5.12, that formed the basis of the analysis carried out in Figures 5.13 and 5.14 was carried out by Emma Condon, who joined the Frenguelli lab as part of her MIBTP doctoral programme miniproject.

None of the work in this thesis has been submitted for any previous degree. All sources of information are acknowledged in the form of references.

Daniel David Cooper

September 2019

Publications arising from this work

1) The immunofluorescence experiments concerning impaired BDNF-induced CREB phosphorylation in MSK1 KD compared to WT mice described in Chapter 3: Figure 3.2 were included within the following publication, which is appended to the end of this document:

DAUMAS, S., HUNTER, C. J., MISTRY, R. B., MORÈ, L., PRIVITERA, L., **COOPER, D. D.**, REYSKENS, K. M., FLYNN, H. T., MORRIS, R. G. M., ARTHUR, J. S. C. & FRENGUELLI, B. G. 2017. The Kinase Function of MSK1 Regulates BDNF Signaling to CREB and Basal Synaptic Transmission, But Is Not Required for Hippocampal Long-Term Potentiation or Spatial Memory. *eNeuro,* 4**,** ENEURO.0212-16.2017.

2) The RNAseq results detailed here in Chapter 4, describing the role the kinase function of MSK1 plays in regulating over half of the transcriptomic response to environmental enrichment, were included as part of the below publication. This publication was not appended to this document due to the current formatting and large size of the early access paper on the Journals website.

PRIVITERA, L., MORÈ, L., **COOPER, D. D.**, RICHARDSON, P., TSOGKA, M., HEBENSTREIT, D., ARTHUR, J. S. C. & FRENGUELLI, B. G. 2020. Experience recruits MSK1 to expand the dynamic range of synapses and enhance cognition. *The Journal of Neuroscience*, JN-RM-2765-19.

Abstract

Cognitive impairment, as a result of developmental issues, age and diseases such as dementia have the potential to affect anyone, and are a significant source of socioeconomic burden to both the healthcare system and the families of those affected. Environmental enrichment has emerged as a non-pharmacological intervention that can improve cognitive function and ameliorate the effects of cognitive impairment. Understanding the mechanisms underpinning these enrichment-mediated benefits are of great interest for designing effective interventions to boost cognitive function. MSK1 is thought to act as a transducer of MAPK signalling to gene expression within neurons, in response to extracellular signals upregulated by environmental enrichment, by phosphorylating the nuclear transcription factor CREB, and modifying chromatin structure through histone H3 phosphorylation. As such, MSK1 is positioned to play an important role in mediating neuronal changes within the hippocampus in response to environmental enrichment by regulating activity-dependent transcriptional changes.

Here, mice homozygous for a kinase-inactivate form of MSK1 fail to phosphorylate CREB in response to BDNF-TrkB stimulation, and the kinase activity of MSK1 is demonstrated to regulate over half of the transcriptional changes induced following 3 months of environmental enrichment. Genes regulated by MSK1 included the IEGs Egr1 and Arc/Arg3.1, and appeared to be involved in restructuring the hippocampal extracellular environment, regulating primary cilium structure and MAPK signalling. Interestingly expression of MSK1 itself and MAPK pathway signalling appeared to be regulated in a homeostatic manner by environmental enrichment.

Further experiments with a shorter 1 week period of enrichment indicated a potential role for the kinase activity of MSK1 in a transient environmental enrichment-induced decrease in AMPAR-mediated glutamatergic transmission and a potential effect in remodelling CA3/CA1 synaptic signalling, however both 1 week and 5 week periods of EE failed to show an MSK1 kinase activity-dependent effect on several aspects of CA1 neuron morphology, synaptic transmission, short-term presynaptic plasticity and synaptic transmission. Exposure to 1 week and 5 week periods of EE was also associated with

decreased postsynaptic expression of calcium-permeable AMPARs which could act as a potential form of EE-regulated metaplasticity at SC/CA1 synapses. Behavioural assays also revealed a novel role for MSK1 in regulating novelty-motivated behaviour, with kinase inactivation associated with reduced object investigation and impaired social memory, regardless of enrichment. This work implicates MSK1 as an important regulator of experience-dependent structural and synaptic changes within the hippocampus, further adding to the body of work characterising the kinase function of MSK1 already established by the Frenguelli lab.

List of abbreviations

μA	Microampere
μm	Micrometer
μl	Microlitre
AC	Adenylate cyclase
AKT	Serine/threonine kinase
Ala	Alanine
AMPA	α-amino-3-hydroxy-5-methyl-4-isoxazolepropionic acid
AMPAR	AMPA receptor
ANOVA	Analysis of variance
AP-1	Activator protein-1
Arc/Arg3.1	Activity-regulated cytoskeletal protein
Asp	Aspartate
ATF-1	Activating transcription factor 1
BAM	Binary Alignment/Map format
BDNF	Brain-derived neurotrophic factor
bp	Base-pair
c-Fos	(cellular) Fos proto-oncogene, AP-1 transcription factor subunit
C/EBP	CCAAT enhancer – binding protein
CA1	*cornu ammonis* 1
CA2	*cornu ammonis* 2
Ca^{2+}	Calcium (divalent ion)
CA3	*cornu ammonis* 3
CaM	Calmodulin
CaMK	Ca^{2+}/calmodulin-dependent protein kinase
CaMKK	Ca^{2+}/calmodulin-dependent protein kinase kinase
cAMP	Cyclic adenosine monophosphate
Ca_V1	L-type voltage-dependent calcium channel 1
CBP	CREB binding protein
Cdh3	Cadherin-3
cFos	(cellular) Fos proto-oncogene, AP-1 transcription factor subunit

CI	Ca^{2+} impermeable
CMKLR1	Chemokine like receptor 1
CNQX	6-cyano-7-nitroquinoxaline-2,3-dione
CP-AMPAR	Ca^{2+}-permeable AMPAR
CRE	cAMP response element
CREB	Cyclic-AMP response element binding protein
CREM	cAMP responsive element modulator
CRTC	CREB-regulated transcriptional coactivator (also known as TORC)
d	day
D-AP5	D-2-amino-5-phosphonovalerate
DAPI	4',6-diamidino-2-phenylindole
DEG	Differentially expressed gene
DG	Dentate gyrus
DGC	Dentate granule cell
DHF	7,8-dihydroxyflavone
DMSO	Dimethyl sulfoxide
DNA	Deoxyribonucleic acid
E-LTP	Early phase LTP
EC	Entorhinal cortex
EE	Environmental enrichment
Egr1	Early growth response 1 (also known as Zif268)
EPSC	Excitatory postsynaptic current
EPSP	Excitatory postsynaptic potential
ERK	Extracellular signal-related kinase
Erk1/2	Extracellular-signal regulated kinases 1/2
fEPSP	Field EPSP
FRS2	Fibroblast growth factor receptor substrate 2
G	Guanine
GABA	Gamma-aminobutyric acid
GluA1	Glutamate ionotropic receptor AMPA type subunit 1
GluA2	Glutamate ionotropic receptor AMPA type subunit 2
GluA3	Glutamate ionotropic receptor AMPA type subunit 3

GluN2A	Glutamate Ionotropic Receptor NMDA Type Subunit 2A
GluN2B	Glutamate Ionotropic Receptor NMDA Type Subunit 2B
GO	Gene ontology
GOTerm	Gene ontology term
GRB2	Growth-factor receptor-bound protein 2
H3K4	Histone 3, lysine 4
HAT	Histone acetyl transferase
I	Current
IEG	Immediate early gene
IGV	Interactive Genome Browser
Ins(1,4,5)P3	inositol-1,4,5-trisphosphate (Ins(1,4,5)P3)
IO	Input-output
IVC	Individually ventilated cage
KDEE	MSK1 Kinase-dead environmentally enriched
KDSH	MSK1 kinase-dead standard housed
Kmt2a	Lysine methyltransferase 2A
KO	Knock-out
L-LTP	Late phase LTP
LEC	Lateral EC
LFS	Low-frequency stimulation
LNGFR	Low-affinity nerve growth factor receptor
LoxP	Locus of X-over P1
LTD	Long-term depression
LTM	Long-term memory
LTP	Long-term potentiation
MAPK	Mitogen-activated protein kinase
MAPKK	Mitogen-activated protein kinase kinase
MAPKKK	Mitogen-activated protein kinase kinase kinase
MEC	Medial EC
MEK	Mitogen-activated protein kinase kinase
mEPSC	Miniature excitatory postsynaptic current
Mg^{2+}	Magnesium (divalent ion)

mGluRs	Metabotropic glutamate receptors
Mll1	Mixed-lineage leukemia 1
mOsm	milliosmoles
mRNA	Messenger RNA
ms	Milliseconds
MSK1	Mitogen- and stress-activated protein kinase 1
MSK1 KD	MSK1 kinase dead
MSK1 KO	MSK1 knock-out
MSK2	Mitogen- and stress-activated protein kinase 2
mth	Month
MWM	Morris water maze
NF-κB	Nuclear factor-κ light-chain enhancer of activated B cells
NGF	Nerve-growth factor
nM	Nanomolar
NMDA	N-methyl-D-aspartate
NMDAR	NMDA receptor
NOR	Novel object recognition
NT3	Neurotrophic factor 3
NT4	Neurotrophic factor 4
NT5	Neurotrophic factor 5
OLM	Object location memory
P2rx6	Purinergic Receptor P2X6
p300	Histone acetyltransferase p300
p38	Mitogen-Activated Protein Kinase 14
pA	Picoampere
PB	Phosphate buffer
PBS	Phosphate buffered saline
PC	Principal component
PCA	Principal component analysis
PCL	Pyramidal cell layer
PCR	Polymerase chain-reaction
pCREB	phosphorylated CREB

PFA	Paraformaldehyde
PI3K	Phosphatidylinositol 3-kinase
PKA	Protein kinase A
PKC	Protein kinase C
PP	Perforant path
PPD	Paired-pulse depression
PPF	Paired-pulse facilitation
PPR	Paired-pules ratio
PSD	Postsynaptic density
PSD95	Postsynaptic density 95
Q	Glutamine
QC	Quality Control
R	Arginine
Raf	Rapidly accelerated fibrosarcoma
Rarres2	Retinoic acid receptor responder 2
Ras	Rat sarcoma
RI	Rectification index
RNA	Ribonucleic acid
RNAseq	RNA sequencing
rRNA	Ribosomal RNA
RSK2	Ribosomal Protein S6 Kinase A3
RT	Room temperature
RTK	Receptor tyrosine kinase
S133A	Serine to alanine point mutation at CREB residue 133
sAPPα	Secreted amyloid precursor protein-alpha
Sb	Subiculum
SC	Schaffer collateral
Ser	Serine
Ser133	Serine 133
SGZ	Sub-granular zone
SH	Standard housed
Shc	Src homology and collagen

SLM	Stratum lacunosum moleculare
SO	Stratum oriens
SOS	Son of sevenless
Spry4	Sprouty 4
SR	Stratum radiatum
SRF	Serum-response factor
STM	Short-term memory
T	Thymine
TA	Temperoammonic
Thr	Threonine
TORC	Transducer of regulated CREB activity
TrkA	Tropomyosin receptor kinase A
TrkB	Tropomyosin receptor kinase B
TTX	Tetrodotoxin
Tyr	Tyrosine
Tyr515	Tyrosine residue 515
Tyr816	Tyrosine residue 816
V	Voltage
wk	Week
WT	Wild-type
WTEE	Wild-type environmentally enriched
WTSH	Wild-type standard housed
αCaMKII	alpha CaMK

Chapter 1: Introduction

1.1 The hippocampus

1.1.1 Functions of the hippocampus

The role of the hippocampus in learning and memory was brought to widespread attention by the observation of patients who underwent a bilateral medial temporal-lobe resection, during which in some cases surgical excision of the anterior hippocampus and hippocampal gyrus occurred. This resulted in the loss of recent previous memories (partial retrograde amnesia) and in the ability to form new ones (anterograde amnesia) (Scoville and Milner, 1957). The most memorable of these cases, patient H.M., underwent the surgery in 1953 in an attempt to control his seizures. Following surgery, H.M. acquired very severe anterograde amnesia and slight retrograde amnesia, though retained immediate memory for as long as 15 minutes. However this could not be linked directly to the hippocampus, due to the removal of several other brain regions such as the amygdala and the parahippocampal gyrus. With the advent reliable animal models developed a decade later, a cause-effect relationship between hippocampal loss and the ability to form memories began to be established (Squire, 2009). Indeed, later studies would demonstrate that due to the removal of the anterior hippocampal gyrus in addition to the hippocampus, H.M.'s memory loss appeared more severe than would be explained by hippocampal lesion alone (Squire, 2009).

Studies of H.M. by Brenda Milner also provided insight into the distinctly different forms of memory, where H.M. displayed the capacity to improve motor skills through practice, though he had no memory of doing so (Squire, 2009). This precipitated a series of studies on amnesic patients, establishing two distinct forms of memory: The hippocampus-dependent declarative memory (which consists of episodic and semantic memory) and non-declarative or procedural memory, a largely hippocampus-independent form of learning from practice or habit such as the ability to draw something accurately or play an instrument (Squire, 2009). The hippocampus was therefore seen to play an essential role in the consolidation of short-term declarative memories into long-term memory.

This process of consolidation is hippocampus-dependent but once complete, the memory is resistant to hippocampal lesion as evidenced by the partial retrograde amnesia observed by Scoville and Milner (1957). This amnesia only went back as far as 4 years in the most extreme case, indicating consolidation is time dependent, and that long-term memories are stored independently of the hippocampus. This has given rise to a systems level model of memory acquisition in which the hippocampus can provide information to other brain areas such as the striatum during learning (Ballard et al., 2019) and consolidation that features cross talk of the hippocampus with many different brain areas especially the neocortex (Squire et al., 2015)

The hippocampus also has a well characterised role in the interpretation of spatial information, allowing navigation of surroundings and in the formation and storage of spatial memory (Andersen et al., 2009). Hippocampal lesions disrupt spatial navigation within rats, resulting in impaired spatial learning in an experimental paradigm known as the Morris water maze (MWM) (Morris et al., 1982). In 1971, using surgically implanted electrodes to measure *in vivo* perception of the environment, O'Keefe and Dostrovsky observed that specific pyamidal neurons within the CA1 region of the hippocampus, termed "place cells", fired only when the rat was simultaneously located in a certain area and oriented towards a particular direction (O'Keefe and Dostrovsky, 1971). The reliance of place cell firing on spatial cues was demonstrated when this effect was abolished in the dark (O'Keefe and Dostrovsky, 1971). O'Keefe and Dostrovsky interpreted their results as a cellular basis of a "cognitive map" generated within the brain, where a physical neuronal map could underlie an abstraction of the environment as a cognitive map (O'Keefe and Dostrovsky, 1971, O'Keefe and Nadel, 1978). The location-specific activity of place cells depends on input from "grid" cells located within the entorhinal cortex (Brun et al., 2002, Fyhn et al., 2004), which fire according to the absolute place of an animal within an environment (Hafting et al., 2005). Place cells and grid cells along with other specialised "border cells: and "head direction-modulated" cells, are thought to represent an entorhinal-hippocampal map of an organisms environment and its place within it (Moser et al., 2015).

Recently, this idea of cognitive maps representing physical space has been generalised to involve the hippocampus in mapping social interactions (Tavares et al., 2015). Utilising fMRI

scanning of brain activity (based on blood flow to brain regions) in human participants whilst they engaged with a role-playing game simulating social interaction, hierarchy and decision making, functional bases for their perception of social position could be observed within the brain (Tavares et al., 2015). Left hippocampal activity corresponded with changes in subject perception of social standing within the activity, and questionnaire based measurements of participants social avoidance and neuroticism showed significant negative correlation with hippocampal activation during the activity (Tavares et al., 2015). Activity in additional brain regions: the left dorsolateral prefrontal cortex, anterior cingulate cortex and left inferior parietal lobule also predicted additional key variables defining social position. Anterior cingulate cortex activation for example predicted the magnitude of the hippocampal-predicted direction of social standing; i.e. the hippocampus predicted whether someone was in a relative position of power or of perceived affiliation from a participant, but dorsal anterior cingulate cortex activity predicted how large or small that power difference or affiliation was perceived to be (Tavares et al., 2015). This study highlights how the hippocampus, in concert with other brain regions, can represent episodic and semantic memories as another kind of cognitive map within the hippocampus. In fact the role of the hippocampus in spatial memory has been hypothesised to be due to this abstracted representation of memory, and not due to any selective disposition for spatial information (Eichenbaum, 2017).

Hippocampal atrophy in humans is associated with Alzheimer's disease (Jack et al., 1999), memory loss, cognitive impairment and dementia (Shi et al., 2009). A decline in hippocampal volume is also associated with impaired cognition, notably episodic memory and working memory in older adult humans (O'Shea et al., 2016). Understanding the mechanisms of normal hippocampal function is vital in designing effective strategies to combat these cognitive impairments, without disrupting the network of activity regulated by the hippocampus.

1.1.2 Hippocampal anatomy and connectivity

Part of the limbic system and located within the medial temporal lobe of the human brain, the mammalian hippocampus is a densely interconnected network of neurons arranged into a folded laminar sheet that can be divided into several distinct anatomical regions (Figure 1). Two hippocampi exist in symmetry with each other within the brain, one in each

hemisphere where each connects to the other contralaterally. The hippocampus is one of the most widely studied areas of the brain, due to its distinct laminar structure that allows for easy identification of pathways for electrophysiological manipulation and recording and for the relatively closed, unidirectional nature of information transfer between different hippocampal regions. Another major reason for hippocampal study is the well characterised role it plays in the acquisition, processing and consolidation of episodic and spatial memories, along with many other functions often performed in concert with other regions of the brain (Andersen et al., 2009).

Two main pathways from the EC provide sensory information input to the hippocampus: Firstly, axons of the perforant path (PP), conveying sensory information mainly from neurons in layer II, and to a lesser extent IV, of the entorhinal cortex to the granule cells of the dentate gyrus (DG) (Neves et al., 2008, Canto et al., 2008). The DG then forms excitatory connections to the apical dendrites of *cornu ammonis* 3 (CA3) region cells within the stratum lucidum via mossy fibre (MF) afferents. The pyramidal cells of the CA3 region project axons onto dendrites of the ipsi- and contralateral CA1 cells via the Schaffer collateral/commissural pathway (SC/AC) within the stratum radiatum (Neves et al., 2008, Andersen et al., 2009). CA1 pyramidal cells then project directly back into the lateral EC (LEC) or the medial EC (MEC) either directly or via the subiculum (Sb) (Canto et al., 2008). In this way, information primarily flows in a loop – from the EC, to the DG, the CA fields and the Sb, and then back to the EC after being altered based on connectivity of the hippocampal regions to each other (Andersen et al., 2009). In addition, the CA1 is also innervated directly within stratum lacunosum moleculare by layer III of the EC via the temperoammonic (TA) pathway (Kajiwara et al., 2008).This is summarised in Figure 1 B. In addition to these classical pathways, pyramidal neurons of the CA2 region, existing between regions CA3 and CA1, also receive input from the mossy fibres of DG granule cells (Lorente De Nó, 1934, Ishizuka et al., 1995). Whereas CA3 neurons primarily innervate CA1 neurons along the apical dendrite within the stratum radiatum (SR), CA2 neurons innervate the basal dendrites of the CA1 neurons within the stratum oriens (SO) (Shinohara et al., 2012).

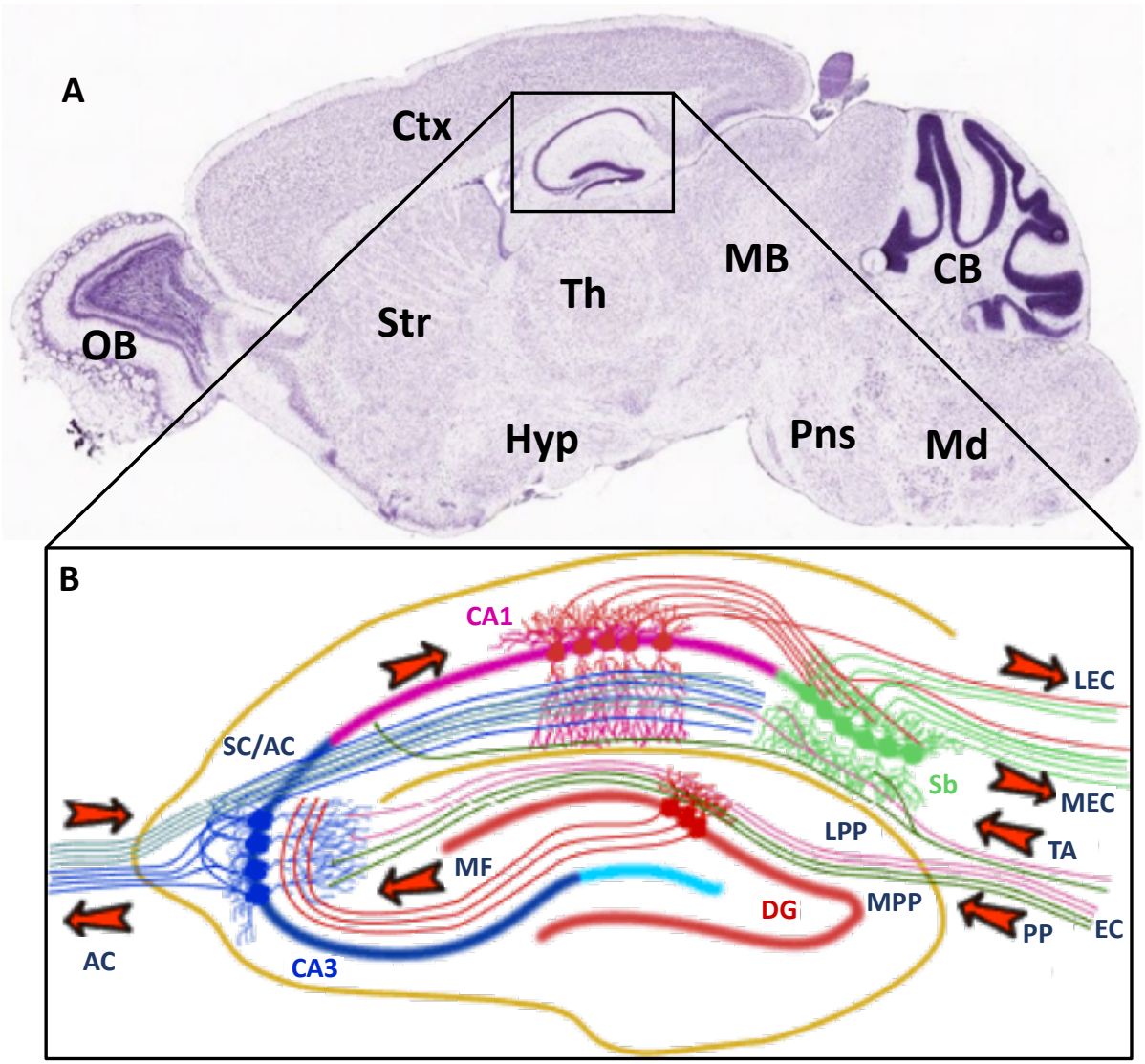

Figure 1.1. The rodent hippocampus and illustration of information processing pathways. A) Nissl-stained nuclei of a slice taken facing the sagittal plane (looking at the side of the head from the left-hand side) approximately halfway through one hemisphere of the brain. Slice was taken from a p56 mouse brain highlighting the distinct cytoarchitecture of the hippocampus. Important brain regions are labelled from left to right: OB, olfactory bulb; Str, striatum; Ctx, cerebral cortex; Hyp, hypothalamus; Th, thalamus; MB, midbrain; Pns, pons; Md, medulla; CB, cerebellum. The hippocampus is highlighted within a black box. **B)** Schematic illustration of information processing pathways within the hippocampus: Information flows from layers II and IV of the entorhinal cortex (EC): from the lateral EC via the perforant pathway (LPP) and the medial EC via the PP (MPP) to granule cells of the dentate gyrus (DG) and CA3 pyramidal cells. The mossy fibre pathway (MF) contains axons projecting from granule cells within the DG which innervate CA3 pyramidal cells. CA3 pyramidal cells then innervate CA1 pyramidal cells via the Schaffer collateral/associational commissural pathway (SC/AC). CA1 pyramidal cells then project directly back into the lateral EC (LEC) or the medial EC (MEC) and the subiculum (Sb). The Sb then sends projections to innervate the LEC and MEC. The Sb and CA1

can also be directly innervated by axons from cells in layer III of the EC via the temporoammonic (TA) pathway. Arrows indicate the largely unidirectional flow of information originating from the EC. Figure A from the Allen Brain Atlas (Lein et al., 2007). Figure 1.1 B reproduced from http://www.bristol.ac.uk/synaptic/pathways/.

1.1.3 Hippocampal cell morphology and characteristics

The hippocampus is subdivided into several distinct regions based on differences in neuronal structure, function and connectivity: The DG, CA1, CA2, CA3 which form a largely unidirectional circuit to and from the EC in part via the Sb. These regions contain distinct neuronal populations characterised by the "principal" excitatory neurons, that are responsible for the primary excitatory synaptic transmission from one region to the next described in Figure 1 B. The principle neurons found in the DG, CA1, CA2 and CA3 are illustrated below in Figure 1.2 A, and an illustration of a CA1 pyramidal cell highlighting key features of its cytoarchitecture is shown in Figure 1.2 B.

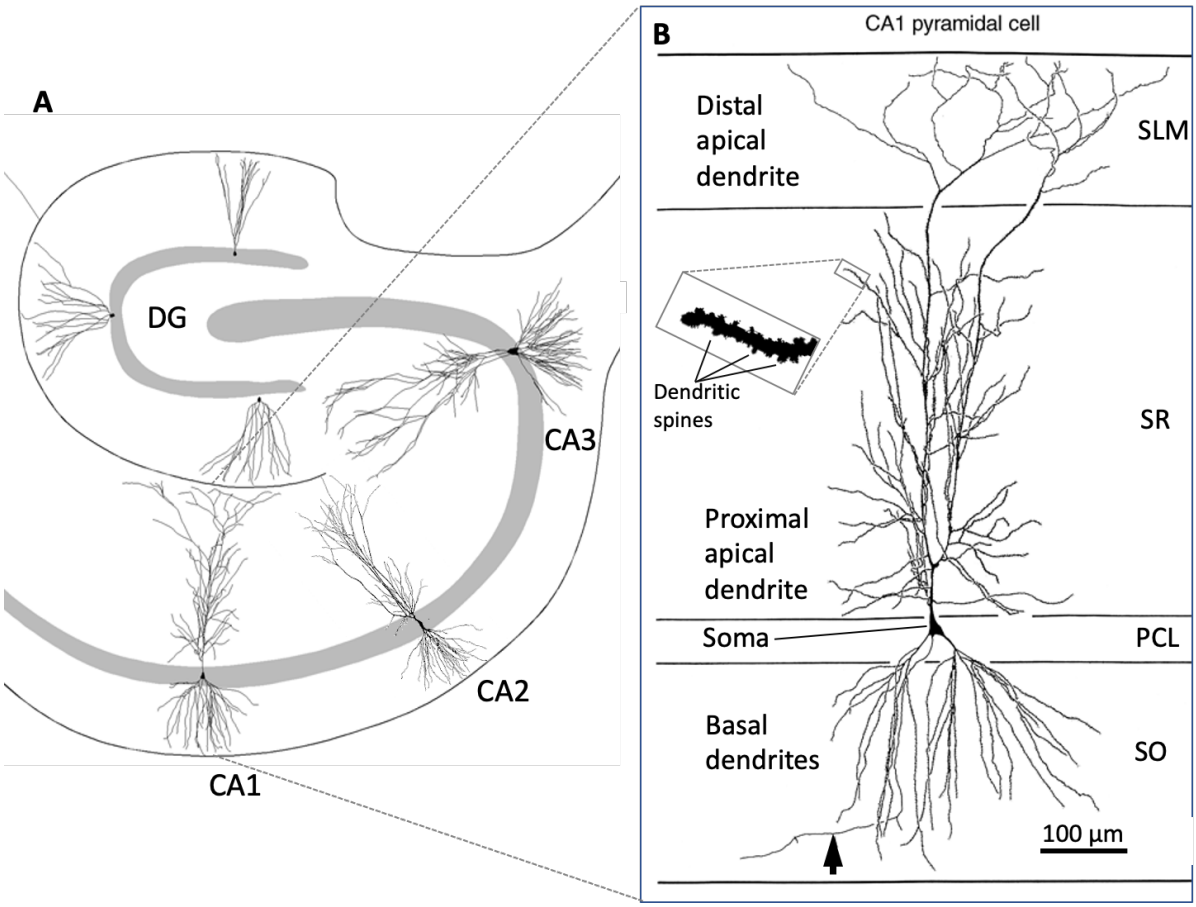

Figure 1.2. Principle cells of the rat hippocampal DG, CA1, CA2 and CA3 regions. A) Dentate granule cells (DGCs), the principle excitatory neuron within the DG display conical dendritic fields, radiating

outwards into the molecular layer of the DG. Pyramidal cells in the CA1 and CA3 layer display broadly similar morphology possessing bipolar extensions of dendrites above and below the soma, within the pyramidal cell layer. CA3 pyramidal cells typically display a larger soma than those found within the CA1. **B)** An illustration of a CA1 pyramidal cell. The soma of the neuron sits within the pyramidal cell layer (PCL) from which basal dendrites protrude into the stratum oriens (SO). A long apical dendrite extends from the soma through the stratum radiatum (SR) and into the stratum lacunosum-moleculare (SLM) at its distal end, branching along the way. Dendritic spines highlighted are seen as small (~ 1 µm) protrusions along the length of dendrites. The axon of this neuron is located at the bottom of the image and is marked with an arrowhead. Bar =100 µm. Figure 1.2 A from Anderson (2009) with CA2 neuron from Ishizuka et al. (1995) and Figure 1.2 B from Ishizuka et al. (1995), dendritic spines in Figure 1.2 B from McEwen et al. (1999).

Dentate granule cells (DGCs), the principle excitatory neuron within the DG, display conical dendritic fields, radiating outwards to the molecular layer of the DG where they form synapses and receive input from PP fibres. The DG also contains pyramidal basket cells, interneurons that form synapses with and inhibit DGC firing through the release of the neurotransmitter gamma-aminobutyric acid (GABA) at inhibitory synapses. Interneurons are present throughout the hippocampus at a proportion approximately 12.5 % to principle cells (Keller et al., 2018) where they exert their inhibitory activity upon principle cells. The dentate gyrus in concert with the CA3 appears to play an essential role in processing spatial pattern separation, where similar environments, objects or other contextual information are discriminated from prior knowledge (Gilbert et al., 2001, Kesner, 2007, Yassa and Stark, 2011).

Unique within the hippocampus, the dentate gyrus contains neural stem cells, and is a site of neurogenesis during adulthood and throughout the lifespan (Palmer et al., 1997, Gage, 2002, Dayer et al., 2003, Moreno-Jimenez et al., 2019). Neurogenesis in the dentate gyrus occurs in humans as well as rodents and is observed to decrease with age (Baptista and Andrade, 2018, Moreno-Jimenez et al., 2019). Additionally, Alzheimer's patients demonstrate significantly lower levels of neurogenesis when compared with healthy individuals (Moreno-Jimenez et al., 2019). Interestingly exercise, which increases levels of neurogenesis within the DG (Kondo, 2017, Liu and Nusslock, 2018, Baptista and Andrade, 2018), improves spatial pattern separation in a manner that is significantly positively correlated with increased DG neurogenesis (Creer et al., 2010). Older mice do not seem to demonstrate exercise-induced

increases in DG neurogenesis or spatial pattern separation (Creer et al., 2010). Ablation of hippocampal neurogenesis, through a neural-precursor cell specific inducible proapoptotic factor which specifically targets new-born cells, results in spatial memory deficits arising from apparent impairments in pattern separation when approaching a Morris water maze task from variable start locations (Dupret et al., 2008). Neurogenesis within the hippocampus may therefore play a key role in the dentate gyrus' proposed ability to discriminating between current and previous information by allowing pattern separation to occur.

Reductions in hippocampal neurogenesis have been linked to many human psychological disorders such as depression and anxiety disorders, and many medications for these disorders work to increase levels of neurogenesis (Schoenfeld and Cameron, 2015). Genetic deletion of a gene that normally inhibits hippocampal neurogenesis has also been seen to result in a significant reduction in symptoms of depression and anxiety in response to treatment with corticosteroid (Hill et al., 2015). One proposed cause of reduced hippocampal neurogenesis seems to be chronic levels of stress (Baptista and Andrade, 2018): Corticosteroids are released during periods of chronic stress as part of the hypothalamus-pituitary axis response (Godoy et al., 2018), and have been to exert an inhibitory effect on hippocampal neurogenesis (Sawamoto et al., 2016).

The principle pyramidal cells of CA3, CA2 and CA1 are located within the pyramidal cell layer, and feature a basal dendritic tree that extends into the stratum oriens (SO), along with an apical dendrite that extends and branches throughout the stratum radiatum (SR) and into the stratum lacunosum-moleculare (SLM) (Figure 1.2 B).Several features distinguish pyramidal cells within each region:

CA1 cells receive different inputs along the length of their apical dendrite: Within the SLM, CA1 dendrites receive input directly from the EC via the TA pathway, and dendrite branches within the SR are innervated by Schaffer collateral/commissural fibres from ispi- and contralateral CA3 pyramidal neurons. CA1 pyramidal neuron dendrites are covered in roughly 30,000 small bulbous protrusions called dendritic spines (Figure 1.2 B) (Andersen et al., 2009). These spines form the postsynaptic terminal of synapses with presynaptic boutons originating from axons, in this case from Schaffer collaterals. SC/CA1 synapses are excitatory,

utilising glutamate as the primary neurotransmitter, and result in the propagation of electrical signals from area CA3 to the CA1. Region CA1 has been studied extensively within the hippocampus, and plays a necessary role in the acquisition and retrieval of spatial memory (Tsien et al., 1996, Place et al., 2012, Brun et al., 2002, Nakazawa et al., 2004, Beer et al., 2018), fear (or contextual) memory (Huerta et al., 2000, Nakazawa et al., 2004, Ji and Maren, 2008) and novel object recognition (Rampon et al., 2000b, Nakazawa et al., 2004). The CA1 appears necessary for temporal pattern separation (Huerta et al., 2000, MacDonald et al., 2011, Beer et al., 2018) (ability to separate similar but different sensory information over time) which is independent of dentate gyrus/CA3 involvement (Gilbert et al., 2001). CA3/CA1 inputs (SC pathway) appear necessary for the recall aspect of spatial memory, whilst direct innervation of area CA1 by the entorhinal cortex (temperoammonic pathway) appear sufficient for the formation of place cell maps (explained later) and the acquisition of spatial memory (Brun et al., 2002).

The function of hippocampal subfield CA2 has received far less attention than either CA1 or CA3, due in part to difficulty distinguishing a clear divide between the other subfields, however recent work has shed light on a role for CA2 distinct of other hippocampal subfields (Dudek et al., 2016). The soma of CA2 and CA3 pyramidal cells are typically much larger than CA1 pyramidal cells, and project very little into the SLM (Ishizuka et al., 1995, Andersen et al., 2009). CA2 pyramidal neurons receive input from CA3 cells via Schaffer collaterals, and also via layers II and II of the entorhinal cortex (Caruana et al., 2012). Axons from CA2 pyramidal neurons innervate CA1 neurons primarily at basal dendrites in the SO, but also at their apical dendrite within the SR (Caruana et al., 2012, Dudek et al., 2016). Impaired CA2 function is associated with impaired social recognition memory in rodents (Stevenson and Caldwell, 2014, Hitti and Siegelbaum, 2014, Tzakis and Holahan, 2019). Using a CA2-specific cre-expressing mouse model, Hitti and Siegelbaum (2014) found that inhibition of CA2 synaptic activity, through the expression of a cre-dependent tetanus neurotoxin light chain, impaired social recognition memory, but not performance on simple object recognition memory tasks nor novel object preference. The tetanus neurotoxin disrupts synaptic vesicle fusion, and so when its expression was induced, CA2 neurons were unable to presynaptically release neurotransmitter, indicating that the postsynaptic signalling from CA2 neurons plays an important role in social recognition memory (Hitti and Siegelbaum, 2014). Social recognition

memory in animals is important for the recognition of mates and offspring, social hierarchy and the establishment and maintenance of groups (Tzakis and Holahan, 2019). Expression of receptors for both vasopressin and oxytocin, crucial neural signalling molecules mediating sociability behaviour in mammals (Donaldson and Young, 2008), are enriched within pyramidal cells of the CA2 compared to other hippocampal subfields (Pagani et al., 2015, Dudek et al., 2016), and the CA2 region preferentially receives vasopressinergic input from the paraventricular nucleus (Zhang and Hernandez, 2013). This role in integrating sensory hippocampal input, with vasopressin and oxytocin signalling may explain the importance of area CA2 for social recognition memory.

Area CA2 also appears to have a role in the processing of some spatial information: Distinct from areas CA1 and CA3, place fields within area CA2 show less stability in their firing response to the environment over time (Mankin et al., 2015). This highlights a potential role for region CA2 in interpreting the change in incoming sensory information from the environment over time (Mankin et al., 2015). This observation of shifting place fields could be explained another observation of region CA2: new granule cells born within the DG appear to form synapses with CA2 neurons directly, bypassing the CA3 (Llorens-Martin et al., 2015). Interestingly, these connections from immature granule cells are increased following a 2 week daily physical exercise regime and are tenfold more increased in area CA2 than CA3 (Llorens-Martin et al., 2015) and can therefore regulated by an organisms experience.

CA2 pyramidal neurons, unlike CA1 neurons, are resistant to long-term potentiation (LTP, discussed in detail later) induction (Lee et al., 2010, Dudek et al., 2016). Underlying this resistance is the gene RGS14, which encodes a scaffolding protein that acts to suppress synaptic plasticity in CA2 neurons by binding to activated Ras G-proteins and inhibiting MAPK activation in response to growth factor stimulation (Lee et al., 2010, Evans et al., 2018, Tzakis and Holahan, 2019). Interaction of RGS14 with the CAMKs CAMKII and Ca2+/CaM and other plasticity-related proteins indicates that RGS14 also functions as an inhibitor of calcium signalling (Evans et al., 2018). Whole brain knockout of RGS14 (RGS14KO) allows CA2 neurons to undergo robust LTP, whilst leaving CA3/CA1 LTP unchanged (Lee et al., 2010). RSG14KO mice possess enhanced spatial and object recognition memory (Lee et al., 2010), however these benefits of RGS14 KO to spatial and memory raise the question of why RSG14 is

expressed within the CA2 at all (Evans et al., 2018). RGS14-mediated CA2 LTP suppression is likely to confer some kind of evolutionary benefit, and one hypothesis for its presence is that of solidifying synaptic changes established during early development (Evans et al., 2018): Expression of RGS14 protein cannot be detected until p7 in the CA2 region of mice, with its expression increasing until adulthood at 2 months of age where it remains stable (Evans et al., 2014). Area CA2 therefore appears to be important for social recognition memory and the temporal discrimination of spatial information in adult animals, and appears to display greater synaptic plasticity during early organism development which appears linked to spatial memory and is suppressed in adulthood. Additionally inputs to the CA2 from the DG are affected in an activity-dependent manner by exercise.

Region CA3 is necessary for the recall of spatial information (Brun et al., 2002, Nakazawa et al., 2002), and appears to have a role in encoding such information, especially over short periods of time where afferents to the CA1 serve to refine place cell mapping (Nakazawa et al., 2003, Nakazawa et al., 2004). Additionally, whilst not required for the acquisition of contextual fear memory, disruption in CA3 synaptic plasticity reduces the speed of this acquisition (McHugh and Tonegawa, 2009). CA3 pyramidal neurons possess unusual multi-headed dendritic spine projections or "thorny excrescences" along their proximal apical dendrite that form the postsynaptic component of synapses within the stratum lucidum, which receive input from granule cells of the DG via presynaptic MF boutons (Ishizuka et al., 1995, Gonzales et al., 2001). Dendritic spines are usually mono-headed, projecting a stalk from the dendrite featuring a single head, which can assume a diverse array of shapes, that can form the postsynaptic component of a synapse (Andersen et al., 2009). The thorny excrescences on the dendrites of CA3 neurons consist of a single stalk containing multiple spine heads which each receive largely unitary input from a single MF axonal bouton (Acsády et al., 1998, Gonzales et al., 2001). This means one axonal bouton could trigger depolarisation at multiple proximal postsynaptic sites, amplifying the received signal with respect to mono-synaptic innervation. Indeed these mossy fibre-thorny excresence DG/CA3 synapses are very effective at depolarising CA3 neurons to above firing threshold (Chater and Goda, 2013). Work performed in cultured hippocampal neurons found that the size of these mossy fibre-thorny excresence DG/CA3 appears to be preferentially bidirectional modulated in response to global activity levels (homeostatic plasticity, discussed later) compared to

other synapses (Lee et al., 2013). This activity-dependent modulation has been hypothesised to play a role in gating the strength of information entering the hippocampal circuit in response to changes in overall activity (Chater and Goda, 2013, Lee et al., 2013).

Each subfield also contains a heterogeneous population of glial cells, a diverse group of cells including microglia, astrocytes and oligodendrocytes which perform a range of functions (Andersen et al., 2009). Across the entire brain, the ratio of glial to neuronal cells is thought to be roughly 1:1 (85 billion to 86 billion respectively) (Haug, 1986, Azevedo et al., 2009, von Bartheld et al., 2016). However within the cortex (including the allocortex, which contains the hippocampus), the ratio of glial to neuronal cells is thought to be closer to 3-4:1, in contrast with the much lower ratio of glial cells to neural cells present in the cerebellum at 0.05/0.23:1 (Azevedo et al., 2009, von Bartheld et al., 2016). Humans possess greater total neural and glial populations relative to mice and other primates, due to the increased brain size of humans relative to other primates and primates possessing increased neuronal density compared with other mammals (Herculano-Houzel, 2012). However proportions of glial cells to neural cells do not appear to differ between humans, mice and other primates (Herculano-Houzel, 2012). Within the hippocampus, approximate glial/neural cell ratios are 0.84:1, however proportions of specific glial cells to neurons are hard to determine due to different methodologies employed in their measure (Keller et al., 2018). Stereology suffers from assumptions of homogeneity when extrapolating from the small volume of tissue within which cells are counted (von Bartheld et al., 2016, Keller et al., 2018). Likewise distinguishing between glial cells and neural cells can be difficult, even when employing neuronal markers such as NeuN to label cells specifically (von Bartheld et al., 2016).

Astrocytes are the most abundant glial cells within the mammalian brain (Keller et al., 2018) and possess many identified functions, contributing to the homeostatic regulation of the extracellular environment through the control of ion concentrations, uptake of amino acids and modulation of blood flow (Kimelberg, 2010, Eroglu and Barres, 2010, Jäkel and Dimou, 2017). Each astrocyte possesses up to 100,000 processes spread throughout the immediate region surrounding itself and importantly, these processes are associated with the synaptic connections between neurons where they can modulate synaptic activity (Kimelberg, 2010, Eroglu and Barres, 2010). Astrocytic processes located near synapses

contain neurotransmitter receptors which bind synaptically released glutamate (Wang et al., 2006), triggering an increase in Ca^{2+} concentration within the astrocyte (Dani et al., 1992, Eroglu and Barres, 2010). Astrocytes are therefore able to respond to synaptic signalling, and can then modulate synaptic activity through the release of co-transmitters such as ATP, D-serine (Eroglu and Barres, 2010) and the neurotrophin brain-derived neurotrophic factor (BDNF) (Lalo et al., 2018). Astrocytic processes also contain glutamate transporters and are thought to "mop up" glutamate spill-over into the perisynaptic space, reducing glutamate diffusion from the synapse to neighbouring areas (Song and Dityatev, 2018). The pre- and post-synaptic neurons their associated astrocytic processes make up the tripartite model of a synapse, where astroglia actively respond to and modulate synaptic activity (Araque et al., 1999).

As part of their role in regulating the microenvironment around synapses, astrocytes, along with neurons, secrete specialised adhesion and signalling glycoproteins which make up the extracellular matrix a protein meshwork surrounding neurons and glial cells (Barros et al., 2011). Around synapses and cell bodies, this extracellular matrix forms perineuronal nets, which stabilise synapses and anchor AMPA glutamatergic receptors within the synapse (Barros et al., 2011, Fawcett et al., 2019). Astrocytes are also involved in regulating the experience-dependent remodelling of the extracellular matrix in response to learning and environmental enrichment (Song and Dityatev, 2018). This occurs through the secretion of matrix metalloproteases to selectively degrade the extracellular matrix, to facilitate the creation and elimination of synapses (Song and Dityatev, 2018). Astrocytes therefore play an important role in synaptic signalling and the remodelling of synapses in response to activity.

Microglia are mobile immunological cells that display phagocytic activity, moving between cells and endocytosing invading bacteria and viruses (Nau et al., 2014) and damaged neurons undergoing programmed cell death (apoptosis) (Bilimoria and Stevens, 2015) such as after injury, and are thought to play a role in synaptic remodelling (Jäkel and Dimou, 2017, Paolicelli and Ferretti, 2017). Microglia are uniformly distributed throughout the hippocampus and appear present at lower numbers than astrocytes (Keller et al., 2018).

In cultures, microglia depletion leads to an increase in functional synapses (Ji et al., 2013). This role of microglia in synapse elimination appears to occur in the animal largely during development and under pathological conditions (Wu et al., 2015, Hong et al., 2016, Paolicelli and Ferretti, 2017). In the healthy post-natel brain, however, depletion of microglia appears to reduce both dendritic spine elimination and formation (Parkhurst et al., 2013). Additionally, microglia depletion resulted in impaired motor-learning, context-dependent fear recall and novel-object recognition (Parkhurst et al., 2013). These behavioural deficits in adult microglia depleted mice were further elaborated through pharmacological depletion within the hippocampus, resulting in behavioural deficits in spatial learning and in both social preference and recognition, an effect that was reversed once microglia numbers were repopulated 20 days later (Paolicelli and Ferretti, 2017, Torres et al., 2016).

The role of microglia in behavioural learning appears to be at least in part mediated by BDNF (Paolicelli and Ferretti, 2017): Inducible selective ablation of BDNF from microglia does not appear to affect BDNF protein levels, synapse or neuron number within the cortex or hippocampus of p30 mice (Parkhurst et al., 2013). However these mice display impaired contextual fear recall, and impaired motor-learning-induced spine formation in the motor cortex, and motor-learning improvement (Parkhurst et al., 2013). Compared with controls, synaptosomes purified from BDNF-lacking microglia mice show decreased levels of phosphylated TrkB (Parkhurst et al., 2013), a key BDNF receptor discussed later, indicating that the loss of microglial BDNF reduces levels of neuronal BDNF signalling, and highlights a role for microglial secreted BDNF in certain forms of learning. Therefore microglia appear to play a beneficial role in learning-mediated synapse remodelling within the adult brain, and at least some of this is mediated by secreted BDNF.

Oligodendrocytes wrap axonal processes from principle cells with an extended multi-layered cell membrane, forming a fatty sheath called myelin. The effects of this are two-fold: First, this insulates the axon and enables “saltatory” conduction of electrical impulses along small sections of un-myelinated axon called nodes of Ranvier, speeding up transmission considerably by about 100-fold (Nave, 2010). Secondly, as action potential conductance is restricted to the ~0.5% of the total axon surface area that is unmyelinated, energy consumption due to resetting ion gradients post-transmission is drastically reduced (Nave,

2010). Additionally, oligodendrocytes appear to export products of glycolysis (pyruvate and lactate) to the surface membrane of insulated axons, which appears to support axonal energy metabolism (Simons and Nave, 2015).

Cells within the hippocampus therefore display a range of morphology and interconnectivity, each specialised for different functions such as excitatory and inhibitory synaptic transmission, information processing, regulation of the cell microenvironment and immune system response and are implicated in the processing, interpretation and storage of experiences within an organism. How this information processing between neurons of the hippocampus occurs is thought to involve activity-dependent changes in the synapses between them (Morris, 2006, Neves et al., 2008), a concept which is explored in the next section.

1.2 Mechanisms underlying hippocampal learning and memory

Utilising an improved method of Golgi's silver nitrate stain Santiago Ramón y Cajal characterised neuronal morphology in great detail throughout the central nervous system. These studies led Ramón y Cajal to propose in 1911 that neurons were discrete entities that, whilst having processes that adjoined other neurons, were themselves independent of each other (Sotelo, 2003). He also postulated that the Information transfer occurred between these neurons in a polarised manner (Sotelo, 2003). This idea of information exchange between discretised neurons was expanded further by Donald Hebb, who theorised that the probability of information transfer between neurons could be increased when a cell is near enough to another that it "repeatedly, or persistently takes part in firing it" through "some growth process or metabolic change" (Hebb, 1949).

In 1973 Tim Bliss and Terje Lømo were able to demonstrate that a repetitive train of electrical stimulation applied to PP fibres from the EC could cause an increase in the strength of transmission to dentate granule cells lasting hours within an *in vitro* preparation of acute hippocampal slices (Bliss and Lomo, 1973). This stimulation-induced increase in transmission strength was also demonstrated to last for days using *in vivo* preparations (Bliss and Gardner-Medwin, 1973). This idea that increased synaptic signalling, through repeated periods of presynaptic stimulation, could result in an increase in synaptic efficacy was developed into

the model of long-term potentiation (LTP) (Bliss and Collingridge, 1993). This model of activity-dependent modification of synaptic stength formed the basis of the modern understanding of synaptic "plasticity" discussed below.

1.2.1 Hebbian plasticity mediates changes in synaptic strength

The majority of excitatory transmission throughout the CNS is mediated by the neurotransmitter glutamate which, at synapses, acts as an agonist for ionotropic glutamate receptors: the N-methyl-D-aspartate receptor (NMDAR) (which is also co-activated by glycine, discussed later), α-amino-3-hydroxy-5-methyl-4-isoxazolepropionic acid receptors (AMPAR) and kainate receptors (Reiner and Levitz, 2018). Glutamate also binds to metabotropic glutamate receptors (mGluRs) which mediate intracellular changes via secondary messenger proteins rather than acting as channels for ions (Reiner and Levitz, 2018). Using electron microscopy and immunogold labelling, mGluRs have been observed to localise perisynaptically, around the specialised area of the postsynaptic membrane directly opposite presynaptic neurotransmitter release sites (Lujan et al., 1996). This has led to the idea that mGluR activation depends on glutamate spill-over from the synaptic cleft after several release events (Viaene et al., 2013, Reiner and Levitz, 2018).

Following presynaptic glutamate release into the synaptic cleft, AMPA and kainate receptors exhibit faster opening (within 1 ms) than NMDARs (which take around 10 ms), but are however inactivated much faster (within milliseconds) once synaptic glutamate concentrations decrease, with inactivation of NMDARs on the order of hundreds of milliseconds (Reiner and Levitz, 2018). As a result, the kinetics of excitatory postsynaptic potentials (EPSCs) mediated by AMPA/kainate receptors displays a fast rise and fast decay as glutamate is cleared from a synapse. These properties of the NMDAR on the other hand are much slower.

1.2.1.1 Long-term potentiation

Typically, activation of AMPARs through the presynaptic release of glutamate into the synaptic cleft allows Na^+ influx and triggering depolarisation of the postsynaptic membrane (Bliss et al., 2018). This removes the voltage-dependent Mg^{2+} block of NMDA receptors (Johnson and Ascher, 1990), thereby allowing Ca^{2+} entry (Mayer and Westbrook, 1987) which

initiates numerous postsynaptic events, including the induction of LTP under certain circumstances (Bliss et al., 2018, Lynch et al., 1983). The majority of excitatory transmission occurs through AMPARs, however these are not very permeable to Ca^{2+}, and LTP induction requires the activation of NMDARs which can conduct Ca^{2+} (Bliss et al., 2018). Induction of LTP *in vitro* is frequency dependent, due in part to the coincident depolarisation necessary for the removal of the Mg^{2+} block of NMDARs and the presence of L-glutamate to keep NMDARs open (Bliss et al., 2018). Examples of LTP inducing stimuli include High-frequency stimulation (250 pulses, at 50Hz), tetanic stimulation (100 pulses, at 100Hz, 3 times with 20s in between) and theta burst stimulation (TBS, 10 bursts of four pulses, at 100 Hz, with 200 ms in between, spaced 10s apart for 1m) (Gärtner and Staiger, 2002). Additionally, mGluR activation by synaptic glutamate release plays a complementary role in CA3-CA1 synapse NMDAR-dependent LTP induction, and is a requirement for LTP induction at mossy fibre-CA3 synapses (Bashir et al., 1993).

An additional level of NMDAR regulation during synaptic transmission occurs due to NMDARs being heteromeric tetramers consisting of four different subunits: GluN1-4, and require L-glutamate binding to the GluN2 subunit, and D-serine or glycine binding to the co-agonist site of the GluN1 subunit to open (Li et al., 2009, Rosenberg et al., 2013). Synaptic release of D-serine and glycine is thought to occur in a synaptic activity-dependent manner (Rosenberg et al., 2013) with astrocytic processes that are associated with a synapse being the major source of D-serine (Li et al., 2013), highlighting an important role for astrocytes in synaptic transmission.

NMDAR-mediated LTP induction was first highlighted by the blockade of glutamate binding at NMDARs by treating *in vitro* hippocampal slices with the NMDAR antagonist D-2-amino-5-phosphonovalerate D-AP5 (previously D-APV), which prevents LTP induction at SC/CA1 synapses whilst preserving synaptic transmission (Collingridge et al., 1983, Morris et al., 1986). Intraventricular application of D-AP5 onto the hippocampus was also seen to impair spatial learning in the MWM task (Morris et al., 1986). As previously mentioned in section 1.1.1, place cells within the CA1 selectively fire depending on the orientation and location of an organism in an environment (O'Keefe and Dostrovsky, 1971, O'Keefe and Nadel, 1978). The experience-dependent mapping of specific place cells to a particular position is

observable as soon as an organism is introduced to a novel environment, however this mapping is refined rapidly (5 - 6 m) after introduction into a stable firing field (here "stability" means consistent reactivation of firing patterns of particular place cells by the same environmental stimulus) (Frank et al., 2004, Moser et al., 2015). This process of refining place cell mapping to a location is disrupted by the addition of NMDA antagonist 3-(2-Carboxypiperazin-4-yl)propyl-1-phosphonic acid (Kentros et al., 1998, Ekstrom et al., 2001). Place cells therefore map to the environment in an experience-dependent fashion, and the long-term stability of place cell maps depends on NMDA receptor activation within the hippocampus. NMDA-mediated synaptic plasticity is therefore thought to underly the experience-dependent refining of place cell maps during spatial learning (Moser et al., 2015).

Genetic knock-out studies of NMDA signalling within the CA1 indicated that activity-dependent changes in CA1 postsynaptic efficacy underpin the acquisition of spatial memory (Tsien et al., 1996, Place et al., 2012), temporal association of memories (Huerta et al., 2000) and regulate how the environment is mapped to CA1 neurons by modifying the size and specificity of their place fields (McHugh et al., 1996). Additionally NMDARs within the CA3 are necessary for pattern matching of spatial cues to occur, and facilitate the recall of spatial memory (Nakazawa et al., 2002, Nakazawa et al., 2004).

LTP is thought to be a key cellular process underlying long-term memory (LTM) formation: As discussed above, pharmacological (Morris et al., 1986, Bye and McDonald, 2019) and genetic disruption (Tsien et al., 1996) of NMDAR signalling within the hippocampus prevents LTP induction and impairs learning and memory in behavioural assays (Nicoll, 2017). Intracellular injection of a Ca^{2+} chelator prevents LTP induction (Lynch et al., 1983) and an inactivating mutation of a calcium sensitive intracellular kinase (which are discussed in greater detail later), CamkIIα, prevents LTP induction at CA3-CA1 synapses and impairs spatial learning in the MWM, despite normal NMDAR function (Giese et al., 1998, Cooke et al., 2006). Synaptic enhancement has also been recorded *in vivo* in response to one-trial inhibitory avoidance learning, through the implantation of a multielectrode array into the stratum radiatum of the CA1 dendrite field of the hippocampus containing CA3-CA1 synapses (Whitlock et al., 2006). This synaptic enhancement was characterised by the same neuronal biomarkers as LTP (increased AMPAR receptor expression and phosphorylation), was blocked

by pharmacological inhibition of NMDARs, and most importantly occluded HFS electrode-induced LTP (Whitlock et al., 2006). The inhibitory avoidance task employed by Whitlock et al. (2006) consisted of pairing an aversive stimulus (foot shock) with context-specific cues (the dark) and associative learning between the two was abolished by pharmacological block of NMDARs. Control animals exposed to only the context or the aversive stimulus did not demonstrate the LTP-like enhancement, and HFS electrode-induced LTP was possible in these animals, in contrast to the conditioned animals in which learning had occurred (Whitlock et al., 2006). These studies demonstrate a necessary role for NMDAR function and NMDAR-mediated activation of Ca^{2+}-sensitive intracellular proteins in both hippocampal learning and LTP induction and that certain forms of hippocampus-dependent learning produce LTP-like changes in synaptic strength, which occlude the effects of electrode-induced LTP itself. This represents compelling evidence for the role of LTP as one of the cellular bases of learning and memory processes within the brain.

In support of the *in vivo* importance of LTP during learning and memory, certain *in vitro* stimulation protocols for LTP induction such as theta-burst stimulation (TBS) successfully induce LTP by mimicking similar synchronised firing patterns (theta waves) that are observed to occur naturally within the hippocampus during learning (Larson et al., 1986, Henley and Wilkinson, 2013, Larson and Munkácsy, 2015).

Induction of LTP results in the strengthening of a synapse, initially through a short-term increase in transmission strength called early phase-LTP (E-LTP) which lasts minutes to hours and involves the transient insertion of additional AMPARs at the postsynaptic membrane, but eventually is converted into late phase-LTP (L-LTP), which lasts hours to days, through the transcription and synthesis of new proteins (Frey et al., 1996, Henley and Wilkinson, 2013, Chater and Goda, 2014). Additionally, an increase in NMDAR-mediated transmission has been reported following LTP induction within the hippocampus (Bashir et al., 1991, Clark and Collingridge, 1995), indicating that increased NMDAR conductance through post-translational modifications or insertion can contribute to LTP-induced changes in synaptic transmission.

E-LTP-induction can also lead to the potentiation of existing “silent synapses”, weaker synapses that initially display only NMDAR-mediated postsynaptic responses, but which can become fully functional through the insertion of functional AMPARs (Isaac et al., 1995, Liao et al., 1995, Morita et al., 2014). Activation of these silent synapses depends on coincident glutamate release at these NMDAR-only containing synapses and depolarisation of the postsynaptic cell (Isaac et al., 1995, Morita et al., 2014), indicating a role for silent synapse activation in coincidence detection between separate synapses on the same neuron. The protein products of LTP-induced gene expression can stabilise and enlarge the synapse and cause both the insertion and concentration of AMPARs at the postsynaptic density (PSD) (Vitureira and Goda, 2013, Chater and Goda, 2014). In addition, LTP induction stimulates BDNF expression within the postsynaptic neuron, which is exocytosed at the synapse where it can mediate presynaptic modifications (Vitureira and Goda, 2013, Chater and Goda, 2014).

L-LTP is dependent on gene expression, as pharmacological inhibition of transcription or translation in *in vitro* slice preparations either before or shortly after (~ 1 hour) LTP induction occludes L-LTP formation, but still allows E-LTP, indicating that products of new gene expression determine the persistence of strength changes to the synapse (Nguyen et al., 1994, Frey et al., 1996, Fonseca et al., 2006, Hernandez and Abel, 2008, Alberini and Kandel, 2014, Daumas et al., 2017). This transcriptional component following LTP induction involves the rapid (within minutes of stimulation) expression of immediate early genes (IEGs) (Sheng and Greenberg, 1990, Minatohara et al., 2015) which contribute to the induction of L-LTP both directly and through the transcriptional regulation of other gene products (Minatohara et al., 2015). These are elaborated on in more detail later. Using *in vitro* preparations, as in the above studies, it is not possible to study the length of LTP maintenance for longer than a few hours due to the short-term viability of slices. *In vivo* studies of LTP induction within the rat hippocampus using implanted microelectrodes have shown that LTP-mediated increases to synaptic efficacy can be maintained for much longer lengths of time, on the order of weeks at CA3-CA1 synapses (Staubli and Lynch, 1987) and months at the dentate gyrus following performant-path simulation (Abraham et al., 2002). The necessity of activity-dependent NMDAR-mediated Ca^{2+} changes within neurons for learning and memory, discussed in the above paragraph, and the long timeframe (days to months) of LTP-induced

changes highlights activity-mediated changes in synaptic strength as a key mechanism underlying learned behaviour.

Induction of new transcription and translation during LTP depends to varying degrees on the activation of intracellular kinases, including calcium/calmodulin-dependent protein kinase II (CaMKII) through a rise in intracellular Ca^{2+} following NMDAR transmission, protein kinase C (PKC), protein kinase A (PKA), the MAPK signalling pathway and the phosphatidylinositol 3-kinase (PI3K) pathway (Andersen et al., 2009, Sweatt, 2016) several of which will be elaborated further in context later in this work. Several different mechanisms therefore contribute to the long-term increase in synaptic transmission following LTP: Greater efficacy of transmission strength at pre-existing synapses through increased total number of ionotropic glutamatergic receptors present at the potentiated postsynapse and in individual channel conductance and an increase in pre-synaptic L-glutamate release probability or through an increase in functional synapse number, either through activation of silent synapses or novel synaptogenesis. Hebbian induction of LTP is summarised below in Figure 1.3.

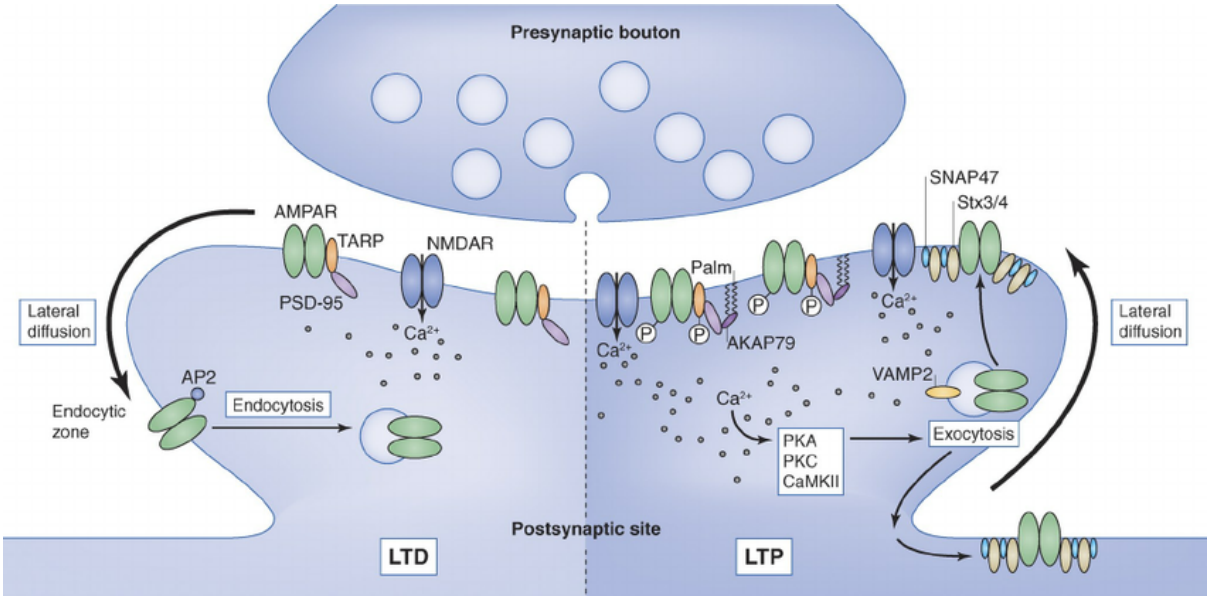

Figure 1.3. AMPAR receptor modulation at the post-synapse during the Hebbian plasticity events LTP and LTD. Left: induction of long-term depression occurs as a result of a small increase in intracellular Ca^{2+} as a result of sporadic, low frequency firing. During endocytosis of AMPARs, bound AP2 functions as an adaptor allowing clatherin recruitment (not shown in figure). **Right:** The large postsynaptic increase in Ca^{2+} concentration following LTP induction activates calcium-dependent

protein kinases such as PKA, PKC and CaMKII resulting in modifications of intracellular vesicular AMPAR subunits already present at the postsynapse. This promotes their exocytosis, and increases AMPAR levels at the postsynapse. Figure reproduced from Vitureira and Goda (2013)

1.2.1.2 Long-term depression

Another form of Hebbian plasticity concerns the reduction in excitatory synaptic strength known as long-term depression (LTD) of which there are two main varieties: NMDAR-LTD and mGluR-dependent LTD (Collingridge et al., 2010): NMDAR-LTD can be induced by several different stimulation patterns (Collingridge et al., 2010), the most commonly employed being that of prolonged repetitive low-frequency stimulation (LFS) of a synapse such as 1 Hz stimulation sustained over a longer period of time (250 pulses at 1 Hz) (Gärtner and Staiger, 2002). This results in a small consistent rise in intracellular Ca^{2+} which is detected by intracellular Ca^{2+} sensitive proteins, that trigger the destabilisation of AMPARs at the PSD through dephosphorylation by protein phosphatases, inducing their endocytosis and reducing glutamatergic transmission at a synapse (Collingridge et al., 2010). mGluR-dependent LTD occurs through activation of second messengers, which regulate the activity of intracellular proteins including, depending on the subtype of mGluR activated, the expression of Arc/Arg3.1 (Collingridge et al., 2010).which mediates the endocytosis of AMPAR receptors at the postsynapse (Park et al., 2008, Corrêa et al., 2012).

LTD reduces the efficacy of synaptic transmission through AMPAR endocytosis (as illustrated in Figure 1.3) and LTD-induced destabilisation of scaffold proteins which can lead to the elimination of a synapse (Collingridge et al., 2010). Low-frequency stimulation (1 Hz) induced-LTD both in *in vitro* (Bastrikova et al., 2008) hippocampal slice preparations and *in vivo* optogenetically within the hippocampus (Wiegert and Oertner, 2013) have been shown to trigger synapse elimination. This functional role for LTD in eliminating synapses is illustrated in behavioural tasks that require the un-learning of a previous learned behaviour or “flexibility”: Mice engineered to express an inhibitor of protein phosphatase 2 (PP2), a Ser/Thr phosphatase involved exclusively in the NMDAR-dependent form of LTD (Collingridge et al., 2010), display normal LTP but impaired NMDAR-LTD (Nicholls et al., 2008). This corresponds with an deficit in spatial memory flexibility during reversal learning in the MWM, where LTD-deficient mice learned the location of a hidden platform normally, but took longer

to correctly learn a new location when this was changed (Nicholls et al., 2008). Spatial inflexibility of LTD-deficient mice was also observed in a T-maze task, where mice learned to find a reward in one arm normally, but displayed increased entries into the wrong arm once the reward location was switched (Nicholls et al., 2008).

1.2.2 Homeostatic plasticity can regulate overall synaptic strength within a neuron

Homeostatic synaptic plasticity describes a process whereby neurons can modulate their cell-wide excitability in response to synaptic input within a dynamic range (Turrigiano, 2008). This prevents over-and under stimulation of the neuron in response to activity-dependent Hebbian changes in synaptic transmission probabilities through LTP and LTD, whilst still maintaining the relative weighting of each synaptic connections strength (Turrigiano, 2008). In an uncorrected system, this could lead to positive feedback, the synapse increasing in transmission efficacy every time it strengthens until a hyper-excitable state is achieved or vice versa resulting in pathogenic synapse elimination (Turrigiano and Nelson, 2000, Collingridge et al., 2010).

Runaway destabilisation of synaptic transmission is prevented by scaling of the whole neuron through “homeostatic plasticity”, such that transmission weight at each synapse is preserved, but global cell excitability returns near a constant level (Turrigiano, 2008, Turrigiano, 2012) as illustrated in Figure 1.4. Prolonged (24-48 hr) activity deprivation with the voltage-gated sodium channel blocker tetrodotoxin (TTX) induces a cell-wide upregulation in excitatory synaptic transmission in both cultured hippocampal (Corrêa et al., 2012, Soares et al., 2017) and cortical (Turrigiano et al., 1998, Rutherford et al., 1998) pyramidal neurons. Likewise, prolonged (24-72 hr) pharmacological inhibition of excitatory transmission by blocking AMPA and NMDA glutamatergic receptors results in a significant upregulation of excitatory transmission along with a proportional increase in AMPAR accumulation at synapses (O'Brien et al., 1998), though this effect is likely primarily mediated by the blockade of AMPA and kainite receptor signalling (Turrigiano et al., 1998)..

Conversely, chronic increases in excitatory transmission through pharmacological blockage of inhibitory GABAergic transmission results in a decrease in excitatory transmission strength of cultured spinal neurons (O'Brien et al., 1998) along with cortical pyramidal neurons (Turrigiano et al., 1998) and hippocampal interneurons (Chang et al., 2010). This reduction in excitatory transmission in response to an increase in global transmission has been observed to accompany a reduction in AMPAR expression at synapses (O'Brien et al., 1998). These activity-dependent changes in excitatory transmission therefore seem to scale overall neuronal activity to maintain a constant level of excitability. At the network level, in organotypic hippocampal slices, chronic inhibition of excitatory transmission was seen up upregulate synaptic transmission at DG-CA3 and CA3-CA1 synapses, which is in line with the above idea of homeostatic scaling (Kim and Tsien, 2008). However recurrent CA3-CA3 synapse transmission was decreased, which appeared to limit potential epileptogenic activity brought about by the increase in synaptic transmission at DG-CA3 and CA3-CA1 synapses (Kim and Tsien, 2008). Homeostatic plasticity therefore appears to be regulated cell-wide, but the activity-dependent modifications are synapse specific.

Another study applied TTX to the hippocampus *in vivo* by implanting a slow release mechanism after 2 days saw an increase in CA3-CA1 excitatory transmission in concordance with the above *in vitro* studies (Echegoyen et al., 2007). In juvenile animals (p15) this increase was associated with an increase in AMPAR expression at the postsynapse, however, increased excitatory transmission in adult animals (p30) appeared to be largely due to increased presynaptic release probability, or synaptogenesis (Echegoyen et al., 2007). Echegoyen et al. (2007) also noted an increase in amplitude of inhibitory GABAergic transmission in both adult and juvenile rats. These results largely replicate the results of the cultured neuronal studies mentioned in the previous paragraph within a more realistic model.

The molecular mechanisms underlying homeostatic modifications are still unclear (Turrigiano, 2012). The dynamic regulation of AMPAR expression at synapses appears to, at least in part, underlie homeostatic synaptic plasticity and several molecules have been proposed to regulate this process including BDNF, the IEG Arc/Arg3.1 and postsynaptic density (PSD) -95 (Turrigiano, 2012). One of these candidates, Arc/Arg3.1, promotes the endocytosis of AMPARs cell-wide in response to activity-dependent changes (Corrêa et al.,

2012, Minatohara et al., 2015) through interactions with endophilin and dynamin (Shepherd et al., 2006). BDNF can also induce the expression of Arc/Arg3.1 (Hunter et al., 2017) and promotes the localisation of PDS-95 to the postsynapse (Yoshii and Constantine-Paton, 2014). PSD-95, a major scaffolding protein which functions to stabilise glutamate receptors at the postsysnaptic density (PSD) present at the psotsynapse of glutamatergic synapses (Chen et al., 2011). PSD-95 is dynamically redistributed across synapses within a cell and longer PSD-95 retention corresponds with an increased PSD size, which is stabilised at synapses that actively receive input (Gray et al., 2006). Arc/Arg 3.1 and PSD-95 therefore appear to work antagonistically, responding to extracellular signals released in an activity-dependent manner such as BDNF, to regulate the strength of synaptic efficacy across synapses neuron-wide.

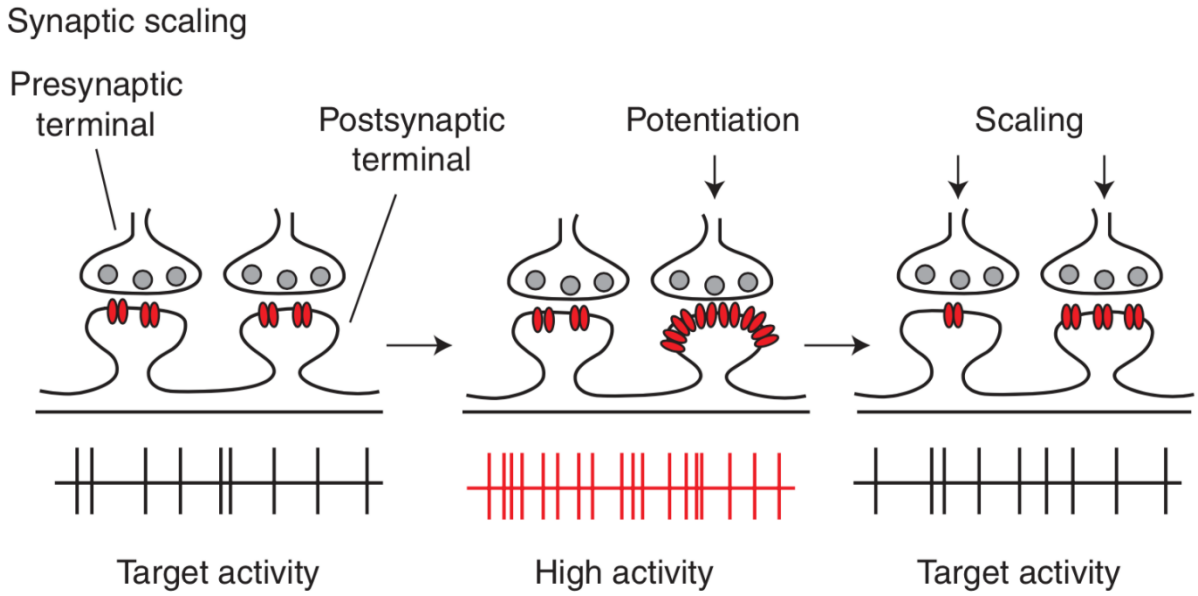

Figure 1.4. An illustration of homeostatic scaling of a neuron in response to Hebbian potentiation at a synapse. AMPAR channels (red) increase in number at a potentiated synapse (right-hand synapse). This increases overall neuronal activity, and so total AMPAR expression at synapses is reduced to return overall neuronal activity to pre-potentiation event levels, whilst maintaining the relative transmission weights between synapses. Figure from Turrigiano (2012).

Induction of homeostatic plasticity in response to changes in global cell excitability is determined by Ca^{2+} influx during neuronal signalling (Turrigiano, 2012). Intracellular Ca^{2+} concentration levels, detected by multiple calcium-sensitive pathways, are thought to determine the strength and direction of global changes in cell excitability (Turrigiano, 2012).

1.2.3 AMPA receptors are key mediators of synaptic plasticity

AMPARs are homomeric or tetrameric assemblies of the GluA subunits: 1, 2, 3 and 4, (encoded by the Gria1-4 genes) that form an ionotropic channel that opens in response to extracellular binding of L-glutamate (Chater and Goda, 2014) (Figure 1.5 A, B). Subunit composition defines the properties of the AMPAR such as conductance, sensitivity to neurotransmitter and interaction with intracellular proteins (Chater and Goda, 2014, Henley and Wilkinson, 2016). The heteromeric GluA1/GluA2 AMPAR is the most commonly expressed subunit assembly throughout the forebrain including the hippocampus (Isaac et al., 2007) (Figure 5.3 B), and is impermeable to Ca^{2+} ions due to post-transcriptional Q/R editing of the GluA2 transcript (Sommer et al., 1991, Cull-Candy et al., 2006, Chater and Goda, 2014). The presence of the edited R residue obstructs divalent cation (including Ca^{2+}) entry through the AMPAR (Figure 1.5 C) due to its proximal location to the channel pore and reduces channel conductance (Swanson et al., 1997, Isaac et al., 2007). The majority of GluA2-containing AMPARs found within the mature brain are calcium-impermeable (>99%) (Greger et al., 2003).

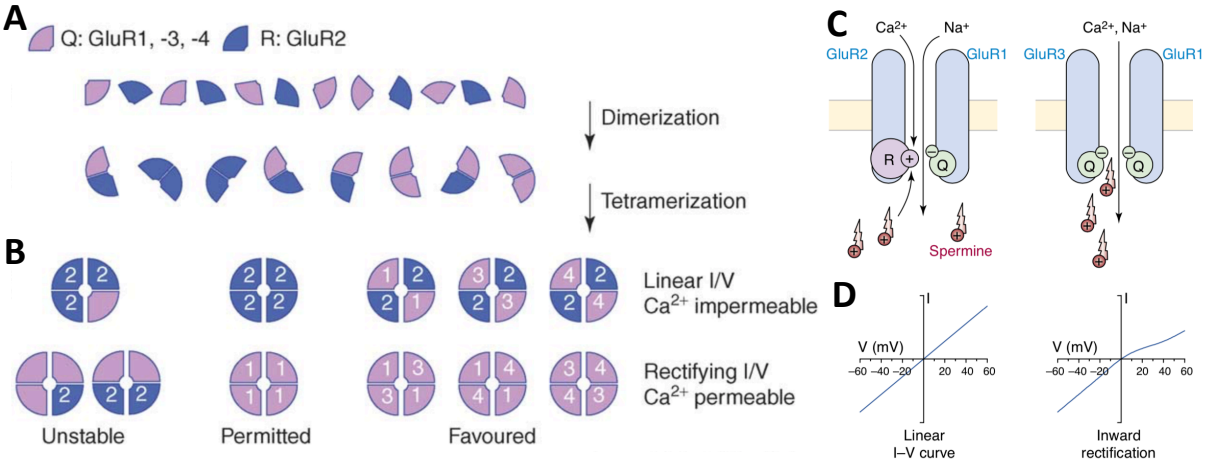

Figure 1.5. Tetramerisation of AMPAR subunits and the effect of GluA2 subunit inclusion on Ca^{2+} permeability. Q(Glutamine)/R(Arginine) editing of GluR2 (GluA2) subunits prevents Ca^{2+} entry when GluA2 is assembled into an AMPAR receptor with other combinations of GluA1-3 subunits and in rare GluA2 homomers. **A)** GluR (GluA) receptor subunits 1, 3 and 4 do not contain an edited R residue, unlike GluA2 and first dimerise and tetramerise to form functional AMPAR receptors. **B)** Certain tetrameric assemblies are inherently unstable, and therefore certain configurations of GluA subunits are favoured in functional AMPARs. GluA2 inclusion in AMPAR assemblies determine channel Ca^{2+}

permeability properties. **C)** AMPAR channels are subject to intracellular spermine block unless their assembly includes the Q/R edited GluA2 subunit. **D)** AMPARs containing edited GluA2 subunits are Ca^{2+} impermeable and present a linear I/V relationship. GluA2-lacking, Ca^{2+} permeable AMPARS display rectifiying I/V relationships due to polyamine block at positive potentials. Figure 1.5 A + B (left) from Cull-Candy et al. (2006) and Figure 1.5 C and D (right) from Domenico E Pellegrini-Giampietro (2003).

GluA1 homomeric or heteromeric assemblies lacking GluA2, however, are permeable to both Na^{+} and Ca^{2+} and are subject to intracellular block by endogenous polyamines such as spermine and spermidine (Jonas et al., 1994, Bowie and Mayer, 1995) (Figure 1.5 C). Ca^{2+} impermeable (CI) AMPARs display a linear current/voltage (I/V) relationship, whereas conductance of Ca^{2+} permeable (CP) AMPARs at positive intracellular potentials is reduced due to intracellular polyamine block and display a rectifying I/V relationship (Pellegrini-Giampietro, 2003) (Figure 1.5 D).

CP-AMPARS are the primary form of AMPAR expressed during early development in cortical pyramidal neurons (Kumar et al., 2002) and immature cultured hippocampal pyramidal neurons (Pickard et al., 2000) due to lack of GluA2 subunit expression. However, GluA2 expression increases quickly following the second week of postnatal development (Kumar et al., 2002). Up to 8-10 % of AMPARs present a basal level within adult CA1 cells of the hippocampus are CP-AMPARS (Rozov et al., 2012). As previously mentioned, dynamic presentation or removal of AMPARs at synapses is thought to underlie both Hebbian and homeostatic synaptic plasticity (Figures 1.3 and 1.6 A respectively) In this way, postsynaptic AMPAR availability for neurotransmitter binding at a specific synapse can be modulated in response to activity.

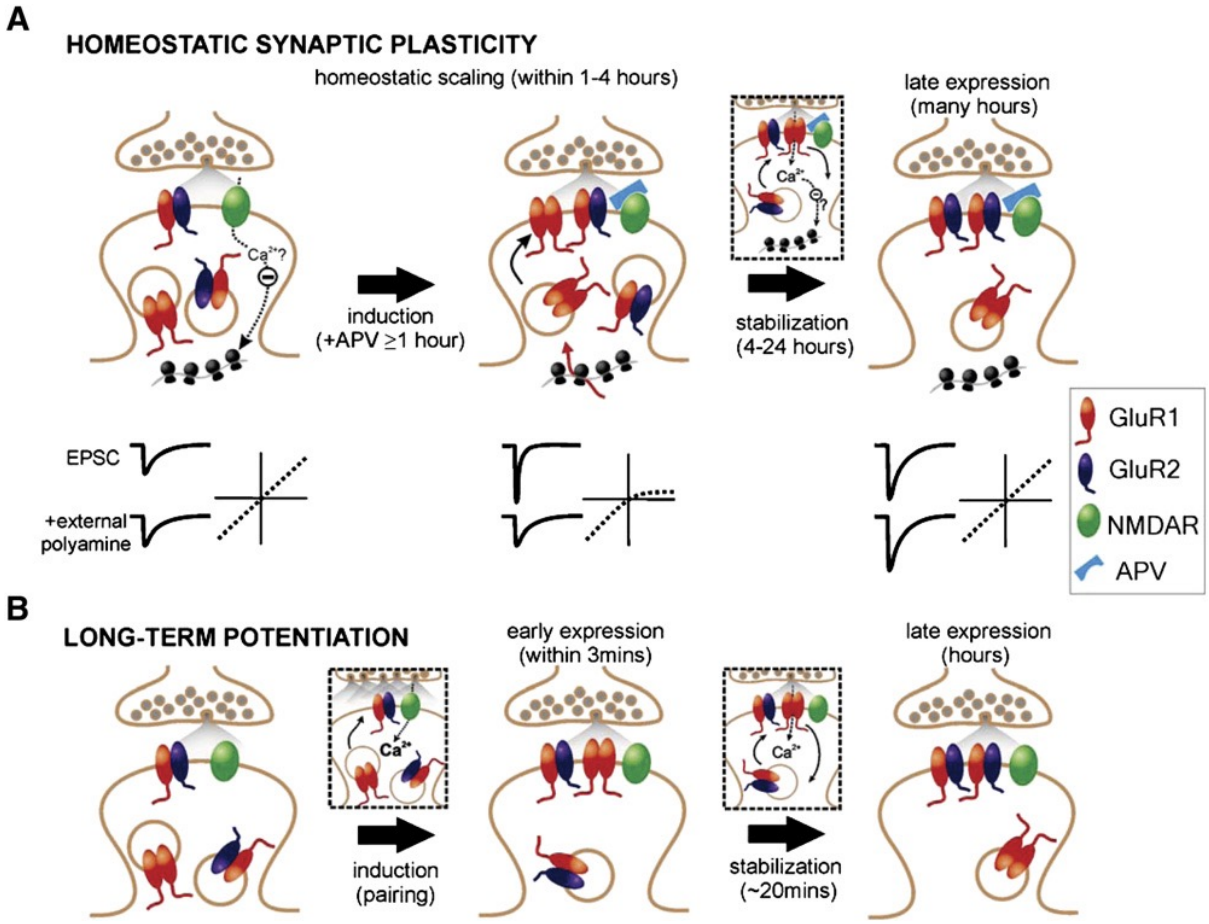

Figure 1.6. Homeostatic plasticity and long-term potentiation induction in CA1 neurons involves the transient recruitment of GluR2 (GluA2) lacking AMPARs: A) Following homeostatic plasticity induction (left) - in this case synaptic scaling in response to block of NMDARs by D-AP5 – an increase in dendritic GluA1 synthesis occurs, leading to an increase in GluA2 lacking AMPARs and their incorporation into the postsynaptic membrane (middle). Stabilisation of synaptic changes then occurs over the next 4-24 hours, and GluA2-lacking AMPARs are replaced by GluA2-containing AMPARs, in a Ca^{2+} dependent mechanism mediated in part by Ca^{2+} influx through CP-AMPARs (right). **B)** During LTP induction (left), Ca^{2+} influx during activation of NMDARs promotes insertion of GluA2 lacking AMPARs into the postsynaptic membrane within minutes (middle). The increase in synaptic strength is then preserved over the next 20 minutes whilst GluA2-lacking AMPARs are replaced with GluA2-containing AMPARs, driven again by Ca^{2+} through CP-AMPARs (right). I/V relationship of postsynaptic cells at each stage of these processes, and the subsequent increase in rectification due to CP-AMPAR presence is displayed in the centre. Figure from Isaac et al. (2007).

Insertion of additional CP-AMPARs can also occur during hippocampal LTP through their transient insertion into the postsynaptic membrane following LTP induction (Plant et al., 2006, Morita et al., 2014) (Figure 1.6 B). preferentially at silent synapses (Morita et al., 2014).

Silent synapses lack sufficient AMPAR expression to respond to presynaptic neurotransmitter release but can rapidly traffic AMPARs to the postsynaptic membrane during LTP events and be rapidly recruited into functional synapses (Liao et al., 1995, Isaac et al., 1995, Morita et al., 2014). CP-AMPARs play an essential role in mediating synaptic plasticity (Cull-Candy et al., 2006, Isaac et al., 2007) and the induction of certain forms of LTP such as PKA-dependent LTP within the hippocampus of rats aged between 3-12 weeks (Park et al., 2016, Park et al., 2018). CP-AMPARs are subject to an activity-dependent block by intracellular polyamines such as spermine, requiring coincident glutamate activation coupled with postsynaptic depolarisation, functioning in a similar manner to Mg^{2+} block of NMDA receptors (Pellegrini-Giampietro, 2003). Expression of CP-AMPARs therefore present an important source of postsynaptic NMDAR dependent synaptic plasticity that is thought to be important for the conversion of E-LTP into L-LTP, dependent on stimulation following their insertion (Park et al., 2018). However, the above studies have focused on rodents <12 weeks of age, and therefore still pre-adulthood and doubts have been raised about the necessity of CP-AMPARs for CA1 neuron LTP induction in adult mice: pharmacological block of CP-AMPAR signalling in 2-3 month old mice did not affect LTP induction (Gray et al., 2007). However, the stimulation strategy employed by Gray et al. (2007) (HFS delivered as a compressed protocol) differed from that of Park et al. (2016) (HFS spaced over 10 min), and a role for CP-AMPARs in the protein-synthesis dependent stage of LTP consolidation has been proposed (Park et al., 2018). Further experiments using adult animals (>12 weeks age), longer (>1 hour) recording times of induced LTP more in line with Park et al. (2016) and LTP induction with and without CP-AMPAR inhibitors are necessary to definitively determine a role for CP-AMPAR necessity in LTP consolidation.

Hebbian modulation of a synapse can therefore lead to an increase or decrease in signal transmission across an individual synapse in response to an activity-dependent presynaptic stimulus. Over- and under-stimulation of a cell through Hebbian processes is prevented by homeostatic scaling, which also occurs in an activity-dependent manner, and dynamic changes in AMPAR receptor expression and composition at a synapse is essential to both forms of plasticity. These changes in synaptic strength in response to external stimuli create new patterns of activation that can be reactivated by those same stimuli; this is thought to directly underlie the storage of learning and memory (Takeuchi et al., 2014, Bliss

et al., 2018). Therefore, these plasticity mechanisms of synaptic strength are thought to play a part in the underlying learning and memory within the hippocampus during *in vivo* learning and memory within an animal.

1.3 Molecular mechanisms underlying memory and synaptic plasticity

1.3.1 Regulation of transcription factors

Consolidation of memory during *in vivo* behavioural trials, like L-LTP, requires transcription (Alberini and Kandel, 2014). This induction and regulation of activity-dependent transcription is mediated by immediate early genes (IEGs), which go on to regulate intracellular pathways and the expression of further transcription factors (Alberini and Kandel, 2014). The expression of IEGs and genes involved in the regulation of learning and memory can be regulated by cyclic-AMP response element binding protein (CREB), serum-response factor (SRF), nuclear factor-κ light-chain enhancer of activated B cells (NF-κB) and activator protein-1 (AP-1) (Alberini and Kandel, 2014) whose binding sites are well conserved within IEG upstream promotor regions (Tullai et al., 2007).

Epigenetic regulation of histones via acetylation and phosphorylation by various intracellular histone acetyl transferases (HATs) and kinases have also been shown to be necessary for the transcriptional response underlying LTP (Levenson and Sweatt, 2005, Alberini and Kandel, 2014). These histone modifications modulate histone interaction with DNA and affect transcription factor access to DNA, either aiding or preventing their recruitment, and thus regulating transcription (Levenson and Sweatt, 2005). CREB-binding protein (CBP) is a prominent HAT, and heterozygous CBP mice suffer impaired declarative memory consolidation (as assessed by novel object recognition and the MWM) but not short-term memory during behavioural tasks, and a reduction in c-Fos expression in CA1 neurons, underlining the role histone regulation plays during memory-dependent transcription (Korzus et al., 2004). Additionally mitogen-and stress-activated protein kinase 1 (MSK1) phosphorylates histone H3 in response to MAPK activation which has been shown to likely underlie Arc/Arg3.1 induction following BDNF signalling (Hunter et al., 2017).

1.3.1.1 CREB and its role in memory and synaptic plasticity

cAMP response element–binding protein (CREB) has been implicated as an important evolutionarily-conserved mediator of synaptic plasticity during the activity-dependent regulation of transcription in response to synaptic signalling events (Sheng et al., 1990, Shaywitz and Greenberg, 1999, Sakamoto et al., 2011, Alberini and Kandel, 2014). CREB is a key mediator of spatial memory (Pittenger et al., 2002, Viosca et al., 2009), fear encoding and retrieval (Kida et al., 2002) and memory consolidation (Yin et al., 1995, Ortega-Martínez, 2015). Functioning as a transcription factor, CREB regulates the expression of immediate early genes (IEGs) such as c-Fos (Ginty et al., 1994, Bito et al., 1996), CCAAT enhancer – binding protein (C/EBP) and Early growth response 1 (Egr1 also known as Zif268) which are involved in regulating further transcription following their activation (Alberini and Kandel, 2014), along with other CRE promotor-containing genes (Barco et al., 2008). This is explored in more detail below.

1.3.1.2 CREB and its role in LTP and long-term memory.

CREBs role in mediating LTP has been controversial: CRE-dependent gene transcription induction was seen to be necessary for memory consolidation to occur in *alpysia* and *drosophila* models when activated through a PKA-dependent pathway (Bito et al., 1996, Silva et al., 1998). Within rodent models, LTP disruption has been observed in loss-of-function hypomorphic mutants of CREB, in which the alpha and delta isoforms of CREB were mutated (CREB$\alpha\delta$) (Bourtchuladze et al., 1994). However later studies using CREB$\alpha\delta$ mice found no LTP deficit, and complete CREB inactivation mutants (CREBnull, featuring disruption of all CREB isoforms including α, δ and β) also displayed normal LTP (Gass et al., 1998), LTD and do not display significantly impaired spatial learning (Balschun et al., 2003). Lack of CREB expression seems to affect other CREB family transcription factors such as cAMP responsive element modulator (CREM), which undergoes a 2-3-fold compensatory increase in expression within the brain in response to CREB $\alpha\delta$ isoform disruption (Hummler et al., 1994) as well as the β isoform of CREB (Blendy et al., 1996). CREM expression is also upregulated CREBnull mice, and mutants experiencing disruption of both CREB and CREM suffer neurodegeneration and apoptosis in hippocampus (Balschun et al., 2003). CREM and Activating Transcription Factor 1 (ATF-1) are CRE-binding, CREB family transcription factors sharing high homology

with CREB, and could compensate for CREB-mediated activity in hypomorphic CREB mutants (Gass et al., 1998, Barco and Marie, 2011, Vogt et al., 2014).

More specific loss-of-function mutations in CREB that disrupt activity and not expression therefore provided a more robust way of testing CREB-mediated LTP. Using a "KCREB" mutant expressing a dominant negative form of CREB that is transcriptionally inactive yet competes for CRE-binding promotor regions, Pittenger et al. (2002) observed deficits in spatial memory and LTM but normal short-term memory (STM). Expression of KCREB inhibited the normal transcriptional activity of CREB, CREM and ATF-1 within the CA1 region of the hippocampus and was doxycycline-controlled, such that upon doxycycline application, behavioural deficits were reversed (Pittenger et al., 2002). In another loss of CREB function study on memory, short-term antisense oligodeoxynucleotide-mediated disruption of CREB expression within the hippocampus was observed to impair LTM formation in spatial memory-dependent tasks, with inhibition only required for a short period following initial exposure to a training stimuli (Guzowski and McGaugh, 1997).

Loss-of-function CREB studies therefore implicate CREB in LTM formation and LTP. However, they have not always seen a necessary role for CREB function and can be confounded by compensation of related genes and the genetic background of animals used. Expression of a constitutively active form of CREB however, has been seen to facilitate LTP within the hippocampus (Barco et al., 2002). This appears to occur due to an enhancement in CBP binding, and c-Fos expression, which resulted in LTP induction after just one train of electrical stimulation, rather than 4 spaced high frequency pulses as is typically required (Barco et al., 2002). Gain of CREB function studies seem to consistently implicate CREB in mediating LTP and LTM formation (Barco and Marie, 2011).

1.3.1.3 Regulation of CREB transcriptional activity within neurons

CREB is localised within the nucleus, and is thought to be constitutively bound to DNA with its transcriptional activity regulated by its phosphorylation state (primarily at Ser133) (Wiggin et al., 2002) (Mayr et al., 2001) and by interactions with other CREB-binding proteins such as the CREB-regulated transcriptional coactivators (CRTCs, previously known as TORCs) (Conkright et al., 2003, Barco and Marie, 2011). Phosphorylation at Ser133 regulates the

interaction between CREB and its co-activator CBP (Chrivia et al., 1993, Mayr et al., 2001). Once in complex together, CBP can recruit RNA polymerase II to the promotor region of CRE-containing genes and CREB-mediated gene expression can take place (Kee et al., 1996).

CREB phosphorylation at Ser133 can occur through the activation of several different pathways leading to changes in intracellular second messengers and the activation of various kinases (Naqvi et al., 2014). Protein kinase A (PKA) is activated by increased intracellular cAMP where it can then act as a CREB kinase (Gonzalez and Montminy, 1989). Elevations in cAMP are mediated by adenylate cyclases, which are regulated by increases in intracellular Ca^{2+} and G protein-coupled receptors (GPCRs) (Poser and Storm, 2001, Lonze and Ginty, 2002). Application of forskolin, which stimulates adenylate cyclase (AC) and thus increases cAMP concentration within cells directly results in an increase in pCREB levels (Sheng et al., 1991).

Protein kinase C (PKC) and Ca^{2+}/calmodulin-dependent protein kinases I, II and IV (CaMK I, II and IV) are activated by an increase in intracellular concentrations of Ca^{2+} and also contribute to CREB phosphorylation (Yamamoto et al., 1988, Sheng et al., 1991, Bito et al., 1996). During an activity-dependent depolarisation event, presynaptic glutamate release activates postsynaptic AMPA receptors, causing an initial elevation of intracellular Na^{+} concentration, which results in the removal of the voltage-dependent Mg^{2+} block of NMDARs through which Ca^{2+} and further Na^{+} influx can occur. Additionally, this depolarisation event activates voltage-sensitive Ca^{2+} channels, which then allows further Ca^{2+} influx. Ca^{2+} influx activates calmodulin (CaM) which binds Ca^{2+} forming Ca^{2+}/CaM. The activated Ca^{2+}/CaM complex can then phosphorylate CaMKII and CaM kinase kinase (CaMKK) which then activates CaMKI and IV, which can then subsequently phosphorylate CREB (Means, 2000). CaMKIV is localised to the nucleus of cells, highly expressed within the brain and is necessary for Ca^{2+}-induced expression of BDNF (Means, 2000). Activation of CaMKIV depends on an isoform of CaMKII: γCaMKII which shuttles Ca^{2+}/CaM from voltage sensitive Ca_V1 Ca^{2+}channels where Ca^{2+} concentration is high, to the nucleus whereupon releasing bound Ca^{2+}/CaM, it induces the activation of CaMKIV via CAMKK and allows CaMKIV to phosphorylate CREB at Ser133 (Ma et al., 2014).

Neurotrophin stimulation of receptor tyrosine kinases (RTKs) can also cause CREB phosphorylation via the phosphatidylinositol 3-kinase (PI3K)/AKT Serine/Threonine Kinase (AKT) signalling pathway (Lonze and Ginty, 2002). Ribosomal S6 kinases (RSKs) can also phosphorylate CREB *in vitro* in response to nerve-growth factor through the neurotrophin-mediated activation of RTKs and subsequent recruitment of a mitogen-activated protein kinase (MAPK) cascade recruiting mitogen-activated protein kinase kinase (MEK) and extracellular signal-related kinases 1/2(ERK1/2) (Lonze and Ginty, 2002).

CREB can also be directly phosphorylated by mitogen- and stress-activated protein kinases 1 and 2 (MSK1/2), which are activated by the MAPK pathway via ERK1/2 (Arthur, 2008). MSK1/2-mediated phosphorylation of CREB at Ser133 does not seem to strongly recruit the CREB co-activators CBP or p300 in contrast to PKA-mediated CREB phosphorylation (Mayr et al., 2001). However, despite this, CREB phosphorylation by MSK1/2 is essential for MAPK-mediated CREB-dependent gene expression (Naqvi et al., 2014). CREB is phosphorylated at serine (Ser) 133 in response to the extracellular neurotrophins: BDNF, nerve growth factor (NGF) and fibroblast growth factor (FGF) (Ginty et al., 1994). MSK1 is believed to be the primary kinase involved in CREB phosphorylation in response to neurotrophin stimulation (Arthur et al., 2004). CREB phosphorylation therefore serves as a signalling hub, integrating a multitude of signalling pathways into a transcriptomic response which can then change the behaviour and structure of synapses. This is summarised in Figure 1.7 below.

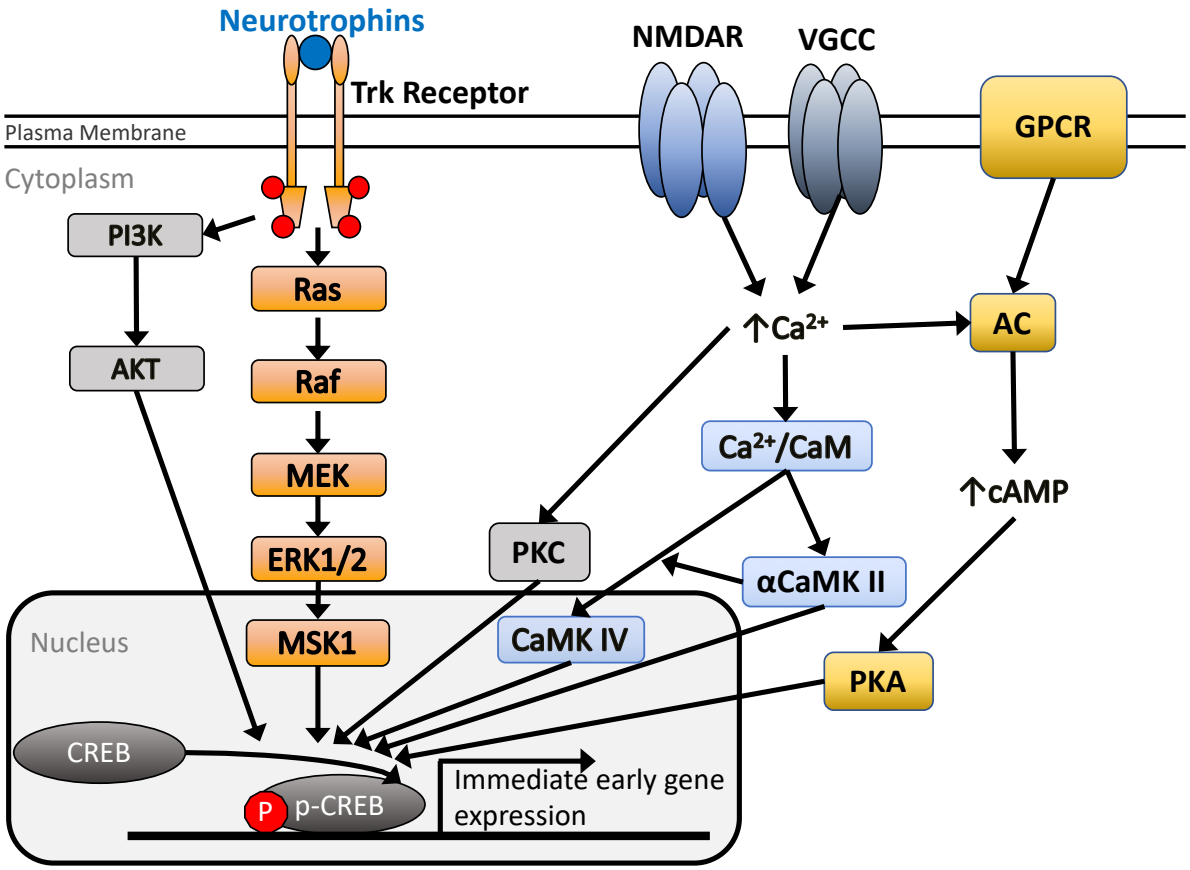

Figure 1.7. Summary of CREB phosphorylation in the mammalian brain by various endogenous signalling pathways. Left to right: Neurotrophin activation of tyrosine-kinase (Trk) receptors can activate the phosphatidylinositol 3-kinase (PI3K)/AKT Serine/Threonine Kinase (AKT) signalling pathway, resulting in CREB phosphorylation. Neurotrophin activation of Trk receptors can also trigger a ras/raf- mediated MAPK signalling cascade that phosphorylates and activates MSK1 via MEK and Erk1/2 (orange). Depolarisation of a neuron triggers the influx of Ca^{2+} through NMDARs and voltage-sensitive calcium channels (VSCCs). Intracellular Ca^{2+} can then bind Calmodulin (CaM) forming the activated Ca^{2+}/CaM complex activating a series of CaM kinases including αCaMKII which shuttles Ca^{2+}/CaM to the nucleus and activates CaMKIV (blue). PKC can also be activated by intracellular Ca^{2}. Adeylate cyclase (AC) converts ATP to cAMP in response to stimulation by GPCRs and intracellular Ca^{2+}, and increases in cAMP activate PKA which can then go on to phosphorylate CREB (yellow).

1.3.2 Immediate early genes in synaptic plasticity

IEGs are a rapidly activated family of genes that constitute the first wave of activity-induced transcription, with nuclear transcript expression appearing within minutes of LTP induction (Minatohara et al., 2015). A significant number of IEGs are transcription factors, or have a role in regulating transcription themselves (Tullai et al., 2007) whereas others can directly affect synaptic transmission in neurons (Minatohara et al., 2015). *In vivo* induction of

IEG expression within a hippocampal neuron is also associated with its involvement in spatial and fear memory processing (Minatohara et al., 2015).

c-Fos, Egr1 and Arc/Arg3.1 are important IEGs involved in the regulation of synaptic plasticity and memory formation (Minatohara et al., 2015, Duclot and Kabbaj, 2017, Wall et al., 2018). Arc/Arg3.1 mRNA can be localised to dendrites after its transcription, where local translation into Arc/Arg3.1 protein can take place (Steward et al., 2014). Arc/Arg3.1 can be translocated to inactive spines and synapses during LTP induction at active synapses, reducing AMPAR content at synapses not undergoing potentiation, which serves to enhance the contrast between potentiated and non-potentiated synapse transmission strengths (Okuno et al., 2012) and is thought to be one mechanism underlying homeostatic plasticity (Turrigiano, 2012). Egr1 and c-Fos display transcription factor activity, with Egr1 targeting the expression of MAPK proteins and neurotrophins (Duclot and Kabbaj, 2017). Egr1 knock-down in the hippocampus has been shown to affect the persistence of memories following consolidation (Duclot and Kabbaj, 2017).

Many IEGs contain CRE promotor sites, and expression of a constitutively active form of CREB in human embryonic kidney (HEK) cells has been shown to affect the expression of cFos and BDNF (Barco et al., 2008). Another IEG regulated by CREB is the CCAAT enhancer-binding protein (C/EPB), the expression of which is upregulated within hippocampal CA1 neurons after LTP induction at CA3/CA1 synapses (Arguello et al., 2013), and whose disruption can block the induction of L-LTP and formation of LTM (Arguello et al., 2013, Alberini and Kandel, 2014). CREB's role in memory is therefore dependent on its ability to modulate the transcription of genes involved in regulating synaptic transmission, which is poised to integrate activity-based changes in synaptic transmission, through regulation of its activity by phosphorylation through multiple signalling pathways.

1.3.3.1 Brain-derived neurotrophic factor within the hippocampus

BDNF is a 14 kDa protein belonging to the family of neurotrophins, signalling molecules that also includes neurotrophic factor 3 (NT3), NT4/5 and nerve-growth factor (NGF) and that share structural homology. BDNF begins as the precursor molecule pre-pro-BDNF synthesised within the endoplasmic reticulum, whereupon, after folding, it is

translocated to the Golgi apparatus (Kowiański et al., 2018). Within the Golgi apparatus, pre-pro-BDNF has its signal localisation region cleaved yielding pro-BDNF 32 kDa in size (Kowiański et al., 2018). As pro-BDNF progresses through the Golgi apparatus through to the trans-Golgi/early secretory vesicle maturation stage, pro-BDNF is cleaved to yield mature BDNF, a 14 kDa protein (Mowla et al., 2001, Kowiański et al., 2018). Both pro-BDNF and mature BDNF are secreted, and pro-BDNF can undergo extracellular cleavage by enzymes including matrix-metalloproteases 2 and 9 (Kowiański et al., 2018). Pro-BDNF appears to function antagonistically to mature BDNF, negatively regulating many BDNF-dependent functions such as dendritic branching and synaptic plasticity (Yang et al., 2014a). pro-BDNF expression in mice appears similar to mature BDNF during early development (p15), but decreases by p42 and further subsequently with age, with mature BDNF levels dominating in adulthood, implying mature BDNF (hereafter referred to as just BDNF) is most important in the adult organism (Yang et al., 2014a).

BDNF is the endogenous ligand for the tropomyosin receptor kinase B (TrkB) receptor, where upon binding, it induces receptor dimerisation triggering autophosphorylation of intracellular tyrosine residues within the TrkB receptor kinase domain. Once phosphorylated, the kinase domain of TrkB then phosphorylates tyrosine (Tyr) residues within its juxtamembrane domain. Phosphorylation of residue Tyr816 triggers intracellular release of calcium via generation of inositol-1,4,5-trisphosphate (Ins(1,4,5)P3) and can activate CREB via CaMKs discussed earlier (Figure 1.7) (Minichiello, 2009). Phosphorylation of Tyr515 at the juxtamembrane domain allows the binding and recruitment of adaptor proteins containing phospho-Tyr-binding domains such as sarcoma (src) homology and collagen (Shc) containing adapter proteins and fibroblast growth factor receptor substrate 2 (FRS2) (Minichiello, 2009). Shc adaptors are then themselves phosphorylated and can then bind growth-factor receptor-bound protein 2 (GRB2) and son of sevenless (SOS) proteins, which themselves trigger a Ras/Raf response activating a MAPK signalling cascade (Minichiello, 2009). FRS2 competes with Shc adaptors for binding to phosphoTyr515 sites and can itself also bind GRB2, triggering Ras/Raf signalling to the MAPK pathway (Minichiello, 2009). The MAPK signalling cascade then activates ERK1/2 (Alonso et al., 2004), which then phosphorylates MSK1 (Arthur, 2008), and results in an upregulation of CREB Ser133 phosphorylation (Arthur et al., 2004).

Physiological concentrations of BDNF are difficult to estimate: Effective increases of BDNF-mediated activity can be observed by bathing slices in concentrations of between 20-50 ng/mL (0.8-2nM) (Kang and Schuman, 1995, Figurov et al., 1996, Ji et al., 2010, Corrêa et al., 2012, Hunter et al., 2017), giving insight to the physiological concentrations of BDNF during active release, however bath application of BDNF must get around sequestering of BDNF by BDNF receptors at the slice surface in order to penetrate to the more active middle of slice.

Application of BDNF to cultured hippocampal DGCs has been seen to induce both axonal and dendritic branching in dentate granule cells, but this effect was not seen in cultured CA1 or CA3 cells (Danzer et al., 2002). This BDNF-induced increase in dendritic complexity within DGCs was abolished with the inclusion of a tyrosine kinase (Trk) receptor inhibitor, highlighting the role BDNF-TrkB signalling plays in regulating hippocampal cell morphological plasticity (Danzer et al., 2002). BDNF application to CA1 neurons does however, increase spine density in an Erk1/2 dependent manner (Alonso et al., 2004). 2 weeks of BDNF application into the adult rat hippocampus increases neurogenesis within the dentate gyrus, increasing numbers of mature dentate granule cells for at least 1 month after application was over (Scharfman et al., 2005).

The hypothesised role of BDNF in learning and memory comes from electrophysiological studies performed using LTP-inducing stimuli and behavioural tasks: BDNF mRNA expression within the hippocampus has been seen to increase following hippocampus-dependent tasks such as during spatial memory acquisition in the MWM or radial maze (Kesslak et al., 1998)}, and contextual fear conditioning (Hall et al., 2000, Lu et al., 2008). BDNF release is necessary for the induction and maintenance of LTP at glutamatergic and GABAergic synapses within the CNS (Gottmann et al., 2009, Lin et al., 2018, Panja and Bramham, 2014). Mice heterozygous for BDNF knockout have shown reduced BDNF expression leads to impaired *in vitro* LTP in the layer IV-III pathway within the visual cortex (Bartoletti et al., 2002) and at CA3-CA1 synapses within the hippocampus (Novkovic et al., 2015). Bath application of TrkB-IgG (which acts to soak up extracellular BDNF) to hippocampal slice preparations disrupts LTP formation, and can even reverse induced LTP within 70m of the inducing tetanic stimuli (Kang et al., 1997, Lu et al., 2008). In addition, application of anti-

BDNF oligo nucleotides (to prevent BDNF synthesis) prevents LTM formation, and infusion after learning can disrupt recall of established spatial memories (Lu et al., 2008). Furthermore, selective genetic deletion of BDNF from either CA1 or CA3 neurons has indicated that the presynaptic release of BDNF is required for LTP induction, but postsynaptic BDNF is required for LTP maintenance (Lin et al., 2018). BDNF activity and expression therefore plays a key role in the formation of LTP and long term memory.

BDNF release occurs from neurons in an activity-dependent manner (Patterson et al., 1992, Tao et al., 1998, Kohara et al., 2001, Gärtner and Staiger, 2002, Matsuda et al., 2009): LTP inducing stimuli, High-frequency (250 pulses, at 50Hz), tetanic (100 pulses, at 100Hz, 3 times with 20s in between) and theta burst stimulation (TBS, 10 bursts of four pulses, at 100 Hz, with 200 ms in between, spaced 10s apart for 1m) are all sufficient to detect significant increases in BDNF secretion from primary cultures of hippocampal neurons (Gärtner and Staiger, 2002). In contrast, LTD inducing stimulation (1 Hz) is insufficient to trigger BDNF release (Gärtner and Staiger, 2002). In response to neuron depolarisation, BDNF is released from vesicles within both the postsynaptic cell dendrites and to a lesser extent, the presynaptic cell axon (Matsuda et al., 2009). Postsynaptic BDNF release is Ca^{2+}-dependent, at least partially as a result of NMDAR activation (Matsuda et al., 2009). This supports the involvement of activity-dependent release of BDNF in LTP induction and L-LTP formation.

The activity-dependent release of BDNF, its structural effects on spine morphology, dendrite branching and neurogenesis, and its ability to modulate AMPAR and Arc/Arg3.1 expression along with PSD-95 localisation in response to neuronal signalling has led to the hypothesised role of BDNF of, at least in part, mediating the effects of homeostatic synaptic plasticity (Turrigiano, 2008, Turrigiano, 2012). BDNF release has also been observed in response to global changes in synaptic activity, from presynaptic to postsynaptic neurons, with less release during global activity deprivation (TTX incubation) and greater release following hyperexcitation (picrotoxin incubation) compared with baseline spontaneous activity (Kohara et al., 2001).

The activity-dependent increase in neuronal transmission strength in response to TTX-mediated activity deprivation is blocked by 48 hr incubation with exogenous 25 ng/ml BDNF (Rutherford et al., 1998). Additionally 48 hr incubation of cultured cortical pyramidal neurons with scavengers of endogenous BDNF (TrkB-IgG) produces the same increase in AMPAR-mediated transmission as seen following TTX incubation (Rutherford et al., 1998). Conversely, 48 hr incubation of these cultured pyramidal neurons with BDNF (25 ng/ml) produces a significant decrease in AMPAR-mediated synaptic transmission (Rutherford et al., 1998). This lead to the hypothesis by Rutherford et al. (1998) that low network levels of neural activity result in low levels of released BDNF, and synaptic upscaling of excitatory neuron activity occurs. When higher levels of neuronal activity occur, greater levels of BDNF are released, and AMPAR-mediated excitatory transmission is downscaled (Rutherford et al., 1998).

Cultured hippocampal pyramidal neurons display BDNF-mediated scaling effects similar to cortical neurons: Incubation (48 hrs) of hippocampal pyramidal neurons with either BDNF (50 ng/ml), or an inhibitor of TrkB (blocking BDNF signalling), decreases or increases excitatory synaptic transmission respectively (Corrêa et al., 2012). Additionally exogenous BDNF incubation has the opposite effect on cortical bipolar interneurons, which form GABAergic synapses onto excitatory cells and therefore inhibit excitatory activity, increasing AMPAR-mediated synaptic transmission strength at interneuron synapses receiving stimulation from excitatory neurons, increasing interneuon activity and thus their ability to inhibit excitatory cells (Rutherford et al., 1998). Incubation with TrkB-IgG however, does not affect AMPAR-mediated transmission (Rutherford et al., 1998). This suggests that endogenous BDNF levels are capable of modulating excitatory neuron transmission, but only elevated levels of BDNF can modulate interneurons, further complicating the interaction of BDNF expression with networks of neurons.

BDNF, released in an activity-dependent manner during neuronal signalling, is therefore poised to modulate neuronal network activity, both in a synapse specific manner through the facilitation of Hebbian plasticity during LTP induction and maintenance, and through the global regulation of excitatory transmission in response to network activity. How BDNF exerts these effects is explored in the next session.

1.3.3.2 Role of BDNF in CREB phosphorylation and activity-dependent synaptic plasticity

As mentioned previously, CREB can be activated through BDNF-TrkB activation and the phosphorylation of TrkB residue Tyr515 via the MAPK pathway. BDNF application onto the hippocampus of a transgenic constitutively active CREB mutant shows a cooperative enhancement of LTM (Suzuki et al., 2011), suggesting extracellular BDNF signalling can work in concert with upregulated CREB function to enhance LTM. Activity-dependent BDNF release therefore plays an important role in regulating synaptic plasticity, and improvements in STM and LTM due to upregulated CREB activity are thought to be due to increased CREB-mediated BDNF-expression (Suzuki et al., 2011). In this way, activity-dependent release of BDNF can induce CREB-mediated transcriptional changes within neurons (Figure 1.8) and is thought to represent a potential link between external stimuli, neural plasticity and learning (Cowansage et al., 2010). A positive feedback loop therefore exists, between activity-dependent BDNF release, BDNF-mediated CREB activation and subsequent BDNF expression, via CREB-mediated expression of C/EPBβ, which promotes BDNF expression (Bambah-Mukku et al., 2014). This feedback loop is necessary for the consolidation of short-term to long-term memory, and lasts between 24 and 48 hours post-learning, before repression of BDNF expression occurs through binding of repressors including histone deacetylase 2 (HDAC2) and methyl-CpG binding protein 2 to the BDNF promotor region (Bambah-Mukku et al., 2014). This positive feedback loop resulting from LTP-inducing activity inducing BDNF expression and release which activates CREB, leading to further BDNF release therefore seems to play an important role in mediating the induction and maintenance of LTP.

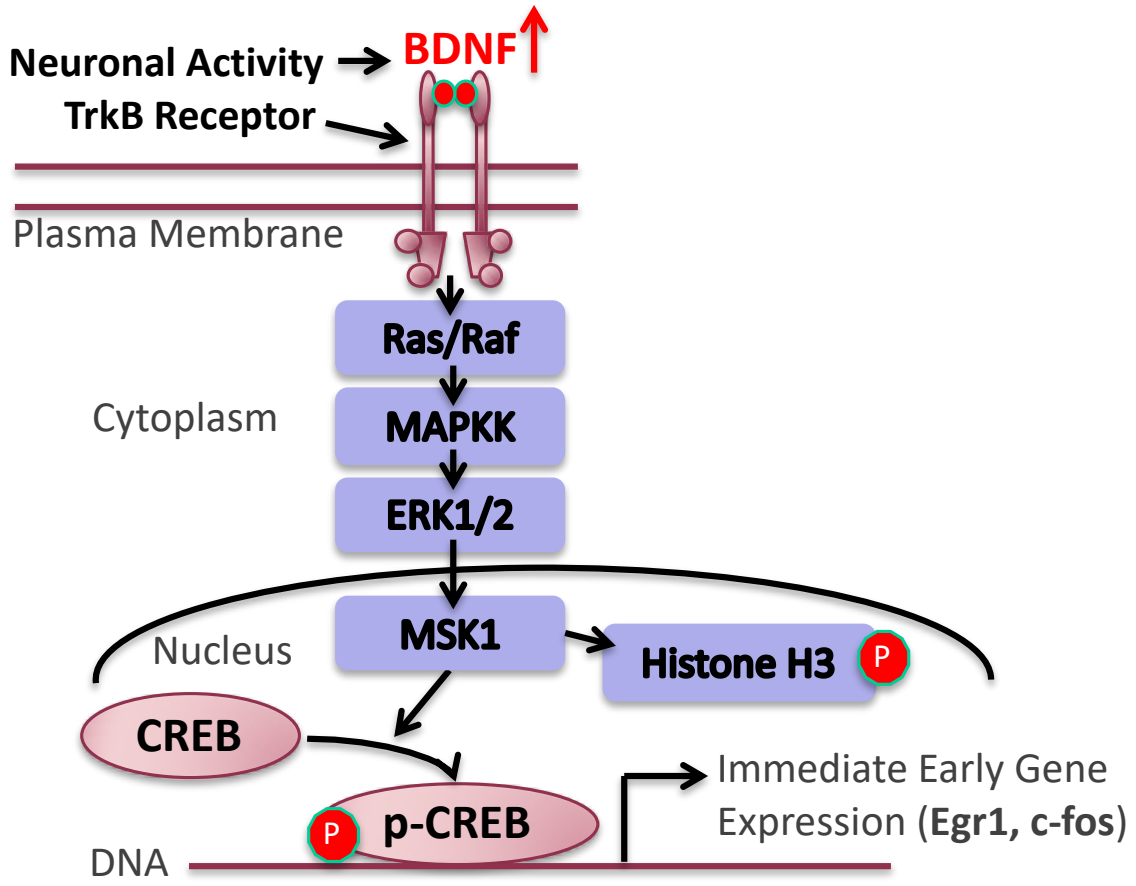

Figure 1.8. A simplified model of MSK1s role in mediating the BDNF-TrkB-dependent activation of CREB transcriptional activity. BDNF binds to TrkB, inducing receptor dimerisation and autophosphorylation of key intracellular Tyr residues. Phosphorylation of Tyr515 activates a MAPK signalling cascade via the recruitment and activation of Ras/Raf through scaffolding proteins. Erk1/2 is activated by the MAPK cascade and phosphorylates MSK1, activating its CREB and histone H3 kinase activity. Phosphorylation of histone H3 can induce a euchromatic open state of chromatin increases, increasing transcription factor access to DNA, where pCREB and other transcription factors can bind and promote transcription.

1.4 The effect of environmental enrichment on the hippocampus, plasticity and memory

1.4.1 Environmental enrichment

Environmental enrichment (EE) has emerged as a potential non-pharmacological intervention to ameliorate the effects of age-related cognitive decline (Sampedro-Piquero

and Begega, 2017, Birch and Kelly, 2019) and cognitive impairment associated with neurological disorders (Nithianantharajah and Hannan, 2006). EE was first described in 1947, when Donald Hebb observed rats exposed to a form of EE (spending ample time outside of their cage exploring his home) to be demonstrably better at problem solving than those raised within cages in the lab (Hebb, 1949). This has been translated into a housing paradigm for research animals, whereby animals are kept in larger cages, featuring many colourful and varied objects and larger social groups to provide extra cognitive stimulation, and exercise wheels for voluntary exercise (Nithianantharajah and Hannan, 2006, Ohline and Abraham, 2019). It can also feature frequent rotation and change of the objects placed within the environment (Ohline and Abraham, 2019) and increased mothering of new-born pups through the inclusion of multiple dams for the same litter (D'Amato et al., 2011).

Discriminating which components of the EE paradigm are responsible for the positive effects of EE is important for both consistency between labs, and for any potential therapeutic application of EE (Sale et al., 2014, McDonald et al., 2018). Key variables between EE paradigms are the inclusion of a running wheel (for voluntary exercise), social enrichment (more cage mates for social stimulation), the creation of a complex environment (toys, balls, tunnels, and regular rearrangement as a source of novelty) and a larger cage. Additionally, the control group being used for comparison against the EE group should be taken into consideration – control groups lacking bedding and individually housing mice may accentuate the effects of EE, by comparing to an impoverished control group. Grégoire et al. (2014) looked at the effects of different EE variables: cognitive stimulation, social stimulation and voluntary exercise, individually and at the interactions between them in order to ascertain their contribution to the phenotypes attributed to EE. They concluded that voluntary exercise was responsible for the positive effects of EE on neurogenesis (confirming results first seen by van Praag et al. (1999)), and that this effect was not affected by increases in levels of corticosteroids in the hippocampus associated with exercise (Grégoire et al., 2014). The complex environment however reduced overall levels of corticosteroids within the bloodstream, and social interaction appeared to increase levels of c-fos expression in the dentate gyrus, a marker of synaptic plasticity (Grégoire et al., 2014). Overall, different components of the EE paradigm appear to underlie different aspects of EE-mediated hippocampal benefit.

An additional consideration of environmental enrichment paradigms is how long animals are exposed to EE. Below in Table 1.1, key studies highlighting the effects of different durations of EE on certain types of hippocampal-dependent learning and memory are summarised in order to help visualise the timeline of EE-mediated effects. Changes in neuron morphology, neurogenesis and BDNF expression within the hippocampus are also shown alongside these, as these have been proposed as cellular and molecular correlates potentially underpinning observed EE-mediated behavioural benefits (Grégoire et al., 2014, Sale et al., 2014, Kelly and Hannan, 2019). Furthermore, what stage in the animals lifespan EE exposure occurs is also an important consideration for evaluating the benefits of EE application. Mice (Gower and Lamberty, 1993) and rats (Frick et al., 1995) display spatial memory differences across the lifespan, with older rodents (24 months) displaying much more severe deficits than middle aged rodents (10-18 months) when compared with those of a young adult age (3-4 months) (Kennard and Woodruff-Pak, 2011). Environmental enrichment has been shown to offset these age-related learning and memory deficits in rat and mouse models (Sampedro-Piquero and Begega, 2017, Kelly and Hannan, 2019, Birch and Kelly, 2019) and so age has been included as a variable in Table 1.1. A final consideration is the species being investigated: Mice and rats appear to exhibit differences in navigating water maze tasks, both species are capable of learning the location of a hidden platform during water maze trials, but rats appear to have an easier time through their larger size and strength, and through greater utilisation of spatial cues(Frick et al., 2000).

Study	Study details					Behaviour			Neuron morphology			
	Age pre-EE (wks)	EE duration (wks)	Species (sex)	Wheel?	Social enrichment?	Contextual Fear Cond.	Spatial learning and/or memory tests	NOR	Spine density	Dendrite	Neuro-genesis	BDNF expression
Novkovic et al., 2015	3	3 - 4	Mice (male)	✓	×			↑ (24hr) , N.D. (1 wk)	-	-		↑ protein (hippo)
Hendershott et al., 2016	4	4	Mice (male)	✓	×	-	↑ acquisition, MWM	-	-	-	-	-
Hendershott et al., 2016	4	4	Mice (female)	✓	×	-	↑ acquisition, MWM	-	-	-	-	-
Mesa-Gresa et al., 2013	4	4	Mice (male)	✓	✓	-	-	↑ (1hr)	-	-	-	-
Falkenberg et al., 1992	7 - 8	4	Rats (N.S.)	×	✓	-	-	-	-	-	-	↑ mRNA (CA1)*
Malik and Chatterji, 2012	3 - 4	6 - 7	Rats (male)	×	✓	↑ (24hr)			↑ CA1 apical	-	-	-
Correa et al., 2012	Born into EE	6 - 7	Mice (male)	✓	✓	-	-	-	↑ CA1 apical	-	-	-
Rampon et al. 2000b	6 - 8	8	Mice (N.S.)	✓	N.S.	↑ (24hr)	-	↑ (24hr)	↑ CA1 apical+ basal	-		-
Duffy et al. 2001	4	8	Mice (female)	✓	×	↑ (24hr), Cued No diff.	-	-	-	-		-
Van Praag et al., 1999	12	8 - 16	Mice (female)	✓	N.S.		↑ acquisition, MWM	-	-	-	↑	-
Gobbo and O'Mara, 2004	N.S.	10	Rats (male)	✓	✓		N.D. acquisition, MWM	↑ (24hr), Object location	-	-		↑ protein (DG)
Speisman et al., 2014	20 - 32	10 (behav. wk 5)	Rats (male)	×	N.S.	-	↑ acquisition, MWM	-	-	-	↑	-
Speisman et al., 2014	78 -86	10 (behav. wk 5)	Rats (male)	×	N.S.	-	↑ acquisition, MWM	-	-	-	↑	-
Mora-Gallegos et al., 2015	4	11	Rats (male)	×	✓	-	↑ performance in radial arm maze	-	-	-	-	-
Mora-Gallegos et al., 2015	31	11	Rats (male)	×	✓	-	N.D. performance in radial arm maze	-	-	-	-	-
Harati et al. 2011	4	12	Rats (female)	×	✓	-	↑ acquisition, MWM	-	-	-	-	-
Faherty et al., 2003	3 - 4	12 - 16	Mice (male)	✓	✓	-	-	-	-	↑ CA1 length (apical+basal); ↑ CA1 volume (apical+basal); ↑ DGCs length	-	-
Birch and Kelly, 2019	12 - 20	35	Rats (male)	×	×	-	N.D. acquisition, MWM	N.D. (24 hr, 2 objects); ↑ (24 hr, 3 objects)	-	-	N.D.	N.D.
Harati et al. 2011	4	48	Rats (female)	×	✓	-	↑ acquisition and retention (24 hrs), MWM	-	-	-	-	-
Birch and Kelly, 2019	12 - 20	76	Rats (male)	×	×	-	↑ retention 48 hrs, MWM	↑ (24 hr, 2 objects); ↑ (24 hr, 3 objects)	-	-	↑	N.D.
Harati et al. 2011	4	96	Rats (female)	×	✓	-	↑ acquisition and retention (24hr), MWM	-	-	-	-	-

Table 1.1: Summary of environmental enrichment experimental study conditions and resultant behavioural effects along with key changes within the hippocampus. Top table (light grey): Shorter periods of EE (<5 weeks); Middle table (grey): Medium periods of enrichment (5 – 11 weeks); Bottom table (darker grey): Longer periods of enrichment (>11 weeks). Table abbreviations: EE (environmental enrichment); Wheel (exercise wheel present in EE); Cond. (conditioning); MWM (Morris water maze); NOR (novel object recognition); N.D. (no difference); N.S. (not specified); hr (hour); wks (weeks).

Environmental enrichment paradigms therefore include several conditions that individually positively modulate hippocampal size in rodent models, however one criticism of paradigm design is the high degree of variability between laboratories due to lack of standardisation (Redolat and Mesa-Gresa, 2012), which can also be seen in Table 1.1. Despite variations in species, sex, age, length of EE, exercise and social enrichment, EE appears capable of robustly

modulating spatial learning: as measured by MWM acquisition (demonstrated by a reduced latency to learn platform location over trials); and spatial memory: as measured by MWM probe trial, (more time in platform quadrant after learning) in addition to hippocampus-dependent memory in contextual fear conditioning experiments that feature a 24 hour delay, and in other forms of memory that may not depend on the hippocampus such as novel object recognition. This may therefore demonstrate a robustness to EE, where variations in the EE paradigm can produce consistent results across multiple laboratories. However variation between paradigms between research groups no doubt contributes to some of the variability between laboratories with regards to the effects of EE, as has also been concluded by others (Redolat and Mesa-Gresa, 2012, Ohline and Abraham, 2019).

1.4.2 The effect of environmental enrichment on behaviour

EE has been seen to improve spatial learning after short (>4 weeks) (Hendershott et al., 2016), medium (5 – 11 weeks) (van Praag et al., 1999, Speisman et al., 2013) and longer (>11 weeks)(Harati et al., 2011, Huttenrauch et al., 2016, Birch and Kelly, 2019) periods of EE (Table 1.1). Spatial memory is also improved following longer periods of EE (Huttenrauch et al., 2016, Harati et al., 2011), though these mice are older (due to the length of EE), and so EE has been suggested to play more of a protective role in preventing performance deficits. Another form of hippocampus-dependent memory developed through contextual fear conditioning (with 24 hour delay), is also seen to improve following 6 -8 weeks of EE (Rampon et al., 2000b, Duffy et al., 2001, Malik and Chattarji, 2012).

Consistent improvements across the lifespan are also observed in 24 hour novel object recognition (NOR) memory after short, medium and longer periods of EE (Rampon et al., 2000b, Gobbo and O'Mara, 2004, Novkovic et al., 2015, Birch and Kelly, 2019). Lesion studies of the hippocampus have typically been shown not to affect NOR (Barker and Warburton, 2011, Cohen and Stackman, 2015) and this has led to the conclusion that NOR is a hippocampus-independent form of memory (Barker and Warburton, 2011, Cohen and Stackman, 2015). Pharmacological inhibition of hippocampal function has however been shown to disrupt NOR, opening up the idea that rodents may develop compensatory learning and memory mechanisms during NOR when hippocampal function is permanently ablated,

though this effect could be due to pharmacological inhibitior spillover into surrounding brain areas (Barker and Warburton, 2011, Cohen and Stackman, 2015). A more sensitive test of hippocampal function involves novel movement of a familiar object (object location experiments) (Barker and Warburton, 2011) and a 10 week period of EE has been seen to improve this also (Gobbo and O'Mara, 2004).

Other benefits of EE are a reduction in anxiety (Huttenrauch et al., 2016, Sampedro-Piquero and Begega, 2017, McQuaid et al., 2018) and improved sociability behaviour (Mesa-Gresa et al., 2013, McQuaid et al., 2018), though this benefit does not seem to be observed without social enrichment (Hendershott et al., 2016). Furthermore, Frick et al. (2003) demonstrated using adult (7 months) and middle-aged/older (72 weeks) mice that even a short period of EE (4 weeks) can prevent age-related impairments in spatial memory in both male and female mice.

1.4.3 Environmental enrichment induces structural and cellular changes within the hippocampus

Behavioural changes influenced by EE are mirrored by structural changes at the neuronal level throughout the brain. Increased angiogenesis, along with both cortical and hippocampal expansion, is observed following EE exposure (Sale et al., 2014, Huttenrauch et al., 2016). Hippocampal CA1 and DG principle neurons themselves also display significant increases in their apical dendrite length and cell volume through greater dendritic branch complexity (Faherty et al., 2003). Additionally, an upregulation of adult hippocampal neurogenesis, through both increased proliferation and survival of new neurons within the DG of animals is also observed (Lehmann et al., 2013, Kempermann, 2019). Increases in glucocorticoid concentration during chronic stress have been shown to reduce hippocampal size and neurogenesis (Sawamoto et al., 2016, McEwen and Akil, 2020). However neurogenesis within the hippocampus in response to environmental enrichment appears to depend on modulation of glucocorticoid concentration in the bloodstream (Lehmann et al., 2013), implying that the enrichment paradigm changes the way that the hippocampus responds to glucocorticoids, or exerts a neuroprotective effect. Within humans, hippocampal

volume has been seen to vary in response to environmental and pathological conditions: exercise and cognitive stimulation appear to increase hippocampal volume, whilst reductions in hippocampal size are associated with chronic levels of stress, diagnoses of dementia and major depressive disorder (McEwen and Akil, 2020).

1.4.4.1 Environmental enrichment alters synaptic plasticity within the hippocampus

Alterations in synaptic plasticity and transmission are also observed in response to EE: Exposure to EE results in greater dendritic spine density in CA1 pyramidal cells (Rampon et al., 2000b, Malik and Chattarji, 2012, Corrêa et al., 2012) and increased synaptogenesis for DG, CA3 and CA1 principle neurons (van Praag et al., 2000, Rampon et al., 2000b). Longer dendritic trees, along with greater spine density and thus sites for new synapse formation could account for this enhanced synaptogenesis following EE exposure. This rise in neural connectivity may also explain why EE has been seen to generally increase synaptic transmission and facilitate LTP at SC/CA1 synapses (Ohline and Abraham, 2019). EE may selectively enhance some forms of LTP and not others: Duffy et al. (2001) observed that in EE mice one burst of HFS (100Hz) was capable of inducing a robust, PKA-dependent potentiation at SC-CA1 synapses that demonstrated no decay 80m after stimulation. Control mice demonstrated only a transient potentiation that had nearly decayed to baseline by 80m, and was unaffected by PKA inhibitors (Duffy et al., 2001). Within *in vitro* hippocampal slices at SC-CA1 synapses, E-LTP induction by a single burst of HFS is thought to last between 1-3 hours and does not require protein transcription, whereas L-LTP induction persists for at least 8 hours and is thought to be protein synthesis dependent requiring PKA activity (Nguyen et al., 1994). Some studies however find that 1 burst HFS is sufficient for L-LTP induction (Sajikumar et al., 2008, Villers et al., 2012), although this discrepancy may be due to differences in slice rest periods post-cutting (Lynch et al., 2015) (longer slice rest times pre-LTP induction may deplete proteins necessary for L-LTP induction and thus require novel translation to occur) or through pre-conditioning of synapses which prime them for LTP induction through CP-AMPAR insertion as a result of an organisms prior experience (Park et al., 2018). Despite the differences observed between labs, within the study by Duffy et al. (2001), due to observing these differences in the same preparation, it is tempting to conclude that EE may decrease

the requirement for L-LTP formation in response to just 1 HFS (100Hz) burst, however Duffy et al. recorded only for 80m, which is not long enough to rule out a deficit in E-LTP induction.

EE has also been seen to regulate the dynamic range of synaptic plasticity, through simultaneous enhancements in both LTD and LTP after short periods of 2 – 3 weeks EE (Artola et al., 2006, Buschler and Manahan-Vaughan, 2012, Stein et al., 2016). Heterozygous BDNF knock-out mice display deficits in LTD and HFS induced LTP and reduced BDNF expression compared to wildtype mice (Novkovic et al., 2015). However, after 3 weeks of EE, BDNF heterozygotes display the same level of LTP, LTD and BDNF expression as WT mice who have not undergone EE (Novkovic et al., 2015), implicating the EE-dependent regulation of BDNF in mediating the benefits of EE to synaptic plasticity. Furthermore knock-out of the NR1 subunit of the NMDA receptor restricted to are CA1 impairs novel object recognition and contextual fear memory, however exposure to environmental enrichment ameliorates this effect (Rampon et al., 2000b). EE therefore appears to play a role in modulating synaptic plasticity and transmission within the hippocampus, and this may underlie the benefits seen in behaviour following EE.

Whole-cell patch clamp recordings performed in hippocampal CA1 neurons indicate that EE can increase miniature excitatory postsynaptic current (mEPSC) frequency, without affecting EPSC amplitude (Malik and Chattarji, 2012). However, exposure to EE has also been seen to significantly increase CA1 pyramidal mEPSC amplitude (Corrêa et al., 2012). This difference could however be due to the different EE paradigms employed, with Malik and Chatterji (2012) employing EE housing from p25 with additional daily environmental stimulation for 4 - 5 weeks, whereas Corrêa et al. (2012) housed mice in EE from birth for 6 - 7 weeks and included additional dams pre-weaning. An increase in mEPSC frequency could indicate a greater number of functional synapses present in CA1 neurons arising either from synaptogenesis - causing more frequent spontaneous pre-synaptic vesicle fusion during TTX application - or potentiation of existing silent synapses which would increase the number of detectable fusion events. An increase in mEPSC amplitude however indicates an increase in glutamatergic receptors at the postsynaptic membrane of synapses. By affecting changes in synaptic plasticity and neuronal structure, EE therefore can alter the network properties of the hippocampus.

1.4.4.2 Molecular changes induced by environmental enrichment are poorly characterised yet likely underlie its effects on the hippocampus

Molecular changes induced by EE are thought to underlie changes in neuronal morphology and plasticity and the exact mechanisms underlying the benefits of EE are still unclear (Sale et al., 2014, Kelly and Hannan, 2019). Exposure to EE causes an upregulation in BDNF mRNA (Frick et al., 2003) and protein (Gobbo and O'Mara, 2004, Novkovic et al., 2015) expression. Concordant with this, 4 weeks of EE exposure leads to an upregulation in CREB phosphorylation within the hippocampus (Hu et al., 2013), a process both regulated by BDNF, and that results in BDNF expression (Tao et al., 1998). Other plasticity-related factors are also modulated by short-term EE, including Egr1 after 1 week of EE (Koh et al., 2005), AMPAR and NMDAR subunits GluA1 and GluN2A and GluN2B after >2 weeks of EE (Tang et al., 2001), PSD-95 after 3 weeks EE (Nithianantharajah et al., 2004), CREB and αCaMKII after 3 – 4 weeks EE (Huang et al., 2006). Additionally, cortical RNA upregulation in 4 month old mice following brief periods of EE (2 and 14 days) includes genes involved in neuronal calcium-signalling (Calmodulin, Calretinin), neuronal structural plasticity (N-cadherin, Cortactin) and PSD-95, indicating that synaptic plasticity is a key target of the molecular changes induced by EE (Rampon et al., 2000a).

A large overlap exists between phenotypes associated with EE exposure and those associated with CREB-mediated transcription. CREB-mediated transcription within the hippocampus underlies benefits to spatial memory (Viosca et al., 2009), LTM (Pittenger et al., 2002), LTP (Barco and Marie, 2011), synaptic plasticity (Barco et al., 2008) and CREB transcription promotes neurogenesis within the hippocampus and greater circuit plasticity as new neurons integrate within neural circuitry (Ortega-Martínez, 2015). In addition to this, CREB binding protein (CBP), which binds CREB, is recruited during CREB-mediated transcription and has a necessary role in regulating EE-induced transcription and neurogenesis (Lopez-Atalaya et al., 2011). Activation of CREB transcriptional activity through phosphorylation is upregulated after 4 weeks of EE (Hu et al., 2013) and CREB is also one of several proteins regulating IEG expression, with IEGs containing a significant enrichment of CRE-promotor sites (Tullai et al., 2007). Expression of the IEGs Arc/Arg3.1, Egr1 and c-Fos is upregulated after exposure to novel environments (Guzowski et al., 2001) and Arc/Arg3.1 and

Egr1 upregulation is observed following EE, although this paradigm relied on comparison to individually housed isolated controls (Koh et al., 2005). Many of the beneficial effects of EE on hippocampal-dependent memory, synaptic plasticity and neurogenesis seem therefore to depend on the induction of CREB-mediated gene expression.

1.5 Mitogen-and stress activated protein kinase 1 plays a key role in the molecular mechanisms of learning and memory

The importance of MSK1 in memory formation and synaptic plasticity was first demonstrated by studying Erk1/MSK1 signalling in response to contextual fear conditioning assays (Sindreu et al., 2007), and in complete MSK1 knock-out (KO) mice (Chwang et al., 2007, Karelina et al., 2012). MSK1 KO demonstrate impaired activity-dependent CREB phosphorylation in addition to spatial and fear memory formation deficiencies (Chwang et al., 2007). Additionally MSK1 KO mice possess a reduction in dendritic complexity in both CA1 and CA3 pyramidal and dentate granule cells, and a decrease in dendritic spine density of CA1 and CA3 pyramidal cells (Karelina et al., 2012). MSK1 knock-out mice also demonstrate a deficit in novel-object recognition (Karelina et al., 2012). Additionally, MSK1 knock out mice fail to upregulate DG neurogenesis nor do they increase DG, CA1 and CA3 principle neuron dendritic complexity following EE (Karelina et al., 2012). MSK1 expression is enriched within the brain, particularly within the hippocampus, compared with rest of the body (Chwang et al., 2007) and is believed to be the primary CREB kinase in response to neurotrophin signalling (Arthur et al., 2004). As mentioned previously, MSK1 is activated by ERK1/2 as a result of BDNF-mediated TrkB activation and can directly phosphorylate CREB and histone H3 (Arthur, 2008, Chwang et al., 2007). In addition to MSK1 activation by the BDNF signalling pathway, 30m following contextual fear conditioning Ca2+-stimulated adenylyl cyclase activity has been seen to activate PKA, Erk1, MSK1 and CREB within CA1 neurons, which is necessary for memory formation during contextual-fear conditioning (Sindreu et al., 2007).

MSK1 therefore seems to play an important role in regulating several elements of hippocampal structural synaptic plasticity via regulation of dendrites and their spines including EE-dependent effects and is also involved in the formation of spatial memory. With its position regulating CREB transcription and histone H3 phosphorylation in response to extracellular BDNF signalling, MSK1 seems poised to regulate neuronal transcription in

response to activity-dependent BDNF stimulation (such as during EE or neuronal activity). However, complete knock-outs of gene function and expression can confound studies of protein function, as has been seen with studies of CREB function in LTP and LTM discussed above (pages 31 – 33). The role of MSK1 as the primary CREB-kinase in response to neurotrophin signalling via the MAPK pathway relies on testing the kinase activity of MSK1. A separate role for MSK1 has been demonstrated in complex with the glucocorticoid receptor and Erk1/2 during behavioural responses to stress (Gutièrrez-Mecinas et al., 2011), indicating that a complete knock-out of MSK1 could have unforeseen effects on signalling pathways beyond the loss of kinase activity. Indeed in contrast to previous studies using MSK1 knock-out mice, the Frenguelli lab have demonstrated that the kinase function of MSK1 is not required for the induction of several forms of spatial memory nor for mGluR LTD and at least two different forms of LTP (Daumas et al., 2017).

Previously generated MSK1 kinase dead (MSK1 KD) mice (Corrêa et al., 2012, Arthur, 2008) are therefore used in this study, which are homozygous for an Asp194Ala mutation in the N-terminal kinase domain of the MSK1 gene. MSK1 KD mice lack detectable MSK1 kinase activity (Corrêa et al., 2012). Primary hippocampal cultures from MSK1 KD mice fail to undergo homeostatic upscaling of synaptic transmission in response to activity deprivation following *in vitro* 24hr treatment with TTX (Corrêa et al., 2012). In addition stimulation and inhibition of the BDNF-TrkB-MAPK signalling pathway failed to alter synaptic properties, in contrast to WT neurons (Corrêa et al., 2012). Importantly, when transfected with wildtype MSK1, MSK1 KD neurons were able to respond as expected to activity deprivation and the electrophysiological phenotypes observed were rescued (Corrêa et al., 2012).

In acute hippocampal slices, MSK1 KD mice display a deficit in basal synaptic transmission at the CA3/CA1 Schaffer collateral pathway (Daumas et al., 2017) and fail to display synaptic enhancement after exposure to EE, a process thought to be regulated by activity-dependent release of BDNF (Corrêa et al., 2012). However MSK1 KD mice undergo normal induction of mGluR LTD and display no difference in response to 1 burst HFS and TBS induced LTP (Daumas et al., 2017). MSK1 KD mice also display an increase in basal dendritic spine density in CA1 neurons, but do not undergo as much of an increase in spine density after EE compared to WT mice (Corrêa et al., 2012).

1.5.1 The kinase function of MSK1 regulates synaptic transmission and activity-dependent homeostatic plasticity within the hippocampus through regulation of Arc/Arg3.1 and CREB phosphorylation

Basal glutamatergic synaptic transmission within acutely-prepared hippocampal slices from MSK1 KD mice is decreased at Schaffer collateral/CA1 synapses (Daumas et al., 2017) and cultured MSK1 KD neurons fail to homeostatically upregulate expression of GluA1 and mEPSC amplitude in response to activity deprivation (Corrêa et al., 2012). This indicates that the kinase activity of MSK1 can regulate synaptic strength in an activity-dependent manner that likely involves modulation of GluA1 expression. In response to EE, MSK1 KD CA1 neurons display a blunted increase in dendritic spine density, and fail to display an increase in amplitude of AMPAR-mediated mEPSCs (Corrêa et al., 2012, Lalo et al., 2018). Deficits in synaptic upscaling in MSK1 KD mice in response to activity deprivation are thought to be caused by dysregulation of Arc/Arg3.1 (Corrêa et al., 2012), which mediates the endocytosis of AMPARs (Chowdhury et al., 2006) (Figure 1.9). Knock out of Arc/Arg3.1 activity increases synaptic AMPAR expression levels (Chowdhury et al., 2006), and Arc/Arg3.1 is normally downregulated in response to activity deprivation by TTX, reducing AMPAR endocytosis and increasing AMPAR surface availability (Shepherd et al., 2006). Cultured MSK1 KD neurons fail to downregulate Arc/Arg3.1 expression in response to 24 hour activity deprivation by TTX, which may underlie their failure to increase AMPAR expression, as occurs in WT mice (Corrêa et al., 2012). Recent work with MSK1 KD mutant mice indicates that Arc/Arg3.1 expression is regulated by MSK1's role in phosphorylating histone H3, and that phosphorylation of CREB is not necessary (Hunter et al., 2017).

Such activity-dependent synaptic scaling in CA1 neurons is thought to be modulated by BDNF (Turrigiano, 2012, Pozo and Goda, 2010, Corrêa et al., 2012) which is in itself regulated in an activity-dependent manner, with a reduction in BDNF release in response to TTX activity deprivation (Rutherford et al., 1998) and increased BDNF expression in EE (Novkovic et al., 2015). TTX-mediated activity deprivation (for 48hrs) causes an increase in excitatory transmission, by reducing the quantal amplitude measured at the postsynapse, as measured by minature excitatory postsynaptic current (mEPSC) amplitude, and this increase

in mEPSC amplitude is blocked by application of exogenous BDNF. Long-term application (24 hr) of BDNF (50ng/ml) has been shown to reduce mEPSC amplitude (Corrêa et al., 2012). Likewise, inhibitors of BDNF signalling through the MAPK pathway targeting TrkB and Erk1/2 cause upscaling of mEPSC amplitudes, the same effect as TTX application, and the opposite effect of BDNF application (Corrêa et al., 2012). BDNF signalling via TrkB and the MAPK pathway therefore appears to be a key regulator of overall excitatory transmission in a neuron in response to overall activity.

On shorter timescales, which may be more relevant to the role BDNF plays in inducing potentiation in response to synaptic activity, 20 min of BDNF application has been seen to increase expression of IEGs including Egr1, c-Fos and Arc/Arg3.1 along with VGF in cultured hippocampal cells in a TrkB/MAPK-dependent fashion (Alder et al., 2003). This upregulation of IEGs including Arc/Arg3.1 is also observed in the hippocampus 24 hrs after a hippocampus-dependent learning task (Alder et al., 2003).

Outside of the role of Arc/Arg3.1 in AMPAR-receptor endocytosis in homeostatic scaling, Arc/Arg3.1 plays an important role in the bidirectional regulation of synapse strength during plasticity events: Arc/Arg3.1 knockout mice demonstrate impaired LTD at SC-CA1 synapses and despite displaying increased E-LTP, fail to convert E-LTP to L-LTP, with facilitation decaying to baseline by 80 min at MPP-DG and 60 min at SC-CA1 synapses (Plath et al., 2006). Arc/Arg3.1 KO mice also demonstrate impairments in many hippocampus-dependent tasks such as contextual fear conditioning (24 hr delay), novel object recognition (24 hr delay), spatial learning (acquisition latency), memory (probe trial) and reversal learning in the MWM (Plath et al., 2006). These results have are supported by *in vivo* intrahippocampal infusion of Arc/Arg3.1 anti-sense oligonucleotides (ODNs, which prevent Arc/Arg3.1 translation) into wildtype rats: HFS (400Hz, 100 pulses) LTP induction 1.5 hours after ODN infusion at PP-DG synapses resulted in intact E-LTP, but impaired L-LTP (Guzowski et al., 2000). Additionally ODN-mediated Arc/Arg3.1 disruption impairs spatial memory but not acquisition in the MWM. LTP-induction of the MPP through HFS appears to result in the synthesis of Arc/Arg3.1 mRNA in the cell body of DGCs, and over the course of 2 hours newly synthesised Arc/Arg3.1 mRNA is localised to the site of postsynaptic activation in the dendrite (Steward et al., 1998). Arc/Arg3.1 synthesis appears necessary for the late stage of LTP in part through

the stabilisation of F-actin and the phosphorylation of cofilin, both proteins involved in the remodelling of the postsynaptic cytoskeleton following L-LTP (Messaoudi et al., 2007). Arc/Arg3.1 therefore plays a necessary role in both LTP and LTD, and in learning and memory.

Finally, as discussed in section 1.3.3.1 (pgs. 39 – 40) induction of L-LTP requires TrkB activation by BDNF, and LTP induced by infusion of exogenous BDNF is both completely blocked by pre-treatment with Arc/Arg3.1 anti-sense ODNs, and reversed by their application up to 2 hrs post-induction (Messaoudi et al., 2007). The role of BDNF in L-LTP induction therefore seems to depend on Arc/Arg3.1 translation, which can then promote stabilisation of cytoskeletal proteins at stimulated synapses.

These observations marry well with the work of Corrêa et al. (2012): MSK1 KD mutation prevents BDNF signalling to CREB, which leads to an insensitivity to activity deprivation brought about by TTX, and results in a dysregulation of Arc/Arg3.1 expression (Figure 1.9). Likewise, this could render the mutant mice insensitive to the long-term stimulation by BDNF brought about by EE, which upregulates BDNF expression, and could result in the stabilisation of F-actin and cofilin at synapses, potentially explaining the greater transmission strength at SC-CA1 synapses following EE in WT but not MSK1 KD mice (Corrêa et al., 2012) (Figure 1.9). However, in later work LTP induction in MSK1 KD mutants was not seen to be impaired, implying that specific BDNF/TrkB signalling to MAPK/MSK1 is not necessary for sufficient Arc/Arg3.1 expression to induce L-LTP following TBS and 1 burst HFS induction (Daumas et al., 2017). This could be due to the several different TrkB intracellular Tyr residues individually activating several different intracellular pathways in response to BDNF stimulation (Minichiello, 2009): residue phosphoTyr515 mediates the activation of the MAPK signalling cascade that involves MSK1 (pg. 39), and so activation of the other residues may be sufficient for sufficient Arc/Arg3.1 expression during LTP induction. Despite this, MSK1 appears to regulate basal glutamatergic transmission at SC-CA1 synapses and CA1 neuron spine density in response to EE (Corrêa et al., 2012, Lalo et al., 2018), and therefore the role MSK1 plays in transducing the effects of environmental enrichment is still of interest.

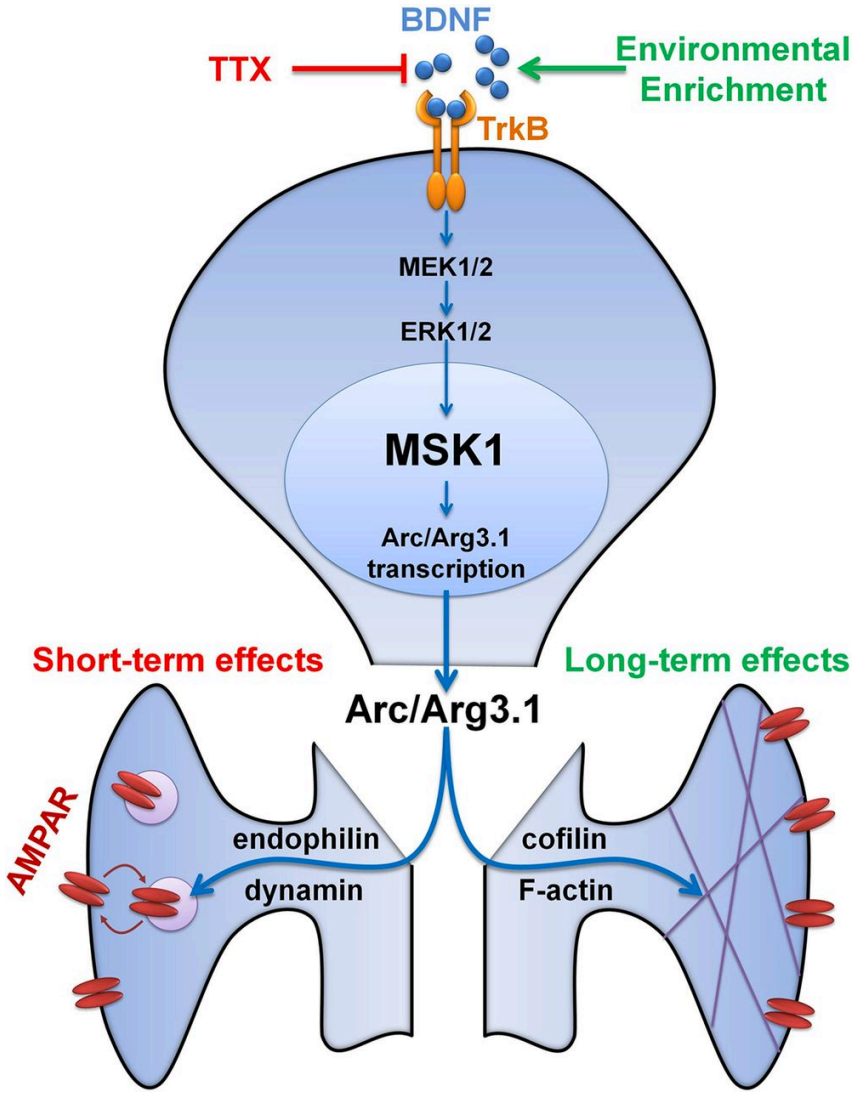

Figure 1.9. Model of MSK1's role in the regulation of homeostatic and experience-dependent synaptic scaling from Corrêa et al. (2012). Activity-dependent release of BDNF stimulates TrkB receptors, triggering a MAPK cascade including kinases MEK1/2 and ERK1/2 that results in the activation of MSK1. MSK1 then phosphorylates CREB and histone H3, modulating the expression of IEGs including Arc/Arg3.1. Arc/Arg3.1 expression promotes the endocytosis of AMPARs through interactions with endophilin and dynamin and consequently the level of AMPAR-mediated transmission at synapses. Longer-term effects of Arc/Arg3.1 expression changes could modulate dendritic spine number and stability through interactions with cofilin and F-actin.

1.6 Aims

Overall, the series of experiments contained within this thesis were conducted to assess what role the kinase activity of MSK1 has in regulating the effects of environmental enrichment within the hippocampus. This was approached at many levels, from the transcriptomic, to cellular and then behavioural with an aim to link observed differences together causally. In order to accomplish this, an MSK1 transgenic mutant mouse lacking MSK1 kinase activity (MSK1 KD) was used. To this end, the following aims were pursued:

1) Establish a direct role for MSK1 in phosphorylating CREB at Ser133 in response to extracellular BDNF stimulation at the TrkB receptor by examining pCREB immunofluorescence changes in acute hippocampal slices during acute BDNF application.

2) Assess what proportion of transcription depends on MSK1 kinase activity as part of BDNF-MSK1-CREB signalling during experience-dependent synaptic plasticity in response to *in vivo* exposure to environmental enrichment.

> **2a)** If deficits are observed in the transcriptional response to environmental enrichment, do they possess a functional commonality that can be related to phenotypes observed in mice featuring MSK1 kinase inactivation?

3) Assess impact of MSK1 kinase activity inactivation on hippocampal Schafer collateral-CA1 synapse AMPAR-mediated transmission along with CA1 neuron morphology both at a basal level in standard housing and following different lengths of environmental enrichment.

4) Assess what impact loss of MSK1 kinase activity has on hippocampal-dependent behaviour both at a basal level in standard housing and following different lengths of environmental enrichment.

1.7 Experimental rationale

MSK1 KD mice do not display impaired hippocampal LTP or LTD and do not display deficits in spatial memory. MSK1 KD mice do, however present a deficit in basal glutamatergic transmission at Schafer-collateral-CA1 synapses within the hippocampus (Daumas et al., 2017) and deficits in the homeostatic scaling of synaptic transmission and GluA1 surface presentation following activity deprivation (Corrêa et al., 2012). MSK1 KD mice also do not undergo an upregulation in synaptic strength in response to environmental enrichment (Corrêa et al., 2012). BDNF is implicated in regulating homeostatic activity-dependent synaptic scaling and in mediating the effects of environmental enrichment. The ability of MSK1 to regulate the phosphorylation of CREB and histone H3 within hippocampal neurons in response BDNF stimulation of the TrkB receptor sets MSK1 up as a powerful modulator of transcription in response to the activity-dependent release of BDNF such as during neuronal activity or experience-dependent stimuli.

Accordingly, these set of experiments were conducted to further examine the differences between WT and MSK1 KD mice and to establish the role of MSK1's kinase activity in modulating the effects of EE. Previous studies on MSK1 using MSK1 KO models may have confounded interpretations of the kinase activity of MSK1 with potential structural roles MSK1 may have in complex with other proteins. Therefore, the use of an MSK1 KD mouse model to test the effects of EE on transcription and relate observed differences back to synaptic, cellular and behavioural observations will help to unravel the molecular mechanisms underlying the beneficial effects of EE which are at present poorly understood.

Chapter 2: Methods

2.1 Experimental animals

2.1.1 MSK1 kinase dead mice

MSK1 kinase-dead (MSK1 KD) mice used in this study were generated and have been described previously (Corrêa et al., 2012). MSK1 KD mice were generated by a mutation of Asp194 to Ala (D194A) in the N-terminal kinase domain of the endogenous MSK1 gene in embryonic stem-cells, which were used to generate mosaic mice by Corrêa *et al.* (2012). These were then backcrossed as previously described in Corrêa *et al.* (2012). Backcrossing from the original C57-Bl/6n strain used by Taconic Artemis to generate the mutant mice was done for at least four generations using female MSK1 KD homozygous mice and male WT C57-Bl/6J mice purchased from Charles River UK. The point mutation was confirmed by genotyping with PCR. PCR was performed using the primer set 5'-CGGCCATGTGGTGCTGACAGC-3' and 5'-GGGTCAGAGGCCTGCACTAGG-3', which generates 529 bp and 378 bp products for MSK1 KD and WT mice respectively (Corrêa et al., 2012). The D194A point mutation was confirmed in this study as a mismatched base in the MSK1 gene observed in hippocampal reverse-transcribed cDNA in Figure 4.2 at bp 100,616,031 within the genome (genome assembly GRCm38.87). This encodes a change in the reverse complement to the cDNA (RNA) from 5'-GAT-3' to 5'-GCT-3', confirming the D194A point mutation**.** MSK1 KD mice were generated on a C57BL/6 genetic background and are homozygous for the MSK1 KD allele (Corrêa et al., 2012). Control mice, homozygous for the wildtype MSK1 allele ("wildtype mice") were generated from littermate mice heterozygous for the MSK1 KD mutation (Corrêa et al., 2012). The homozygous MSK1 KD and wildtype (WT) mice were then kept and maintained as independent colonies. Approximately every 6 months, the homozygous MSK1 KD and wildtype mouse colonies were interbred with C57/BL6 mice to generate heterozygotes, which were then bred to rederive both homozygous colonies. This was done to avoid genetic divergence between the homozygous MSK1 KD and wildtype colonies.

2.1.2 CREB S133A mice

The CREB S133A conditional mutant mice used in this study were generated from CREB S133A mice described previously (Wingate et al., 2009), crossed with a mouse line

expressing the Tg(Camk2a-cre)159Kln CaMKIIα promoter (Minichiello et al., 1999). CREB S133A mice were previously generated from a C57BL/6 genetic background by mutating ser133 to alanine in exon 5 of the CREB gene which is present in all 3 CREB isoforms (Wingate et al., 2009). A cassette containing a CREB minigene and a neomycin resistance gene was inserted before the mutated exon 5 to allow selection of transfected embryonic stem-cells, which were used to generate mosaic mice (Wingate et al., 2009). The CREB minigene contained the wildtype exons 5-11 of CREB. The neomycin/minigene cassette was flanked by LoxP sites, allowing excision by Cre recombinase (Wingate et al., 2009). Crossing these CREB S133A mice with a mouse line expressing the Tg(Camk2a-cre)159Kln CaMKIIα promoter (Minichiello et al., 1999) (Cre expression regulated by CamKIIa promoter) generated transgenic mice expressing only the excised S133A CREB gene in a forebrain-specific (hippocampus, amygdala and neocortex) manner after post-natal day p20. Expression of Cre recombinase was controlled for by using mice homozygous for WT CREB (bred from $CREB^{fl/WT}$ heterozygotes) expressing Cre recombinase through the same cross with Tg(Camk2a-cre)159Kln mice. These CREB S133A mice were generated previously within the Frenguelli lab without my involvement. In this study, CREB S133A conditional mutant mice are referred to as CREB WT ($Cre^{+}CREB^{WT/WT}$ mice) and CREB S133A ($Cre^{+}CREB^{fl/fl}$).

2.2 Animal housing and care

Mice were kept in individually ventilated cages (IVCs) with water and food provided *ad libitum* with paper shavings, sawdust substrate and a cardboard tunnel. For standard-housed (SH) mice, a maximum of five mice per cage were housed together in Tecniplast sealsafe 1284L cages (36.5 x 20.7 x 14.0 cm). Environmentally enriched (EE) mice were housed in larger Tecniplast sealsafe 1500U cages (48.0 x 37.5 x 21.0 (h) cm), supplemented with brightly coloured ladders, tunnels, a seesaw, a running wheel and a two-tier house. These were housed with extra cage mates (max 7 to a cage) to provide increased social stimulation. EE cages had their contents rotated once per week with different toys and different positions to provide environmental stimulation. This EE paradigm was chosen to keep results consistent with EE paradigms employed by previous studies using MSK1 KD mice (Corrêa et al., 2012, Lalo et al., 2018). Single housing of animals was minimised where possible to prevent social deprivation, however when mice were taken for tissue, due to mice being taken in an experimentally blind fashion, the final mouse of a cage could occasionally be left on its own

for up to two weeks. Mice were never raised without cagemates, and mice used for behavioural experiments were never single housed. All mice were maintained on a 12/12 h light/dark cycle with lights on at 7 A.M within IVCs. The care and accommodation of all the animals held within the facility complied with the standards set out in relevant codes of practice for the housing and care of animals used for scientific purposes. Behavioural studies were conducted under the auspices of PPLs 70/7821 and PA69C1971.

WT and MSK1 KD mice were housed in EE from birth for 3 months for transcriptomic experiments in Chapter 4. In Chapters 5 and 6 WT and MSK1 KD mice were housed in SH until transfer to EE or remained in SH housing for 1 or 5 wks prior to experimentation depending on experimental group. Adult mice were used in Chapters 5 and 6 aged between 12 – 24 wks of age.

2.3 Acute hippocampal slice preparation:

Mice were killed by cervical dislocation in accordance with Schedule 1 of the United Kingdom Animals (Scientific Procedures) Act 1986. The animals were decapitated and the brain was then removed and immediately immersed in oxygenated ice-cold high-magnesium aCSF (composition in mM: 124 NaCl, 4.4 KCl, 1.0 Na_2HPO_4, 25.0 $NaHCO_3$, 12.0 $MgCl_2$, 2.0 $CaCl_2$, 10 $C_6H_{12}O_6$). A razor blade was used to take a thin slice from the lateral side of each hemisphere to make a flat base to mount to the metal cutting platform for slicing. The brain was then bisected along the midline, and hemispheres mounted for slicing upon a metal platform medial-side up using cyanoacrylate glue (RS Components Ltd., CP 1252). The mounted hemispheres were then immersed within a bath of oxygenated (gassed with 95 % O_2/5 % CO_2) ice-cold aCSF and attached to the vibratome (Campden Instruments, 7000smz2). 300 μm slices were then prepared using the following parameters: frequency: 75 Hz, amplitude: 1.25 mm, blade advance speed: 0.08 mm/s. Slices were then left to recover in a 250 ml beaker containing oxygenated aCSF (containing normal magnesium concentrations, 2.0 mM $MgCl_2$) at 34 °C. Slices were supported on a mesh to allow for adequate perfusion of the oxygenated aCSF around the slice. Oxygenated aCSF was kept circulating in the beaker via a plastic syringe “chimney” into which a fine aeration candle was inserted which continuously drew aCSF from the bottom of the beaker to the top.

2.4 Immunohistochemistry

2.4.1 Slice acquisition and staining

300 µm sagittal sections of mouse brain (WT or KD) were acquired and slices with an intact hippocampus (visible and distinct CA1-3 regions and dentate gyrus) were randomly allocated to treatment groups: No Treatment (CTRL) or Treatment (BDNF: 50 ng/ml or dihydroxyflavone (DHF): 2 mM). Experiments were conducted blind to genotype. The slices were left for 3 hrs in a 50 mL beaker of oxygenated aCSF (in mM: 124 NaCl, 4.4 KCl, 1.0 Na_2HPO_4, 25.0 $NaHCO_3$, 2.0 $MgCl_2$, 2.0 $CaCl_2$) at 34 °C after cutting to allow time to recover from slice cutting and return to a baseline level of CREB phosphorylation. CREB phosphorylation levels had previously been seen to elevated following cutting, decreasing over time and becoming reliably stable 3 hrs post-slice preparation as the slices stabilise in their new environment (Frengeulli lab, unpublished). This minimised the measurement of any increase in pCREB levels arising in response to the acute trauma of slice preparation. Slices were then treated after this period had elapsed.

After 10 min of treatment with 50 ng/ml recombinant human BDNF (Cell guidance systems, GFH1, 100 µM stock in distilled water), 500 nM DHF (Sigma-Aldrich, D5446, 2 mM stock in distilled water containing 4 % DMSO (in which the 7-8 DHF was initially dissolved to a concentration of 50mM)) or an equivalent volume of vehicle: 25 µl distilled water for BDNF experiments, 125 µl of 4 % DMSO in distilled water for DHF experiments (0.01% DMSO concentration in final volume). Treatment or vehicle control was premixed with 1.5 ml of bath aCSF prior to addition. The slices were fixed in 4 % PFA in PBS, pH = 7.4. The slices were then blocked for 1.5hrs in a solution consisting of 10 % goat serum (Sigma Aldrich, G9023), 0.4 % Triton X-100 and PBS to prevent non-specific antibody binding. Three more washes with PBS were then carried out, and slices were incubated with the primary antibody: rabbit derived anti-pCREB (Cell Signalling Technology, 9198L) diluted 1:400 in 10 % goat serum and 0.4 % Triton X-100 in PBS for 3.5 hrs at room temperature including half an hour at 4°C halfway through the incubation. Slices were then twice washed in PBS and incubated with Alexa Fluor 488 nm goat anti-rabbit IgG antibody (Molecular Probes, A11008) diluted 1:800 in 10 % goat serum and 0.4 % Triton X-100 in PBS for 1.5 hrs at room temperature. The slices were then washed in PBS a further three times and mounted for confocal microscopy analysis using

Fluoroshield (Sigma Aldrich, F6182) or Fluoroshield + DAPI (Sigma Aldrich, F6057) to preserve fluorescence.

2.4.2 Image acquisition

Images were acquired from the CA1 region of slices using identical settings with the ZEN2 software package (Zeiss) on an LSM 880 laser confocal-scanning system coupled to a Zeiss inverted microscope. Images to be analysed were visualised under a 40X oil-immersion objective, with an average of 4 scans collected for each image. Z-stacks were obtained from the CA1 region (15 images) and a maximum intensity projection image generated from each which was then used for cell intensity quantification.

2.4.3 Image analysis

Images were analysed in ImageJ by first splitting the colour channels and keeping only the 8-bit green channel. Images were then auto-thresholded using Otsu's algorithm (Otsu, 1975) to determine the optimal threshold level by maximising the inter-group variation to distinguish two populations of pixels. ImageJ's "Analyze Particles" command was then used to identify ROIs corresponding to individual cells (cell minimum size = 45 pixels, maximum = Infinity). The mean pixel intensity of the regions identified as "cells" was then calculated by multiplying the average total intensity per cell by the number of identified cells and dividing by the total pixel area across all cells (to prevent bias from larger cells). To obtain a value for the background fluorescence of the cell, the auto-threshold method used above was inverted to recognise background as foreground and vice-versa setting an upper exclusion threshold before measuring the fluorescence of the image.

To obtain the total fluorescence of each image the average pixel intensity of the background image was subtracted from the average pixel intensity identified within the region of interest defined as cells. Next, the image average pixel fluorescence values were averaged on a per day basis to acquire a measure of average fluorescence per animal for treatment and control, which were then compared to yield the percentage difference of treatment/control slice and thus the effect of treatment upon the slice. This was performed by a custom java macro within ImageJ which can be provided upon request. Significant difference between size of MSK1 KD treatment effect and size of WT treatment effect was

assessed using an unpaired Student's T-test (alpha = 0.05) and using the non-parametric Kruskal-Wallis rank-sum test between ECDFs: on calculated % differences between treatments and control after image processing. This was performed in Microsoft Excel and in Origin respectively.

2.5 RNAseq experiments

2.5.1 Experimental Design

Mice were split into 4 different groups based on genotype (WT or MSK1 KD), and housing condition (environmental enrichment (EE) or standard housing (SH)).Wild-type standard housing (WTSH), wild-type environmental enrichment (WTEE), MSK1 kinase-dead standard housing (KDSH) and MSK1 kinase-dead environmental enrichment (KDEE) mice were raised in the appropriate housing condition for 3 months after birth. At 3 months of age, the mice were killed and one brain hemisphere hippocampus was used for electrophysiological recordings, with the other used for RNA extraction (Figure 4.1 A). Samples were analysed blind, 6 samples to a group, 4 groups in total, with two housing conditions (Figure 4.1 B).

2.5.2 RNA extraction and library preparation

Mice were killed by cervical dislocation, one hippocampus extracted, and then rapidly homogenized in Trizol (Invitrogen, #15596018). Total RNA was then precipitated using isopropanol following manufacturers protocol. RNA quality was checked using Nanodrop and a Qubit 4 fluorometer (Invitrogen). mRNA libraries were prepared using the TruSeqv2 (Illumina, #RS-122-2001) LS protocol in-house by the School of Life Sciences Genomics Department. Briefly, poly-A mRNA was pulled down using poly-T magnetic beads, fragmented, and primed with random hexamers before first-strand synthesis. Following second-strand synthesis, blunt end repair was performed with a 3' to 5' exonuclease, and 3' ends adenylated. Adaptors were then ligated to the cDNA. All 24 library samples were quality checked on a 2100 bioanalyser (Agilent) and assayed on a Qubit 4 fluorometer (Invitrogen) before being multiplexed 6 samples to a lane, and sequenced at 150 bp paired end (PE) on an Illumina HiSeq 4000. An average of 41.76 M reads per sample were obtained (Appendix Table i).

2.5.3 Quality control and trimming

Samples were de-multiplexed and the raw fastq files quality checked using FastQC v0.11.3 (Andrews, 2010). Adaptor contamination was removed using Skewer v0.2.2 (Jiang *et al.* 2014), with Illumina TruSeq v2 adapter lists, including reverse complements and theoretical PCR product. Fastq files were also trimmed if the mean quality of bases dropped below 10 (4 bp window) and only reads >50 bp were kept. Adapter contamination removal was confirmed using FastQC. Paired fastq files for each sample (forward and reverse) were aligned to the mouse genome (GRCm38) using STAR aligner v2.5 (Dobin et al., 2013), and annotated (GRCm38.87). Aligned BAM files were then loaded into IGV v2.3.65 (Robinson et al., 2011) and compared at the MSK1 gene locus, to check for a mismatch in the kinase domain of the MSK1 gene introduced as a point mutation into the kinase dead mutants (Corrêa et al., 2012)**.** Basic QC metrics were calculated for each sample using SeqMonk (Babraham Inst., N.P.), looking for high probe read counts across ribosomal RNA, mitochondrial genes, and observing how many reads fall within genes and exons. HtSeq v0.6.1p1 (Anders et al., 2015) was then used to quantify read counts for individual genes, using default parameters, specifying unstranded reads and only unique read alignment. A minimum average PHRED quality score of 10 was necessary for reads to be counted.

2.5.4 RNAseq differential expression analysis

Principal component analysis of gene expression values across samples was conducted in R v3.5.0 (Core-Team, 2018) using the DEseq2 package v1.20.0 (Love et al., 2014). Differential gene expression testing statistical comparisons were conducted using the Wald test statistic with a Benjamini-Hochberg-corrected p.value cut-off of $\leq$0.05 to control for false discovery rate. A log2 fold-change cut-off of 0.38 (corresponding to a 1.3 fold increase/decrease) was used to further define significant differentially expressed genes. Gene ontology enrichment analysis was performed using the topGO package v2.32.0 (Alexa *et al.*, 2006) using the "classic" algorithm and Fisher's exact test for enrichment scoring against the ontology org.Mm.eg.db v3.6.0 (Carlson, 2018). Multiple-testing correction was carried out using Benjamini-Hochberg correction, and GO-terms were considered significant at a corrected p-value $\leq$0.01. GOTerm analysis compared a list of DEGs with an annotated ontology of gene function collected into terms. A term was determined to be significantly enriched if a significantly large amount to genes belonging to it were present in the tested

DEG list. Some GOterms contain more genes than others, and so an expected number of genes based on the size of the submitted DEG list was calculated for each GOTerm and compared with the number of DEGs in the submitted list. Enrichment for a GOterm within the DEG list was therefore calculated as a fold-change of the number of significant genes annotated to each term present within the DEG list / number of significant genes annotated to GO term if transcriptome randomly sampled with same number of genes. Unless explicitly stated, default parameters were used for all tools, scripts used for these analyses can be provided upon request.

2.6 Whole-cell patch-clamp electrophysiology

300 μm sagittal slices were prepared from mouse brains and left to recover for 1 hr in 34 °C oxygenated aCSF before transfer to recording chamber. The recording chamber was perfused with aCSF preheated to 34 °C at a rate of 2 ml/min. aCSF composition (in mM): 124 NaCl, 4.4 KCl, 1.0 Na_2HPO_4, 25.0 $NaHCO_3$, 2.0 $MgCl_2$, 2.0 $CaCl_2$. Recordings were made using borosilicate glass pipettes with a resistance of 3-5 MΩ, and cells held at -70 mV in voltage-clamp. The signal was sampled at rate of 10 kHz and amplified on an AxoPatch200b amplifier (Molecular Devices, UK). No online filtering was used, but an offline low-pass filter of 2 kHz was applied when reanalysing files. Recordings were only accepted for analysis if Rs values were <20 MΩ, and if whole-cell capacitance and Rs values varied by <20 % over the course of the experiment. All electrophysiology experiments were conducted and analysed blind to genotype and housing condition.

2.6.1 Excitatory postsynaptic current recordings

AMPAR-mediated excitatory postsynaptic currents **(**EPSCs) were pharmacologically isolated by applying a non-competitive antagonist of $GABA_A$ receptors, picrotoxin (50 μM, Acros Organics, 131210050), and the competitive NMDAR antagonist D-AP5 (25 μM, Hello bio HB0225) to the perfused aCSF. Patch pipettes were filled with an internal solution consisting of: (in mM) 145.0 CsCl, 2.5 NaCl, 1.0 EGTA, 10.0 HEPES, 4.0 MgATP, 5.0 QX 314 chloride (Hello bio, HB1030), 0.1 spermine (when included (Sigma Aldrich, S2876)) and made up to pH 7.2 using CsOH (approximately 0.31 mM). Patch solution osmolarity was 295+/-2 mOsm as assessed using a Type 13 osmometer (Roebling). CNQX (Hello bio, HB0204) was included with some recordings to assess the AMPAR contributing portion of evoked currents and minature EPSCs (mEPSCs), and was used at a final concentration of 10 μM. DMSO was used as a vehicle for both picrotoxin and CNQX; DMSO concentration in bath aCSF was 0.05% when using solely with picrotoxin, and 0.075 % when CNQX and picrotoxin were used. Liquid-junction potential was calculated at 3.9 mV and was not corrected**.** Neurons were held at -70 mV and series-resistance compensation was not performed.

2.6.2 Stimulation of evoked excitatory postsynaptic current recordings

Evoked EPSCs were induced using a constant-current isolated stimulator (Digitimer Ltd., DS3). Stimulation entailed a 100 μs injection of current (strength depending on experiment) onto Schaffer collateral axons within the *stratum radiatum* by a bipolar electrode placed onto the slice. Evoked EPSCs were stimulated 15 s apart. Due to previous observations of basal synaptic-transmission differences in MSK1 KD mice versus WT mice (Corrêa et al., 2012, Daumas et al., 2017), rectification and paired-pulse ratio (PPR) experiments used varying stimulation strengths to achieve a ~100 pA response to ensure consistent response strength across recordings between genotypes. This was chosen based on the input-output profile obtained for both genotypes (WT and MSK1 KD) under standard housing conditions, such that a reliable postsynaptic depolarisation could be detected upon each stimulation, yet was below 75% of the maximal response (see Figure 5.2 for input-output curves). Rectification index was calculated using the following: $RI=((I_{+40} – I_0)/(I_0 - I_{-70}))*7/4$.

2.6.3 Miniature excitatory postsynaptic current recordings

mEPSCs were recorded using identical solutions to those used for evoked current detection with the addition of tetrodotoxin citrate (1 μM) (HelloBio, HB1035) to the aCSF bath solution. mEPSCs were identified using miniAnalysis (Synaptosoft Inc., USA) using AMPAR EPSC automatic detection parameters and a threshold of >5x RMS noise of traces. Identified traces were then manually inspected to add any obvious mEPSCs below the noise threshold, and subsequently alter the threshold to ensure mEPSCs smaller than the calculated noise threshold were detected. Auto-detection was then carried out, and detected mEPSC events inspected by eye. mEPSCs were rejected based on visual appraisal of shape (Figure 4.1), and data was exported into Excel. mEPSCs were then rejected if rise>decay. Individual mEPSC amplitudes were averaged across a recording (per cell) and each cell average was treated as an individual n. mEPSC frequency was calculated as number of events/min. Statistical analysis of differences between groups was conducted in Origin and consisted of 2-way ANOVAs run between conditions for housing and genotype effects. Alpha level was set to 0.05.

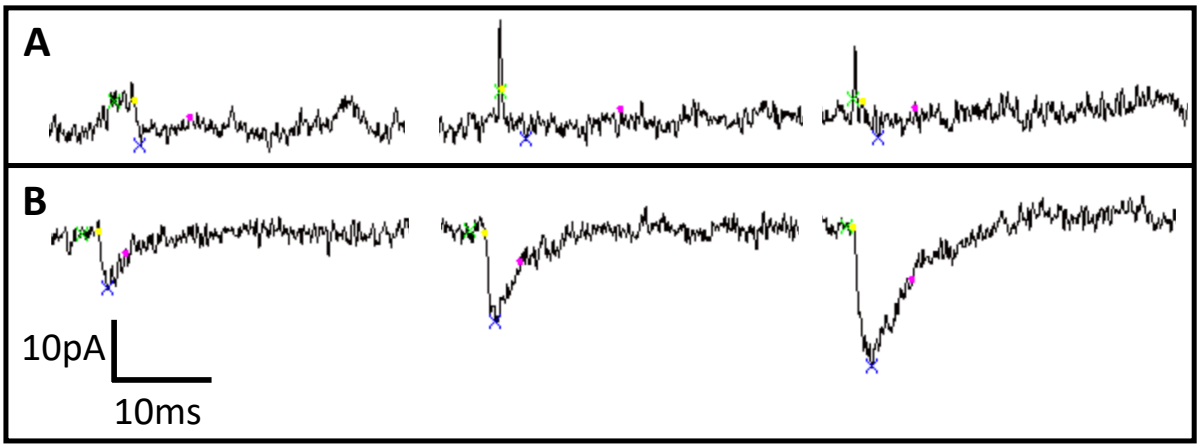

Figure 2.1: Visual appraisal of mEPSCs auto-detected using miniAnalysis program. A) Examples of rejected mEPSCs that despite detection, are clearly due to artefacts. **B)** Examples of accepted mEPSCs clear of artefacts and displaying a distinct rise and decay phase.

2.7 Neurolucida neuronal reconstruction

2.7.1 Staining of CA1 neurons

Biocytin (Sigma Aldrich, B4261) was included at 3-5 mg/ml with the internal patch-solution as per established protocol (Marx et al., 2012) for certain electrophysiology experiments blind to genotype or housing. 5 week EE experiment CA1 neurons were filled

during electrophysiology experiments performed using each mouse used for behavioural experiments. 1 week EE experiment CA1 neurons were opportunistically filled during some electrophysiology experiments from mice raised in their respective housing conditions. The decision to fill certain 1 week EE CA1 neurons was undertaken only for some experiments to achieve the same number of reconstructions to the 5 week EE reconstructions, and was decided at the start of the days recordings.

Immunohistochemical staining methodology was adapted from Marx *et al.* 2012: Cells were filled for a minimum of 20 min, during which time electrophysiological recordings were made. After patch-pipette removal, cells were left for 10 min to allow excess extracellular biocytin to wash from the slice, after which slices were transferred to 4 % PFA in phosphate buffer (PB, 100 mM, pH 7.4) and left to fix overnight at 4 °C. The following day, slices were washed 6-7x for 10 min per wash in PB, before incubation in 2 ml of 3 % H_2O_2 or 2 ml of 1.6 % H_2O_2 in 50 % methanol (the latter of which resulted in far superior background stain reduction), for 20-30 min to quench endogenous peroxidase activity within slices. This process was repeated until bubble formation ceased. Slices were then washed 6x for 10 min in PB. Slices were then incubated in a 1 % avidin-biotinylated horse-radish peroxidase (ABC) solution (Vector Laboratories, PK6100) containing 1 % Triton X-100 at room temperature (RT) for 1 hr in darkness. Slices were then incubated in this solution for 30 min on a shaker at RT and left overnight at 4°C.

The following day, slices were left at RT for 1 hr, and then washed in PB 6-7x for 10 min per wash. Slices were then incubated on a shaker in a solution of 3.3'-diaminobenzadine tetrahydrochloride (Sigma Aldrich, D5905-50TAB) made up as 1 tablet (10 mg substrate) in 15 ml of Tris-buffered saline, pH 7.6 containing 3 μl of 1 % $CoCl_2$, and 6 μl of 1 % $NiCl_2$. The chromogenic reaction was then initiated by adding 4.5 μl of 3 % H_2O_2 (prepared fresh). The reaction was monitored using a light microscope and stopped as soon as the dendritic branch structure was clearly visible. Slices were transferred to 100 mM PB to stop the reaction and washed immediately 3x in PB. Slices were afterwards washed 3-4x times more, 10 m per wash. Slices were then transferred to labelled glass slides and left in an 80 % humidity chamber for 3 hrs. Slices were then subject to progressive ethanol dehydration (10 m in 10 %->90 %

ethanol at 10 % steps), left in 100 % ethanol twice more for 10 m, and then xylene for 10 m more. Eukitt mounting medium (Fluka Analytical, 03989, Aldrich) was then added to the slices, and a glass cover slip (thickness No.1) applied and sealed with nail polish. This long dehydration process was intended to prevent "corkscrewing" of the dendrites (see Figure 2 of Marx *et al.* 2012).

2.7.2 Reconstruction and analysis of stained CA1 apical dendrites

Mounted slices were then reconstructed using Neurolucida at 100X magnification on a Zeiss light microscope. A reference point would be set, the soma outlined, and tracing begun from the base of the apical dendrite. All branch points were treated as bifurcating nodes, and the dendritic tree traced as one entity to allow branch order comparisons. Sholl analysis (Sholl, 1953) was performed using 10 μm concentric rings emanating from the cell soma and total dendritic volume, number of bifurcations (nodes), surface area and length quantified. All samples were stained, traced and analysed blind to genotype and treatment. Neurolucida reconstruction was performed blind to housing, genotype and date slices obtained.

2.8 Behavioural experiments

2.8.1 Housing and handling

Animals were separated into experimental groups 5wks prior to experiments, and housed 2 mice to each SH cage, and 4 mice to each EE cage. A plastic tunnel was added to each cage 2 wks before testing, and animals handled twice weekly to allow mice to get used to both tunnel handling and the experimenter. Animals were tunnel handled in accordance with the recent NC3R recommendations to minimise anxiety effects observed with tail handling (Gouveia and Hurst, 2017) which can confound behavioural assays.

2.8.2 Open field and object location memory assays

Open field and object location memory assays were conducted within a grey 44x44x30 cm chamber (Ugo Basile, #47432) containing a single yellow striped wall to provide spatial memory cues. The chamber floor was coated in a layer of wood shavings, which were retained across all tests for each cohort of animals. Indirect lighting was provided by floor-lamps spaced evenly around the apparatus and kept between 30-35 LUX for the centre, and 20-25

LUX for corners (corners no more than +/- 1 LUX from each other). Object location assay was conducted following a protocol provided by Dr Gareth Barker (Bristol University, UK) (Barker and Warburton, 2011). A retention time of 24 hrs was chosen for the object location memory task to ensure that long-term memory performance was assessed. Object location memory assays were performed in 3 stages, one stage a day for 3 days:

During stage 1 (habituation/open field), the animal was placed in the centre of the chamber containing no objects facing the striped wall. The animal was then left to freely explore the chamber and recorded for 5 min. Time spent in the centre of the chamber vs. time spent near the chamber walls was measured to provide an assessment of anxiety. The centre of the chamber was defined by sectioning the chamber into 16 equal 11 x 11 cm squares and monitoring the time spent the centre 4 squares as highlighted below in Figure 2.2, in which the striped wall (used as a spatial cue) is visible. Animals were also observed for any inherent bias for spending time in a particular area of the chamber (north, south, east or west (8 square chunks)) but none was observed.

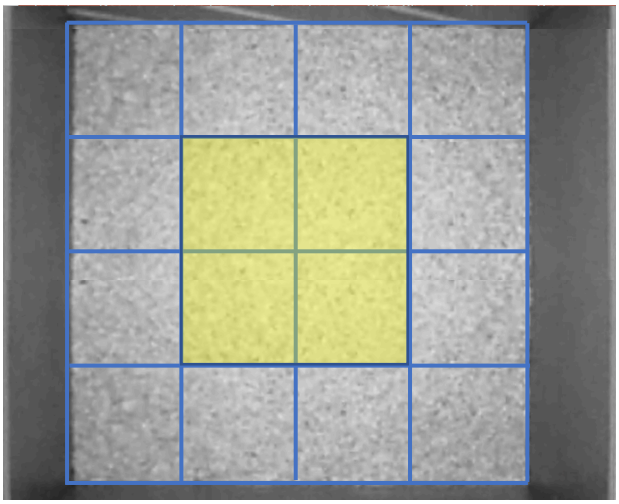

Figure 2.2: Sectioning of chamber used for open field and object location assays. During open field trials, time in the centre 4 squares (highlighted) was used as a measure of anxiety.

Stage 2 (baseline) introduced two identical objects placed 5 cm away from the walls, on the opposite side of the chamber to the striped wall. The animal was then placed within the chamber again facing the striped wall and left to freely explore the chamber for 5 min. Time spent investigating the objects was scored (see behavioural analysis below for details on scoring) and animal locomotion tracked.

Stage 3 (test) was conducted 24 hrs after stage 2. One object was placed in the previous location (away from the striped wall) and the other moved next to the striped wall.

Movement of the left or right object was randomised between animals. However the total number of left/right object movements within a group was kept even. The animal was

then placed into the chamber facing the striped wall and left to freely explore for 5 min. As with stage 2, time spent investigating the objects was scored and animal locomotion tracked. Between tests, objects were washed with 100% ethanol using a paintbrush in order to remove olfactory cues, and soiled shavings were removed along with visible fecal boli. The shavings were mixed to dissipate any location-specific olfactory cues. Animals were tested sequentially, with animals interleaved by group. Test order within each group was random, but order of testing across the three days was kept the same to ensure the 24 hrs retention time stayed the same across animals. All behavioural experiments were conducted blind to animal genotype

2.8.3 Social preference and social novelty preference

A 3-chamber apparatus was used (Ugo Basile, #46503, 60x40x22 cm - external cage, internal cage 20x40x22 cm) to assess social interaction between a test mouse and two novel mice never before encountered by the test mouse, following Crawley's 3-chamber paradigm (Kaidanovich-Beilin et al., 2011, Crawley, 2004). Chambers were separated by two removable doors opening onto the central chamber, which were open or closed depending on the stage of testing (see below). Mice used as social interaction partners were restrained under wire cups (15 cm tall, 7 cm diameter) and were habituated to the cups across 2 days prior to testing (2x 10 min and 20 min sessions each day for each mouse). The chambers and doors were washed with 70 % ethanol between tests to prevent olfactory cues from affecting subsequent tests, and the test area was surrounded by a partition to minimise external cues. Wire cups were wiped with a paintbrush and 100 % ethanol to eliminate odours and facilitate quick drying between tests as these could not be adequately dried with tissue. Testing was carried out in three stages, each following the last:

Stage 1 (habituation) consisted of placing the mouse into the central chamber and allowing free roam for 5 min. Both doors were closed, but rooms visible to the test mouse, inside each were empty wire cups.

Stage 2, ("stranger1") introduced social interaction partner 1 to one of the side chambers (location left or right randomised, with an equal distribution of each within each group) and both doors were opened. The animal was then free to explore both rooms, one with the stranger 1 mouse restrained within a wire cup, and the other containing the empty

wire cup. 10 minutes of recording the time the animal spent in each chamber and actively investigating each wire cup was then performed.

Stage 3 ("stranger2") introduced the second social interaction partner placed within the other unoccupied wire cup. The test mouse was then recorded for a further 10 min, observing the same parameters as stage 2: time the animal spent in each chamber and time spent actively investigating each wire cup.

Longer periods of habituation for both the object location memory test and social interaction tests were initially considered. However there were concerns that this could lead to unintentional "enrichment" of the standard housed mice. Open field testing was therefore conducted to observe any extraneous effects of anxiety to testing that this may have produced between conditions. Social preference testing was always performed one week after object location memory testing, so that the mice were more accustomed to the testing environment and experimenter. During testing, animals were monitored for signs of distress and weighed over the course of experimentation, however no weight loss >5% of pre-test weight was observed. In line with project license limits, mice used as social interaction partners who were kept restrained under wire cups during sociability experiments were not restrained for longer than 30 min/trial, nor for longer than 2 hours/day total. Social interaction partners were rotated between tests, so that each mouse received a break between trials. All behavioural experiments were conducted blind to animal genotype

2.8.4 Behavioural analysis

Behavioural analysis was carried out using ANYmaze (Stoelting Labs). During object investigation and sociability experiments, the animal was considered to be investigating the object/wire cup if its head was aligned towards the centre, was no more than 2.5 cm from the edge of the object/wire cup, and the animal's body was oriented towards the object. During manual and supervised automated scoring, if the mouse had not approached the object/wire cup and had instead rotated in such a way that it was only facing briefly, or it performed repetitive behaviour whilst facing the object/wire cup such as digging, rearing grooming, or mounting the object, this was not counted as investigation and was not scored. ANYmaze automated tracking analysis used the animals head to measure zone entries, and orientation of the animal's head to the centre of the object to determine whether the mouse was actively investigating the object. Statistical analysis using a 2-way ANOVA was performed

between groups in order to observed effects of housing or genotype and any potential interaction effect. When appropriately required by ANOVA significance, Bonferroni post-hoc testing was employed to test for difference between conditions. Alpha level was set to 0.05 for both ANOVA and post-hoc testing. All analysis was carried out blind to housing treatment and genotype.

Chapter 3: Investigation of MSK1s role in transducing extracellular BDNF signalling to CREB.

3.1 Introduction:

3.1.1 Using an MSK1 KD mouse to probe the role of MSK1 kinase function on CREB phosphorylation in response to extracellular BDNF signalling

BDNF is released in an activity-dependent manner within the hippocampus (Matsuda et al., 2009, Patterson et al., 1992), where it binds to its receptor TrkB and can trigger both MAPK signalling cascade and Pi3k/Akt pathways (Minichiello, 2009). BDNF-TrkB signalling is required for hippocampal-dependent learning (Minichiello et al., 1999, Minichiello, 2009) and synaptic function and plasticity within the brain (Gottmann et al., 2009, Cowansage et al., 2010). BDNF is also implicated in regulating homeostatic synaptic plasticity within neurons (Turrigiano, 2012) and BDNF can increase AMPAR-mediated synaptic transmission likely through regulation of AMPAR trafficking (Bolton et al., 2000).

cAMP response element–binding protein (CREB) is implicated as an important mediator of synaptic plasticity and learning and memory through its activity-dependent regulation of transcription (Sheng et al., 1990, Sakamoto et al., 2011, Alberini and Kandel, 2014, Kida, 2012). The transcriptional activity of CREB is regulated by its level of phosphorylation (primarily at Ser133) and activation of transcriptional co-activators (Barco et al., 2008, Johannessen et al., 2004, Naqvi et al., 2014). Phosphorylation of CREB at Ser133 occurs in response to MAPK pathway activation and this activation is sufficient to initiate CREB transcription (Naqvi et al., 2014). CREB phosphorylation therefore represents an important step in converting neuronal activity into lasting transcriptional changes that underlie the formation of memory and the regulation of synaptic plasticity.

MSK1 is a Ser133 CREB kinase whose activity is modulated by the mitogen-activated protein kinase (MAPK) pathway via extracellular signal-related kinases 1/2(ERK1/2) (Arthur et al., 2004) and is believed to be the primary CREB kinase activated in response to BDNF-signalling within the brain (Arthur, 2008, Reyskens and Arthur, 2016). In support of this, MSK1 KO mice display a deficit in activity-dependent CREB phosphorylation 1 hr following

contextual fear conditioning (Chwang et al., 2007). that are likely mediated by the kinase activity of MSK1.

Accordingly, to confirm that MSK1 has a direct effect as the exclusive CREB kinase in response to BDNF stimulation and that the kinase-disruption reported in MSK1 KD mice (Corrêa et al., 2012) directly affects its ability to phosphorylate CREB, acute hippocampal slices were prepared and levels of pCREB immunoreactivity compared in both MSK1 KD and control WT mice with and without application of BDNF or the selective TrkB agonist 7,8-dihydroxyflavone (DHF) (Jang et al., 2010). Using an MSK1 KD mice as opposed to the knock out mice mentioned in the previous paragraph will serve to confirm that the effects of direct BDNF-mediated CREB phosphorylation are due to the kinase activity of MSK1, and not due to another unknown function of MSK1, nor due to any compensatory effects that may have occurred in a complete knock out. It was hypothesised that MSK1 KD slices would display a deficit in both BDNF-mediated and DHF-mediated upregulation of CREB phosphorylation when compared to WT immunoreactivity.

3.2 Results:

Acute hippocampal slices were prepared from both WT and MSK1 KD genotypes and treated with either BDNF (50 ng/ml) or an equivalent volume (25 µl) of distilled water control (vehicle for BDNF), before fixation and staining using a primary anti-pCREB (phospho S133) antibody, and then a 488 nm secondary antibody (Figure 3.1). This concentration of BDNF was chosen as it was within the range of previous experiments demonstrating BDNF-mediated effects (section 1.3.3.1, pg. 38) and due to the previous observation that 50 ng/ml of BDNF can induce CREB phosphorylation in hippocampal slices (Finkbeiner et al., 1997) and cultured neurons (Corrêa et al., 2012).

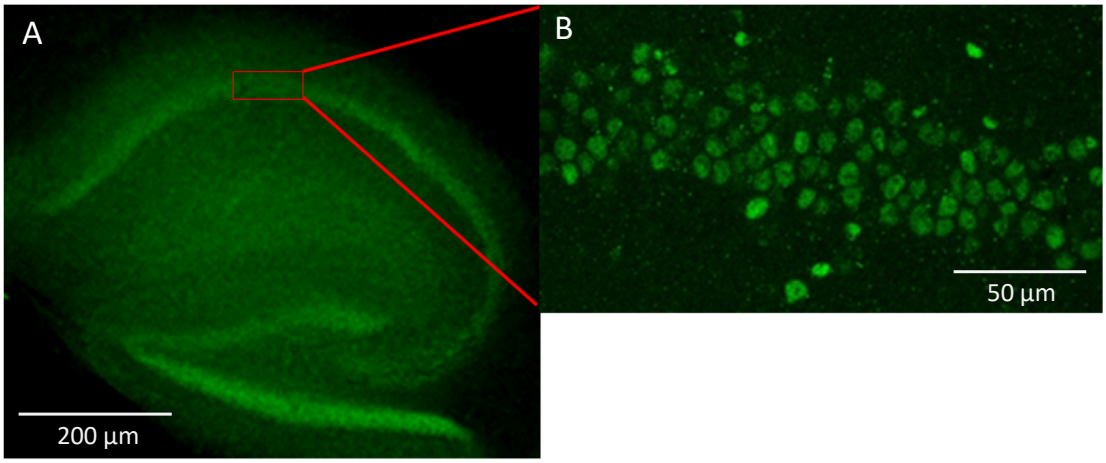

Figure 3.1. Immunofluorescence Images stained for pCREB from a sagittal slice of WT mouse hippocampus. A) 5X Image of whole hippocampus. **B)** 40X Image taken of the CA1 region showing localisation of pCREB within hippocampal pyramidal neurons.

3.2.1 MSK1 KD mutants fail to phosphorylate CREB in CA1 neurons in response to BDNF stimulation:

BDNF-treated WT slices displayed an increase in levels of pCREB in CA1 neurons compared to vehicle control slices (Figure 3.2A, top panels). In contrast, pCREB levels in area CA1 of MSK1 KD mice did not appear to change as a result of BDNF treatment (figure 3.2 A, bottom panels). Quantification of the BDNF-induced change in immunofluorescence showed a significant BDNF-dependent increase (slices averaged for each animal) in CREB phosphorylation in WT MSK1 mice (132.8 ± 9.1 %, n = 21 slices from eight mice (figure 3.2B), but no overall change in pCREB immunoreactivity in the CA1 region of slices taken from MSK1 KD mice (96.8 ± 10.2 %, n = 20 slices from 10 mice (figure 3.2B) ($p = 0.0184$, unpaired T-test, two-tailed) as quantified on a per animal basis. This increase in WT but not MSK1 KD animals can be visualised on a per slice basis, both in % BDNF treated slice fluorescence intensity change (Figure 3.2 C) and with empirical cumulative probability distributions (ECDFs) of raw slice pCREB intensity values illustrating overlap between control groups and rightwards shift of WT BDNF treated slices (Figure 3.2 D). Baseline levels of pCREB did not appear to be different between MSK1 KD and WT mice (Figure 3.2D), as untreated slices showed no difference in pCREB levels. ($p = 0.55$, Kruskal-Wallis rank-sum test).

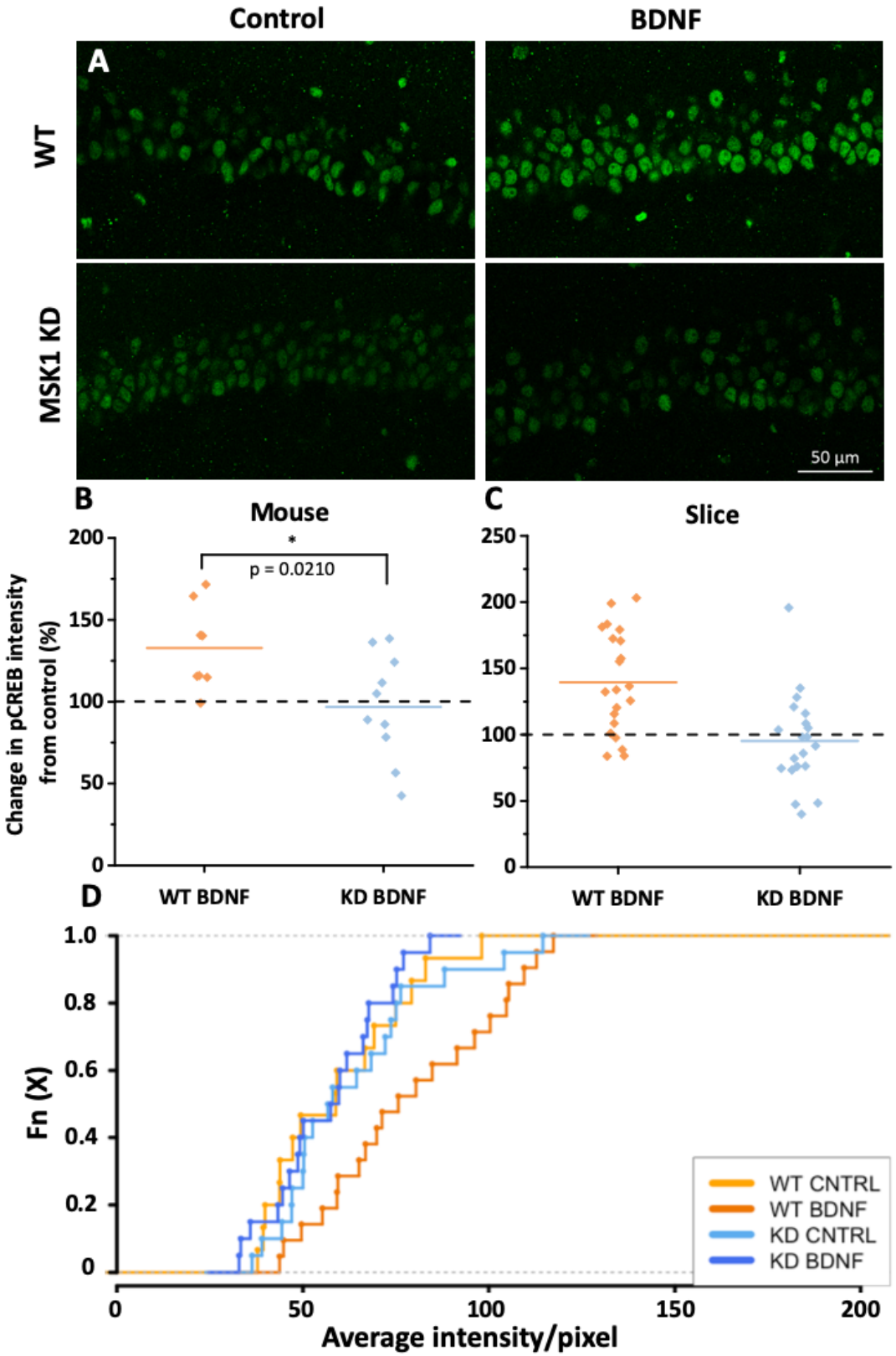

Figure 3.2. CREB phosphorylation in CA1 neurons is significantly increased in WT mice, but not in MSK1 KD mutants in response to BDNF stimulation A) Immunofluorescence images of slices from WT and MSK1 KD mice treated with either control (distilled water) or BDNF (50 ng/ml) resulting in an increase in pCREB immunoreactivity in WT mice, but not in MSK1 KD mice. (40X magnification) **B, C)**

Data points showing % change in pCREB fluorescence in BDNF treated slices/average intensity from control untreated slices for WT (21 slices, 8 mice) and MSK1 KD mice (20 slices, 10 mice) per mouse (B) (two-sample T.test, p = 0.0210) or per slice (C). Line indicates mean of data points. **D)** ECDF plots for each group from slice pixel intensity values to illustrate overlap between control groups and rightwards shift of WT BDNF treated slices. Statistical testing was carried out between % response averaged between animals (each n is an averaged response between slice intensities per animal, Figure 3.2 B).

3.2.2 MSK1 KD mutant mice display deficit in CREB phosphorylation in response to the TrkB-specific agonist 7,8-dihyroxyflavone in CA1 neurons.

BDNF has also been observed to bind the low-affinity nerve growth factor receptor (LNGFR) in addition to the TrkB receptor (Squinto et al., 1991), so a more specific probe of the pathway involved in pCREB upregulation observed in response to BDNF application was undertaken. DHF, a TrkB-specific agonist known for its nootropic effects (Jang et al., 2010, Castello et al., 2014), was applied (2mM) to slices from both WT and MSK1 KD mice and levels of pCREB immunoreactivity again measured via fluorescence (Figure 3.3 A). DMSO vehicle control (0.25%) was applied to untreated control slices. Quantification of the DHF-induced change in pCREB immunofluorescence showed a significant DHF-dependent difference in CA1 CREB phosphorylation in WT mice (160.8 ± 19.9 %, n = 16 slices from 5 mice, but not MSK1 KD mice (104.1 ± 12.7%, n = 18 slices from 5 mice (Figure 3.3 B) (p = 0.1203, unpaired T-test, two-tailed). These changes were observed on a between-animal basis (Figure 3.3 B) and also can be seen on a per slice basis, both in % treated slice fluorescence intensity change (Figure 3.3 C) and with ECDFs derived from raw intensity values (Figure 3.3 D). Overlap between WT and KD control group and KD DHF treated slices can be observed in Figure 3.3 D, along with a rightwards shift in the WT DHF group, indicating greater pCREB immunofluorescence.

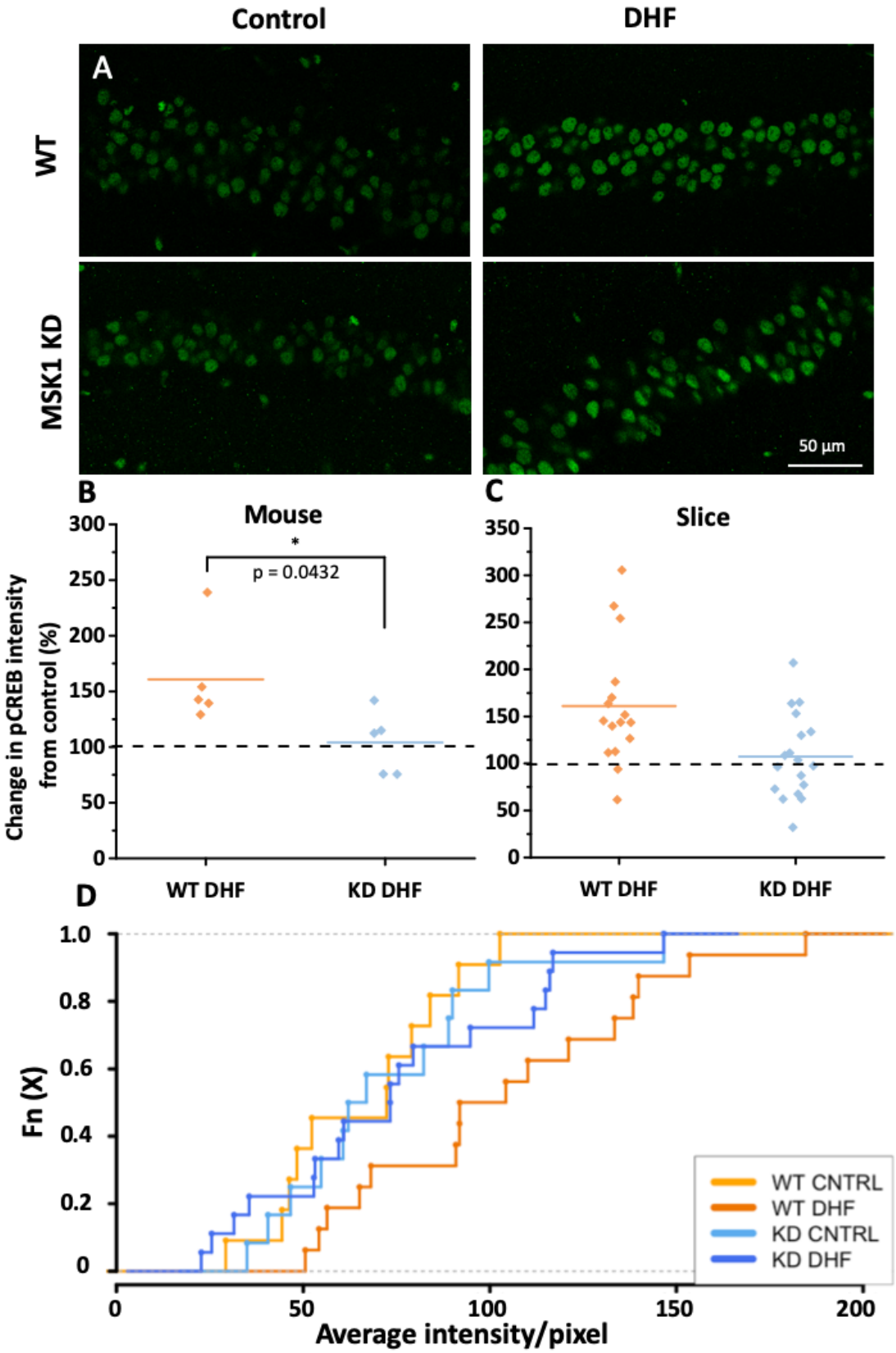

Figure 3.3. CREB phosphorylation in CA1 neurons is significantly increased in WT mice, but not in MSK1 KD mutants in response to DHF stimulation A) Immunofluorescence images of slices from WT and MSK1 KD mice treated with either DMSO (0.01%, vehicle control) or DHF (2mM) resulting in an

increase in pCREB immunoreactivity in WT mice, but not in MSK1 KD mice. (40X magnification) **B, C)** Data points showing % change in pCREB fluorescence in DHF treated slices/average intensity from control untreated slices for WT (16 slices, 5 mice) and MSK1 KD mice (18 slices, 5 mice) per mouse (B) (two-sample T.test, p = 0.0432) or per slice (C). Line indicates mean of data points. **D)** ECDF plots for each group from slice pixel intensity values. Statistical testing was carried out between % response averaged between animals (each n is an average of treated slice intensities compared with averaged control slice intensities from the same animal) (B) showing a significant change between WT CTRL slices and WT DHF slices.

3.2.3 Increased CREB phosphorylation detected in WT mice is not due to lack of specificity of the anti-pCREB Ser133 antibody.

Specificity of the anti-pCREB antibody was called into question by the product sheet provided by the manufacturer. When used for western blot analysis, two distinct bands close to the molecular weight for pCREB could be observed: One for pCREB S133, and another for phosphorylated activating transcription factor 1 (ATF-1), a CREB-related protein. Both CREB and ATF-1 possess a conserved kinase activating region that share a high degree of similarity. To ensure the MSK1 kinase activity-specific effect seen in Figures 3.2 and 3.3 were due to elevated levels of pCREB in the wildtype animal and not due to a second substrate recognised by the antibody, a second mutant mouse model was utilised. This mouse was homozygous for expression of a serine to alanine point mutation at CREB residue 133 (S133A) (Wingate et al., 2009) in exon 5 of the CREB gene (which is common to all 3 isoforms of CREB) that was restricted in expression to post-natal day 20 and limited to the forebrain. Full details on this mouse can be found in the previous methods chapter and describe the expression strategy behind this restricted expression. In Figure 3.4, binding of the anti-pCREB antibody within cells of the CA1 region can be observed in CREB WT mice (homozygous for the wildtype CREB allele), as would be expected. However, in S133A CREB mice (homozygous for the mutated S133A CREB allele), no visible 488 nm fluorescence staining of cells within the CA1 can be observed (Figure 3.3). A 4',6-diamidino-2-phenylindole (DAPI) stain was included to highlight the nuclei of cells, and which displays colocalisation with pCREB fluorescence. This was repeated across 5 additional slices from 3 different mice in which the same lack of pCREB staining was observed. Lack of pCREB staining in combination with a DAPI stain highlighting

cell nuclei within S133A CREB mutants indicated that the anti-pCREB antibody was specific for pCREB.

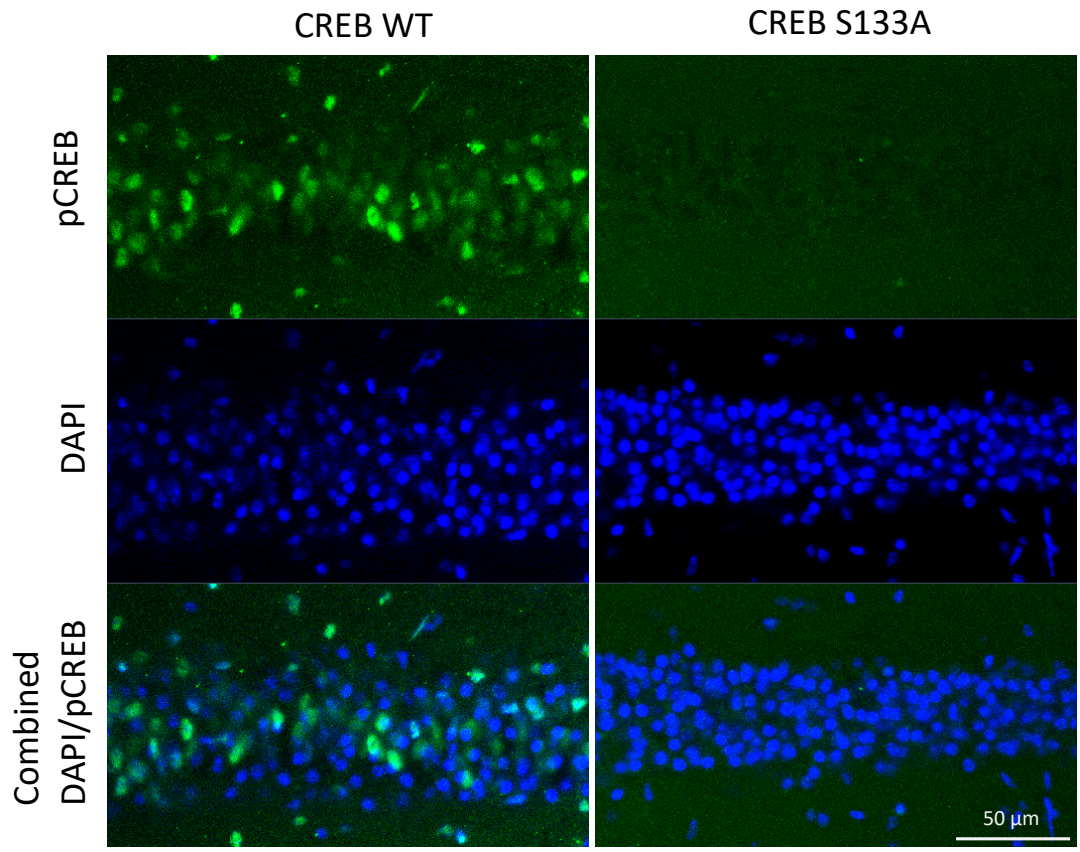

Figure 3.4. CREB mice homozygous for S133A point mutation fail to bind anti-pCREB antibody within CA1 pyramidal cells. Immunofluorescence images obtained from mice homozygous for wildtype CREB allele (CREB WT) and mice homozygous for S133A point mutation (CREB S133A) stained with anti-pCREB antibody and 488 nm secondary. DAPI channel is shown to indicate positions of nuclei and demonstrate overlap with pCREB expression in CREB WT mice.

3.3 Discussion

3.3.1 Phosphorylation of CREB at S133 in response to BDNF is MSK1-dependent and likely occurs via the TrkB receptor

Failure to upregulate CREB phosphorylation at Ser133 in response to BDNF treatment in MSK1 KD animals (Figure 3.2) suggests that the kinase activity of MSK1 is required for CREB phosphorylation in response to BDNF. The increase in pCREB levels following application of BDNF to *in vitro* brain slices is therefore largely MSK1-dependent. The similar significant increase in pCREB immunofluorescence observed following DHF application (Figure 3.3) also indicating that BDNF-mediated MSK1-dependent CREB phosphorylation occurs primarily via the TrkB receptor.

Control WT and MSK1 pCREB immunofluorescence was observed to be similar (Figure 3.2 D), indicating that MSK1-dependent CREB phosphorylation is relatively low under basal conditions. Since MSK1 controls the increase in CREB phosphorylation in response to BDNF, this highlights a role for MSK1 in regulating BDNF-dependent CREB-mediated transcription in response to activity-dependent release of BDNF. This disruption of BDNF-CREB signalling means that MSK1 KD mice provide a novel insight into how both BDNF and MSK1 control CREB-mediated transcription. Previously observed phenotypes within the MSK1 KD mice may therefore be explained by study of neurotrophin-induced CREB-mediated transcription in both WT and MSK1 KD mice.

3.3.2 MSK1 KD mice can still phosphorylate CREB at S133 through MSK1-independent pathways

Basal CREB phosphorylation levels of MSK1 KD mutants did not appear to be different from WT animals (Figure 3.2 D; Figure 3.3 D), indicating CREB phosphorylation was still possible through MSK1-independent pathways, (such as cAMP- or Ca^{2+}-dependent kinases). CREB phosphorylation therefore still appears possible via MSK1-independent kinases in the MSK1 KD mutant. This has also been tested experimentally using the adenyl-cyclase activator forskolin which, when applied to slices from both WT and MSK1 KD mice, caused a significant and comparable increase in pCREB in both genotypes (Daumas et al., 2017).

In summary, MSK1 KD mice display an inability to phosphorylate CREB in response to the extracellular neurotrophin BDNF likely primarily via the TrkB receptor within the CA1 field of the hippocampus. By regulating CREB phosphorylation in this manner, MSK1 plays a key role in transducing activity-dependent neurotrophin changes within the hippocampus into transcriptomic changes within CA1 neurons. MSK1 KD mice are therefore an ideal model for testing the effects of experience-induced BDNF expression on CREB and histone H3 transcription.

The work covering the pCREB immunofluorescence in response to BDNF application in this chapter has been published in (Daumas et al., 2017). The work covering the S133A CREB mutant (here used as an antibody control) is included in a paper from the Frenguelli lab currently under review.

Chapter 4: Utilisation of RNAseq to elucidate the role of MSK1 kinase-activity in mediating the transcriptomic response to environmental enrichment

4.1 Introduction:

The role of MSK1 in regulating the response to environmental enrichment has previously been examined in MSK1 KO mutants. Compared to WT mice, MSK1 KO mice present with a significant decrease in spinogenesis and dendritic branching complexity in hippocampal DG, CA1 and CA3 principle neurons and progenitor cell proliferation in the sub-granular zone (SGZ) of the DG (Karelina et al., 2012). Following 40 day exposure to EE, MSK1 KO mice failed to demonstrate the spatial memory enhancement seen in WT mice, and showed reduced levels of EE-mediated spinogenesis and SGZ progenitor proliferation (Karelina et al., 2012). MSK1 KD mutants have also been exposed to EE, where they fail to display an increase in mEPSC amplitude compared to WT mice (Corrêa et al., 2012), indicating that the benefits of EE are mediated at least in part specifically by the kinase activity of MSK1.

Expression of both BDNF (Novkovic et al., 2015, Cowansage et al., 2010) and the TrkB receptor (Hu et al., 2013) have been observed to increase as a result of EE, and BDNF-mediated signalling plays an important role in mediating the beneficial effects of EE (Sale et al., 2014, Novkovic et al., 2015). Likewise, CREB-mediated transcription, and the phosphorylation of histone H3 have been repeatedly implicated in the regulation of synaptic transmission, plasticity and learning and memory (Deisseroth et al., 1996, Chwang et al., 2006, Crosio et al., 2003, Lisman et al., 2018, Kandel, 2012). EE increases levels of CREB itself (Huang et al., 2006) and enhances both LTP and LTD (Irvine et al., 2006, Artola et al., 2006). CREB transcriptional co-activator CBP has also been implicated in regulating the transcriptional response to EE (Lopez-Atalaya et al., 2011). Histone H3 phosphorylation by MSK1 has also been seen to regulate hippocampal-dependent memory formation through chromatin remodelling (Chwang et al., 2007).

MSK1 KD mutants also display deficits in activity-mediated homeostatic enhancements in synaptic transmission such as upregulation of Arc/Arg3.1 expression in response to activity-deprivation (Corrêa et al., 2012). Arc/Arg3.1 upregulation in response to activity deprivation is thought to rely on activity-dependent BDNF expression (Turrigiano,

2012). Therefore perhaps environmental enrichment (EE), known to upregulate expression of BDNF in an activity-dependent manner (Novkovic et al., 2015) relies on MSK1-mediated CREB/histone H3 phosphorylation and subsequent transcriptional activation.

The inability of MSK1 KD mice to phosphorylate CREB at Ser133 or histone H3 in response to BDNF-mediated stimulation of the TrkB receptor (Arthur et al., 2004, Arthur, 2008) led to the question of how the transcriptomic response to EE would be affected by MSK1 kinase inactivation. If MSK1 cannot phosphorylate and activate CREB and histone H3 transcriptional activity, and CREB and histone H3 are involved in the regulation of the transcriptional response to EE, then MSK1 KD mice would display a transcriptional deficit after EE. Both MSK1 KD and WT mice were observed to have no difference in basal CREB phosphorylation levels (Fig 3.2 D; WTCTRL and KDCTRL), and so would be expected to display relatively little transcriptomic difference under conditions that are not expected to stimulate BDNF expression (standard housing). However MSK1 KD mutants fail to increase CREB phosphorylation in response to BDNF (Figure 3.2), perhaps indicating a deficit in CREB activation following BDNF upregulation.

Therefore, in order to better understand the deficits in the response of MSK1 mutant mice to EE (Karelina et al., 2012, Corrêa et al., 2012) and the transcriptional underpinnings of EE and the role MSK1 may play in mediating their effects, RNAseq was employed. Using RNA harvested and sequenced from whole individual hippocampi of MSK1 KD and WT mice kept in SH and EE housing conditions from birth to 3 months, differential gene expression testing was conducted.

4.2 Results:

4.2.1 Experimental set-up and quality control of RNAseq data

Mice were split into 4 different groups based on genotype: Wildtype standard housed (WTSH), wildtype environmentally enriched (WTEE), MSK1 kinase-dead standard housed (KDSH) and MSK1 kinase-dead environmentally enriched (KDEE) mice were raised in the appropriate housing condition for 2 months after birth, before undergoing 4 weeks of

behavioural assays. At 12 weeks, the mice were killed and a hippocampus from one hemisphere used for electrophysiological recordings, with the other whole hippocampus was homogenised and used for RNA extraction (Figure 4.1 A). The behavioural and electrophysiological experiments these mice were used for were performed by different researchers within the Frenguelli lab and were published along with this RNAseq experiment together in Privitera et al. (2020)

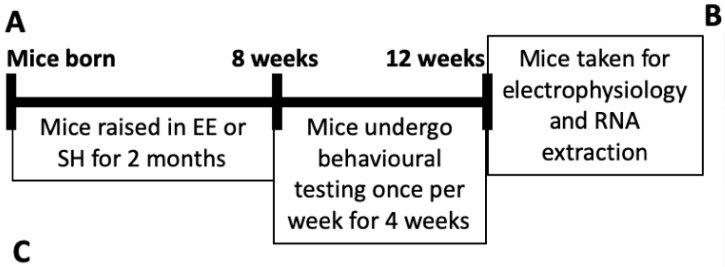

B

Genotype	Housing Condition	Sample No.
KD	SH	1, 3, 4, 5, 6
KD	EE	7, 8, 32A, 36A
WT	SH	10, 11, 13, 14, 15
WT	EE	16, 17, 33A

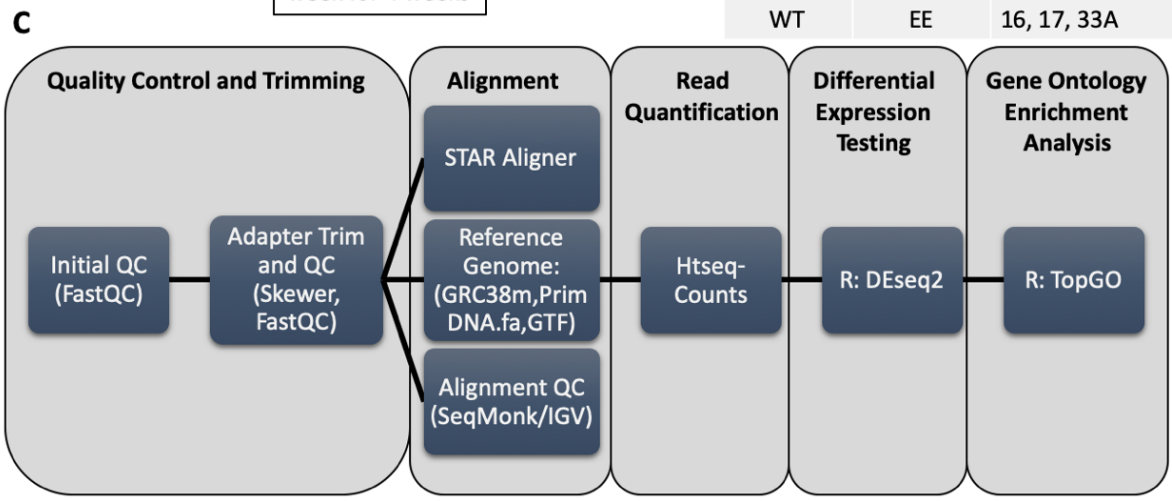

Figure 4.1. RNAseq experimental summary. A) Experimental Timeline. Mice were split into 4 different groups based on genotype (WT or KD), and housing condition (EE or SH). Mice in each group were raised for 2 months in their corresponding housing condition before undergoing 4 weeks of behavioural testing. Afterwards, mice were used for electrophysiological experiments at which time RNA from an intact hemisphere of the hippocampus was extracted and used for library preparation. The behavioural and electrophysiological experiments these mice were used for were conducted by different researchers and are covered in Privitera et al. (2020). **B)** Final sample table containing all samples used for differential expression analysis. Samples failing quality control (QC) and displaying poor intragroup correlation were removed. **C)** Summary visual of RNAseq analysis pipeline detailing software used for each stage of data processing. For full details please see Chapter 2: Methods.

Raw read fastq files were quality checked, trimmed to remove low quality reads and Illumina adapters, aligned to the mouse genome (GRC38m.8) and reads mapping to each gene quantified as a measure of expression. Average mapping of samples that passed quality

control (QC) was 92.29% (Appendix Table i). Samples were analysed blind, 6 samples to a group, for a total of 24 samples. Aligned sample reads were compared at the MSK1 gene locus using the interactive genomics viewer (IGV), to check for a mismatch in the kinase domain of the MSK1 gene introduced as a point mutation into the kinase dead mutants (Corrêa et al., 2012). The base mismatch (G for T point mutation) at chr12:bp100616031 (within the MSK1 gene, resulting in a Asp194Ala amino acid substitution) was detected for all KD samples (Figure 4.2), confirming that no sample mislabelling had occurred, at least with respect to genotype.

Figure 4.2. Integrative genome browser displaying loaded sample tracks at exon1 of MSK1 gene indicates half of the samples are of MSK-KD genotype. Highlighted in orange are base-pair mismatches at chr12:bp100616031. Half of the samples contain a majority G alignment instead of T, indicating presence of the D194A mutation characterised in Corrêa et al. 2012.

Quality control of sample data for the RNAseq experiment was performed, trimming low-quality reads and removing contaminants before checking sample reads against various quality metrics: Sample 34B was excluded due to ribosomal RNA (rRNA) contamination

(Figure 4.3) and very few reads having survived the QC process (Table 4.1, Appendix table i). Sample 33B was also excluded due to suffering excessive rRNA contamination (>25%) (Figure 4.3, Table 4.1, Appendix table i). Intragroup sample variation was observed to be quite high for some samples, and this interfered with obtaining good quality distinct expression. Therefore, samples 12 (WTSH), 31B and 35A (WTEE), 2 (KDSH) and 9 (KDEE) were removed due to poor intra-group correlation (Figure 4.4, Table 4.1, Appendix table i). After removal of samples that failed quality control (QC) and displayed excessive within group variation, the number of samples for each condition was as follows: KDSH n = 5; KDEE n = 4; WTSH n = 5; WTEE n = 3 (Figure 4.1 B, Table 4.1, Appendix table i).

Sample	Condition	Data QC Fail?	Removed from analysis?	Reason for removal
Sample_1	KDSH	N	N	N/A
Sample_2	*KDSH*	*N*	*Y*	*Poor Intra-group correlation of gene expression*
Sample_3	KDSH	N	N	N/A
Sample_4	KDSH	N	N	N/A
Sample_5	KDSH	N	N	N/A
Sample_6	KDSH	N	N	N/A
Sample_7	KDEE	N	N	N/A
Sample_8	KDEE	N	N	N/A
Sample_9	*KDEE*	*N*	*Y*	*Poor Intra-group correlation of gene expression*
Sample_10	KDEE	N	N	N/A
Sample_11	KDEE	N	N	N/A
Sample_12	*KDEE*	*N*	*Y*	*Poor Intra-group correlation of gene expression*
Sample_13	WTSH	N	N	N/A
Sample_14	WTSH	N	N	N/A
Sample_15	WTSH	N	N	N/A
Sample_16	WTSH	N	N	N/A
Sample_17	WTSH	N	N	N/A
Sample_31B	*WTSH*	*N*	*Y*	*Poor Intra-group correlation of gene expression*
Sample_32A	WTEE	N	N	N/A
Sample_33A	WTEE	N	N	N/A
Sample_33B	*WTEE*	*Y*	*Y*	*rRNA contamination and poor intra-group correlation*
Sample_34B	*WTEE*	*Y*	*Y*	*mitochondrial RNA contamination and low quality reads left trimmed reads too short for accurate unique alignment.*
Sample_35A	*WTEE*	*N*	*Y*	*Poor Intra-group correlation of gene expression*
Sample_36A	WTEE	N	N	N/A

Table 4.1. Summary of RNAseq sample quality control outcome and reasons for exclusion from analysis. Most samples passed quality control of raw read data with only two failures: sample_33B and sample 34B. Several other samples were removed that displayed poor gene expression correlation within conditions.

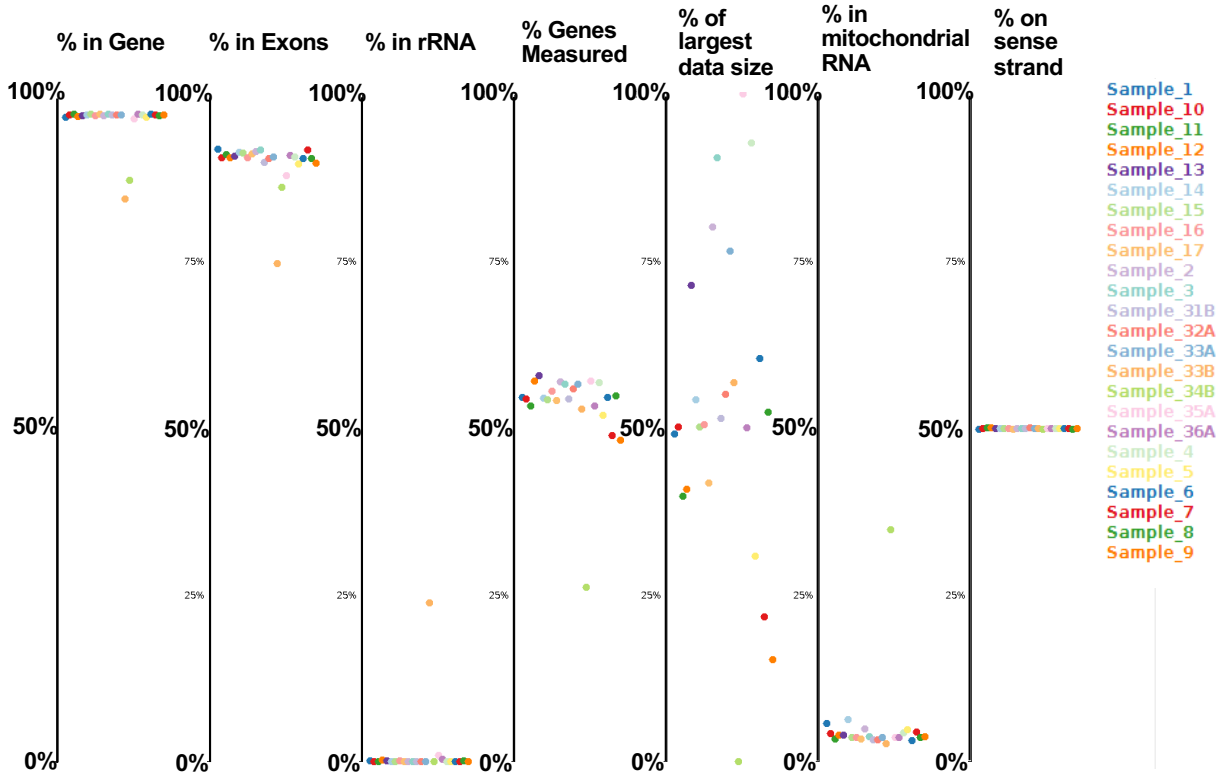

Figure 4.3. RNAseq quality control plot generated by SeqMonk. Here reads aligned to specific genome features as a percentage of total reads can be observed. Each column corresponds to a different QC metric, and the percentage of reads in each sample aligned to each genome feature is represented by the height of the colour for each sample within a column. From left to right: % reads mapping to gene features, % mapping to exons, % mapping to ribosomal RNA, % of genes with reads mapping to them, % when comparing reads in sample to reads of largest sample, % reads mapping to mitochondrial (non-genomic) RNA, % reads on sense strand. All samples are colour coded, and the left-most sample in a column corresponds to the top-most sample in the legend.

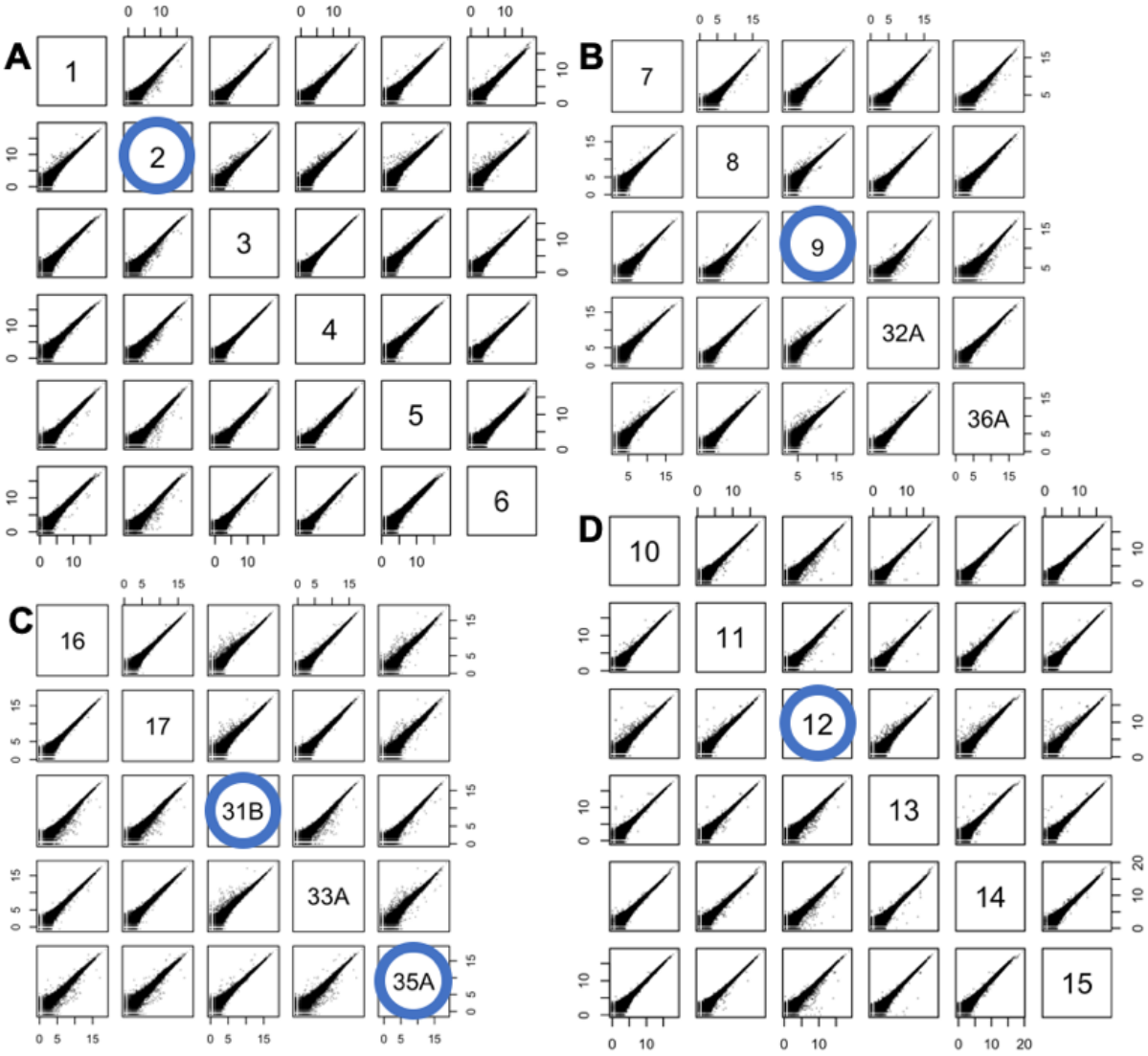

Figure 4.4. Intra-group scatter plots of gene expression excluding samples that failed quality control. Highlighted in blue circles are samples removed from analysis due to poor intra-group correlation. **A)** MSK1 kinase-dead standard housed (KDSH) mice. **B)** MSK1 kinase-dead environmentally enriched (KDEE) mice. **C)** Wildtype environmentally enriched (WTEE) mice. **D)** Wildtype standard housed (WTSH) mice.

4.2.2 More than half of environmental enrichment-mediated transcriptomic changes are MSK1-dependent.

Samples were grouped according to their genotype/housing condition (Figure 4.5 A), and subjected to principle component analysis (PCA). PCA was conducted on gene counts normalised on a per-gene basis between samples for the top 500 genes by expression variation between samples. Principal component (PC) 1 and PC 2 accounted for 73 % and 8 % respectively of total variation and displayed distinct clustering between each condition (Figure 4.5 B). PCs 3 to 15 individually accounted for a very low percentage (<5%) of total variation (Figure 4.5 C), and displayed little distinct clustering of groups in any meaningful way. Groups separated very distinctly along PC1 seemingly in response to EE (Figure 4.5 B). MSK1 KD mice appear to demonstrate a weaker mixed response to EE, with KDEE being more spread out across PC1 than the tighter cluster of WTEE on the right-most side (Figure 4.5 B). This could indicate an uncoordinated response of KD mice to EE when compared with WT mice. In concordance with this, the standard housed conditions (KDSH and WTSH) display relatively little separation along PC1 (Figure 4.5 B).

A

Genotype/ Housing	Standard Housing (SH)	Enriched Environment (EE) (3mths from birth)
Wildtype (WT)	WTSH	WTEE
MSK1-KD (KD)	KDSH	KDEE

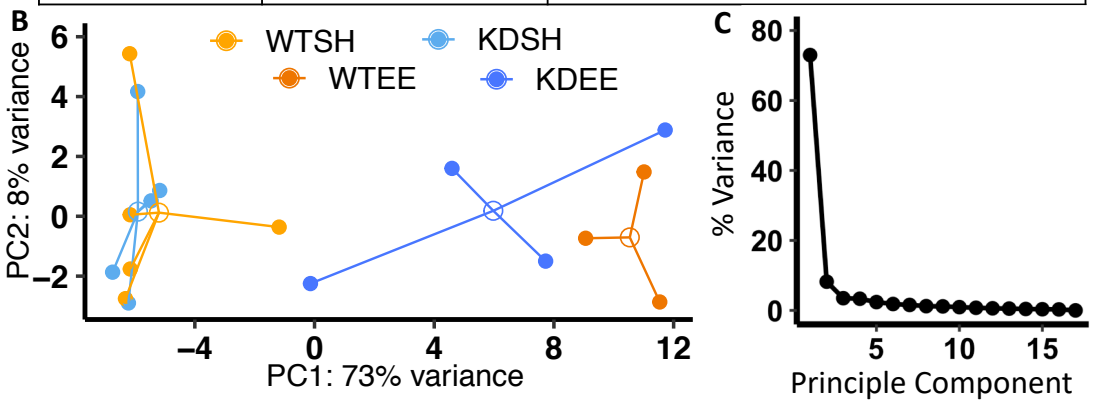

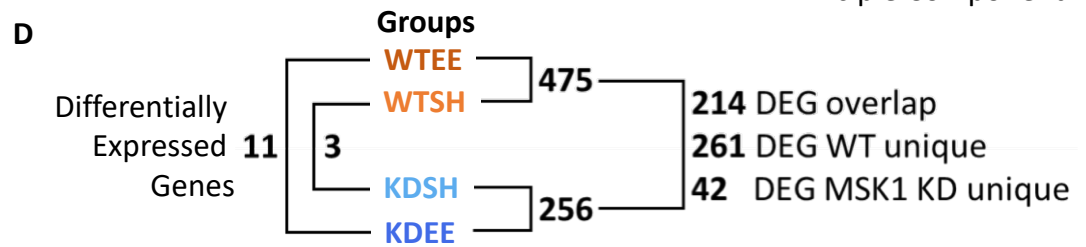

Figure 4.5. RNAseq reveals over half of the transcriptional response to 3mths of environmental enrichment is MSK1-dependent. A) Summary of genotype and housing conditions and group abbreviations. **B)** Principal component analysis of gene expression variation of the top 500 genes between groups for the first and second principle components. **C)** Scree-plot of gene expression variation percentage of the top 500 genes vs. principle component number **D)** Summary of differential gene expression testing between groups. Numbers of differentially expressed genes between groups are summarised, as well as overlap of DEGs identified between WTSH-WTEE and KDSH-KDEE groups.

Differential expression testing revealed very little difference between both SH conditions: between the baseline genotypes KDSH and WTSH only 3 DEGs were detected: two ribosomal proteins and an uncharacterised protein (Figure 4.5 D, Appendix Table iii and v). This is in line with another study that looked at gene expression in standard housed behaviourally naïve CREBS133A mutant and WT mice, which showed no detectable differences in gene expression between CREBS133A and WT mice (Briand et al., 2015). The study by Briand et al. (2015) was however performed with a microarray, and so was limited in the scope of genes that could be detected. Much stronger, however, was the robust response to enrichment that both WT and KD mice underwent. 475 DEGs were detected in WT mice in response to enrichment (WTEE vs. WTSH, Appendix Table s iii and vi), and only 256 DEGs detected in KD mice (KDEE vs. KDEE Appendix Table s iii and vii) as seen in Figure 4.5 D. Of these, 214 DEGs were common to both mice (Figure 4.5 D), responding to enrichment in an MSK1-independent manner. However 261 genes were differentially expressed in only WT mice and therefore, in an MSK1-dependent manner. This means greater than half of the observed significant transcriptomic change in response to enrichment was mediated by the kinase activity of MSK1 (Figure 4.5 D).

4.2.3 Differential gene expression testing between WT and KD mice reveals genotype-dependent differences in modulation of the MAPK pathway and Egr1 expression in response to EE.

Differential gene expression testing between both WT and KD genotypes after exposure to EE (WTEE vs. KDEE) yielded 11 significant DEGs (Figure 4.6 A, B; Table 4.2; Appendix Table iv). Egr1 and Sprouty RTK signalling antagonist 4 (Spry4) were downregulated in WTEE mice compared with KDEE mice (Figure 4.6 A, B; Table 4.2). Egr1, as mentioned in

the introduction section, is an IEG important in activity-dependent changes in synaptic strength (pg 37) and whose expression is upregulated in response to neuronal stimulation by BDNF (pg 54), and can be seen to be upregulated within the hippocampus 24 hrs after a hippocampus-dependent learning task (Alder et al., 2003). Spry4 is an inhibitor of ras signalling during nerve growth factor (NGF) activation of the TrkA-mediated Erk/MAPK pathway (Alsina et al., 2012). NGF is another neurotrophin, which promotes neuronal differentiation in development (Alsina et al., 2012). More interestingly in the adult animal, NGF appears to promote plasticity within the hippocampus, as bilateral hippocampal blockade of NGF signalling *in vivo* results in spatial memory impairments (while preserving acquisition), along with impairing *in vivo* induction of LTP at PP-DG synapses (Conner et al., 2009).

In contrast, 9 genes were upregulated in WTEE mice compared to KDEE mice Figure 4.6 A, B). These nine genes (Table 4.2) include a ATP-gated ion channel: P2rx6, whose gene expression has been seen to increase after 6 weeks of exercise (Cardoso et al., 2019) and can form heteromeric P2rx6/P2rx4 receptors that are permeable to Ca^{2+} and that also respond to extracellular cations (Kaczmarek-Hájek et al., 2012). However the function of P2rx6 receptors within the brain are still largely unknown (Kaczmarek-Hájek et al., 2012), with P2rx6 knockout mice developing normally, appearing physiologically normal, displaying normal locomotion in openfield testing and not displaying compensatory increased expression of other P2x receptors in kidney or heart tissue (except P2rx2 in the heart; additionally the brain has not been tested) (de Baaij et al., 2016). Also upregulated was a cadherin-related protein, Cdhr3, which is not well characterised within the brain, but is used as a marker of ciliated epithelial cells due to its high abundance within them (Lutter and Ravanetti, 2019). Cadherins are thought to mediate stabilisation of cell-cell contacts between pre- and post-synaptic cells at the synapse and mediate structural changes at the synapse following plasticity events (Arikkath and Reichardt, 2008). and

Two other genes upregulated in WT mice compared to MSK1 KD mice following EE were dynein axonemal intermediate chain 1 (Dnaic1) and PIH1 Domain Containing 2 (Pih1d2). Pih1d2 appears to be part of a complex that regulates the formation of axonemal dynein arms, a key structural component of cilia (Fabczak and Osinka, 2019) and Dnaic1 is required

for functional cilium assembly (Ostrowski et al., 2010) (Table 4.2). Another gene upregulated in WTEE mice compared with KDEE mice was the retinoic acid receptor responder protein 2 (Rarres2) also known as "Chemerin" (Table 4.2), the endogenous ligand of the GPCR chemokine-like receptor 1 (CMKLR1) which upon activation by Rarres2, can stimulate the phosphorylation of ERK1/2 (Goralski et al., 2007). Rarres2 has a neuroendocrine role in food intake and can stimulate angiogenesis in epithelial cells through the activation of MAPK and ERK pathways (Helfer and Wu, 2018). Finally, Hist1hc, a histone linker protein that regulates chromatin condensation, and the genes Gm11992, Gm28578 and Vwa5b1 (whose functions are currently poorly characterised), were also significantly upregulated in WTEE mice compared with KDEE mice (Table 4.2).

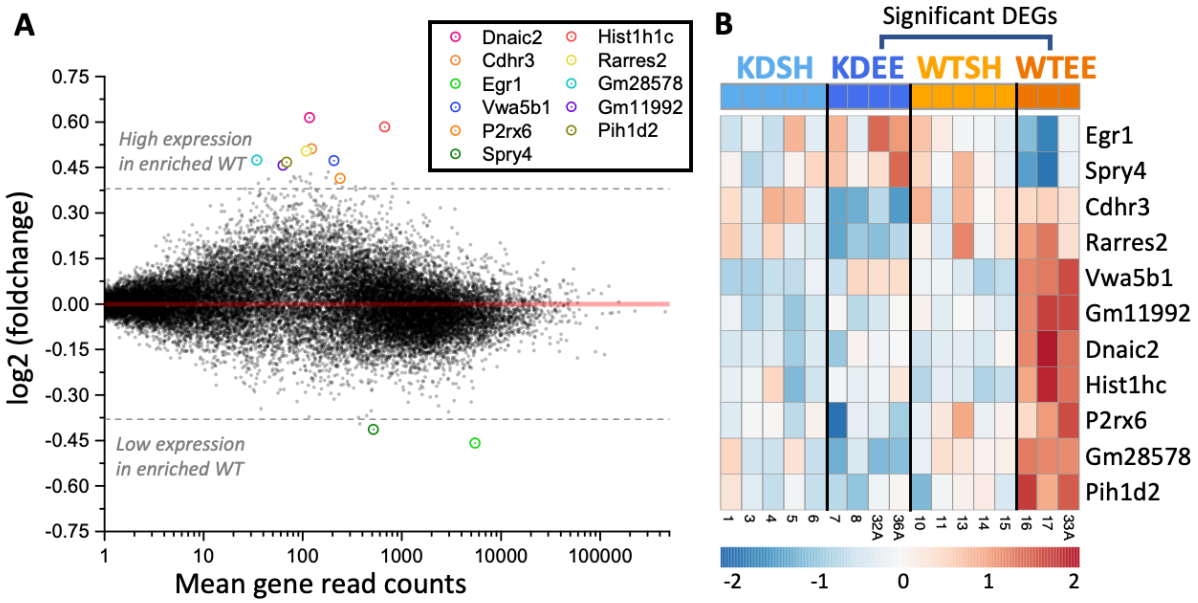

Figure 4.6. Expression summary of 11 differentially expressed genes identified as significant between WTEE and KDEE conditions. A) MA plot of average gene expression across all samples against log_2 fold change between WTEE and KDEE conditions. The 11 DEGs identified between WTEE and KDEE conditions are circled in colours corresponding to plot legend. Dotted horizontal lines indicate the +/- 0.38 log2 fold-change cut-off threshold used in DEG testing. Other genes above the dotted lines but not highlighted do possess log2 fold-changes above the cut-off threshold, but did not achieve statistical significance due to variable expression between samples. **B)** Heatmap of gene expression variation between samples for the 11 DEGs identified between WTEE and KDEE groups. Red indicates high levels of expression, blue indicates low expression. Colour scale is based on gene variance calculated as sample expression deviation from average gene expression across all samples for gene.

Gene symbol	Full name	Alternative names	Functional description	Biological function
Egr1	Early growth response 1	Zif268 (zinc finger protein 268); NGFI-A (nerve growth factor-induced protein A)	The protein encoded by this gene belongs to the EGR family of C2H2-type zinc-finger proteins. It is a nuclear protein and functions as a transcriptional regulator. **(NCBI, 03/05/20)**	Synaptic function and plasticity: Regulation of genes involved in presynaptic vesicular trafficking, neurotransmitters, synapse formation and assembly, and protein translation and degradation (Duclot and Kabbaj, 2015, 2017) Maintenance of L-LTP and consolidation of spatial LTM (Jones, 2001)
Spry4	Sprouty RTK signaling antagonist 4	N/A	The encoded protein is an inhibitor of the receptor-transduced mitogen-activated protein kinase (MAPK) signaling pathway. Activity of this protein impairs the formation of active GTP-RAS. **(NCBI, 03/05/20)**	Associated biological processes (NCBI, 03/05/20) GO:0046580: Negative regulation of Ras protein signal transduction GO:0070373: Negative regulation of ERK1 and ERK2 cascade GO:0043407: Negative regulation of MAP kinase activity
Cdhr3	Cadherin related family member 3	N/A	Cadherins are calcium-dependent cell adhesion proteins. They preferentially interact with themselves in a homophilic manner in connecting cells **(UniProt, 03/05/20)**	Associated biological processes (NCBI, 03/05/20) GO:0098609: Cell-cell adhesion GO:0035249: Synaptic transmission, glutamatergic GO:0043083: Synaptic cleft
Rarres2	Retinoic acid receptor responder 2	Chemerin; Retinoic acid receptor responder (tazarotene induced) 2	Adipocyte-secreted protein (adipokine) that regulates adipogenesis, metabolism and inflammation through activation of the chemokine-like receptor 1 (CMKLR1). Its other ligands include G protein-coupled receptor 1 (GPR1) and chemokine receptor-like 2 (CCRL2). **(UniProt, 03/05/20)**	Associated biological processes (NCBI, 03/05/20) GO:0031012: Extracellular matrix GO:0001934: Positive regulation of protein phosphorylation GO:0062023: Collagen-containing extracellular matrix GO:0006954: Inflammatory response GO:0010759: Positive regulation of macrophage chemotaxis
Vwa5b1	von Willebrand factor A domain-containing protein 5B1	N/A	Function unknown. Diseases associated with VWA5B1 include Usher Syndrome, Type If and Usher Syndrome, Type I (**GeneCards, 03/05/20)**	Associated biological processes (NCBI, 03/05/20) GO:0005576: Extracellular region Vwa5b1 (along with Spry4 and Vgf) identified as a target of transcription factor CIC, which regulates neuronal differentiation of neuroblasts to immature neurons in mouse hippocampus (Hwang et al., 2020)
Gm11992	Uncharacterized protein C7orf57 homolog	Predicted gene 11992	Function unknown.	Function unknown.
Dnaic2	Dynein, axonemal, intermediate chain 2	Dnai2; Gm728	The protein encoded by this gene belongs to the dynein intermediate chain family, and is part of the dynein complex of respiratory cilia and sperm flagella. Mutations in this gene are associated with primary ciliary dyskinesia type 9. **(NCBI, 03/05/20)**	Associated biological processes (NCBI, 03/05/20) GO:0045504: Dynein heavy chain binding GO:0060271: Cilium assembly GO:0007018: Microtubule-based movement GO:0030030: Cell projection organization
Hist1hc	Histone Cluster 1 H1 Family Member C	H1.2 linker histone, cluster member (H1-2)	Histone H1 protein binds to linker DNA between nucleosomes. Histones H1 are necessary for the condensation of nucleosome chains into higher-order structured fibers. Acts also as a regulator of individual gene transcription through chromatin remodeling, nucleosome spacing and DNA methylation **(UniProt, 03/05/20)**	Associated biological processes (NCBI, 03/05/20) GO:0030261: Chromosome condensation GO:0031936: Negative regulation of chromatin silencing GO:0006355: Regulation of transcription, DNA-templated GO:0080182: Histone H3-K4 trimethylation GO:0098532: Histone H3-K27 trimethylation
P2rx6	P2X purinoceptor 6	P2x6	Receptor for ATP that acts as a ligand-gated ion channel. **(UniProt, 03/05/20)**	Associated biological processes (NCBI, 03/05/20) GO:0004931: Extracellularly ATP-gated cation channel activity GO:0001614: Purinergic nucleotide receptor activity GO:0005524: ATP binding
Gm28578	Predicted gene 28578	N/A	Function unknown	Function unknown
Pih1d2	PIH1 domain containing protein 2	N/A	PIH1D2 (PIH1 Domain Containing 2) is a Protein Coding gene. Diseases associated with PIH1D2 include Pyruvate Dehydrogenase E2 Deficiency and Primary Ciliary Dyskinesia. (**GeneCards, 03/05/20)**	Chaperones Hsp90 as part of a complex that regulates axonemal dynein arms, a structural component of cilia (Fabczak et al., 2019) Associated biological processes (NCBI, 03/05/20) GO:0006364: rRNA processing GO:0017160: Ral GTPase binding

Table 4.2: Table describing information for each of the 11 genes identified as significantly differentially expressed between WTEE and KDEE mice.

4.2.4 MSK1 plays a key role in regulating genes associated with EE-induced extracellular structural changes within the hippocampus and the assembly and activity of neuronal primary cilia

To gain a greater understanding of the function of genes differentially expressed in response to EE, GO term functional analysis was carried out the TopGO package within the statistical environment R. Overlap of the 475 DEGs identified in WT and 256 DEGs detected within KD mice in response to EE, was visualised using a Venn diagram (Figure 4.7 A). Three lists of genes were then tested for gene ontology term (GOTerm) functional enrichment: The 214 MSK1-independent DEGs (differential expression in both genotypes after EE) as seen in Figure 4.7 B and Appendix Table viii; the 261 MSK1-dependent DEGs (differential expression unique to WT animals after EE) as seen in Figure 4.7 C and Appendix Table ix; and the 42 MSK1 KD unique DEGs (differential expression unique to MSK1 KD animals) which did not possess any significant enrichment for GOTerm functionality but are presented in Appendix Table x.

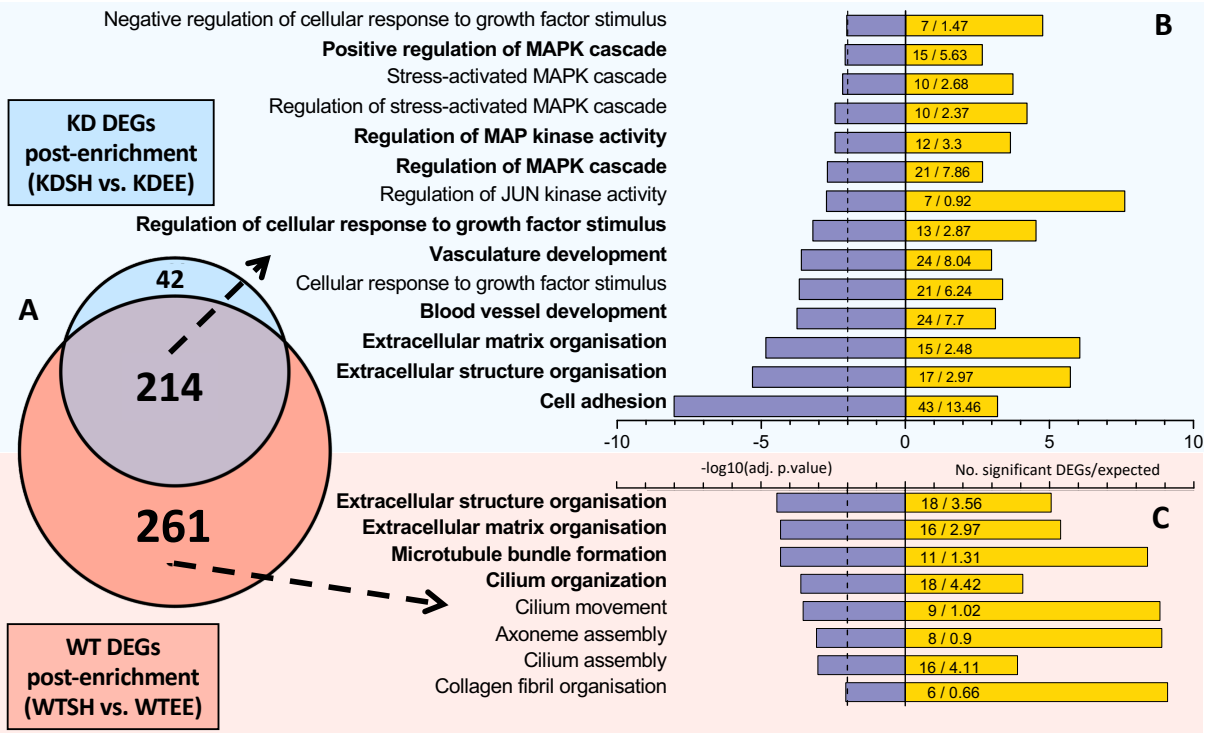

Figure 4.7. Functional GOTerm analysis of differentially expressed genes shows common upregulation of MAPK pathway in both MSK1-KD and WT mice, but a failure of MSK1-KD mice to respond fully to enrichment. A) Venn diagram comparing DEGs in response to enriched-environment (EE) compared to standard-housed controls. Top (blue): DEGs in MSK1-KD mice exposed to EE (256 genes). Bottom (orange): DEGs in wildtype mice exposed to EE (475 genes).**B, C)** Back-to-back barplots

of significantly enriched GO terms against Benjamini-Hochberg adjusted p. values, along with the number of significant genes contributing to each term and the number of significant genes expected from the GO term if the transcriptome was randomly sampled with the same number of genes. **B)** A subset of significantly enriched GO terms common to both wildtype and MSK1-KD mice exposed to EE (from 214 DEGs). **C)** A subset of significantly enriched GO terms unique to wildtype mice exposed to enrichment (from 261 DEGs). Interesting GOTerms discussed later are highlighted in bold. Broken vertical lines in B and C indicates adj. p-value cutoff of 0.05.

GOTerm enrichment analysis of the 214 overlapping DEGs differentially expressed in both WT and MSK1 KD in response to EE (Figures 4.2 D, 4.4 A) revealed many pathways that were regulated in an MSK1-independent manner (Figure 4.7 B; Appendix Table xi). These 214 genes were assigned to 152 significantly enriched GOTerms which included "positive activation of the MAPK cascade", "blood vessel development", "extracellular matrix organisation", "cell adhesion" and "cellular response to growth factor stimulus" (Figure 4.7 B).

261 DEGs were identified uniquely in the WT response to EE, and not in MSK1 KD mice (Figures 4.2 D, 4.4 A). Differential expression of these genes to EE was in an MSK1-dependent manner, and, despite accounting for over half of the transcriptional response to EE in WT mice, these 261 genes were assigned to only 10 GOTerms. Gene-ontology terms highlighted as being regulated in an MSK1-dependent manner included: additional cell adhesion terms, extracellular matrix remodelling terms, "microtubule bundle formation" and "collagen fibril organisation" (Figure 4.7 C; Appendix Table xii). EE induced MSK1-dependent regulation of various primary cilium-related GOTerms governing: "cilia organisation, movement and assembly" were also observed (Figure 4.7 C; Appendix Table xii). This demonstrates good overlap with the several DEGs that experienced the most significant differential expression between WTEE and KDEE mice(Figure 4.6 A, B; Table 4.2): Both Pih1d2 (Fabczak and Osinka, 2019) and Dnaic1 (Ostrowski et al., 2010) are required for functional cilium assembly. Within the mature brain, each neuron contains a primary cilium, where they are involved in transducing extracellular signals, cell migration during neurogenesis and ciliopathies in humans are related to hippocampal volume loss and learning disabilities (Guemez-Gamboa et al., 2014). Additionally Rarres2 and Spry4 activate and inhibit MAPK signalling and are

upregulated and downregulated respectively in WTEE mice compared with KDEE mice (Figure 4.6 A, B; Table 4.2), suggesting an increased activation of MAPK signalling in WT mice following EE that MSK1 KD mice are unable to accomplish.

4.2.5 The majority of genes involved in synaptic plasticity genes do not appear to undergo expression changes following chronic EE exposure in either MSK1 KD or WT mice.

Comparison of DEGs between conditions yielded a surprising lack of GOTerms associated with synaptic activity or plasticity. An obvious test of the hypothesis of whether MSK1 kinase activity is involved in synaptic plasticity improvements after exposure to EE was then to see how the expression of synaptic plasticity genes is affected across conditions. “Synaptic plasticity” (GO: 0048167) and “Regulation of long-term synaptic plasticity” (GO:0048169) gene ontologies were merged to create a list of genes with an annotated function involved in synaptic plasticity. Gene expression variation for each gene was similar between conditions (Figure 4.8 A), which was unsurprising given the lack of GOTerms identified in DEG testing. Here however, even a pathway-wide small-scale change in gene expression regulation cannot be observed in any condition.

Expression levels from individual genes within the ontology known to be regulated by EE (BDNF) or synaptic activity (GluA1, GluA2) were then plotted. Upregulated BDNF mRNA levels have previously been observed in EE conditions (Frick et al., 2003) and in Figure 4.8 C, a slight increase in average expression can be observed here after EE, but this was not significantly different between genotype, or housing conditions. GluA1 protein expression has previously been observed to be regulated by MSK1 kinase activity in response to activity deprivation in cultured primary hippocampal neurons (Corrêa et al., 2012). Additionally, neither activity deprivation, nor MSK1 have been observed to have an effect on GluA2 protein expression (Corrêa et al., 2012). In the present study, no differences in GluA1 mRNA expression were observed between conditions (Figure 4.8 B). GluA2 expression was however significantly lower in both EE conditions compared with SH (2-way ANOVA, $p= 0.00162$).

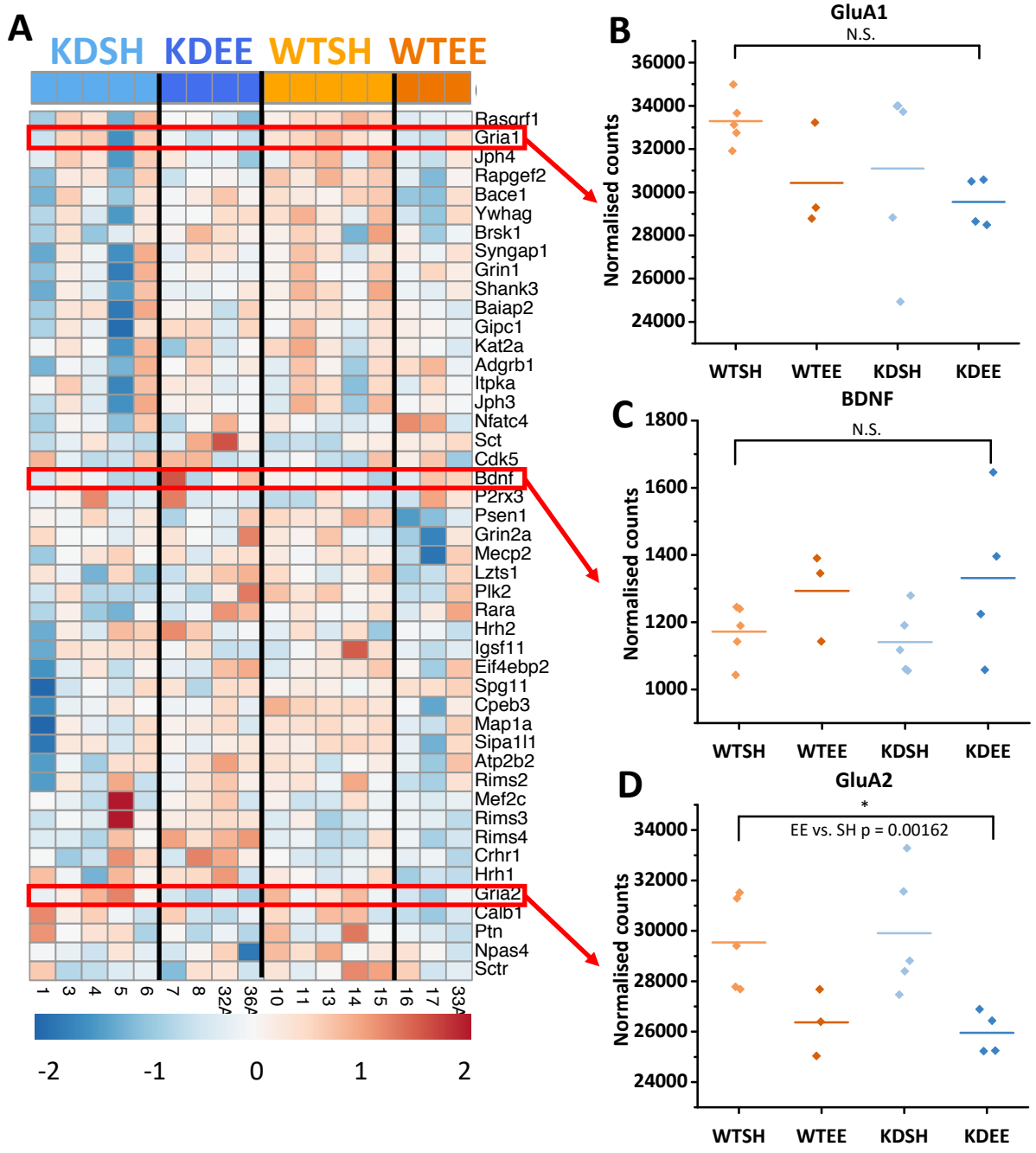

Figure 4.8. Expression summary of genes annotated for synaptic plasticity function show that the majority display no difference in response to EE or MSK1 kinase activity, however GluA2 expression is regulated by EE in an MSK1-independent manner. A) Heatmap of gene expression variation between samples for synaptic plasticity genes from: GO: 0048167 and GO:0048169. Colour scale is based on gene variance calculated as sample expression deviation from average gene expression across all samples for a gene. Red indicates high levels of expression, blue indicates low expression **B, C, D)** Gene expression count plot of samples by group for: **B)** GluA1. **C)** BDNF. **D)** GluA2. GluA2

expression was significantly downregulated in EE conditions compared to SH (2-way ANOVA, p = 0.0162). Lines for each condition in gene count plots represent mean expression for condition.

4.2.6 Expression of IEGs Egr1 and Arc/Arg3.1 are regulated by EE in an MSK1-dependent manner

As previously mentioned, BDNF signalling via the TrkB receptor activates intracellular Ras/Raf, triggers a MAPK cascade activating Mek1/2 which then activate Erk1/2, which then phosphorylates and activates MSK1 allowing CREB phosphorylation and promotion of CREB-mediated transcription including the IEGs Egr1, Arc/Arg3.1 and c-Fos (Figure 1.8). Key genes from this pathway are highlighted in Figure 4.9 A. Upstream of MSk1 signalling, BDNF, TrkB, Mek1/2, Erk1 and MSK1 expression do not appear different between EE groups. However there appears to be a down-regulation of Erk2, p38 MAPK, CREB, Egr1 Arc/Arg3.1 and c-Fos in WTEE mice compared to KDEE mice (Figure 4.9 A). Whilst not all identified as being significantly differentially expressed in the genome-wide differential gene expression analysis, the consistent decrease in expression in WTEE mice of these genes compared to KDEE mice is interesting as it appears to be primarily occurring downstream from MSK1 signalling.

Expression levels of IEGs Egr1 (Figure 4.9 B) and Arc/Arg3.1 (Figure 4.9 C) were significantly affected by an interaction effect of genotype on housing (Egr1, 2-way ANOVA, p = 0.008; Arc/Arg3.1, 2-way ANOVA, p = 0.0289) with expression upregulated in MSK1 KD, and downregulated in WT animals after EE compared to respective genotype SH controls. Egr1 expression was also significantly different between WTEE and KDEE conditions (post-hoc Bonferroni, p = 0.0186). Egr1, identified earlier as being significantly different between both WT and MSK1 KD animals after EE exposure, is a major regulator of synaptic plasticity in response to activity-dependent signaling (Duclot and Kabbaj, 2017). Likewise, Arc/Arg3.1 also has a major role in the activity-dependent regulation of AMPAR receptors at the postsynaptic membrane (Minatohara et al., 2015). Arc/Arg3.1 expression has previously found to be disrupted in MSK1 KD mice, and a role for Arc/Arg3.1 modulating the synaptic transmission deficit in MSK1 KD mice has been proposed (Corrêa et al., 2012). Expression of Egr1 and Arc/Arg3.1 in response to EE therefore appears to be MSK1-dependent. Expression level of

IEG c-Fos (Figure 4.9 D), a marker of neuronal activation such as LTP (Gallo et al., 2018), was however not significantly different between conditions (2-way ANOVA). Lack of c-Fos expression may not be surprising however, as it is typically induced immediately following periods of neuronal activation (Gallo et al., 2018), there may not be a difference in c-Fos induction between samples due to a lack of inducing stimuli such as a behavioural task.

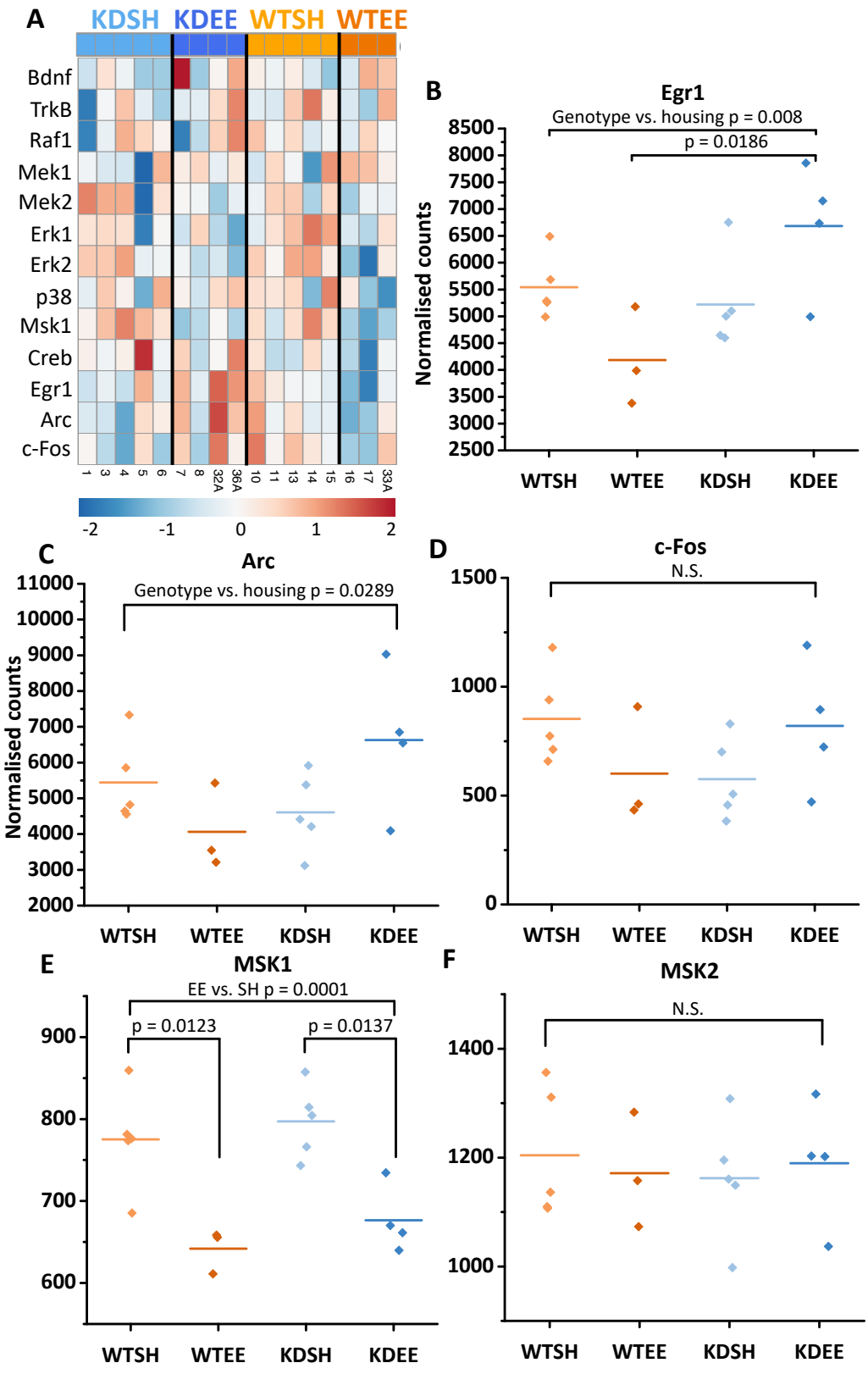

Figure 4.9. Expression summary of genes involved in the BDNF-TrkB-MSK1-CREB signaling pathway, IEGs Egr1, Arc/Arg3.1 and c-Fos and of MSK1 and related family gene MSK2 A) Heatmap of gene expression variation between samples for key genes mediating MSK1-dependent BDNF signaling to

CREB. Colour scale is based on gene variance calculated as sample expression deviation from average gene expression across all samples for a gene. Red indicates high levels of expression, blue indicates low expression **B, C, D, E, F)** Gene expression count plot of samples by group for: **B)** Egr1. Egr1 expression was significantly affected by an interaction effect of genotype on housing (2-way ANOVA, p = 0.008) and also significantly different between WTEE and KDEE conditions (post-hoc Bonferroni, p = 0.0186). **C)** Arc. Arc/Arg3.1 expression was significantly affected by an interaction effect of genotype on housing (2-way ANOVA, p = 0.0289). **D)** c-Fos. **E)** MSK1. MSK1 expression was downregulated in EE conditions vs. SH for both genotypes (EE vs. SH 2-way ANOVA, p = 0.0001), WTSH vs. WTEE (post-hoc Bonferroni, p = 0.0123) and KDSH vs. KDEE (post-hoc Bonferroni, p = 0.0137). **F)** MSK2. Lines for each condition in gene count plots represent the mean.

This downregulation of the IEGs Arc/Arg3.1 and Erg1 (Figure 4.9 B, C), and the apparent downregulation of MAPK signalling (Figure 4.9 A) in WT compared to MSK1 KD mice following EE was surprising. The initial hypothesis explored with this RNAseq experiment predicted that there would be an increase in BDNF-mediated signalling, particularly that of the MAPK pathway, and specifically the IEGs Egr1, which is regulated by CREB activity and Arc/Arg3.1, which is regulated by MSK1 kinase activity (Hunter et al., 2017). BDNF expression was not however seen to be upregulated by 3 months of EE (Figure 4.8 C). This apparent downregulation of the MAPK pathway in WT but not MSK1 KD mice following EE, whilst not predicted by the initial experimental hypothesis, was matched by Egr1 and Arc/Arg3.1 expression differences between WT and MSK1 KD mice. Due to the activity-dependent nature of IEG induction, including Arc/Arg3.1 and Egr1, this may represent a new homeostatic resting state of MAPK pathway and IEG expression that is primed for response to activity. This idea explored further in the discussion section of this chapter.

4.2.7 MSK1 expression appears to be regulated by EE in an MSK1-independent manner and MSK2 expression does not change to compensate for MSK1 kinase inactivation after 3 mths of EE.

Differences downstream of MSK1 signalling in MSK1 KD mice could be due to compensatory upregulation of homologous CREB-kinase gene MSK2 in response to MSK1 activity disruption. Previous studies have looked at the effect of MSK1 deletion on the

expression levels of homologous gene MSK2 which displays CREB kinase activity *in vitro*. In mice homozygous for MSK1 deletion there is no significant compensatory increase in MSK2 expression (Wiggin et al., 2002). MSK1 is also the primary MSK expressed within the CNS, and is believed to be the primary *in vivo* CREB-kinase within neurons in response to neurotrophins (Arthur, 2008). Therefore in MSK1 KD mice, expression levels of MSK1 and MSK2 were looked at. Surprisingly a significant effect of housing was observed on MSK1 expression levels (2-way ANOVA, $p = 0.0001$) and post-hoc testing revealed significant differences between WTSH and WTEE conditions (post-hoc Bonferroni, $p = 0.0123$) and between KDSH and KDEE conditions (post-hoc Bonferroni, $p = 0.0137$) (Figure 4.9 E). MSK1 is downregulated in both Both WT and MSK1 KD indicating that MSK1 downregulation in response to EE occurs independent of MSK1 kinase activity. Expression levels of MSK2 however, were not significantly different between conditions (Figure 4.9 F).

4.3 Discussion:

4.3.1 The kinase activity of MSK1 regulates the majority of the transcriptional response to EE

MSK1 KD mice display a clear deficit in the transcriptional response to EE. Over half of all genes differentially expressed in response to EE reported here were regulated by the kinase function of MSK1 (Figure 4.5). This suggests that MSK1 plays an important role in integrating the response to external stimuli and regulating the transcriptional response to environmental experience. No compensatory upregulation of MSK2 in MSK1 KD mutants (Figure 4.9 F) was observed in response to loss of MSK1 kinase-activity, in concordance with results obtained with MSK1 KO mice (Wiggin et al., 2002). Additionally neither did EE exposure change the expression of MSK2 (Figure 4.9 F). Surprisingly, MSK1 was downregulated following 3 mths of EE from birth (Figure 4.9 E). MSK1 modulation by EE, and lack of expression changes in closely related CREB-kinase MSK2 reinforce prior conclusions that MSK1 is the primary CREB-kinase within the brain (Arthur, 2008) and indicate that MSK1 is necessary for the normal transcriptomic response to EE.

4.3.2 Downregulation of MSK1 in both MSK1 KD and WT mice in response to EE and general downregulation of MAPK pathway signalling in WT mice could indicate a genomic homeostatic response to EE which is impaired in MSK1 KD mice.

The surprising downregulation of MSK1 in response to EE in an MSK1-independent manner after 3 mths of EE (Figure 4.9 E) indicates that a reduction in hippocampal MSK1 activity could be advantageous for the maintenance of EE-induced improvements. BDNF, important for regulating the synaptic plasticity effects of EE and upregulated after acute 3 wk periods of EE (Novkovic et al., 2015) was not observed to be upregulated following 3 mths of EE (Figure 4.8 C). This reduction in BDNF-MAPK-MSK1-mediated signalling was also observed in the synaptic plasticity factors Egr1 and Arc/Arg3.1. Arc/Arg3.1 expression is stimulus- and MSK1-dependent, upregulation occurring in response to BDNF stimulation (Hunter et al., 2017), or during activity-dependent homeostatic plasticity (Corrêa et al., 2012) where it can then regulate synaptic transmission through the synapse-specific endocytosis of AMPAR

receptors (Minatohara et al., 2015) or through the promotion of synaptic function through the stabilisation of F-actin or cofilin at the postsynapse.

Likewise, expression of Egr1 is acutely upregulated following neuronal signalling and the induction of LTP (Chen et al., 2017), where it is plays a key role mediating the induction of synaptic changes (Duclot and Kabbaj, 2017). Egr1 expression, along with that of other IEGs, is controlled by CREB (Section 1.3), which we have previously shown is activated by BDNF in an MSK1-dependent manner (Figure 3.2, Daumas et al., 2017).

To put these results into further context, as mentioned in Figure 4.1, the same mice used for RNA extraction and sequencing were used for behavioural and electrophysiological experiments by other experimenters within the Frenguelli lab (Privitera et al., 2020). This was done to comprehensively evaluate the effects of MSK1 kinase inactivation on the response to 3 months of EE. When tested, the WTEE mice discussed in this chapter displayed an increased dynamic range of synaptic plasticity at SC-CA1 synapses (displaying increased LTP facilitation in response to TBS, and increased magnitude of depression after LTD induction by LFS) compared to WTSH and KDSH controls (Privitera et al., 2020). These WTEE mice also displayed enhanced spatial working and reference memory (tested by spontaneous alternation and MWM probe test respectively) (Privitera et al., 2020). This is in line with the previously observed effects of EE, on improving LTP facilitation (Ohline and Abraham, 2019) and spatial memory (Table 1.1).

MSK1 KD mice housed in EE for 3 months however, displayed no enhancement to LTP or LTD compared to WTEE mice (Privitera et al., 2020). MSK1 KD mice also did not demonstrate the EE-mediated improvement in spatial reference and working memory as WTEE mice did. Furthermore, Privitera et al. (2020) tested cognitive flexibility in these mice using a platform location reversal task, where mice would need to re-learn the position of a platform essentially overwriting or unlearning the previous platform location before learning the new one. WTEE mice learned the location of the new platform significantly faster than WTSH, KDSH and KDEE mice, which all performed comparably (Privitera et al., 2020). This demonstrates a necessity for MSK1 kinase function in mediating the beneficial effects of EE on spatial reference and working memory, on cognitive flexibility and in the bi-directional

expansion of activity-dependent synaptic transmission strength changes (Privitera et al., 2020).

Similar to the RNAseq study presented in this chapter which demonstrated minimal transcriptional differences between WTSH and KDSH mice (Figure 4.5), no significant difference was seen between WTSH and KDSH control mice in spatial memory and electrophysiology plasticity experiments (Privitera et al., 2020). Interestingly, the simultaneous enhancement of both LTP and LTD following EE, effectively increasing the dynamic range of stimulus-induced Hebbian synaptic plasticity changes appears to have been reported for the first time by Privitera et al. (2020), likely due to a general lack of testing for both LTD in addition to LTP in other studies, rather than an observation of a lack of change in both concurrently (Ohline and Abraham, 2019).

EE could therefore increase the dynamic range of IEG signalling, by keeping expression levels of Arc/Arg3.1 and Egr1 low, allowing subsequent stimulus-dependent upregulation of IEG expression to have a much larger fold-change effect on IEG signalling. In this way EE could prime neurons to respond to novel stimuli by enhancing the contrast between non-potentiated and potentiated synaptic signalling, whilst simultaneously preserving an expanded and enhanced hippocampal environment. In support of this, despite a reduction in Egr1 expression in WT mice after EE, expression of synaptic plasticity genes was unchanged (Figure 4.8 A), even when comparatively high levels of Egr1 expression were detected in MSK1 KD mice (Figure 4.9 B). Additionally, a recent TRAP-seq experiment looking exclusively at excitatory cells within the hippocampus found that after forskolin-simulated LTP induction, sequenced transcripts from CA1 and CA3 cells 2 hours-post LTP induction were significantly enriched for the terms cell adhesion, extracellular matrix interactions and MAP kinase signalling (Chen et al., 2017). This highlights the importance of cellular remodelling for the efficacy of synaptic plasticity, and is concordant with MSK1-dependent GO terms identified in Figure 4.7 C. Additionally, Chen *et al.* (2017) found Egr1 to be one of the most significantly upregulated transcripts observed in response to LTP stimulation.

4.3.3 Disruption of MSK1 signalling impairs induction of primary cilia and extracellular remodelling genes in response to EE, potentially disrupting angiogenesis and neurogenesis

MSK1-KD mice fail to alter expression of extracellular structural-, cilium-, and microtubule-related pathways within the hippocampus (Figure 4.7 C). The significant enrichment of a large number of cilia related GOTerms within MSK1-dependent EE-induced genes was unexpected. Most neurons within the CNS possess a primary cilium, an outgrowth from the membrane of the neuronal soma that is supported by a specialised microtubule known as an axoneme (Lepanto et al., 2016). The primary cilium plays an important role in neuronal development and post-natal hippocampal neurogenesis (Lepanto et al., 2016).

Dysregulation of the primary cilium in adult-born hippocampal granule cells disrupts glutamatergic synaptogenesis and dendrite refinement (Kumamoto et al., 2012). Additionally, within mature neurons, the primary cilium has been seen to regulate dendritic branching and extension in response to extracellular cues (Lepanto et al., 2016) and disruption of primary cilia in mature hippocampal dentate granule cells impairs context-dependent fear-related memory and increases LTP at mossy fibre-CA3 synapses (Rhee et al., 2016). The primary cilia are therefore capable of modulating both neurogenesis and dendritic complexity, both processes enhanced by exposure to EE (Faherty et al., 2003, Kempermann, 2019, Lopez-Atalaya et al., 2011). MSK1-dependent regulation of the primary cilia following EE may therefore affect the ability of new neurons to integrate correctly into hippocampal circuits, or affect the connectivity of these circuits themselves.

EE is also associated with the expansion of the cortex and hippocampus (Eckert and Abraham, 2013) and promotion of angiogenesis (van Praag et al., 2000, Sale et al., 2014) as expanded brain regions and new neurons require blood supply. Genes belonging to “Vasculature development” and “cellular response to growth factor” terms were highlighted as being differentially expressed in both WT and MSK1 KD mice here after EE exposure (Figure 4.7 B). However, correct regulation of extracellular matrix remodelling is necessary for angiogenesis and cell migration to occur correctly (Neve et al., 2014) and MSK1 KD mice showed transcriptional deficits in both “extracellular matrix organisation” and “extracellular

structure organisation" in response to EE. Perhaps MSK1 complements EE-induced blood vessel growth and development by regulating extracellular remodelling? In support of this, expression of Spry4 was downregulated in in WT mice after EE when compared with MSK1 KD mice (Figure 4.6 A). A reduction in Spry4 function has been shown to promote survival in CA1 and CA3 neurons (Thongrong et al., 2016) and is associated with the promotion of axonal outgrowth (Hausott et al., 2012) and angiogenesis (Taniguchi et al., 2009).

Additionally, as a negative mediator of ras function following TrkA stimulation by NGF (Alsina et al., 2012), Spry4 downregulation could increase NGF signalling efficacy within the hippocampus. NGF signalling is strongly associated with angiogenesis within the brain (Calzà et al., 2001, Moser et al., 2004, Hansen-Algenstaedt et al., 2006). NGF signalling has also been shown to be necessary for LTP induction at PP-DG synapses and for spatial memory (Conner et al., 2009). Spry4 could then feasibly, through its downregulation, remove a blockade upon this form of NGF-TrkA-MAPK signalling, thereby facilitating plasticity within the hippocampus. This may encourage activation of the MAPK pathway by other neurotrophins such as NGF via TrkA.

MSK1-dependent regulation of Spry4 expression, extracellular remodelling processes and primary cilia in response to EE could work in concert with MSK1-independent angiogenic and cellular growth factor pathways to underpin the positive structural changes observed after EE through blood vessel growth and neurogenesis. Inability to activate of some but not all of these pathways in MSK1 KD mice may also explain observed deficits in the response of MSK1 KD mice exposed to EE. Conducting blood vessel analysis of MSK1 KD mice and WT mice after 3 months of EE would therefore be interesting to evaluate this theory. This could be achieved using cardiac perfusion with paraformaldehyde and subsequent clearing of brain tissue (eg. Following the CLARITY protocol) followed by staining for blood vessel endothelial cell-specific factors such as lectin (Di Giovanna et al., 2018).

4.3.4 Homeostatic regulation of Egr1, Arc/Arg3.1 and MAPK signalling may underlie EE mediated improvements in hippocampal circuits.

MSK1-dependent downregulation of Egr1, an IEG that is acutely upregulated in response to synaptic plasticity induction (Duclot and Kabbaj, 2017), and Spry4, a MAPK inhibitor that can inhibit neurite outgrowth in response to neurotrophin activation (Alsina et al., 2012) led to an investigation of keys genes involved in MAPK-MSK1 signalling. In keeping with the "MAPK signalling" GOTerms identified in both WT and MSK1 KD animals following EE exposure (Figure 4.7 B), BDNF-mediated MAPK signalling upstream of MSK1 did not appear to be different between the two enriched conditions (Figure 4.9 A). However, an apparent downregulation of genes downstream from MSK1 signalling included the MSK1 target CREB was observed in WT but not MSK1 KD animals following EE conditions (Figure 4.9 A). The synaptic plasticity genes Egr1 (Figure 4.9 B) and Arc/3.1Arg (Figure 4.9 C) were significantly downregulated in WT mice following EE compared with MSK1 KD.

WT mice therefore downregulate Egr1, Arc and Spry4 in a MSK1-dependent manner following 3 mth exposure to EE. This downregulation of Egr1 and Arc/Arg3.1 was surprising, as mice exposed to EE consistently present improvements to hippocampal-dependent spatial memory (Eckert and Abraham, 2013; Table 1.1), and the cellular correlate for memory formation is thought to be activity-dependent changes in synaptic strength (Takeuchi et al., 2014, Whitlock et al., 2006). Indeed, genes annotated with the gene ontology biological function synaptic plasticity displayed little overall difference in MSK1-dependent regulation after EE (Figure 4.8), despite MSK1-dependent expression differences in the synaptic plasticity genes Arc/Arg3.1 and Erg1. Western blotting to test protein expression levels of Egr1 and Arc/Arg3.1 was therefore undergone to confirm the transcriptomic changes reported here. Using contemporaneous tissue of MSK1 KD and WT mice from SH and following 3 months EE, another member of the Frenguelli lab observed the same expression changes across all samples (Privitera et al., 2020), confirming that these transcriptomic results are translatable to the protein level at least for Egr1 and Arc/Arg3.1.

One way to explain this unexpected result is to re-evaluate what activity-dependent modifications have taken place following EE. A recent review looked at the effects of EE

duration on common measures of synaptic plasticity, LTP and LTD and synaptic transmission changes within the hippocampus (Ohline and Abraham, 2019). Looking at a broad range of EE durations across a variety of studies, Ohline and Abraham (2019) observed that the excitability of CA1 and DG cells increases during short periods of EE exposure (3-5 wks) however during longer periods of enrichment (8-12 wks) little difference is observed. Additionally facilitation of LTP at CA1 neurons is generally observed to occur following acute periods (2–6 wks) of EE, however after 8-12 wks of EE, this form of facilitation was often observed to take the form of increased LTP duration, rather than an increase in initial induction as observed at 2-6 wks of EE (Ohline and Abraham, 2019). This would indicate that longer periods of EE favour increased L-LTP induction, which is dependent on intracellular signalling pathways, *de novo* transcription and translation, rather than modulating E-LTP, which is associated more with short-term postsynaptic receptor trafficking and post-translational modifications.

This differential facilitation of LTP by shorter (2-6 wks) and longer (8-12 wks) durations of EE (Ohline and Abraham, 2019), indicates that the hippocampus adapts to enrichment exposure, first increasing excitability in response to activity-dependent stimulation which could increase LTP induction in the short-term (2-6 wks) and gradually scaling down cell excitability through a form of homeostatic adaptation whilst maintaining facilitation of LTP, potentially through another mechanism. This homeostatic adaptation to EE has been observed in real-time through *in vivo* field EPSP (fEPSP) recordings made in freely-moving rats: An initial increase in DG cell excitability was observed over 10-14 days post-EE exposure, followed by a gradual decline in fEPSP amplitude during subsequent EE (Irvine et al., 2006).

The downregulation of MSK1 in both WT and MSK1 mice in response to EE, and the MSK1-dependent downregulation of genes including Egr1, Spry4 and Arc/Arg3.1 observed here could be responsible for orchestrating a general homeostatic decrease in cell excitability and dynamic modulation of plasticity after chronic (3 mth) EE exposure. Downregulation of MAPK pathway targets Egr1 and Arc/Arg3.1 may serve to stabilise changes at synapses not currently undergoing a plasticity event, where their expression can be rapidly upregulated in response to plasticity inducing stimuli. This homeostatic regulation could be important in preserving network level improvements in connectivity brought about by long-lasting EE.

Alternatively, upon induction of a plasticity event by the appropriate stimuli, provided in the form of LTP or LTD induction, greater synaptic transmission changes are observed in WT mice following this 3 month period of EE, but MSK1 KD mice (Privitera et al., 2020) implicating this homeostatic downscaling of MSK1, MAPK signalling and IEG expression in facilitating these increased synaptic changes.

4.3.5 Exposure to EE from birth for 3 months appears to be too long of a period of EE to observe acute changes in synaptic plasticity gene expression

The above data highlight a role for MSK1 in mediating the effects of EE after chronic (3 months) life-long exposure. Upregulation of BDNF and plasticity changes have been associated with shorter timepoints of EE (Novkovic et al., 2015) and changes in cell excitability within hippocampal CA1 neurons have been consistently observed after 4-6 wks of EE (Ohline and Abraham, 2019). One complication with the EE paradigm tested here is that this EE housing paradigm was conducted from birth. EE is often described as a non-pharmacological treatment to ameliorate the effects of age-related cognitive decline (Sampedro-Piquero and Begega, 2017) or pathological conditions within the brain (de la Tremblaye et al., 2019). Within a hypothetical human subject, the voluntary application of EE would then typically be after reaching adulthood preferably as early as possible. In order to understand how MSK1 exerts its effects on hippocampal signaling, and the effect of EE when applied as an intervention and not as a life-long housing paradigm, a new round of experimentation was designed. Mice were kept in SH and transferred to enrichment for more acute time periods: 1 week and 5 weeks of EE, in an attempt to capture an earlier time point of dynamic change occurring in response to enrichment that is MSK1-dependent.

Other transcriptomic experiments that have looked at the effects of EE on gene expression have also looked at signalling relevant to CREB-mediated gene expression: Mice heterozygous for a knock-out of CREB-binding protein (CBP), a histone acetyl-transferase that acts as a regulator of CREB transcription factor activity and is recruited by CREB Ser133 phosphorylation(Chrivia et al., 1993, Mayr et al., 2001), have demonstrated little basal difference in transcriptional profile under standard housing conditions, but display an impaired transcriptional response to 2 weeks of EE (Lopez-Atalaya et al., 2011). These mice

display an impairment in contextual fear conditioning and spatial learning and memory that is partially recovered when exposed to 2 weeks of EE (Lopez-Atalaya et al., 2011). Key GO Terms upregulated in WT but not $Cbp^{-/+}$ mice following 2 weeks of EE in the study by Lopez-Atalaya et al. (2011) included "Neurogenesis and neuron differentiation, Ion transport and homeostasis and Synaptic transmission". This is interesting within the context of the RNAseq experiment presented within this chapter for two key reasons:

Firstly, the majority of the transcriptomic response to 2 weeks of EE in $Cbp^{-/+}$ mice was attenuated (Lopez-Atalaya et al., 2011), and since Cbp is involved in CREB-mediated transcription following recruitment via CREB Ser133 phosphorylation, this could be the result of a similar disruption of the signalling pathway impaired in MSK1 KD mice. This may explain why despite seeing MAPK activity decrease in WTEE mice, and no difference in BDNF expression following EE, a lasting change in gene expression response to EE mediated by MSK1 can be observed. Lopez-Atalaya et al. (2011) observed a significant increase in histone acetylation of histone H2B and H3 at key CREB promotor containing genes (DCX and nestin, important for neurogenesis and CREB-regulated (Herold et al., 2011, Merz et al., 2011, McPherson and Lawrence, 2007)) following 2 week EE that were not present in $Cbp^{-/+}$ mice. Cbp functions as a histone acetyl-transferase, and directly binds to CREB following activation, which may serve to target Cbp to CREB transcriptional targets following activation. This means that lasting epigenetic modifications based on previous experience of the mouse can modulate future gene transcription efficacy. Testing histone acetylation of the genes Egr1, Arc/Arg3.1 or other plasticity-related factors in MSK1 KD mice before and after EE using chromatin immunoprecipitation (ChIpSeq) would validate any role the preceding hypothesis may play in mediating the effect of previous environmental exposure on present transcriptional expression.

Secondly, this indicates that shorter, more acute periods of EE appear to induce different transcriptomic changes more oriented to alterations in synaptic transmission (Lopez-Atalaya et al., 2011) compared with 3 months of EE as presented here in Figure 4.7 (B and C) which seemed primarily involved in regulation of the MAPK pathway, extracellular matrix and blood vessel formation.

To summarise this chapter, the kinase activity of MSK1 seems to plays a role in regulating over half of 3 month EE-induced gene transcription. Functional characterisation of MSK1-regulated 3 month EE-induced genes indicated an enrichment for extracellular matrix organisation microtubules and clilium function, which were related back to neuronal function and signalling and synaptic organisation. The synaptic plasticity immediate early genes Egr1 and Arc/Arg3.1 were seen to be regulated in an MSK1-dependent manner following EE. Whereas, GluR2 expression, a subunit of the AMPA receptor that control Ca^{2+} permeability, and MSK1 itself were seen to decrease following EE independent of MSK1 function. This indicates that MSK1 regulates gene expression relevant to synaptic function in response to EE and can perhaps prime transcriptomic responses to EE by modulating MAPK pathway expression levels. Whether MSK1-dependent changes occurs via CREB and histone H3 has not been directly investigated. Indeed, whilst regulation of CREB and histone H3 via phosphorylation in response to MAPK activation by BDNF is an attractive explanation, due to the overlap between CREB and BDNF mutant phenotypes, phosphorylation of other transcription factor targets by MSK1, or even posttranslational modification of histones cannot be excluded. Phosphorylation assays of CREB-related proteins such as CREM, ICER or CBP could further elucidate the relationship of CREB to MSK1. Likewise CHIPseq assays in MSK1 KD mice could highlight changes in transcription factor or histone binding to DNA as a result of MSK1 activation.

The RNAseq experiment covered in this chapter was published as part of the paper by Privitera et al. (2020).

Chapter 5: Electrophysiological investigation of the kinase activity of MSK1 in glutamatergic synaptic transmission within the hippocampus

5.1 Introduction

As previously mentioned in Section 1.4, EE has been shown to improve learning in hippocampal-dependent memory tasks (Ohline and Abraham, 2019, Nithianantharajah and Hannan, 2006). Changes in synaptic connectivity are thought to underlie the benefits of EE (Nithianantharajah et al., 2004, McDonald et al., 2018), however the underlying molecular mechanisms behind EE-induced improvement are at present poorly understood (Sale et al., 2014, Kelly and Hannan, 2019). Exposure to EE can increase CA1 pyramidal cell dendritic spine density (Corrêa et al., 2012, Malik and Chattarji, 2012) and dendritic complexity (Faherty et al., 2003, Beauquis et al., 2010). EE also modulates synaptic plasticity, generally being seen to facilitate LTP at CA1 neurons (Ohline and Abraham, 2019). An increase in E-LTP has been observed following shorter (2-6 wks) of EE: 2 wks of EE in 8-9wk old mice (Buschler and Manahan-Vaughan, 2012), 3wks of EE in 15-23wk old mice (Huang et al., 2006), 5 wks of EE in 8-10 wk old rats (Artola et al., 2006) and 5 wks of EE in 8-9 wk old rats (Malik and Chattarji, 2012). An increase in L-LTP has also been observed following EE: 3-4 wks of EE in 6-7 wk old mice (Novkovic et al., 2015) and in work from our lab following 12 wks of EE from birth (Privitera et al., 2020); but not in some experiements: 2 wks of EE in 8-9wk old mice (Buschler and Manahan-Vaughan, 2012). On the opposite end of the spectrum of Hebbian plasticity changes, Artola et al. (2006) also observed significantly greater LFS-induced LTD following 5 wks of EE in 8-10 wk old rats. Privitera et al. (2020) have also observed an enhancement of LTD in mice following 12 wks of EE from birth using a more conventional LFS induction protocol for LTD (LFS from Artola et al. (2006): 2 x 15m 1Hz stimulation; from Privitera et al. (2020) 15m 1Hz stimulation).

EE has been seen to alter the requirements for LTP induction also: In 12 wk old mice following a 1xburst HFS stimulation protocol, Duffy et al. (2001) observed a significant facilitation of E-LTP after housing in EE for 8 wks. In addition, in aged (21 month old) rats, 3 weeks of EE was seen to convert failed LTP to robust E-LTP following 1x burst HFS, and failed

LTD following 15m LFS to LTD (Stein et al., 2016), indicating that even short periods of EE can help ameliorate age-related declines in synaptic plasticity.

Under basal SH conditions, the kinase activity of MSK1 is not implicated in the induction of LTP via theta-burst stimulation (TBS), or high frequency stimulation (HFS), nor the induction of mGluR-dependent LTD (Daumas et al., 2017) indicating mice are still capable of performing Hebbian plasticity events. However, homeostatic scaling of GluA1 and Arc/Arg3.1 during activity-deprivation is impaired within MSK1 KD mice, as is the EE-induced upregulation of mEPSCs (Corrêa et al., 2012). Acute (3 – 4 wks) periods of EE result in an increase in hippocampal BDNF expression (Novkovic et al., 2015). BDNF is thought to mediate homeostatic synaptic scaling during activity deprivation (Turrigiano, 2012) and homeostatic plasticity changes induced by EE (Cowansage et al., 2010). Activity-dependent release of BDNF during EE appears to derive at least in part from MSK1-dependent astroglial BDNF exocytosis (Lalo et al., 2018), and MSK1 kinase activity is necessary for an EE-mediated increase in glutamatergic transmission (Lalo et al., 2018). Taken together, the kinase activity of MSK1 could be positioned as an important regulator of activity-dependent homeostatic up- and down-scaling of glutamatergic transmission in response to EE-mediated changes in BDNF expression.

The observation that the kinase function of MSK1 regulates over half of transcription in response to 3 months of EE from birth including the IEGs Egr1 and Arc/Arg3.1 (Chapter 4) - presumably through its ability to phosphorylate transcriptional regulators CREB (Chapter 3, Daumas et al., 2017) and histone H3 (Soloaga et al., 2003, Reyskens and Arthur, 2016, Hunter et al., 2017) – along with corresponding behavioural and synaptic plasticity improvements (Privitera et al., 2020) highlighted a key role for MSK1 kinase activity in mediated EE-induced improvements.

Given this role for MSK1 in regulating the IEG-inducing transcription factors CREB- and histone H3 in response to BDNF signalling, lack of change in both BDNF and the expression of large numbers of synaptic plasticity genes after 3 months of EE (Figure 4.5) was unexpected. An enrichment of many extracellular structural regulation gene ontologies was however observed in the DEGs from WT mice but not MSK1 KD after 3 months EE. It was therefore

hypothesised that the RNAseq experiment captured late-stage effects of EE, potentially missing interesting earlier EE-induced BDNF-mediated synaptic transmission changes that could be MSK1 regulated. As discussed in the preceding paragraphs of this chapter, EE-induced synaptic plasticity changes have been observed as early as 2 – 5 wks of EE, and MSK1 KO mice fail to enhance dendritic complexity following 5 wks of EE suggesting that electrophysiological changes occur on such a timescale. To test this, more acute time periods of EE lasting 1 week or 5 weeks were investigated electrophysiologically and with dendrite reconstruction to ascertain the effect of MSK1 kinase inactivation on glutamatergic synaptic transmission differences following acute EE timepoints within the hippocampus. Concurrent RT-qPCR analyses for key genes identified in the RNAseq screen were planned, and during electrophysiology experiments tissue was split: one hemisphere used for slice prep, and one homogenised in Trizol, flash-forzen and saved for RNA extraction. However, unfortunately due to time constraints, RT-qPCR experiments could not be conducted, however as the tissue was saved, this is to be followed up within the lab.

Additionally, the MSK1-dependent regulation of GluA1 and Arc/Arg3.1 expression during synaptic scaling in response to activity-deprivation (Corrêa et al., 2012) raised questions about the proportion of AMPARs containing GluA2 subunits within MSK1 KD mice. MSK1 KD cultured hippocampal neurons display increased surface expression of GluA1 compared to WT neurons, and do not upregulate GluA2 expression (Corrêa et al., 2012) however it is not clear how well these expression differences translate to slices or the *in vivo* brain. Regardless, MSK1 does seem to have a role in the activity-dependent regulation of GluA1 surface expression without affecting GluA2. An increase in GluA1 subunit expression, without a corresponding increase in GluA2 could lead to presentation of GluA2-lacking or Ca^{2+} permeable AMPARs (CP-AMPARs). Investigation of the Ca^{2+} permeability of AMPARs at CA3-CA1 synapses was therefore also conducted by measuring the rectification properties of CA1 pyramidal cells in whole-cell voltage-clamp.

5.2 Results

5.2.1 Experimental set-up

Male mice, 10 – 22 wks old at time of rehousing, were split into 4 experimental conditions for each timepoint of EE assessed: 1 wk and 5 wks, resulting in 8 experimental conditions split between the two groups (Table 5.1). While SH groups were recorded in parallel with EE conditions, experiments were conducted in two batches, one for each EE timepoint. All mice were therefore between the ages of 12 – 24 wks (3-6 months, adult age) at the time of tissue harvest for electrophysiology experiments. Acutely-prepared hippocampal brain slices were used to assess electrophysiological and morphological properties of CA1 neurons *in vitro*. Schaffer collateral (SC) fibres were stimulated using a conical bipolar electrode placed in the stratum radiatum and evoked EPSCs recorded from whole-cell patch-clamped CA1 pyramidal neurons. CA1 neurons were identified visually under 40X magnification by their location within stratum pyramidale and their prominent apical dendrite. Stimulation strength for rectification index (RI) and paired-pulse ratio (PPR) experiments were determined on a per mouse basis due to previous observation of basal synaptic transmission differences in MSK1 KD mice (Corrêa et al., 2012) and experiments being conducted blind to mouse housing and genotype. During some experiments, the patch pipette solution included biocytin to allow filling and subsequent staining of recorded cells for later morphological reconstruction (Section 5.2.6).

1 wk EE		
Condition	Genotype	Housing Condition
WTSH	WT	SH
WTEE	WT	EE
KDSH	MSK1 KD	SH
KDEE	MSK1 KD	EE

5 wks EE		
Condition	Genotype	Housing Condition
WTSH	WT	SH
WTEE	WT	EE
KDSH	MSK1 KD	SH
KDEE	MSK1 KD	EE

Table 5.1: Experimental condition summary for electrophysiological and morphological investigation of acute periods of EE on MSK1 kinase function. Whether a condition belongs to either 1 wk or 5 wks EE experimental group is clearly indicated below.

5.2.2 Environmental enrichment causes a decrease in AMPAR calcium permeability within CA1 neurons, independent of MSK1 kinase function.

Cultured MSK1 KD neurons express significantly more cell surface GluA1 than WT mice, without a corresponding increase in GluA2, which appears to occlude their ability to upscale AMPAR expression at synapses in response to activity-deprivation (Corrêa et al., 2012). This overexpression of GluA1 seemed to be expressed functionally within AMPARs at the postsynapse, due to a corresponding increase in MSK1 KD mEPSC amplitude (Corrêa et al., 2012). Increased GluA1 expression without change in GluA2 could disrupt the normal proportion of GluA1/GluA2 subunits comprising AMPARs in MSK1 KD mice. This could result in an increase in the proportion of GluA2 lacking Ca^{2+}-permeable AMPARs (CP-AMPARs) present at synapses, increasing Ca^{2+} conductance. This could then affect synaptic plasticity induction as discussed in section 1.2.3 (pgs 29-30).

To test whether MSK1 kinase activity affects the Ca^{2+} permeability of AMPAR receptors in CA1 neurons, the amplitude of evoked EPSCs at two holding potentials of the cell (-70 mV and +40 mV) were compared. Comparison of these currents allows calculation of the RI, which displays an approximately linear relationship in GluA2 subunit-containing AMPA receptors (Pellegrini-Giampietro, 2003). In contrast, AMPA receptors lacking GluA2 are predominantly comprised of GluA1 subunits which display a non-linear relationship, as the entry of cations (Na^+ and Ca^{2+}) is affected by the voltage-dependent block of AMPA receptors by intracellular polyamines such as spermine (Isaac et al., 2007, Isa et al., 1995, Bowie and Mayer, 1995). This means that CP-AMPAR conductance is blocked by intracellular polyamines at depolarised (positive) neuron potentials, but not at negative potentials. Calculation and comparison of the RI therefore allows subunit composition elucidation of AMPA receptors within MSK1 KD mice.

A significant increase in rectification index was observed in both WT and MSK1 KD mice in response to 1 wk (EE vs.SH: $F(1,100) = 7.53$; $p = 0.0072$), and 5 wks EE (EE vs. SH: $F(1,59) = 8.38$; $p = 0.0053$) as shown in Figure 5.1 A and B. Representative traces for each condition are displayed below in Figure 5.1 C and D, and the current/voltage relationship for neurons from each condition for both 1 wk and 5 wks EE experiments are also displayed in

Figure 5.1 E and F. This indicates that the proportion of CP-AMPARs to Ca^{2+}-impermeable AMPARs (GluA2 subunit containing) is decreased at SC/CA1 synapses occurs after short-term 1 wk, and 5 wks, EE exposure independent of MSK1 kinase activity. This could indicate that there is a reduction in CP-AMPAR expression following both EE timepoints, or that there is an increase in Ca^{2+}-impermeable AMPAR expression.

This result was the opposite of what would be predicted following the observation of GluA2 expression downregulation following 3 months of EE seen in Figure 4.8 D. With less GluA2 but not GluA1 expression, it could be reasonably supposed that there would be more GluA2-lacking AMPAR receptors assembled from this mix of subunits. However protein level data from contemporaneous mice to those used for the sequencing experiments in Chapter 4 show that the protein level expression of GluA2 appears to be MSK1-dependent, with increased GluA2 protein expression in WTEE mice compared to WTSH mice (control 3 month EE response), and decreased GluA2 protein expression in KDEE mice compared to KDSH mice (MSK1 KD 3 month EE response) (Privitera et al., 2020). The total protein level expression of GluA2 in WT mice before and after 3 months of EE appears to match the pattern of RI results in Figure 5.1 A + B, however, the expression pattern in MSK1 KD mice was the opposite. Perhaps in a similar cohort of mice as that used in the RNAseq study in chapter 4 (3 months EE from birth), MSK1-dependent differences in RI would be observed. Additionally, disruption of MSK1 kinase activity has previously been seen to significantly increase GluA1, but not GluA2 expression at the cell surface in cultured hippocampal neurons (Corrêa et al., 2012). Here, under neither SH, nor EE conditions, did MSK1 KD mice seem to express any greater level of CP-AMPARs than WT mice at the postsynapse of CA1 pyramidal neurons (Figure 5.1 A + B). This discrepancy could be a result of the expression systems seen here (cultures as in Corrêa et al. (2012) and acute hippocampal slices here).

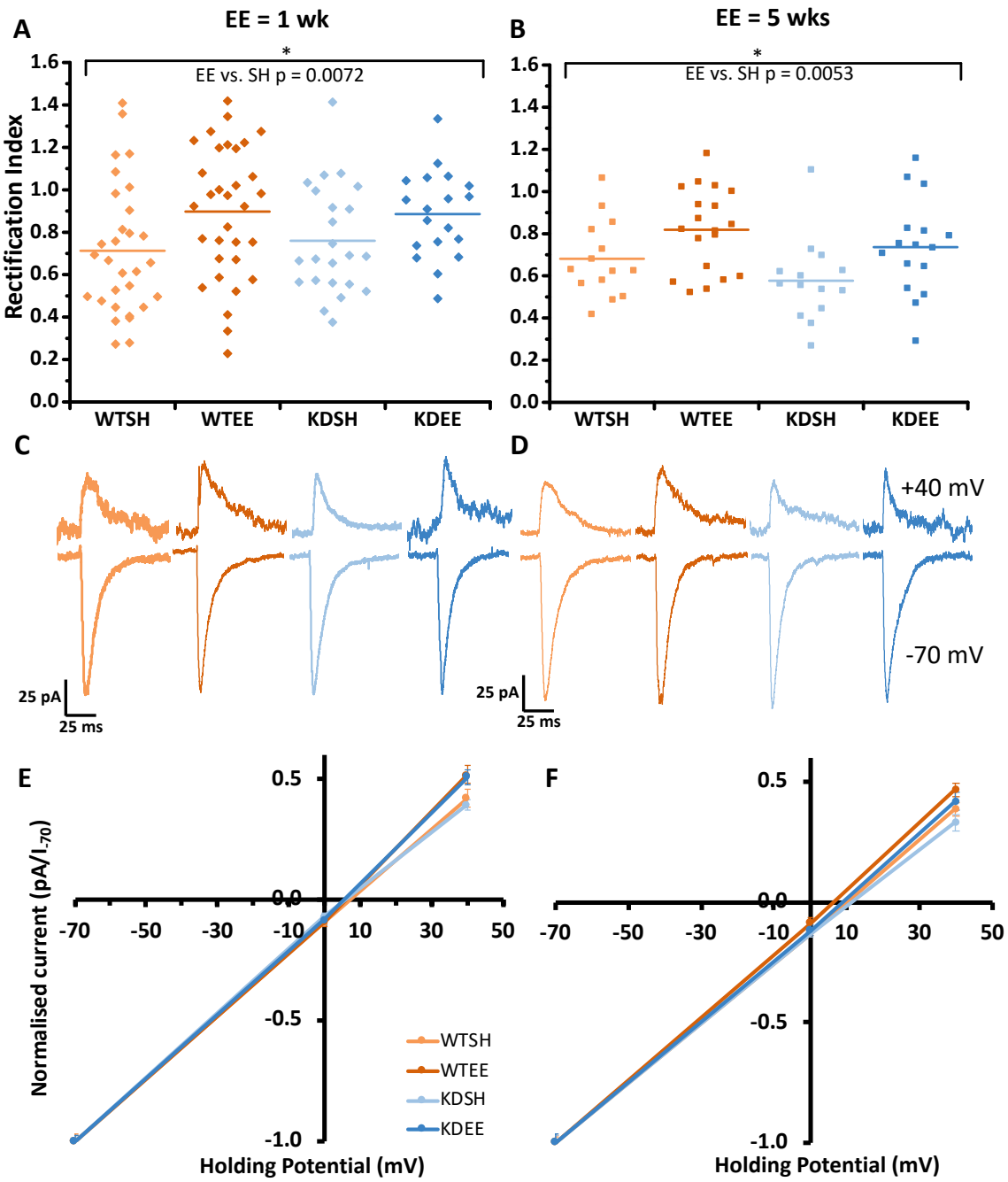

Figure 5.1. Rectification at Schaffer collateral/CA1 pyramidal neuron synapses is affected by both 1 wk and 5wks of EE independent of genotype. A +B) 1 wk (A) of EE causes an increase in rectification index independent of genotype (EE vs.SH: $F(1,100) = 7.53$; $p = 0.0072$) as well as 5 wks of EE (EE vs. SH: $F(1,59) = 8.38$; $p = 0.0053$). n for each group: 1 wk: WTSH = 30; WTEE = 32; KDSH = 23; KDEE = 19; 5wks: WTSH = 15; WTEE = 19; KDSH = 14; KDEE = 16. Horizontal lines indicates mean of data points. **C + D)** Representative average trace of currents obtained at -70mV and +40mV for 1 wk EE (C) and 5 wks (D) experimental conditions. **E + F)** Current response in CA1 neurons at different holding potentials (mV) normalised to current response at -70mV. Stimulation strength was normalised to each neuron such that a 100pA response was obtained at -70mV and that stimulation strength was maintained

throughout the rectification experiment. Normalised current response is shown for 1 wk EE experiment (E) and 5 wk EE experiment (F). Error bars in E and F are +/- SEM.

5.2.3 Whole-cell patch-clamp recordings of input-output responses at SC/CA1 pyramidal neuron synapses do not appear to be different between MSK1 KD nor WT conditions at either the 1 wk or 5 wk EE timepoints.

Decreased basal glutamatergic synaptic transmission at SC/CA1 synapses, as measured by fEPSP input-output measurements, has been observed in MSK1 KD mice under standard housing conditions (Daumas et al., 2017, Privitera et al., 2020). Conversely, AMPAR-mediated quantal amplitude at MSK1 KD SC-CA1 synapses (as measured by mEPSC amplitude) appears to be larger than WT animals (Corrêa et al., 2012). These basal differences between MSK1 KD mice and WT mice indicate that MSK1 kinase activity could play a role in modulating AMPAR activity at the postsynaptic membrane, whether by affecting expression directly, subunit composition, localization of AMPARs or pre-synaptic release probability. EE itself can affect synaptic presentation of GluA1 (Ohline and Abraham, 2019) and so the effect of EE on synaptic transmission was assessed between both WT and MSK1 KD mice after 1 wk and 5wks of EE, in order to ascertain any role played by MSK1 in mediating EE-induced changes.

Response to stimulation was very variable across both genotypes as can be seen in representative traces for each condition for 1 wk (Figure 5.2 A) and 5 wks (Figure 5.2 B) EE groups, peak amplitude was contaminated for some peaks by a second slower component especially at higher stimulation strengths. The initial slope of excitatory postsynaptic currents (EPSCs) averaged from 5 traces was therefore calculated from between 10 – 45 % of the EPSC peak. In Figure 5.2 C it initially appeared that there were genotype and housing-dependent differences. However the response from SH mice in both 1 wk and 5 wk EE groups was very different, with KDSH seeming to display much greater basal synaptic transmission than WTSH mice in the 1 wk EE groups (Figure 5.2 C), but with WTSH appearing to have greater transmission than KDSH in the 5 wk EE groups (Figure 5.2 D). Without getting consistent control SH group responses between 1 wk and 5 wk EE exps, drawing comparisons within groups seemed invalid. The heterogeneity of responses between slices could have been due to variable electrode placement as this was placed based on field of view within the slice and

cells only rejected based on input-output properties if it was not possible to elicit a 100pA response at any stimulation strength between 20-300μA. Due to this heterogeneity, the slope of current response to stimulation was therefore normalised to the current response at 100μA stimulation.

Consistent scaling of current response to input-stimulation was observed. However, overall, very little difference was seen between genotypes or housing conditions after both 1 wk (Figure 5.2 E) or 5 wks of EE (Figure 5.2 F) at any stimulation strength (2-way ANOVAs conducted at each stimulation strength. See Table 5.2). A significant interaction effect between housing and genotype was observed for 1 wk EE conditions in response to 50μA of stimulation (2-way ANOVA: genotype x housing $F(1,99) = 4.94$, $p = 0.029$). However, post-hoc testing failed to identify significant difference between conditions (Table 5.2, top). Likewise, a significant housing effect was observed after 5 wks EE in response to 20 μA of stimulation (2-way ANOVA: EE vs. SH, $F(1,59) = 7.53$, $p = 0.008$). However, post-hoc testing failed to identify significant difference between conditions (Table 5.2, bottom). Previous observations demonstrate that MSK1 KD mice display a deficit in basal synaptic glutamatergic transmission (Daumas et al., 2017, Privitera et al., 2020). Differences here between conditions were not consistent across stimulation strengths, and control (SH) conditions displayed differences between experimental batches (group 1 wk EE vs. group 5 wk EE). Therefore whatever differences may exist between groups, they do not appear to be large enough to detect against the background of such variability between experimental replicates. Whilst this data is not enough to contradict there existing a difference between WT and MSK1 KD basal transmission, no difference between conditions after 1 wk or 5 wks of EE was observed.

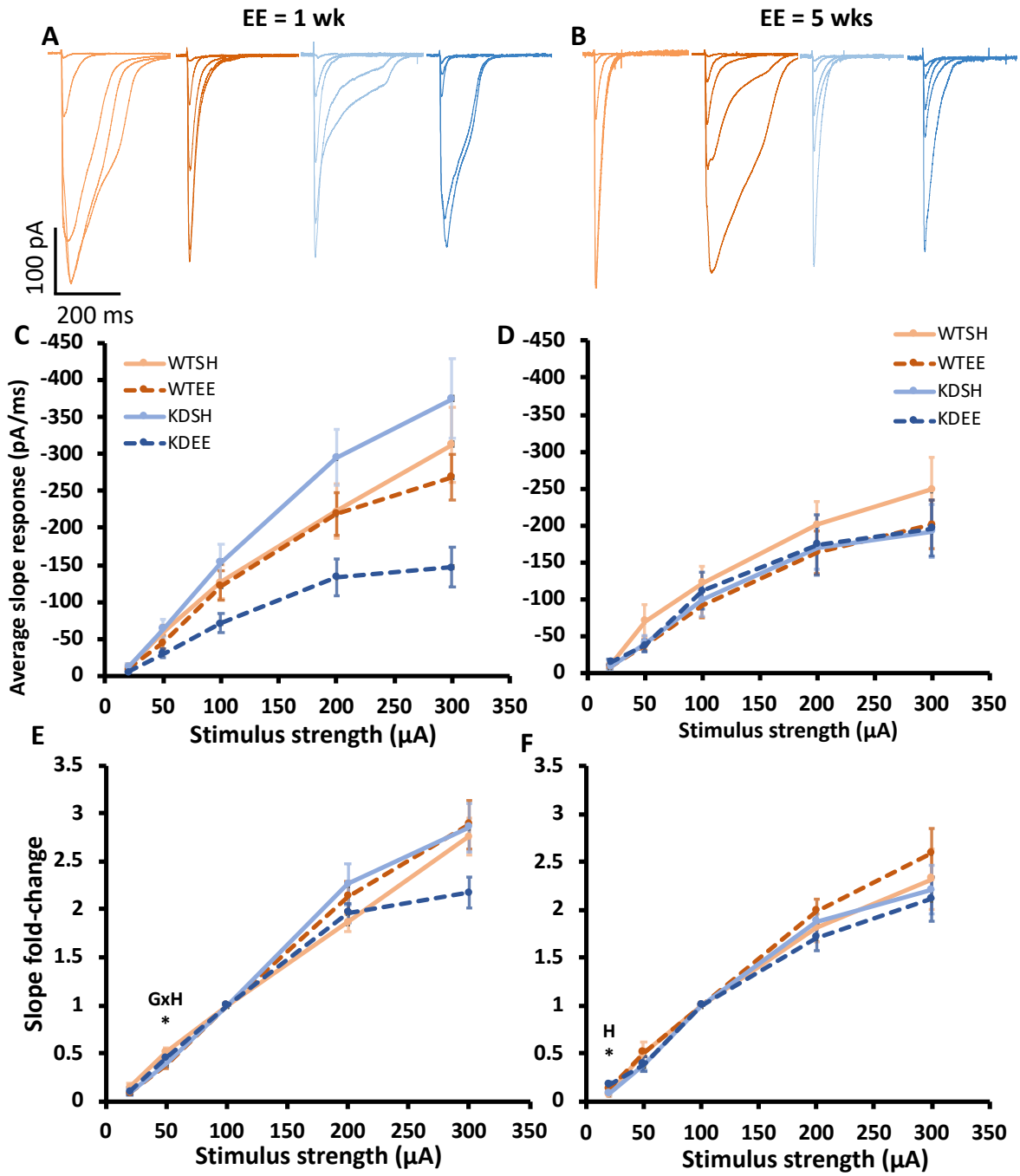

Figure 5.2. Whole-cell patch-clamp recordings of input-output response at Schaffer collateral/CA1 pyramidal neuron synapses do not demonstrate significant differences between conditions at either the 1 wk or 5 wk EE timepoints. A) Representative average traces of recorded currents elicited with 20, 50, 100, 200 and 300 µA stimulating current for 1 wk EE experimental conditions. **B)** Representative average of 5 traces of recorded currents elicited with 20, 50, 100, 200 and 300 µA stimulating current for 5 wk EE experimental conditions. **C + D)** Initial slope (measured between 10 to 45 % of peak) of EPSCs evoked at each stimulus intensity **C)** after 1 wk of EE **D)** after 5 wks of EE. **E + F)** Ratio of the initial slope of EPSCs evoked at each stimulus intensity Normalised to the slope of

evoked EPSC at 100μA **E)** Normalised Initial slope ratio of EPSC at each stimulus intensity of recorded currents showed a significant interaction between housing and genotype on EPSC response at 20 μA of stimulation (2-way ANOVA: genotype x housing F (1,99) = 4.94, p = 0.029) after 1 wk EE. n for each group: WTSH = 28; WTEE = 33; KDSH = 23; KDEE = 19. **F)** Normalised Initial slope ratio of EPSC at each stimulus intensity of recorded currents showed a significant effect of housing on EPSC response at 20 μA of stimulation (2-way ANOVA: EE vs. SH, F (1,59) = 7.53, p = 0.008) after 5 wks EE. n for each group: WTSH = 14; WTEE = 20; KDSH = 14; KDEE = 15.Representative traces display slope fold-change values close to plotted averages. Error bars represent SEM. Asterisk indicates a significance of p <0.05. GxH: genotype x housing interaction effect. H: significant effect of housing.

1 wk EE conditions	2-way ANOVA statistics		
Stimulus strength (μA)	**Genotype (WT vs. MSK1 KD)**	**Housing (SH vs. EE)**	**Interaction (geno x housing)**
20	F (1,99) = 0.404, p = 0.527	F (1,99) = 0.554, p = 0.456	F (1,99) = 1.24, p = 0.269
50	F (1,99) = 0.374, p = 0.542	F (1,99) = 0.963, p = 0.329	**F (1,99) = 4.94, p = 0.029**
100	N/A	N/A	N/A
200	F (1,99) = 0.540, p = 0.464	F (1,99) = 0.005, p = 0.943	F (1,99) = 3.28, p = 0.073
300	F (1,99) = 1.71, p = 0.193	F (1,99) = 1.37, p = 0.244	F (1,99) = 2.91, p = 0.091

5 wks EE conditions	2-way ANOVA statistics		
Stimulus strength (μA)	**Genotype (WT vs. MSK1 KD)**	**Housing (SH vs. EE)**	**Interaction (geno x housing)**
20	F (1,59) = 1.05, p = 0.311	**F (1,59) = 7.53, p = 0.008**	F (1,59) = 0.499, p = 0.483
50	F (1,59) = 2.56, p = 0.115	F (1,59) = 0.012, p = 0.915	F (1,59) = 0.0004, p = 0.985
100	N/A	N/A	N/A
200	F (1,59) = 0.566, p = 0.455	F (1,59) = 0.002, p = 0.968	F (1,59) = 1.53, p = 0.221
300	F (1,59) = 1.35, p = 0.250	F (1,59) = 0.121, p = 0.729	F (1,59) = 0.538, p = 0.466

Table 5.2. Summary of two-way ANOVA statistics between conditions for input-output experiments for 1 wk EE group (top) and 5 wks EE group (bottom).

5.2.4 Neither the kinase activity of MSK1, nor environmental enrichment affect the paired-pulse ratio at SC/CA1 synapses

Synaptic plasticity changes can modulate the presynaptic release probability of glutamate, and measuring facilitation of paired-pulses can measure this (Jackman and Regehr, 2017). Shorter pulse intervals encourage facilitation of the second pulse due to the presence of residual presynaptic Ca^{2+} from the first pulse which, combined with the calcium influx of the second pulse, results in a larger vesicle fusion event via activation of calcium-sensitive proteins (Jackman and Regehr, 2017). Longer inter-pulse intervals see a decay of this effect, due to the buffering and export of the residual intracellular Ca^{2+} (Jackman and Regehr, 2017).

Inactivation of MSK1 kinase function has been previously seen to have no effect on paired-pulse ratio (PPR) under basal SH conditions (Daumas et al., 2017). Additionally EE is not typically seen to modulate PPR (Ohline and Abraham, 2019). However if any changes in transmission were observed in MSK1 KD mice in response to EE, the presynaptic component of any modulation of transmission strength should be ruled out (Citri and Malenka, 2008). Paired-pulse recordings were conducted alongside input-output experiments so although no definite differences in synaptic transmission strength were observed between conditions, this data was also collected.

To evaluate the effect of MSK1 kinase inactivation on pre-synaptic release probability, SC fibres were stimulated with a paired-pulse at different inter-pulse intervals whilst recording from CA1 neurons. As with rectification experiments, stimulation was normalised between slices by using a stimulation intensity that consistently elicited a 100pA response. Seen below in Figure 5.3 A, after 1 wk of EE there is no detectable difference in PPR at any inter-pulse interval between either EE or MSK1 KD conditions and WT slices (two-way ANOVA at each inter-pulse interval, summarised in Table 5.3 below). Likewise at 5 wks of EE, no difference in PPR at any inter-pulse interval can be observed between conditions in Figure 5.3 B. This corroborates the same observations of no effect of MSK1 kinase activity on PPR seen between standard housed WT and MSK1 KD mice in Daumas et al. 2017.

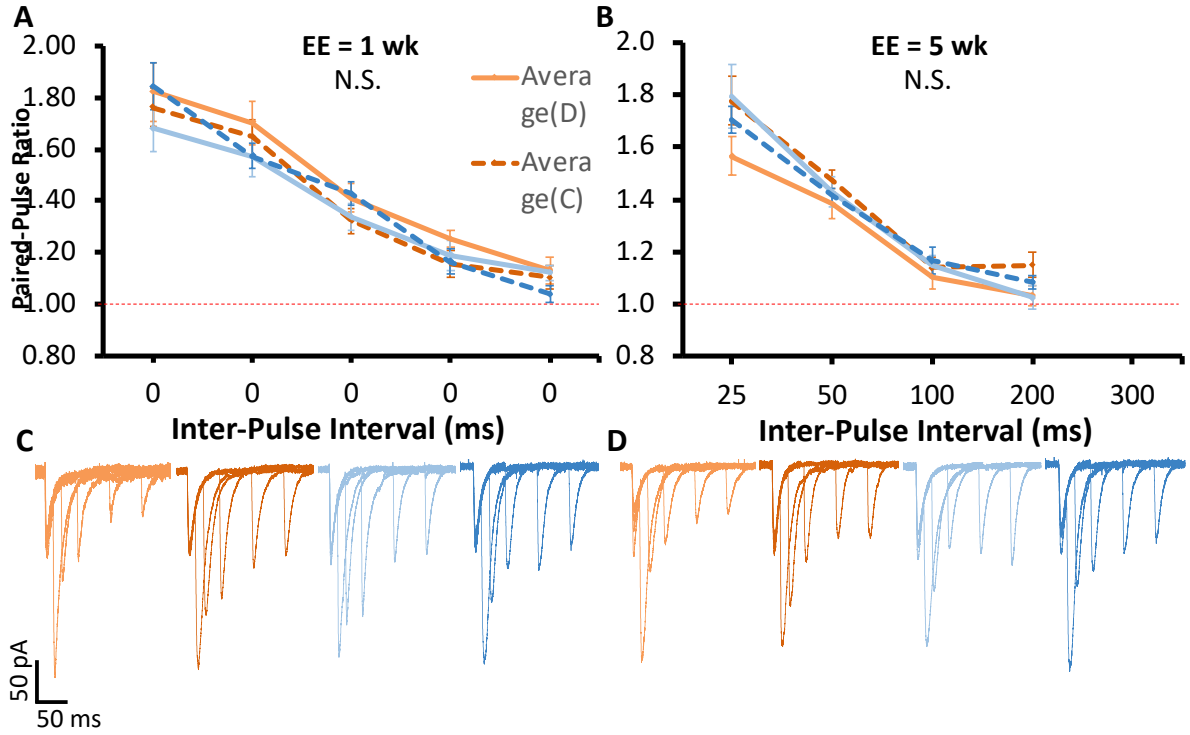

Figure 5.3. No effect of either EE or genotype was seen on presynaptic release probability as measured by paired-pulse ratio (PPR). PPR was measured by dividing second evoked EPSC amplitude by the first, separated by varying inter-pulse interval (ms, x axis). **A + B)** PPR was not significantly different between WT or MSK1 KD mice after 1 wk (A) or 5 wks (B) of EE. Error bars represent SEM. n for each condition: 1wk EE: WTSH = 13; WTEE = 25; KDSH = 11; KDEE = 17; 5 wks EE: WTSH = 14; WTEE = 18; KDSH = 12; KDEE = 12 **C + D)** Representative traces from CA1 neurons of each condition for 1 wk EE group (C) and 5 wk EE group (D).

1 wk EE conditions	Paired-pulse ratio 2-way ANOVA statistics		
Inter-pulse interval (ms)	**Genotype (WT vs. MSK1 KD)**	**Housing (SH vs. EE)**	**Interaction (geno x housing)**
25	F (1,60) = 0.0002, p = 0.990	F (1,60) = 0.011, p = 0.915	F (1,60) = 0.180, p = 0.673
50	F (1,60) = 0.502, p = 0.482	F (1,60) = 0.006, p = 0.937	F (1,60) = 2.86, p = 0.096
100	F (1,60) = 0.083, p = 0.774	F (1,60) = 0.109, p = 0.742	F (1,60) = 1.32, p = 0.255
200	F (1,60) = 0.012, p = 0.912	F (1,60) = 0.205, p = 0.652	F (1,60) = 0.0004, p = 0.983
300	F (1,60) = 0.176, p = 0.676	F (1,60) = 2.00, p = 0.162	F (1,60) = 1.16, p = 0.286

5 wks EE conditions	Paired-pulse ratio 2-way ANOVA statistics		
Inter-pulse interval (ms)	**Genotype (WT vs. MSK1 KD)**	**Housing (SH vs. EE)**	**Interaction (geno x housing)**
25	F (1,52) = 0.212, p = 0.647	F (1,52) = 0.473, p = 0.495	F (1,52) = 1.12, p = 0.294
50	F (1,52) = 2.18, p = 0.146	F (1,52) = 0.084, p = 0.774	F (1,52) = 0.083, p = 0.775
100	F (1,52) = 0.035, p = 0.851	F (1,52) = 0.035, p = 0.851	F (1,52) = 2.62, p = 0.111
200	F (1,52) = 0.324, p = 0.572	F (1,52) = 1.41, p = 0.241	F (1,52) = 0.454, p = 0.503
300	F (1,52) = 0.788, p = 0.379	F (1,52) = 1.74, p = 0.193	F (1,52) = 0.443, p = 0.508

Table 5.3. Summary of two-way ANOVA statistics for paired-pulse ratio experiments between conditions for 1 wk EE group (top) and 5 wks EE group (bottom).

Loss of MSK1 kinase activity therefore does not seem to affect presynaptic release probability between either baseline standard housing conditions, nor did it affect any response to EE in either genotype. This agrees with previous field excitatory field potential (fEPSP) PPR experiments performed in region CA1 wherein there was no difference in PPR between MSK1 KD and WT mice (Daumas et al., 2017). Lack of PPR difference within CA1 neurons following EE agrees with other studies which typically find no change in paired-pulse facilitation after short (4-8 wks) (Malik and Chattarji, 2012, Parsley et al., 2007) or long (3 mths) (Eckert and Abraham, 2013) periods of EE in CA1 neurons.

5.2.5 Analysis of mEPSCs reveals a possible deficit in MSK1 KD response to EE at 1 wk, but not 5 wks of EE

5.2.5.1 mEPSC amplitude and frequency was not affected by TTX incubation time in acute hippocampal slices

AMPAR-mediated mEPSCs were recorded from hippocampal CA1 cells in the presence of tetrodotoxin (1μM). Initially, potential synaptic scaling-related differences between MSK1 KD and WT mice were evaluated in slices, in an attempt to recapitulate the increased mEPSC amplitude phenotype observed in cultured pyramidal cell after 24 hr TTX incubation (Corrêa et al., 2012). However due to potential loss of viability of acute hippocampal slices, the timescale of TTX incubation was not greater than 6 hrs, and neither WT nor MSK1 KD CA1 neurons displayed a difference in either mEPSC amplitude (Figure 5.4 A) or frequency (Figure 5.4 B) over this period. This was not unexpected, as cultured neurons were used by Corrêa et al. (2012) for exactly this reason, however this meant that during evaluation of mEPSC recordings here, length of TTX application was able to be ruled out as a confounding variable.

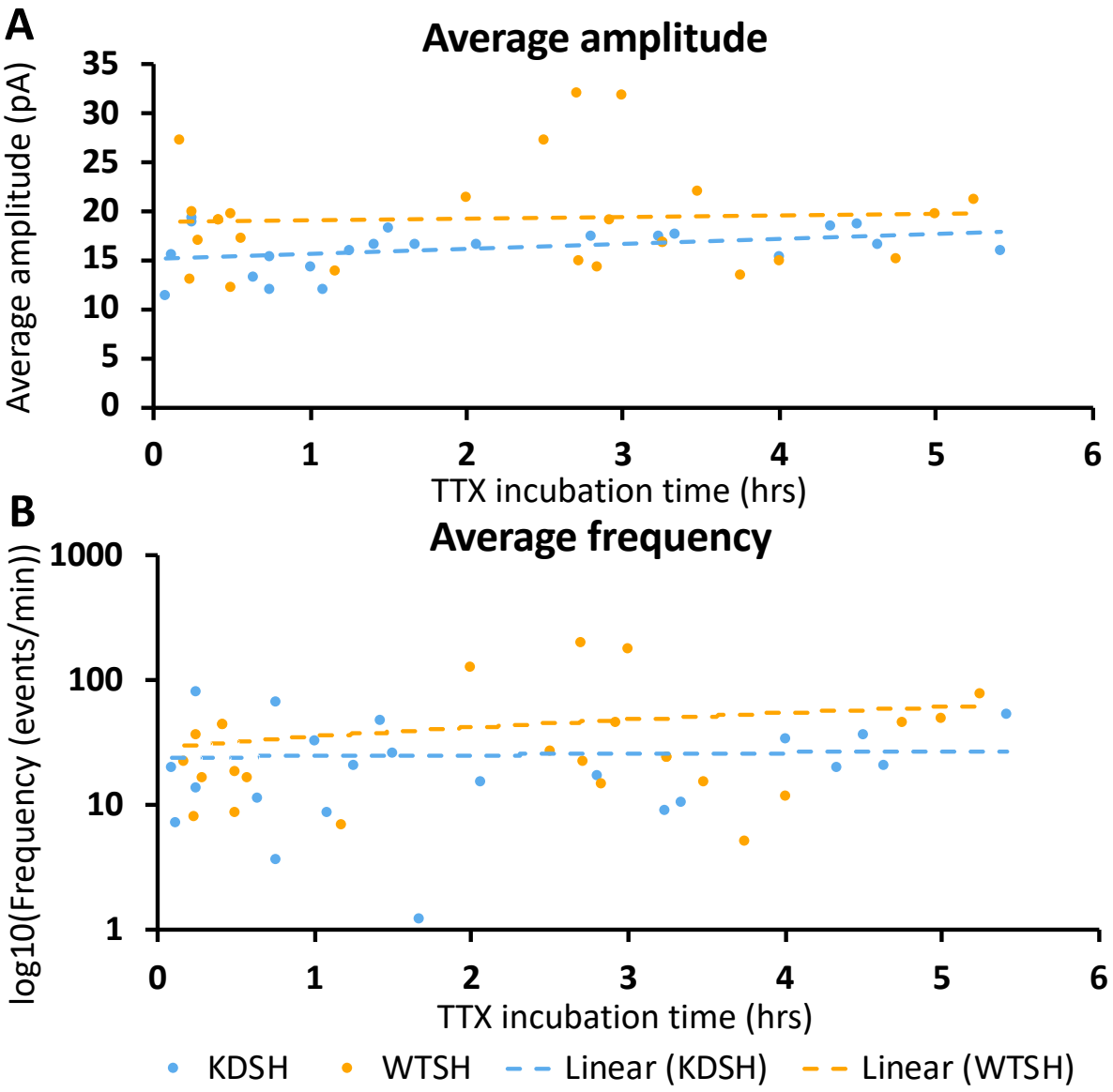

Figure 5.4. No effect of TTX incubation time from 0-6hrs is apparent on mEPSC amplitude or frequency in CA1 neurons recorded from acute hippocampal slices. A + B) Average amplitude (A) and frequency (B) of mEPSCs recorded from both WT and MSK1 KD slices in SH shows no difference in response to TTX incubation time.

5.2.5.2 A significant reduction in mEPSC amplitude was observed in WT but not MSK1 KD mice following 1 wk but not 5 wks of EE, however this difference in genotype response may be exaggerated by "outlier" data points.

The effect of acute periods of EE on levels of AMPAR-mediated glutamatergic transmission in MSK1-KD mice were examined by observing mEPSC amplitude and kinetics of patched cells. As seen in Figure 5.5 A, 1 wk of EE exposure resulted in an overall decrease in mEPSC amplitude (EE vs. SH: $F(1,75) = 11.14$; $p = 0.0013$). Post-hoc testing revealed that this difference was due to a decrease in average mEPSC amplitude for WT mice (WTSH = 19.2 ± 1.1; WTEE = 15.2 ± 0.8; Bonferroni $p = 0.0091$), but not MSK1 KD mice (KDSH = 16.1 ± 0.5; KDEE = 14.3 ± 0.7; Bonferroni $p = 0.902$). Previously, WT mice exposed to EE from birth for 6-8wks have been shown to experience a significant increase in mEPSC amplitude, whereas MSK1 KD mice do not (Corrêa et al., 2012). Longer periods of 8-12 wks EE however do not seem to show a difference (Duffy et al., 2001, Eckert et al., 2010). This decrease in mEPSC amplitude at 1 wk in WT mice may therefore be part of a normal MSK1-dependent response to EE that eventually leads to an increase during periods of longer exposure. However, in the set of experiments performed following 5 wks of EE, no significant difference was observed in mEPSC amplitude. One reason for this discrepancy may be the experience of the mice prior to electrophysiological testing: the 5 wk SH groups underwent behavioural testing two weeks prior to being taken for electrophysiology. BDNF signalling plays an important role in memory consolidation and learning during behavioural tasks (Cowansage et al., 2010, Novkovic et al., 2015) and an increase in BDNF expression following behavioural testing has been observed before, albeit within EE animals compared to impoverished housing animals (Falkenberg et al., 1992). It is therefore possible that this *in vivo* assessment served as a form of MSK1-independent enrichment for the 5 wk SH conditions, possibly occluding the expected effects of EE at this timepoint. Repeating this experiment without the prior behavioural experience confound would aid in discriminating between these effects, or alternatively the measurement of BDNF expression levels before and after behavioural testing in SH animals could potentially resolve this discrepancy.

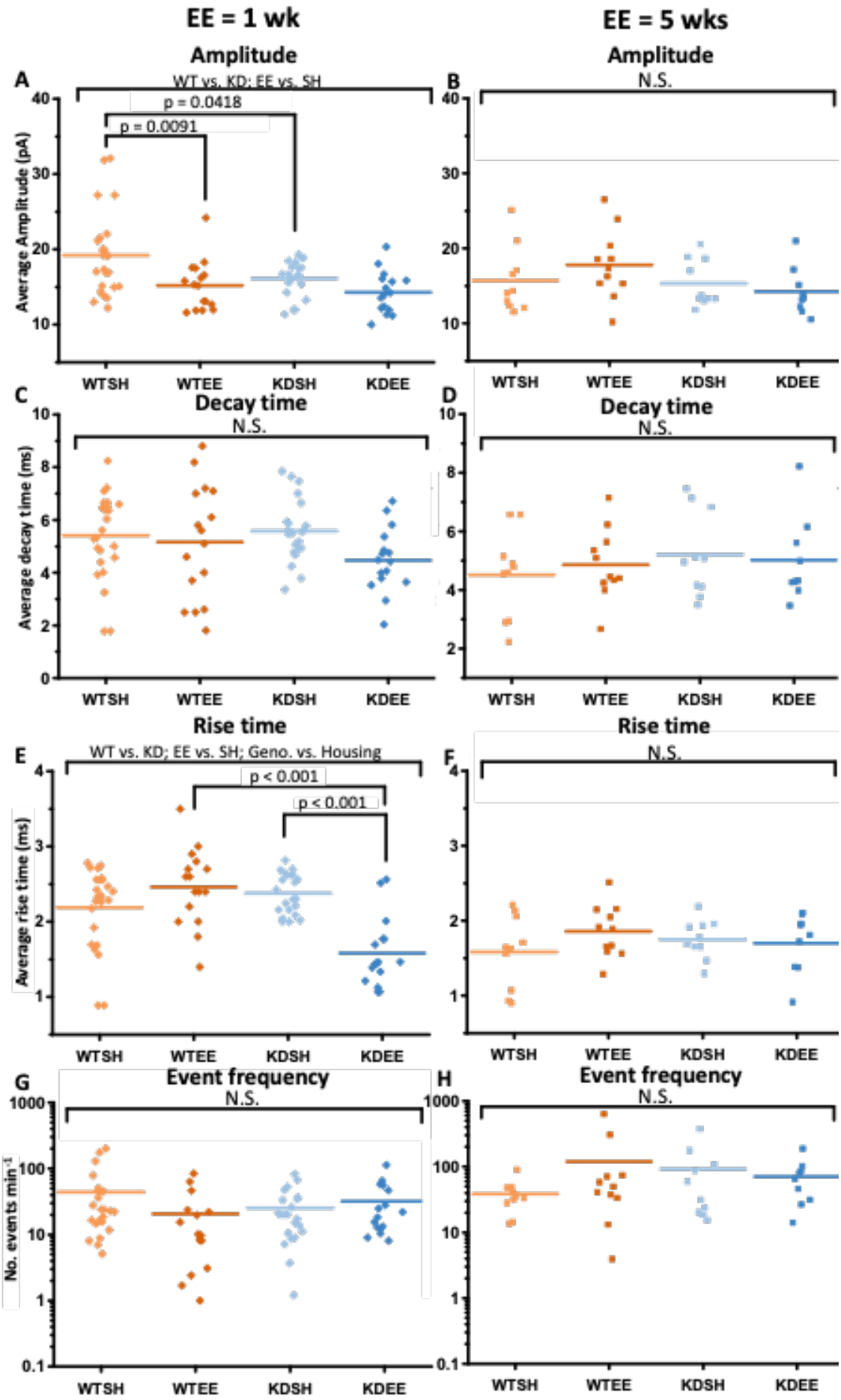
EE = 1 wk
EE = 5 wks
Amplitude
A
WT vs. KD; EE vs. SH
p = 0.0418
p = 0.0091
Average Amplitude (pA)
B
N.S.
Decay time
C
N.S.
Average decay time (ms)
D
Rise time
E
WT vs. KD; EE vs. SH; Geno. vs. Housing
p < 0.001
p < 0.001
Average rise time (ms)
F
Event frequency
G
No. events min-1
H
WTSH
WTEE
KDSH
KDEE

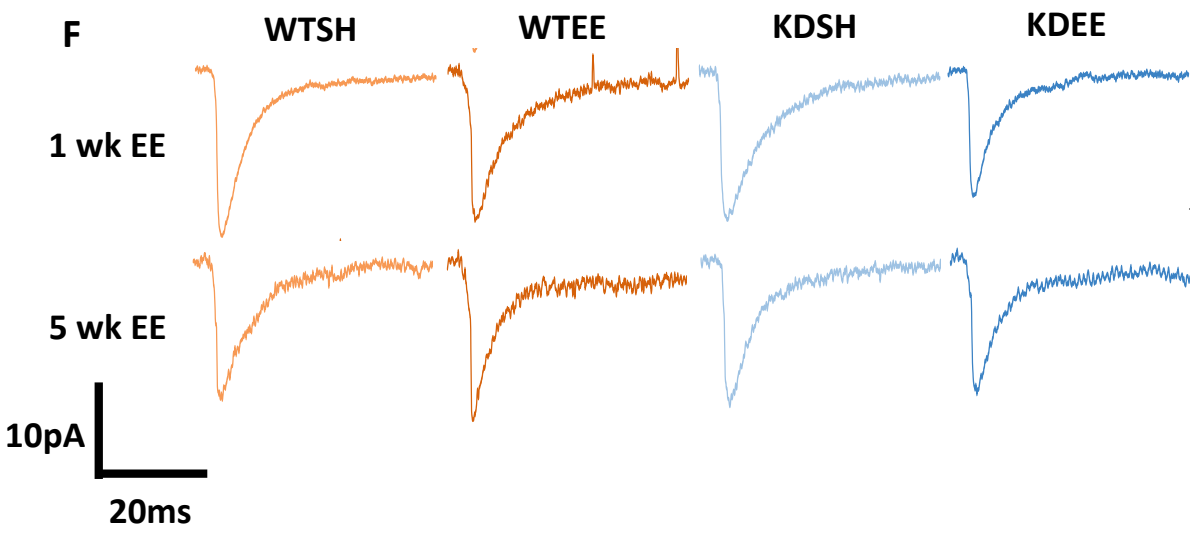

Figure 5.5. Summary of average mEPSC parameters across both 1 wk and 5 wks EE timepoints. A) Average peak amplitude of mEPSCs in 1 wk group conditions. Amplitude was lower in WT mice following 1 wk EE (EE vs.SH: $F(1,75) = 11.14$; $p = 0.0013$; Bonferroni $p = 0.0091$), but not MSK1 KD mice (Bonferroni $p = 0.902$). WT mice also displayed greater mEPSC amplitude compared to MSK1 KD (WT vs. MSK1 KD: $F(1,75) = 5.20$; $p = 0.025$). **B)** No difference in average peak amplitude was observed between conditions following 5 wks of EE. **C, D)** No difference in average decay time was observed between 1 wk (C) and 5 wk (D) EE conditions. **E)** Average rise time of mEPSCs in 1 wk EE conditions showed significant effects of housing (EE vs. SH: $F(1,75) = 6.40$; $p = 0.013$) and genotype (WT vs. MSK1 KD: $F(1,75) = 11.18$; $p = 0.0013$) and an interaction effect between them (genotype vs. housing: $F(1,75) = 26.64$; $p = <0.001$). Post-hoc testing revealed an impaired response of MSK1 KD mice to 1 wk of EE, with a decrease in rise time in MSK1 KD mice in response to EE (KDSH vs. KDEE: Bonferroni $p = <0.001$) but not WT mice (WTSH vs. WTEE: Bonferroni $p = 0.380$). A significant decrease in enriched MSK1 KD compared with enriched WT conditions was also observed following 1 wk of EE (WTEE vs. KDEE: Bonferroni $p = <0.001$). **F)** No difference in rise time was observed between conditions following 5 wks of EE. **G, H)** No difference in rise time was observed between 1 wk (C) and 5 wk (D) EE conditions. **I)** Representative traces for mEPSCs from each condition across both 1 wk EE and 5 wk EE experiments. Traces were averaged from at least 50 events. Scale bars as labelled in figure. n for each condition: 1 wk EE group: WTSH = 25; WTEE = 16; KDSH = 22; KDEE = 16; 5 wks EE group: WTSH = 10; WTEE = 9; KDSH = 11; KDEE = 10.

In Figure 5.5 A, a decrease in mEPSC amplitude within the 1 wk group SH control mice (WTSH = 19.2 +/- 1.1; KDSH = 16.1 $\pm$ 0.5; genotype: $F(1,75) = 5.20$; $p = 0.025$), but not 5 wk group SH control mice (WTSH = 15.7 $\pm$ 1.4; KDSH = 15.3 $\pm$ 1.0) was observed (genotype: $F(1,36) = 0.0034$; $p = 0.954$). This difference was surprising, as both groups of WTSH conditions were

expected to represent the same effect of standard housing, and both KDSH groups show similar values. Animals were aged between 12-24 wks for the 1 wk group of WTSH animals and 12-18 weeks for the 5 wk groups of WTSH animals so this is unlikely to be an age effect. mEPSC amplitudes were therefore compared between SH control groups used in both 1 wk EE and 5 wk EE experiments.

As can be seen in Figure 5.6 A below, whilst effect of experimental group came close to achieving significance, there was no significant difference between SH conditions used across 1 wk and 5 wk EE experiments (EE control group, $F(1,63) = 3.80$; $p = 0.056$). Despite this, the four apparent outliers (amplitude >25 pA) in the "1 wk EE WTSH" control group were looked at for any common confounding variables. The four data points were obtained using 4 hippocampal slices from 3 different experimental animals aged 13, 17 and 18 wks. Two of these results were therefore obtained from a single experimental animal, albeit from separate slices. Additionally, 2 of these 3 mice were from the same litter, however the other 3 mice from this litter gave mEPSC amplitudes <25 pA, more in line with all other experimental groups. Removal of the 4 outlier data points from the "1 wk EE WTSH" control group yielded a new mean amplitude for the 1wk WTSH group of 17.3+/- 3.0, compared with the previous mean amplitude of 19.2 +/- 5.4 when outliers were included (Figure 5.6 B). Each of the 4 "outlier" data points >25 pA would lie >2 standard deviations above a mean of 17.3 +/- 3.0 pA, indicating the abnormally large amplitude of these 4 data points could be the result of a batch effect. However due to no identifiable source of such an effect, nor the observation of any significant difference between groups, the data were included in the analysis performed in Figure 5.5 A. Analysis mean mEPSC amplitude data following 1 wk of EE with the 4 "outliers" excluded (figure 5.6 A) still found significant decrease in mean mEPSC amplitude following enrichment that was not genotype-dependent (EE vs. SH $F(1,59) = 8.70$; $p = 0.004$; Figure 5.6 B). Therefore despite the observation of a reduction in mEPSC amplitude in WT and not MSK1 KD mice following 1 wk of EE, it is difficult to conclude honestly that this is an effect of MSK1 kinase inactivation, and is more likely due to a general decrease in mEPSC amplitude in both genotypes following 1 wk of EE.

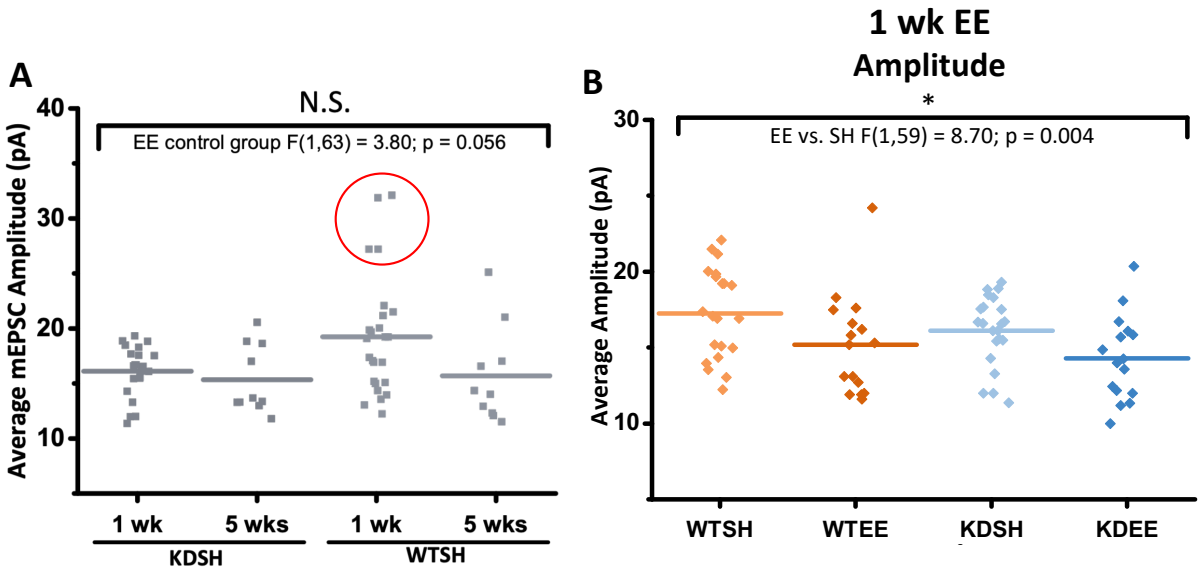

Figure 5.6. Comparison of control (SH) groups between EE experiments, and effect of outlier exclusion from "1 wk EE WTSH" control group. A) All standard housed (SH) experimental groups (WT and MSK1 KD) used as control comparisons during 1 wk and 5 wk EE experiments. No significant difference is observed between the groups. Highlighted by the red circle are the 4 "outliers" with a mean amplitude of >25pA. **B)** Alternative analysis of mean mEPSC amplitude data from the 1 wk EE experiment used in Figure 5.5 A following the removal of 4 datapoints identified as potential "outliers" (in Figure 5.6 A) from the group WTSH, used as the control WT group. A significant effect of housing can still be observed (EE vs. SH $F(1,59) = 8.70$; $p = 0.004$).

This extra analysis in Figure 5.6 A indicated that the observations of potential differences between SH control groups caused by outliers in the "1 wk EE WTSH" group may not be of concern to the interpretation of the reduction in AMPA-mediated excitatory transmission observed after 1 wk of EE in in Figure 5.5 A. However, Figure 5.6 B indicates that regardless of "outlier" inclusion, an observation of a decrease in AMPAR-mediated quantal amplitude following 1 wk of EE at SC-CA1 synapses across both WT and MSK1 KD genotypes is present. Another independent experiment would be useful to confirm these results, and further ascertain the involvement of MSK1 kinase function in regulating AMPAR transmission strength differences following a short (1 wk) period of EE.

5.2.5.3 The kinase function of MSK1 did not affect mEPSC decay time or frequency following either 1 wk or 5 wks of EE.

No difference was observed in either decay or frequency of mEPSCs in any condition following 1 wk or 5 wks of EE (Figure 5.5 C, D, E, H). Due to the lack of difference in paired-pulse ratio (PPR) observed in all conditions for both periods of EE, no difference in mEPSC frequency was not surprising, and indicates that pre-synaptic release probability in these mice is unaffected which is consistent with the PPR data in Figure 5.3 and previous PPR experiments in MSK1 KD mice (Daumas et al., 2017). Other mEPSC experiments have observed EE-mediated increases in frequency following 4-8 wks of EE, but have concluded that this is due to increased functional synapse number, rather than an increase in presynaptic release probability (Malik and Chattarji, 2012).

5.2.5.4 Rise time of mEPSCs was significantly reduced in MSK1 KD mice following 1 wk, but not 5 wks of EE.

Following 1 wk of EE, MSK1 kinase inactivation significantly altered the rise time of mEPSCs compared to WT mice (Figure 5.5 E): an interaction effect between genotype and housing was observed for mEPSC rise time (genotype x housing: $F(1,75) = 26.64$; $p < 0.001$). Post-hoc testing revealed an enrichment-dependent reduction in rise time for MSK1 KD mice (KDSH = 2.4 $\pm$ 0.1; KDEE = 1.6 $\pm$ 0.1; Bonferroni p = <0.001) and between enriched WT and MSK1 KD mice (WTEE = 2.5$\pm$0.1; KDEE = 1.6 $\pm$ 0.1; Bonferroni p = <0.001).

This highlights an MSK1-dependent effect of EE on the kinetics of AMPAR mediated currents in which a decrease in rise time, but not decay time is observed. CA1 neurons make synaptic connections across the length of their dendritic tree, but postsynaptic potentials at synapses more distal to the soma are affected by dendritic filtering, that is they have to travel further along the dendrite to reach the soma than potentials at more proximal synapses (Smith et al., 2003). This results in an increase in rise and decay time due to the postsynaptic potential becoming spread out and reaching the soma over a longer period of time (Smith et al., 2003). Neurons compensate for this by increasing AMPAR receptor density as synapses become more distal from the soma, and potentially, by desensitisation of proximal synapses

to increase their decay time to match distal synapses, thus scaling postsynaptic potential strength in a spatial manner (Smith et al., 2003).

The decrease in rise time observed here in MSK1 KD mice following enrichment therefore could indicate a shift in AMPAR-mediated transmission origin to more proximal locations with respect to the soma (Basu and Siegelbaum, 2015) compared to the WT response to EE: Pyramidal cells within the CA1 receive two primary inputs as discussed in section 1.1.2, axons from CA3 neurons via the SC/AC pathway, and from EC neurons via the temporoammonic pathway. SC/AC pathway axons synapse with CA1 cells in a layer proximal to the cell body, the stratum radiatum, whereas TA/CA1 synapses exist at a more distal location from the CA1 soma, the stratum lacunosum moleculare (Basu and Siegelbaum, 2015). This potential proximal shift in CA1 synaptic signalling could indicate greater stratum radiatum synaptic transmission weight over the SLM in MSK1 KD mice following acute enrichment (1 wk); Disruption of MSK1 kinase activity has been seen to partially occlude the EE-mediated increase in dendritic spine density within the stratum radiatum following 6 wks of EE (Corrêa et al., 2012). This could indicate that the initial (1 wk) response to EE regulates an shift in CA1 input weights from the SR to more distal connections originating in layer III of the EC via the TA pathway in the SLM, and that this is impaired in MSK1 KD mice. The kinase activity of MSK1 has been seen to regulate spine density of CA1 neurons within the stratum radiatum, under baseline standard housing conditions: Corrêa et al. (2012) observed that the spine density of MSK1 KD mice CA1 neurons was greater (1.21 ± 0.08 spines/µm) than that of wild-type (0.97 ± 0.08 spines/µm) ($p = 0.044$). MSK1 therefore could play a role in the activity-dependent re-organisation of CA1 neuron dendrites, an observation that is explored more in the next section.

5.2.6 Reconstruction of CA1 pyramidal cell apical dendrites reveal no gross dendrite morphological differences between conditions and but revealed an effect of EE on proximal-distal dendrite complexity

Following the observation that a significant number of extracellular remodelling GOTerms were uniquely regulated by MSK1 in response to 3 mths of EE (Figure 4.4), and the previously observed role of MSK1 kinase function in regulating dendritic spine density (Corrêa

et al., 2012), CA1 apical dendrite morphology was examined to determine a timescale for EE-mediated structural changes, and the role the kinase activity of MSK1 plays in mediating these changes. Increases in CA1 apical dendrite complexity have previously been observed following periods of EE (Faherty et al., 2003) and previous work with MSK1 KO mice has shown these mice fail to increase in CA1 apical dendrite complexity following 5/6 wks of EE (Karelina et al., 2012). To test the specificity of MSK1 kinase activity on apical dendrite complexity, biocytin was included with the patch solution during electrophysiology experiments conducted above, and later used to stain CA1 apical dendrites for subsequent reconstruction.

Overall, no differences in CA1 apical dendrite volume, surface area, nodes or length were observed between WT and MSK1 KD mice following 1 wk (Figure 5.7, 5.9 B-E) and 5wks (Figure 5.8, 5.10 B-E) of EE (2-way ANOVA comparing genotype and housing). This was surprising, as structural GOTerms featured high levels of enrichment in the MSK1-regulated differentially expressed genes following EE. However this could represent a difference in the EE timepoints measured here (shorter periods of EE 1 + 5 wks) vs. the longer period studied in chapter 4 (3 mths EE). As can be seen in Table 1.1 which presented a summary of EE effects on various physiological aspects, changes in CA1 neuron overall dendritic complexity are generally observed after longer durations of EE (12-16 wks) (Faherty et al., 2003). This is in line with the above hypothesis, that the gene expression changes following 12 wks of EE in Chapter 4 could represent dendritic complexity differences. The data presented here indicate that these dendrite complexity changes may not have occurred yet at more acute periods of EE (1 – 5 wks), but as can be seen in Table 1.1, changes in dendritic complexity are rarely looked at shorter periods of EE, and so this data helps map the timeline of structural changes.

Interestingly however, Table 1.1 highlights that changes to dendritic spine density seem to occur within CA1 neuron apical dendrites following periods of 6 – 8 wks EE (Rampon et al., 2000b, Malik and Chattarji, 2012, Corrêa et al., 2012). Unfortunately, the staining technique employed here did not provide sufficient contrast to accurately quantify dendritic spine density within these samples, however Sholl analysis was conducted, and yielded significant differences in dendrite complexity at different locations across the proximal-distal length of the apical dendrite. Both WT and MSK1 KD mice exposed to EE for 1 week demonstrated a significant reduction in apical dendrite complexity within the region *stratum*

lacunosum moleculare (specifically between 440 – 580 µm from the soma) compared to SH controls (Figure 5.9 A; Table 5.4). Furthermore following 5 wks of EE, WT mice, but not MSK1 KD mice appear to demonstrate a reduction in SR apical dendrite complexity (Figure 5.10 A) however, the data were very variable: This interaction effect between housing and genotype was only observed at 90 µm from the soma, and post-hoc testing was not significant (Table 5.5). Further interaction effects were observed within the SR at 220 and 250 µm from the soma (Figure 5.10 A) where MSK1 KD mice appeared to display the opposite response to EE compared to WT, however again, post-hoc testing was not significant (Table 5.5). Oddly, all mice within the 5 wk group appeared to display Sholl analysis distributions most closely resembling 1 week EE cohort WTEE and KDEE mice (WTEE and KDEE groups from Figure 5.9 A compared with all 4 experiment groups in Figure 5.10 A). This similarity could be due to the two-week period of behavioural testing that the 4 experimental groups of mice from the "5 wk EE" cohort underwent (covered in Chapter 6). A recent study by (Villanueva Espino et al., 2020) demonstrated a robust effect of 27 days of behavioural testing, including hippocampus-dependent tasks, on increasing CA1 neuron apical dendrite branching, primarily within the SR. The behavioural testing that the "5 wk EE" cohort of experimental animals underwent could therefore have occluded any effect of EE that may have been observed between the "5 wk EE" experimental groups.

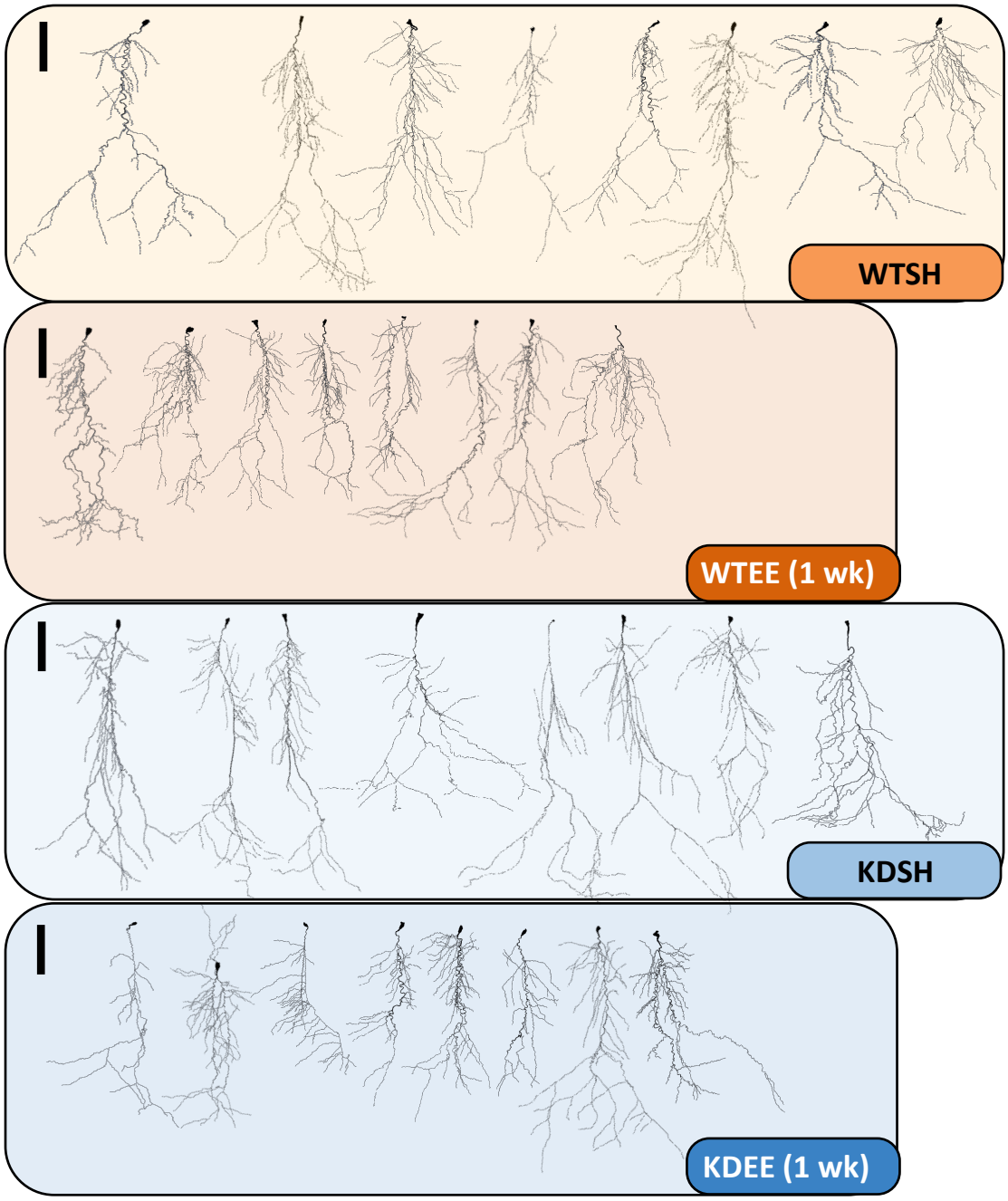

Figure 5.7 . Reconstructed hippocampal CA1 neuron apical dendrite morphologies from WT and MSK1 KD mice post-1 wk EE (WTEE, KDEE) along with SH controls (WTSH, KDSH) from neurons recorded during patch-clamp electrophysiology experiments. All reconstructions performed by Emma Condon (MIBTP). Black scale bar to the top left of each experimental group = 100 µm.

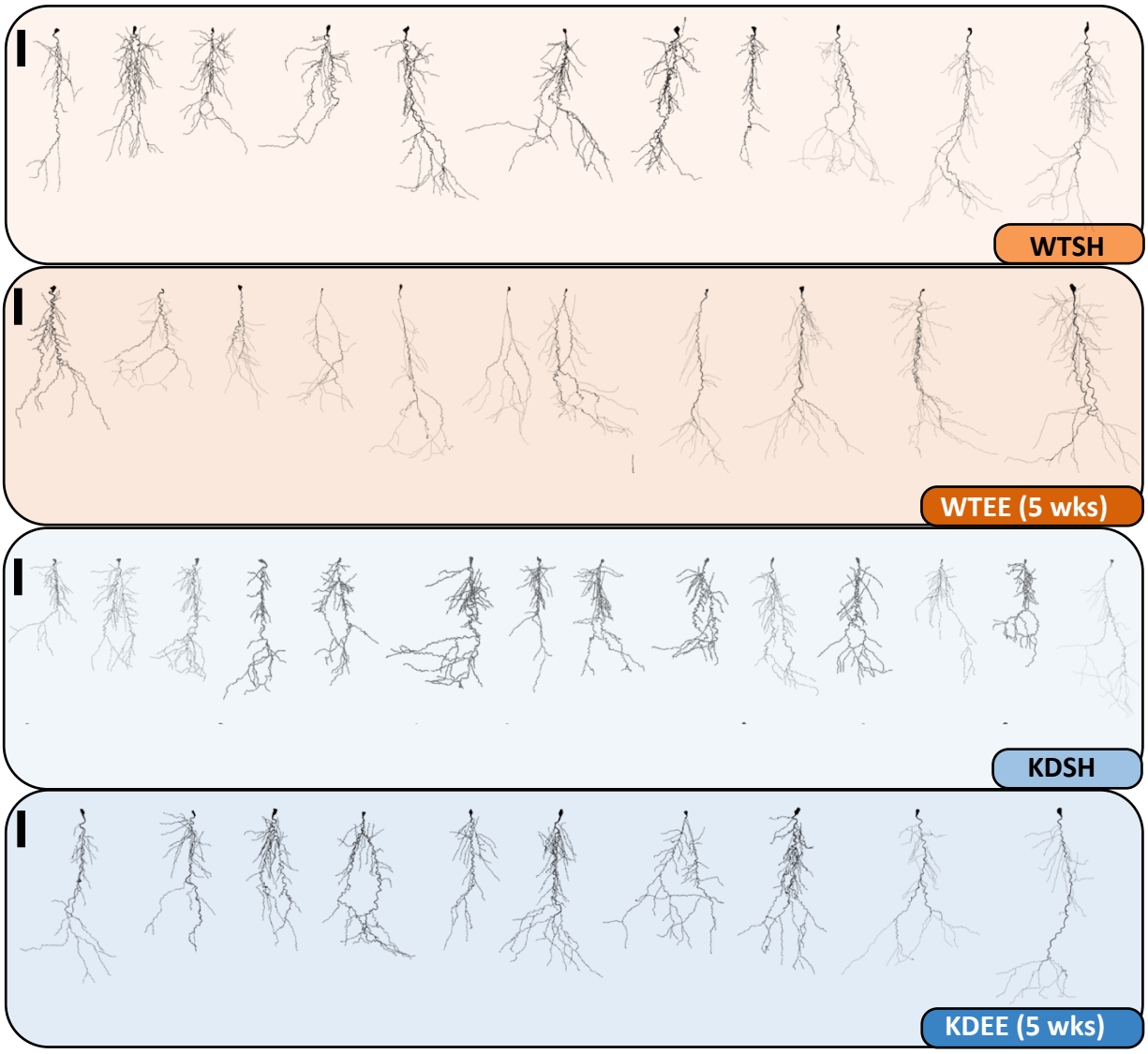

Figure 5.8. Reconstructed hippocampal CA1 neuron apical dendrite morphologies from WT and MSK1 KD mice post-5 wk EE (WTEE, KDEE) along with SH controls (WTSH, KDSH) from neurons recorded during patch-clamp electrophysiology experiments. All reconstructions performed by Emma Condon (MIBTP). Black scale bar to the top left of each experimental group = 100 µm.

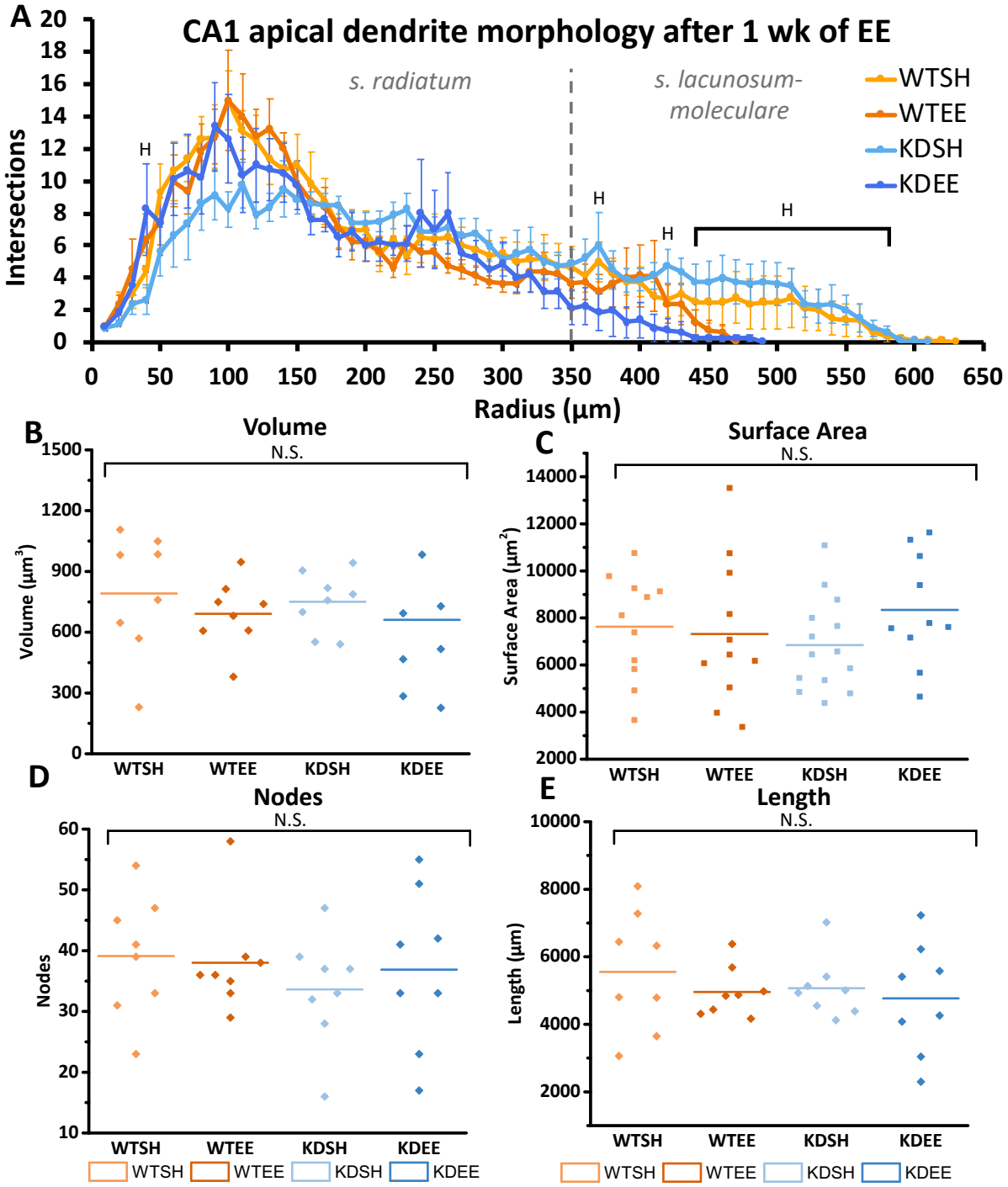

Figure 5.9. Reconstructed hippocampal CA1 neuron apical dendrite morphologies from WT and MSK1 KD mice post-1 wk EE (WTEE, KDEE) along with SH controls (WTSH, KDSH) from neurons recorded during patch-clamp electrophysiology experiments. A) Sholl analysis of CA1 neuron apical dendrites for each condition. Error bars are SEM. The symbols " H " above datapoints represents a significant effect of housing as measured by 2-way ANOVA. ANOVA statistics summarised in Table 5.4. **B, C, D, E)** Data points plotted for volume (B) surface area (C) branch point nodes (D) and length (E) of CA1 neuron apical dendrites. Lines indicate mean of data points. All reconstructions performed by Emma Condon (MIBTP).

1 Week EE Exps.: Sholl analysis intersection 2-way ANOVA statistics			
Radius	**Genotype (WT vs. MSK1 KD)**	**Housing (SH vs. EE)**	**Interaction (geno x housing)**
40	N.S.	$F(1, 32) = 4.44$, $p = 0.044$	N.S.
370	N.S.	$F(1, 32) = 4.33$, $p = 0.047$	N.S.
420	N.S.	$F(1, 32) = 4.35$, $p = 0.046$	N.S.
440	N.S.	$F(1, 32) = 6.17$, $p = 0.019$	N.S.
450	N.S.	$F(1, 32) = 7.00$, $p = 0.013$	N.S.
460	N.S.	$F(1, 32) = 7.11$, $p = 0.013$	N.S.
470	N.S.	$F(1, 32) = 8.66$, $p = 0.006$	N.S.
480	N.S.	$F(1, 32) = 8.08$, $p = 0.008$	N.S.
490	N.S.	$F(1, 32) = 8.91$, $p = 0.006$	N.S.
500	N.S.	$F(1, 32) = 8.61$, $p = 0.007$	N.S.
510	N.S.	$F(1, 32) = 8.63$, $p = 0.007$	N.S.
520	N.S.	$F(1, 32) = 7.52$, $p = 0.011$	N.S.
530	N.S.	$F(1, 32) = 6.34$, $p = 0.018$	N.S.
540	N.S.	$F(1, 32) = 6.01$, $p = 0.021$	N.S.
550	N.S.	$F(1, 32) = 6.14$, $p = 0.020$	N.S.
560	N.S.	$F(1, 32) = 4.63$, $p = 0.040$	N.S.
570	N.S.	$F(1, 32) = 5.54$, $p = 0.026$	N.S.
580	N.S.	$F(1, 32) = 4.63$, $p = 0.040$	N.S.

Table 5.4: Summary statistics for 2-way ANOVA testing between housing and genotype dendrite intersections at each Sholl radius distance from the soma for 1 week EE experimental groups. For clarity, only radial increments are shown that were statistically significant for an effect of genotype, housing or genotype x housing interaction. Statistical output shown to 3 significant figures (s.f.), or 2 decimal places (d.p.) as appropriate.

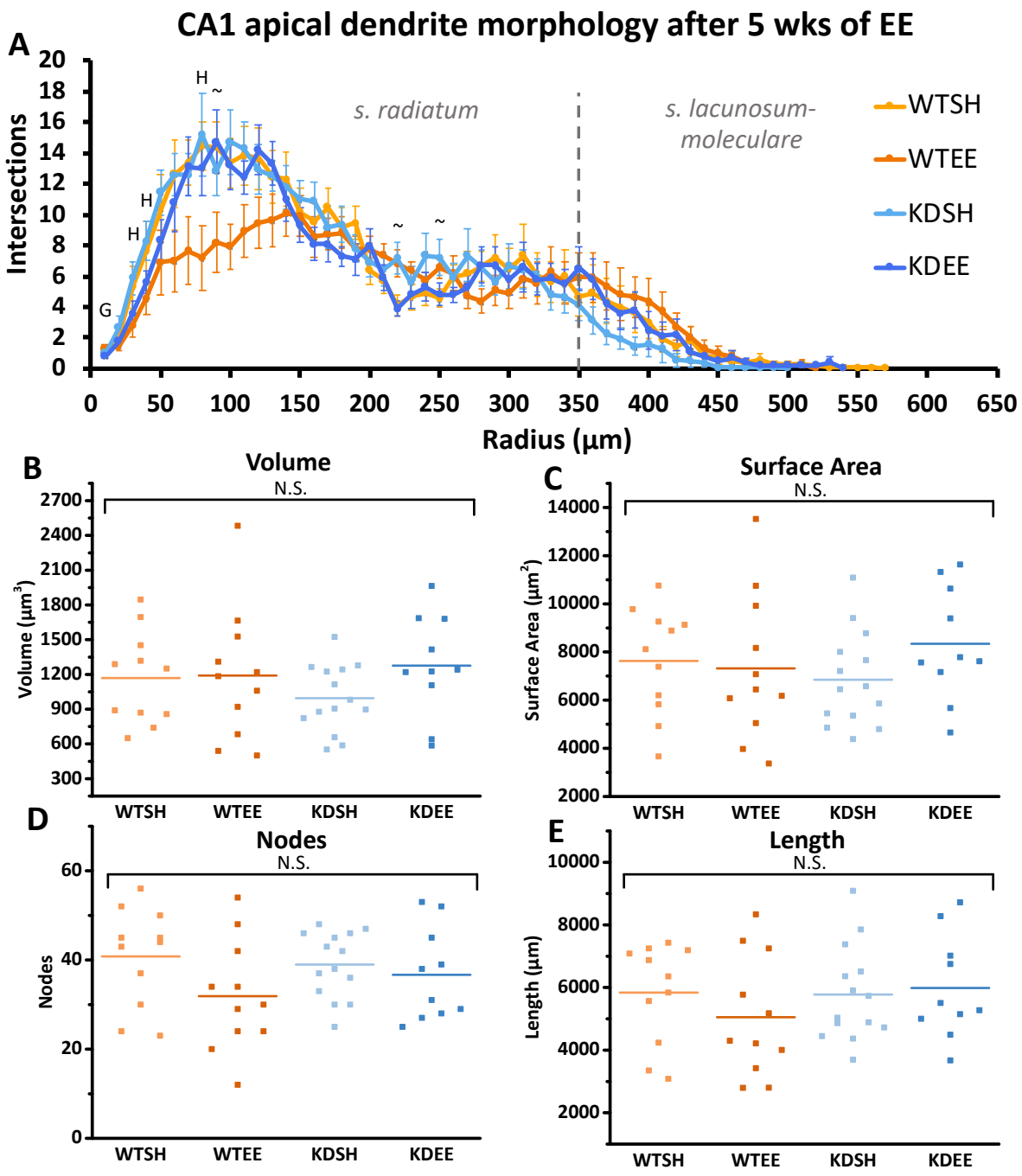

Figure 5.10. Reconstructed hippocampal CA1 neuron apical dendrite morphologies from WT and MSK1 KD mice post-5 wk EE (WTEE, KDEE) along with SH controls (WTSH, KDSH) from neurons recorded during patch-clamp electrophysiology experiments. A) Sholl analysis of CA1 neuron apical dendrites for each condition. Error bars are SEM. The symbols " H ", " G " and " ~ " above datapoints represents a significant effect of housing, genotype or genotype vs. housing respectively, as measured by 2-way ANOVA. ANOVA statistics summarised in Table 5.5. **B, C, D, E)** Data points plotted for volume (B) surface area (C) branch point nodes (D) and length (E) of CA1 neuron apical dendrites. Lines indicate mean of data points. All reconstructions performed by Emma Condon (MIBTP).

5 Week EE Exps.: Sholl analysis intersection 2-way ANOVA statistics				
Radius	**Genotype (WT vs. MSK1 KD)**	**Housing (SH vs. EE)**	**Interaction (geno x housing)**	**Post hoc. (bonf.)**
10	$F(1, 46) = 5.63$, $p = 0.022$	N.S.	N.S.	N.S.
30	N.S.	$F(1, 46) = 5.00$, $p = 0.031$	N.S.	N.S.
40	N.S.	$F(1, 46) = 4.54$, $p = 0.039$	N.S.	N.S.
80	N.S.	$F(1, 46) = 4.59$, $p = 0.038$	N.S.	N.S.
90	N.S.	N.S.	$F(1, 46) = 4.96$, $p = 0.031$	N.S.
220	N.S.	N.S.	$F(1, 46) = 12.57$, $p = <0.001$	N.S.
250	N.S.	N.S.	$F(1, 46) = 6.14$, $p = 0.017$	N.S.

Table 5.5: Summary statistics for 2-way ANOVA testing between housing and genotype dendrite intersections at each Sholl radius distance from the soma for 5 week EE experimental groups. For clarity, only radial increments are shown that were statistically significant for an effect of genotype, housing or genotype x housing interaction. Statistical output shown to 3 s.f., or 2 d.p. as appropriate.

5.3 Discussion

5.3.1 Calcium permeability of AMPAR expression is decreased following exposure to EE in an MSK1-independent manner

The significant increase in rectification shown in WT and MSK1 KD mice following both acute 1 wk and 5 wk periods of EE indicates that EE can induce an MSK1-independent decrease in CP-AMPAR expression at SC/CA1 synapses. This decrease begins after up to 1 wk of EE and may be sustained for at least 5 wks. This decrease in CP-AMPAR expression however was the opposite of what was predicted based on the RNAseq expression data of GluA1 and GluA2 in Figure 4.8 of Chapter 4: After 3 months of EE, GluA2 RNA expression is downregulated, and GluA1 expression unchanged. This would imply an increased expression of CP-AMPARs lacking the GluA2 subunit, due to the GluA2 subunit-mediated block of Ca^{2+} entry when incorporated into heteromeric GluA2/GluA1-3 receptors (Swanson et al., 1997, Cull-Candy et al., 2006), is taking place following 3 months of EE. This perhaps indicates a biphasic response to EE, whereupon CP-AMPAR expression is decreased during the early periods (weeks) of EE and increased over longer (months) of EE.

CP-AMPARs are implicated in the induction of LTP and subsequent conversion of E-LTP into L-LTP: mice lacking GluA2 subunit expression can undergo NMDA-independent LTP (Jia et al., 1996, Mainen et al., 1998) presumably due to their ability to conduct Ca^{2+} in an activity-dependent fashion due to voltage-dependent block by intracellular polyamines (Pellegrini-Giampietro, 2003). LTP induction without blocking NMDARs in GluA2-lacking mice results in LTP facilitation from the additive effects of NMDA-dependent and CP-AMPAR-induced LTP (Jia et al., 1996), suggesting CP-AMPARs can work alongside NMDARs to increase the strength of LTP. After induction of LTP, transient trafficking of CP-AMPARs to the postsynaptic membrane has been observed (Plant et al., 2006, Park et al., 2016). Low frequency stimulation after induction is then necessary to convert E-LTP, which is independent of *de novo* transcription, into L-LTP, which is PKA dependent and relies on *de novo* transcription (Huang et al., 1996, Park et al., 2016). If this extra low frequency stimulation was not provided, or blockers of CP-AMPAR activity were included, L-LTP was not induced (Park et al., 2016). This led the authors to conclude that the insertion of CP-AMPARs post-LTP induction was necessary to increase Ca^{2+} entry which facilitates the induction of L-

LTP in response to the low frequency stimulation, and that if this stimulation were not provided, only E-LTP was induced (Park et al., 2016).

However by contrasting two of their previous studies Park et al. (2018) demonstrated that sometimes this extra low frequency stimulation is not necessary (Park et al., 2018). They conclude that "metaplastic effects" could prime for the conversion of E-LTP into L-LTP without needing extra stimulation post-CP-AMPAR insertion, due to CP-AMPARs already being present in the postsynaptic membrane (Park et al., 2018). CP-AMPAR insertion has been seen to occur following acute stress or glucocorticoid application in a PKA-dependent manner (Whitehead et al., 2013) and following exposure to secreted amyloid precursor protein-alpha (sAPPα) (Mockett et al., 2019) and in both cases results in the facilitation of E-LTP conversion to L-LTP.

The rectification experiments presented here in Figure 5.1, and the gene expression data from Chapter 4 (Figure 4.8) demonstrate a clear role for EE in modulating the expression of CP-AMPARs both at the functional synaptic level and the genetic level. This effect is MSK1-independent, and electrophysiologically, does not appear to have been reported before. A previous study demonstrated that following 40 days (5-6 wks) of EE, 9-10 wk old mice significantly upregulate GluA2 mRNA expression within the hippocampus (Naka et al., 2005). This result by Naka et al. (2005) matches the rectification index experiments presented here in mice following both 1 wk and 5 wks of EE, and demonstrates that the mRNA expression profile at earlier stages of EE (5-6 wks) is the opposite of that described here at 3 months of EE. EE in this regard may function as a metaplasticity event able to regulate the presence of CP-AMPARs present at the postsynaptic membrane before LTP induction occurs. Conversely, EE could regulate the GluA2 subunit composition of the intracellular pool of AMPARs. Due to the general facilitation of LTP in WT mice observed following EE (Ohline and Abraham, 2019, Privitera et al., 2020), and the emerging importance of transiently inserted CP-AMPARs in LTP formation (previous two paragraphs), of great interest would be performing LTP induction experiments in CP-AMPAR blockers in animals from both a EE and SH. Perhaps the EE-dependent regulation of CP-AMPARs may underlie the enhancement in LTP generally displayed following EE.

5.3.2 Neither the kinase activity of MSK1, nor environmental enrichment affect pre-synaptic release probability at SC/CA1 synapses

As expected, due to lack of a basal difference in SH conditions between WT and MSK1 KD mice (Daumas et al., 2017), and consistent prior observations of a lack of modulation by EE (Ohline and Abraham, 2019), paired-pulse ratio was unchanged by either loss of MSK1 kinsase activity, acute (1 wk) or more standard periods of EE (5 wks), or any interaction between the two. This experiment was conducted to parallel Input-output experiments, to ensure any change observed in synaptic transmission was due to postsynaptic receptor differences. This observation was further strengthened by a lack of difference in mEPSC frequency between either genotype, nor as a result of either 1 wk, or 5 wks of EE. This result was in line with previous observations with MSK1 KD mice and comparable periods of EE (Corrêa et al., 2012, Lalo et al., 2018) and was conducted here to rule out a pre-synaptic role in any observed changes in synaptic transmission.

5.3.3 EE induces a temporary reduction in excitatory transmission at glutamatergic synapses in response to EE following 1 wk of EE, that is not present by 5 wks of EE and this may be regulated by MSK1.

A significant reduction in AMPAR-mediated glutamatergic transmission was observed in WT but not MSK1 KD mice following 1 wk (Figure 5.5 A) but not 5 wks of EE (Figure 5.5 B), indicating that MSK1 may have short-term role in reducing glutamatergic transmission immediately after entry into a novel or complex environment, which is not present by 5 wks of EE. This decrease in mEPSC amplitude at 1 wk in WT mice may therefore be part of a normal MSK1-dependent response to EE that eventually leads to an increase during periods of longer exposure. However as explored in Figure 5.6, despite the significance of this observed effect, removal of just 4 outlier points (Figure 5.6 A) is enough to abolish this effect (total n for 1 wk WTSH group = 35), instead revealing that 1 wk of EE results in a significant reduction of mEPSC amplitude in both WT and MSK1 KD mice (Figure 5.6 B). This effect of housing, independent of genotype, was also seen in Figure 5.5 A.

No difference in mEPSC amplitude after 5 wks of EE was unexpected, as previously, WT mice housed in EE from birth for 6-8wks have demonstrated a significant increase in mEPSC amplitude, whereas MSK1 KD mice do not (Corrêa et al., 2012)(Lalo et al., 2018). This could be a reflection of the type of EE used (acute EE where adults were transferred from SH instead of being born there). Other EE paradigms that utilise EE periods of 4-5 wks beginning at a postnatal stage (housing from p25) demonstrate no effect on mEPSC amplitude, but an increase in frequency (Malik and Chattarji, 2012), which was also not demonstrated here. This discrepancy between these results and Corrêa et al., (2012) (6-8 wks EE from birth) and Lalo et al. (2018) (6-12 wks EE; 9-15months EE from birth) demonstrating mEPSC amplitude increases following EE could also be due to the shorter lengths of EE used, however 8-12 wk periods of EE (not from birth) have failed to show an increase in CA1 mEPSC amplitude (Duffy et al., 2001, Eckert et al., 2010) and so the duration of EE utilised here is unlikely to be an issue, instead the differences are likely to come from the postnatal housing of the mice used here, rather than exposure to EE from birth as in (Corrêa et al., 2012) and (Lalo et al., 2018).

5.3.4 1 wk and 5 wks of EE may be too short to observe gross apical dendrite structure changes, however MSK1 may regulate dendrite reorganisation from layers stratum radiatum to lacunosum moleculare following acute periods of EE

8-10 wk old MSK1 KO mice have previously demonstrated decreased dendritic complexity in CA1 neurons compared to WT mice after housing in both a basal SH condition and also after 5 – 6 wks of EE (Karelina et al., 2012). In this Chapter, no effect of MSK1 kinase inactivation on gross dendritic complexity was observed following neither 1 wk, nor 5 wks of EE, calling into question the involvement of MSK1 kinase activity with the large effect of MSK1 knock out mutation previously observed on dendritic branching complexity (Karelina et al., 2012) . Regardless of any effect of EE, MSK1 KD mice do not display the basal dendrite complexity deficit observed in MSK1 KO mice when compared with WT controls under standard housing conditions. This implies that MSK1 does not regulate CA1 basal dendrite complexity, in contrast to the phenotype observed (Karelina et al., 2012) in MSK1 KO mice.

Additionally, as can be seen in Figure 5.9 and 5.10, neither 1 wk nor 5 wks of EE was sufficient to increase dendritic branching complexity compared to standard housed controls. In the above study by Karelina et al., (2012), WTSH and WTEE neurons were not directly compared statistically after EE, but there does appear to be a small increase in WT CA1 neuron complexity after 5 – 6 weeks of EE (Karelina et al., 2012). This indicates that the length of EE used here was sufficient to observe an overall dendritic differences in WT mice, but this was not the case (Figure 5.9 B-E; Figure 5.10 B-E). Consistent increases in dendritic branch complexity have been observed in CA1 neurons after 3 months of EE (15 wk old mice) (Lauterborn et al., 2013) and 4-5 months of EE (18-22 wk old mice) (Faherty et al., 2003). One explanation for the lack of difference in overall dendritic morphology seen in this study between WTSH and WTEE mice it that the length of EE was therefore not long enough at 5 wks of EE. 10 days of EE, whilst sufficient to observe increases in DGC dendrite complexity, is insufficient to significantly increase dendritic complexity in WT CA1 pyramidal neurons (Beauquis et al., 2010). Perhaps dendritic changes are more robust after longer periods of EE such as the 4 – 5 months of EE employed by Faherty et al. (2003), which would actually be consistent with the large number of structural GOTerms observed after 3 months of EE in Chapter 4. In this case, maybe 5 wks of EE not long enough to observe structural plasticity of CA1 apical dendrites, but is long enough to observe the synaptic transmission changes described above. Repeating this study with a 3 month EE timepoint would both aid in comparison to the RNAseq experiment in chapter 4, and would help answer this question.

An additional explanation - provided here as a possibility and not to disparage former studies - is that CA1 reconstructions following EE tend to be performed using the Golgi-Cox method of immunostaining (Faherty et al., 2003, Karelina et al., 2012) which could be vulnerable to selective bias due to the unknown mechanism of neuronal selection for staining and the manual selection of neurons. Golgi staining may preferentially stain more complex neurons, or manual selection of neurons may be biased towards the most complex, especially if experimenters are not blind to condition. Here neurons were filled and stained with no knowledge of their dendritic complexity. The random sampling of neurons stained here may underlie the lack of an effect of acute enrichment on WT neurons observed.

Here two observations were made that, whilst not particularly compelling on their own, may indicate an underlying shift in dendrite distribution between different layers of the hippocampus. The decrease in mEPSC rise time observed in MSK1 KD but not WT mice following 1 wk of enrichment in Figure 5.5 E could indicate that an MSK1-dependent distal shift in synaptic connections to SLM from the SR occurs in response to acute enrichment. Likewise in Figure 5.9 A, an apparent shift in the distribution of apical dendrites belonging to WT and MSK1 KD mice after 1 wk of EE occurs, with significant reductions in dendrite complexity occurring in 1 wk EE mice throughout the SLM despite no increase in total size or complexity of the apical dendrite. This could indicate that acute periods of EE cause a shift in synaptic input of CA1 pyramidal cells from the SLM to the SR, featuring synaptic reorganisation starting at 1 wk EE. This may result in a shift in the kinetics of dendritic signalling, with shorter rise times due to the more proximal location of input relative to the soma, that is somehow compensated for by MSK1 kinase activity. This may be related to MSK1's role in modulating the increase in dendritic spine density in the SR in response to EE (Corrêa et al., 2012) – occurring in tandem with dendritic reorganisation. This would decrease the proportion of postsynaptic potentials from layer III of the EC via the Temporoammonic pathway, perhaps biasing CA1 neurons to SC input. As discussed in Section 1.1.3, pgs 9-11 the SC pathway contains afferents from CA2 and CA3 neurons which synapse with CA1 neurons. Signalling from CA3 neurons appears to underlie the recall of spatial information (Brun et al., 2002, Nakazawa et al., 2002), encoding spatial information (Nakazawa et al., 2003, Nakazawa et al., 2004) and the acquisition of contextual fear memory (McHugh and Tonegawa, 2009). Signalling from area CA2 may play a role in spatial memory (Lee et al., 2010) and social recognition memory (Stevenson and Caldwell, 2014, Hitti and Siegelbaum, 2014, Tzakis and Holahan, 2019). This could therefore underlie part of the improvements in spatial learning and memory observed after EE exposure (Huang et al., 2006, Hendershott et al., 2016). MSK1 KD mice do not display a deficit in spatial learning or memory under basal SH conditions (Daumas et al., 2017). Therefore it would be interesting to test the spatial memory of MSK1 KD mice after these acute (1 wk and 5 wks) periods of EE and to repeat input-output experiments performed by stimulating the SR, here (Figure 4.3) and by others (Daumas et al., 2017), in the SLM, to confirm synaptic and behavioural consequences of such a shift.

Overall, this chapter demonstrates that exposure to EE for a period of 1 wk is enough to see changes in glutamatergic synaptic transmission strength, however by 5 wks, this effect is no longer visible. This effect may be MSK1-dependent, but further experimentation is required to confirm this. MSK1 kinase activity is also implicated in regulating dendritic reorganisation, but not gross complexity changes in response to EE that may favour SC over TA input to CA1 neurons. Neither the kinase activity of MSK1, nor EE affected presynaptic release probability, and the results of Input-output experiments designed to measure basal synaptic transmission were inconsistent between experimental groups. Also seen is that acute exposure to EE for 1 wk and 5 wks decreases functional expression of CP-AMPARs at glutamatergic synapses in contrast to the downregulation of GluA2 observed after 3 months of EE from the RNAseq results in chapter 4. This biphasic regulation of CP-AMPAR expression across EE timepoints, that is independent of MSK1 function, could be important as an underlying mechanism for EE-induced plasticity changes.

Chapter 6: Evaluating the role of MSK1 kinase activity in regulating the effect of EE on hippocampus-dependent spatial memory, social preference and social novelty

6.1 Introduction

So far in this thesis the role of MSK1 kinase activity has been investigated in the transcriptomic, cellular and synaptic response to EE. Translation of these changes to the behavioural level is essential in understanding the functional outcome of these observed differences mediated by the kinase activity of MSK1. Exposure to EE has been shown to enhance learning and memory in many different behavioural tasks (Sampedro-Piquero and Begega, 2017, Hendershott et al., 2016). EE improves performance in the MWM spatial memory-dependent task (Falkenberg et al., 1992, Hendershott et al., 2016, Frick et al., 2003) and in novel object recognition (NOR) (Novkovic et al., 2015, Mesa-Gresa et al., 2013). EE has also been seen to reduce anxiety (Sampedro-Piquero and Begega, 2017, McQuaid et al., 2018) and improve sociability behaviour (McQuaid et al., 2018, Gubert and Hannan, 2019). Exposure to EE has also been seen to ameliorate certain pathology-related behavioural deficits in rodent models of disease including epilepsy, Alzheimer's disease and traumatic brain injury (Nithianantharajah and Hannan, 2006, de la Tremblaye et al., 2019).

Previous work with MSK1 KO mice has highlighted a role for MSK1 in the regulation of several types of behaviour affected by EE (Reyskens and Arthur, 2016). MSK1 KO mice display normal motor and cerebellar function and have been reported to show normal locomotion and anxiety, however MSK1 KO mice present deficits in MWM spatial memory and contextual fear conditioning (Chwang et al., 2007) and fail to demonstrate EE-induced improvement in NOR and Barnes maze performance compared to WT mice (Karelina et al., 2012). Interpretation of these MSK1 KO-mediated behavioural deficits has however been performed on the assumption that observed deficits are due to loss of MSK1 kinase activity effect (Karelina et al., 2012, Chwang et al., 2007), and are not due to other potential functions of MSK1 such as protein interactions or mediating interactions between other proteins, compensatory effects in related kinases resulting from gene knockout, or another unknown effect unrelated to kinase activity. This assumption has been tested through the selective

inactivation of the kinase domain of MSK1 in MSK1 KD mice: MSK1 KD mice fail to recapitulate the deficits in spatial memory observed in the MWM by MSK1 KO mice, with MSK1 KD mice performing normally at multiple different kinds of MWM assay designed to test both spatial working memory and learning (Daumas et al., 2017).

Spatial memory differences between MSK1 KD and KO mice could be due to another structural role of MSK1 independent of its kinase domain, such as the structural role for MSK1 in complex with the glucocorticoid receptor and Erk1/2 during behavioural responses to stress (Gutièrrez-Mecinas et al., 2011). Alternatively, In mouse embryo fibroblast cell lines, phosphorylated MSK1 has been shown to physically interact with a complex between the H3K4-specific methyltransferase lysine methyltransferase 2A (Kmt2a) and mixed-lineage leukemia 1 (Mll1) where MSK1 contributes to Kmt2a-dependent transcription (Wiersma et al., 2016). Ablation of the nuclear localised Mll1 in the prefrontal cortex of adult mice disrupts the Kmt2a/Mll1 complex, and results in impaired spatial working memory and deficits in the activity-dependent expression of Arc/Arg3.1 (Jakovcevski et al., 2015). Forebrain ablation of Kmt2a - resulting in knock-down of expression within the hippocampus - however presented spatial memory deficits in the MWM, and impaired fear conditioning, though object recognition was unaffected (Kerimoglu et al., 2017). Additionally, the Mll family have been shown *in vitro* to bind CBP cooperatively with CREB (Ernst et al., 2001). It is therefore possible that MSK1 interacts with this Kmt2a/Mll1 complex within hippocampal neurons *in vivo* and could regulate its transcriptional activity or provide a role stabilising the whole complex.

To better understand the role the kinase activity of MSK1 plays in spatial memory, a hippocampus-specific spatial memory task: Object-location memory (OLM) (Barker and Warburton, 2011), in which performance has previously seen to be improved after EE (Gobbo and O'Mara, 2004), was performed to try to relate hippocampal signalling to behavioural output. In addition to testing hippocampus-dependent spatial memory, the role of MSK1 KD in a more complex behaviour modulated by EE was also investigated. Rodents are naturally social creatures, displaying a preference for social interaction and novel social interactions, behaviours (Moy et al., 2004, Hendershott et al., 2016) that seem to be regulated by circuits involving the hippocampus, medial amygdala and prefrontal cortex (Bicks et al., 2015). Social isolation causes a reduction in BDNF expression within the hippocampus (Murínová et al.,

2017), in contrast with the increase in BDNF expression typically experienced by enriched rodents (Novkovic et al., 2015). One of the characteristics of the EE housing paradigm is an increase in social stimulation through the inclusion of additional cage mates. Previous work has observed that mice exposed to EE display an enhanced preference for social interaction (social preference) (Rae et al., 2018, Redolat and Mesa-Gresa, 2012) and a preference for social interactions with mice that are novel to the EE mouse (social novelty) (Hendershott et al., 2016, Gubert and Hannan, 2019). Here, the effect of EE on the spatial memory dependent task object location memory and on social preference and social novelty of WT and MSK1 KD mice was assessed in order to better understand the role MSK1 may play in modulating these behaviours and any improvement conferred by EE.

6.2 Results

6.2.1 No effect of MSK1 kinase activity was observed in regulating the effect of EE on a primarily hippocampus-dependent spatial-memory task.

WT and MSK1 KD mice were standard housed to approx. 2.5 mths of age before being split into EE and SH groups. Mice were housed in EE, or continued SH for a further 4 weeks, before being taken for OLM testing. A summary of the OLM testing employed is presented in Figure 6.1 A. MSK1 KO mice have previously been observed to show no anxiety differences compared to WT animals during open field testing (Chwang et al., 2007). MSK1 KD mice also do not display anxiety differences compared with WT animals when tested using the open plus maze (Frenguelli lab, unpublished). To ensure any behavioural effects observed here were not due to anxiety differences between groups induced by either experimenter or experimental set up, WT and MSK1 KD mice were placed into an open-field chamber and allowed to freely explore during the habituation stage of the OLM assay. Due to the thigmotaxic preference of rodents, time spent in the centre of the chamber was used as a metric for anxiety.

No differences in anxiety were observed between conditions as shown in Figure 6.1 B (2-way ANOVA, housing vs genotype). Total distance moved was not significantly different between conditions during the “habituation” and “baseline” OLM trials, however a significant effect of both genotype ($F(1,27) = 5.95$, $p = 0.023$) and housing ($F(1,27) = 5.99$, $p = 0.022$) was observed during the “test” OLM trial (Figure 6.1 C). Due to a lack of interaction effect, post-hoc testing was not performed, however the mean distance travelled by the WTSH group (24m +/-1.53) appeared greater than the other three groups which displayed comparable means (18.25 +/- 1.22, WTEE; 18.26 +/- 1.13, KDSH; 16.84 +/- 1.83, KDEE). This suggests that the significantly reduced movement seen in both MSK1 KD mice, and mice after EE (genotype and housing effects) observed here are primarily determined by the increased movement of WTSH mice.

Total object investigation time was next looked at in “Baseline” (both objects, not moved) and “Test” (both objects, one moved) trials in order to ascertain differences between

conditions in exploring the objects. During the “Baseline” trial, total object investigation time was not significant between condition, however a significant effect of genotype was observed on total object investigation time during the test trial (2-way ANOVA; $F(1, 27) = 15.34$, $p = <0.001$), with MSK1 KD mice spending significantly less time investigating either the moved or unmoved object than WT mice (Figure 6.1 D). In addition to this, 4 mice (3 x KDSH, 1 x KDEE) did not meet the minimum object investigation criteria of 10s total investigation during baseline or test trial necessary to ensure proper object investigation had occurred, and were removed from further object discrimination index analysis (Figure 6.1 E). These excluded mice are highlighted with red circles in Figure 6.1 D, along with the object investigation time cut-off. On average, all conditions showed a preference for investigating the moved object instead of the stationary object, displaying an average discrimination index >0 which would indicate no preference for either object (Figure 6.1 E). However, no significant effect of housing or genotype was observed on discrimination index, which represents the preference of a mouse for investigating the moved object (due to novel position), between conditions between conditions (2-way ANOVA, housing vs genotype). Preference for the moved object in EE conditions may be occluded by the EE housing paradigm itself, within which objects are moved regularly and do not confer reward upon investigation.

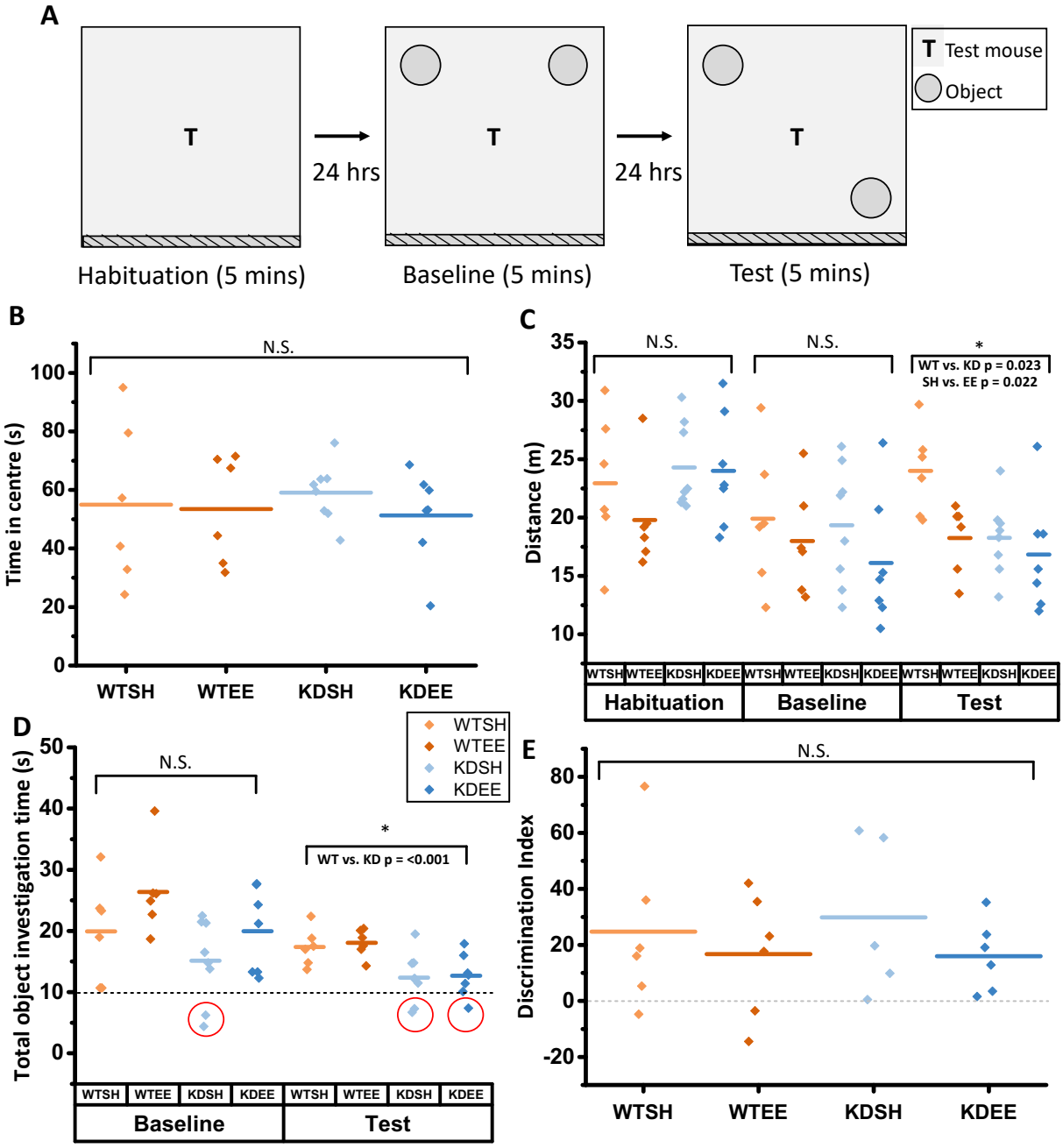

Figure 6.1. Summary of object-location memory (OLM) experiments. A) Graphical summary describing order of testing: Habituation (5 mins) of the test mouse to the test chamber was followed 24 hrs later by baseline testing (5 mins) where the mouse freely explored the chamber with two identical objects present placed opposite a striped wall (for spatial reference). On the final day, 24 hrs after baseline assay, the test phase was conducted (5 mins). Two objects (identical to the ones already seen in baseline assay) are placed, one in the previous position away from the striped wall, and one "moved" object diagonally across the chamber and the mouse left to freely explore the chamber. Left/right object movement was randomly assigned to first animal of a group and then alternated within group. **B)** No difference in anxiety was observed between groups as measured by total time (s)

spent in the centre of the empty chamber during habituation phase. **C)** Mean speed (m/s) of test mice from EE conditions (WTEE, KDEE) was overall slightly lower across the three test phases but was comparable across groups. **D)** Total object investigation time (s) appeared variable between conditions. Grey line represents 10s threshold for minimum total investigation time of both objects in baseline and test phases. **E)** Discrimination index for moved object vs. stationary object (arbitrary units). No significant difference in preferential investigation of the moved object could be observed between conditions. n for each condition: WTSH = 6; WTEE = 6; KDSH = 5; KDEE = 6.

6.2.2 Effect of MSK1 kinase activity in regulating the effect of EE on social preference and social novelty

One week following OLM testing, sociability and preference for social novelty were assessed for WT and MSK1 KD mice housed either in EE for 5 wks, or SH. Social preference and social novelty were assessed using a three-chamber design (Kaidanovich-Beilin et al., 2011) based on the assay developed by Crawley and colleagues (Moy et al., 2004) which is summarised in Figure 6.2 A below. Following habituation of test mice to the chamber, novel WT mice never before encountered by the test mice were used to gauge social interaction preference. Test mice were offered a choice between interacting with an empty wire cup, or a cup containing: “Stranger 1” for 10 mins. Time in each chamber and interaction with each cup were measured to get a preference index for sociability. The empty cup was then replaced with a second novel WT mouse not previously encountered by the test mouse: “Stranger 2”. Preferential interaction with Stranger 2 over Stranger 1 was used as a metric for social novelty, due to the mouse already having interacted with Stranger 1 for 10m.

As seen in Figure 6.2 B, during the “habituation” stage of testing, MSK1 KD mice (KDSH + KDEE) travelled a significantly greater distance (as measured by average speed) than WT mice (WTSH +WTEE) (WT = 0.362m/s +/- 0.030 vs. MSK1 KD = 0.442m/s +/- 0.026: $F(1,27) = 4.48$, $p = 0.045$). Average speed was used as a metric of distance in this experiment, by dividing the total distance travelled by the different test trial time lengths (5m, 10m and 10m), to facilitate distance visual comparison between each trial (Figure 6.2 B). No significant genotype differences in average distance travelled were observed during later trials (“stranger 1” and “stranger 2”; Figure 6.2 B). However a significant EE-dependent reduction in average movement speed for both WT and MSK1 KD mice was observed across all testing

trials (“habituation”: SH = 0.461 +/- 0.030 vs. EE = 0.348+/- 0.022 (F(1,27) = 9.09, p = 0.006); “stranger 1”: SH = 0.486 +/- 0.011 vs. EE = 0.433 +/- 0.058 (F(1,27) = 6.74, p = 0.016); “stranger 2”: SH = 0.376 +/- 0.019 vs. EE = 0.296 +/- 0.014 (F(1,27) = 10.42, p = 0.004), Figure 6.2 B) which is consistent with other studies (Rae et al., 2018). Time spent in each room (containing either empty cup (EC), stranger mouse 1 or stranger mouse 2 depending on trial), during the latter two trials: “stranger 1” and “stranger 2” is displayed as paired data in Figures 6.2 C and 6.2 D respectively to visualize the raw data, however analysis was carried out by taking ratios of these data points and is explored below.

To more accurately quantify differences between conditions, a preference index was calculated for time spent in each chamber containing Stranger 1 (social preference) or Stanger 2 (social novelty) normalised to time spent with the empty cup and Stranger 1 respectively. Despite an increased preference for time spent in the chamber containing Stranger 1 vs. empty cup in both WT and MSK1 KD mice following EE compared to SH controls (WTSH = 6.8 $\pm$ 6.0; WTEE = 21.6 $\pm$ 6.7; KDSH = 6.25 $\pm$ 6.7; KDEE = 21.8 $\pm$ 5.7), no significant effect of housing or genotype was observed as assessed with 2-way ANOVA (Figure 6.2 E). Neither was an effect of genotype or housing found in time spent in the chamber containing Stanger 2 during social novelty assay (WTSH = 17.4 $\pm$ 9.1; WTEE = 15.6 $\pm$ 5.1; KDSH = 7.0 $\pm$ 5.5; KDEE = 25.6 $\pm$ 5.6) as seen in Figure 6.2 F.

Quantification of cup investigation by the test mouse however revealed housing and genotype differences in both social preference and social novelty: Social preference testing as shown in Figure 6.2 G, showed EE mice spent significantly more time investigating Stranger 1 than the empty cup (SH vs. EE, F(1, 23) = 4.47, p = 0.046; WTSH = 25.9 $\pm$ 5.2; WTEE = 45.1 $\pm$ 5.5; KDSH = 18.0 $\pm$ 10.3; KDEE = 36.1 $\pm$ 5.8), indicating an EE-induced increase in sociability occurs independently of MSK1 kinase function. Social novelty preference was significantly reduced in MSK1 KD mice compared to WT mice independent of EE (WT vs. KD, F(1, 23) = 7.06, p = 0.014, WTSH = 43.8 $\pm$ 9.6; WTEE = 20.8 $\pm$ 6.0; KDSH = 14.1 $\pm$ 4.2; KDEE = 1.8 $\pm$ 10.5) demonstrating a basal deficit in MSK1 KD mice in preference for social novelty (Figure 6.2 H).

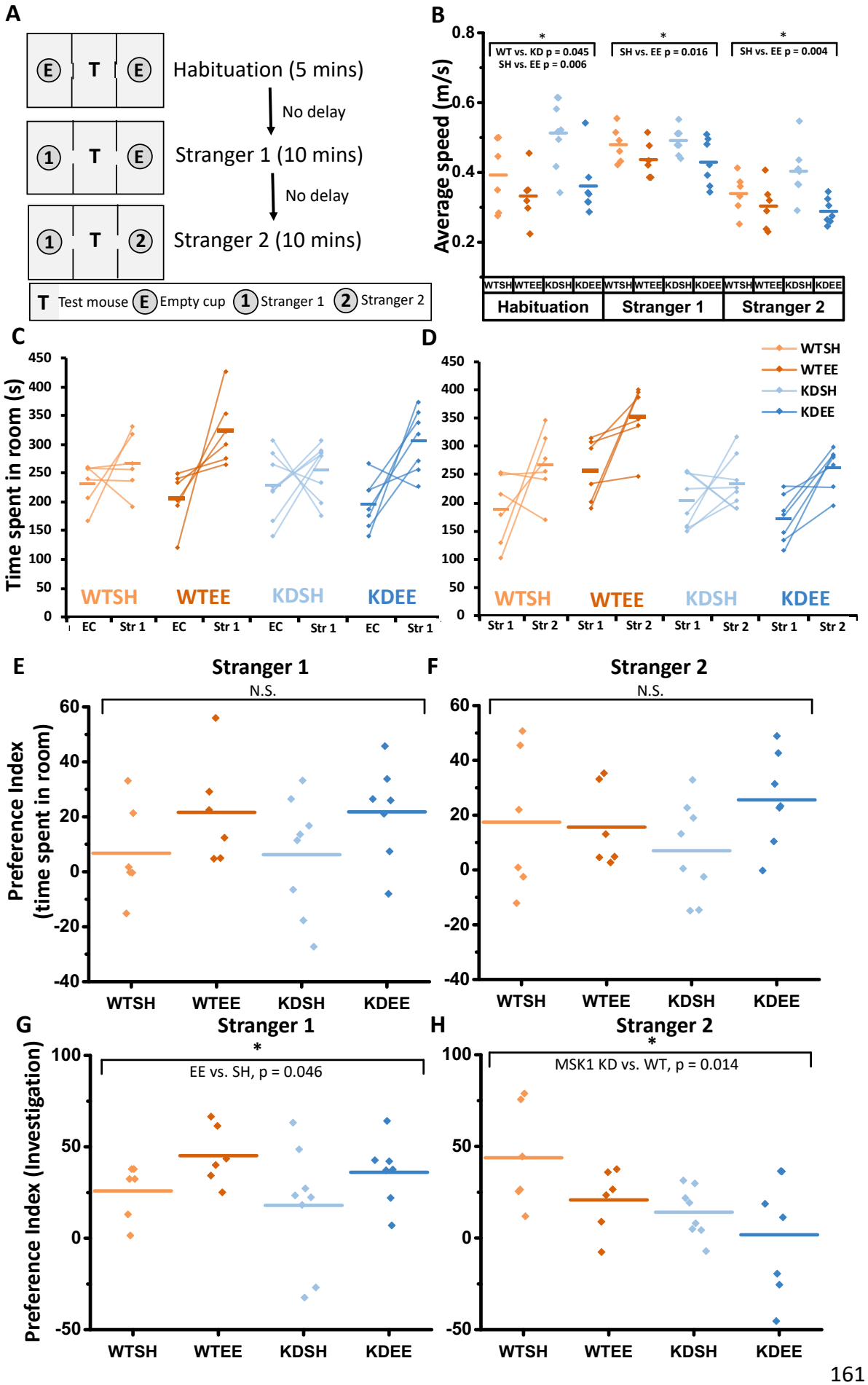
A
E T E
Habituation (5 mins)
No delay
1 T E
Stranger 1 (10 mins)
No delay
1 T 2
Stranger 2 (10 mins)
T Test mouse E Empty cup 1 Stranger 1 2 Stranger 2
B
Average speed (m/s)
WT vs. KD p = 0.045
SH vs. EE p = 0.006
SH vs. EE p = 0.016
SH vs. EE p = 0.004
WTSH WTEE KDSH KDEE
Habituation
Stranger 1
Stranger 2
C
Time spent in room (s)
WTSH WTEE KDSH KDEE
EC Str 1
D
WTSH
WTEE
KDSH
KDEE
Str 1 Str 2
E
Stranger 1
N.S.
Preference Index (time spent in room)
F
Stranger 2
N.S.
G
Stranger 1
EE vs. SH, p = 0.046
Preference Index (Investigation)
H
Stranger 2
MSK1 KD vs. WT, p = 0.014

Figure 6.2. Summary of social preference and social novelty experiments. A) Graphical summary describing order of testing: Habituation (5 mins) of the test mouse to the central room was then followed by replacing one of the empty cups with a cup containing stranger 1 (left/right position alternated within experimental group), and removal of doors to left and right rooms. The test mouse was then allowed to freely explore both rooms for 10 mins, one containing an empty cup, the other stranger 1, allowing observation of test mouse's preference for social interaction. The remaining empty cup was then replaced with a cup containing stranger 2, and the test mouse allowed to explore both rooms freely once more, allowing observation of test mouse's preference for social novelty.
B) Average movement speed (m/s) of each experimental group (WTSH, WTEE, KDSH, KDEE) across each test stage. Average move speed was used to represent overall mouse locomotion due to the different lengths of the habituation (5 mins) and stranger 1 and stranger 2 testing stages (10 mins each). EE groups (WTEE, KDEE) display slightly lower average movement speed compared to SH groups (see text for statistics).
C) Stranger 1 trial: Time spent in each room (s) containing either empty cup (EC), or stranger 1 (Str 1).
D) Stranger 2 trial: Time spent in each room (s) containing either stranger 1 (Str 1), or stranger 2 (Str 2).
E + F) Preference index for time spent in Stranger 1 room over empty cup room: No significant difference preference for time spent in room with stranger 1 over empty cup was observed between conditions (E). No significant preference for time spent in room with stranger 2 over stranger 1 was observed between conditions (F).
G)Both WT and MSK1 KD mice display significantly increased preference for investigating stranger 1 over empty cup following EE (Effect of housing: SH vs. EE, $F(1, 23) = 4.47$, $p = 0.046$) (G).
H) WT mice display significantly increased preference for investigating novel stranger 2 over familiar stranger 1 compared to MSK1 KD mice (Effect of genotype: WT vs. KD, $F(1, 23) = 7.06$, $p = 0.014$) (H).
n for each condition: WTSH = 6; WTEE = 6; KDSH = 8; KDEE = 7.

6.3 Discussion

6.3.1 The kinase function of MSK1 does not regulate spatial memory acquisition and retrieval during an object-location memory task, but may play some role in novelty motivation during investigation.

Due to a lack of significant effect between conditions on preferential investigation of the moved object (Figure 6.1 E), the kinase activity of MSK1 does not seem to underlie hippocampal-dependent spatial memory in an OLM assay. All conditions in the OLM assay did appear to display an apparent overall preference for investigating the moved object, as the average discrimination index for each group >0 (Figure 6 E), indicating that there was sufficient time to form a spatial reference memory during the baseline stage and that a 24hr delay was not too challenging. However this may mean that the assay was not challenging enough to expose subtle differences between genotypes. In support of this, a 5m baseline trial, used in these series of experiments, is typically long enough to form 24hr object location memory retention in WT mice, and sufficient to detect the significant effects of both a gross knockout mutation affecting Erk1/2 signalling (Haettig et al., 2011) and pharmacological blockade of histone acetylation modifications (Seese et al., 2014). However other OLM assay protocols using a similar set up to that used here, but with a 10m baseline and test trial time have displayed greater preference index sizes for the moved object than those obtained here, indicating that longer trial times may increase the effect size, perhaps highlighting more subtle differences between conditions (Au - Denninger et al., 2018). Conversely, a 3m baseline trial is usually not enough to form an adequate memory of object location however, 3 weeks of voluntary exercise, in the form of a running wheel included in housing condition (a key component of the EE paradigm), enables significant discrimination of the moved object in an OLM task with 3m baseline, and is accompanied with an increase in BDNF expression in the hippocampus (Intlekofer et al., 2013). Therefore perhaps increasing baseline trial time to 10m could encourage more successful memory consolidation, whilst conversely decreasing baseline exposure to 3m could increase differences between groups by facilitating significant OLM object discrimination only in EE groups.

Exposure to EE did not have any significant effect on object investigation in the OLM assay for either genotype and actually seemed to slightly decrease preference for the moved object, which was unexpected. This contrasts with studies observing enhanced 24hr inter-trial interval OLM performance following 2-3 weeks of exercise (Intlekofer et al., 2013, Butler et al., 2019). An explanation for the discrepancy between the effect of exercise and the results here, perhaps the preference for the moved object in EE conditions may therefore be occluded by the EE housing paradigm itself, within which objects are moved regularly and do not confer reward upon investigation and thus the movement-induced novelty of the object may provide less motivation for exploration in EE mice. In line with this idea, a reduction in novelty motivation as assessed by exploration of, and locomotion within, a novel environment has been seen to reduce following 2 months EE (de Carvalho et al., 2010). This is likely an effect of the complex environment element of EE, as social enrichment alone (more cagemates only) for 3 months improves OLM performance with a 1 hr inter-trial interval (Smith et al., 2018). This behavioural assay here may therefore not have been appropriate to discriminate the effect of MSK1 kinase inactivation on EE-mediated hippocampus-dependent spatial memory enhancement. A future experiment utilising some form of reward, such as a baited Y-maze wherein mice are allowed to explore both arms during a baseline phase, and the % of correct arm entries (to the arm containing a treat) is monitored in a testing phase after a 24hr delay may be more appropriate. One conclusion that is possible from this OLM assay however, is that the effect of MSK1 kinase inactivation does not appear to significantly affect hippocampus-dependent spatial memory at a baseline (standard housed) level.

An additional consideration of the OLM assay presented here are the sample sizes utilised: WTSH = 6; WTEE = 6; KDSH = 5 (8 tested, 3 removed for low total investigation); KDEE = 6 (7 tested, 1 removed for low total investigation). Other object recognition assays typically utilise around 10-12 animals per condition (Barker and Warburton, 2011, Vogel-Ciernia and Wood, 2014) however, significant differences in OLM performance after 3 weeks exercise have been observed in groups as low as n = 8 (Intlekofer et al., 2013). It is clear that the group sizes employed here of 5 – 6 (after removal of mice below investigation time threshold) are low in comparison to comparable studies. Low sample sizes reduce study power, resulting in detection of only larger effect sizes, and not smaller more subtle differences between conditions (Cohen, 1988). An obvious improvement to this study would be to increase the

group sample sizes to at least 10 animals a group. This was unfortunately not possible during this study due to breeding difficulties and time constraints, but would ensure any missed effects if they exist, are detected.

The effect of genotype on total investigation time observed in Figure 6.1 D occurred in response to a significant reduction in total object investigation time during only the test trial, and not the baseline trial (Figure 6.1 D) in MSK1 KD mice. This may indicate an aversion to the novelty of object positioning, however due to the lack of significant difference in MSK1 KD preference index (Figure 6.1 E) this is unlikely. Perhaps this difference in total object investigation during the test trial, but not baseline trial indicates that MSK1 KD mice experience a lack of motivation to investigate the objects over time. It is not possible from this data to determine whether this is a general effect of repeated exposure to the testing environment, or a product of the novel object positioning in the test trial, but this appears to represent a marked departure from WT behaviour. Perhaps the MSK1 KD mice display a reduction in motivation for object investigation over time compared with WT mice, finding exploration less rewarding. Testing this would be simple through the employ of exploration tests utilising environmental exploration itself as a reward (capitalizing on the rodent desire to reduce environmental uncertainty through exploration) }, or through food rewards of different magnitudes (Spangenberg and Wichman, 2018).

In conclusion, this OLM assay indicated that the kinase inactivation of MSK1 does not significantly affect spatial memory acquisition or recall in an object location task, which is in line with previous studies demonstrating that, under standard housing conditions, MSK1 KD mice perform comparably to WT mice in spatial memory acquisition assays (Daumas et al., 2017, Privitera et al., 2020). 5 weeks of environmental enrichment did not significantly alter object discrimination in response to novel location positioning in either MSK1 KD nor WT mice, however this may have been due to the length of time used for the baseline trial for reference memory formation. The additional observed effect of MSK1 kinase inactivation on total object exploration during OLM test trials may indicate an effect of MSK1 kinase activity on object exploration motivation in general however, a more specific assay to test this behaviour is desired.

6.3.2 The kinase function of MSK1 is implicated in the regulation of social novelty behaviour, but this effect is not EE-dependent.

Social novelty preference was not increased by 5 weeks of EE as expected (Hendershott et al., 2016), but actually seemed to decrease in both genotypes following EE (Figure 6.2 H). Interestingly however, irrespective of housing condition, an MSK1-dependent decrease in social novelty preference was observed (Figure 6 H) which does not seem to be due to a fear of the novel mouse, as mice did not display significantly less time in the chamber containing Stranger 2 compared to WT mice (Figure 6.2 F). Addtionally, as hypothesised, EE significantly enhanced social interaction behaviour (Figure 6.2 G), however this effect was independent of MSK1 kinase activity.

MSK1 KD mice could therefore present a mild form of autistic-like behaviour, and which may manifest itself in complex social interactions which can be a result of neurodevelopmental differences (Moy et al., 2004). However caution should be used when interpreting this observation of social novelty preference reduction in MSK1 KD mice as a study utilising a modified version of this paradigm - in which Stranger 2 swaps position with Stranger 1 upon introduction - saw a loss of the social novelty effect (Pearson et al., 2010) implying this behaviour was more dependent on spatial memory than preference for social novelty. Validation of these results with the same paradigm modification would therefore be necessary to establish whether this effect is due to spatial, or social memory differences.

Overall, the sociability behaviour assays conducted here demonstrate a novel role for MSK1 in potentially influencing social recognition and novelty in mice that has not been demonstrated previously, and more specifically implicate the kinase activity of MSK1 in mediating this behvaiour, distinct from other structural roles for the MSK1 protein potentially disrupted in MSK1 KO mice. MSK1 KD mice still respond to EE, exhibiting an increased preference for sociability with other mice in line with WT mice post-EE (Figure 6.2 G) however the normal preference for novel social interactions is lost in MSK1 KD mice, possibly due to either deficts in social memory, or in motivation to seek out novel encounters. However a spatial memory component to this cannot be ruled out, and further experiments are required to sufficiently validate this.

Chapter 7: Overall Discussion

7.1 Summary of experimental rationale and perspective

Environmental enrichment has emerged as a tool for understanding what effects increased cognitive engagement, social stimulation and exercise have in reducing the pathologies of various neurological diseases such as Parkinson's disease, amyotrophic lateral sclerosis, fragile X syndrome, Huntington's disease and Down syndrome (van Praag et al., 2000, Nithianantharajah and Hannan, 2006) and neurological damage such as ischemic stroke and other forms of brain injury (McDonald et al., 2018, Quattromani et al., 2018). EE has also been seen to ameliorate age-related cognitive decline (ARCD) and dementia by observing its effects on aged animals alongside pharmacological and genetic models of dementia diseases (Nithianantharajah and Hannan, 2006, Redolat and Mesa-Gresa, 2012). Improvements in outcome for such models after exposure to environmental enrichment highlight the benefits that can be derived from this non-pharmacological intervention in the prevention and management of such diseases (Sampedro-Piquero and Begega, 2017). Higher levels of education, higher IQ and social stimulation are thought to form a "cognitive reserve" within humans that has been likened to a form of human environmental enrichment and are associated with a lower risk for developing Alzheimer's disease, and a reduction in morbidities associated with ARCD (Stern, 2012, Thow et al., 2017). By understanding the beneficial effects environmental enrichment can exert on the brain, both in general and within disease models, perhaps the mechanistic basis underlying such improvements in cognitive function can be elucidated and potentially used to inform pharmacological or experiential interventions for various neurological impairments, whether associated with disease, damage or age.

This thesis has looked at one such mechanism implicated in underlying some of the positive effects of environmental enrichment on the hippocampus: the MSK1-mediated phosphorylation of CREB and histone H3 in response to the neurotrophin BDNF, known to be upregulated as a result of enrichment (Novkovic et al., 2015, Gobbo and O'Mara, 2004). The hippocampus plays a well characterised role in the processing and storage of spatial learning and memory (Andersen et al., 2009) and as discussed earlier, is subject to alterations in synaptic plasticity, transmission and structure by EE (Mora et al., 2007, Ohline and Abraham,

2019). These changes are hypothesised to underlie the positive effects of EE on learning and memory, however how these are regulated at the molecular level is still unclear.

BDNF signalling via the TrkB receptor has been implicated in regulating several kinds of learning and memory (Minichiello et al., 1999, Yamada and Nabeshima, 2003, Minichiello, 2009, Schildt et al., 2013) and deficits in BDNF expression impair synaptic plasticity and spatial memory in NOR assays (Novkovic et al., 2015). The downstream target of the TrkB receptor Erk1/2 (Minichiello, 2009) activates MSK1 and phosphorylates histone H3 and the transcription factors CREB and ATF-1 (Arthur, 2008). CREB phosphorylation and IEG expression in response to BDNF stimulation has been observed to require MSK1 (Arthur et al., 2004, Soloaga et al., 2003), and MSK1 is also implicated in mediating environmental enrichment-induced improvements in spatial memory and dendritic spine density (Karelina et al., 2012, Corrêa et al., 2012).

MSK1 is the predominant MSK isoform expressed within the brain (Arthur et al., 2004) and is localised to the nucleus of neurons (Frenguelli and Correa, 2012). MSK1 KO mutants display deficits in hippocampal-dependent fear conditioning and spatial memory tasks and in both CREB and histone H3 phosphorylation (Reyskens and Arthur, 2016, Karelina et al., 2012, Chwang et al., 2007). CREB is an evolutionarily conserved transcription factor that is heavily implicated in regulating gene expression necessary for learning and memory (Alberini and Kandel, 2014, Lisman et al., 2018, Sakamoto et al., 2011). MSK1 is therefore well positioned to regulate transcriptomic changes that are implicated in learning and memory in response to activity-dependent changes in BDNF expression, such as occurs during environmental enrichment.

Previous studies with MSK1 KO mice have, however been unable to show that the kinase activity of MSK1, and not a structural role exclusively regulates these changes. This is supported by recent work with a mouse homozygous for a kinase inactivating mutation of MSK1 (MSK1 KD). MSK1 KD mice no not display basal deficits in spatial learning and memory (Daumas et al., 2017) in contrast with previous studies using MSK1 KO mice (Karelina et al., 2012). The kinase activity of MSK1 has been observed to regulate homeostatic plasticity changes including dendritic spine density and synaptic upscaling within the hippocampus in

response to environmental enrichment (Corrêa et al., 2012) and MSK1 KO mice display deficits in both recognition and spatial memory along with CA1 neuronal morphology and fail to see improvements in these following environmental enrichment. MSK1 KD mice are therefore an appropriate model for assessing the regulatory role that MSK1 kinase activity plays in environmental enrichment-induced changes within the hippocampus.

In this vein, several questions were asked about the role the kinase activity of MSK1 plays in regulating the response to environmental enrichment and tested over the course of this thesis which will be discussed here.

7.2 MSK1 phosphorylates CREB S133 in response to BDNF signalling via the TrkB receptor, and this presumably underlies the role MSK1 plays in regulating over half of the transcriptional response to EE.

In Chapter 3, phosphorylation of CREB at S133 in response to BDNF-TrkB receptor signalling was seen to be MSK1-dependent. Specificity for the TrkB receptor was assessed using the selective TrkB agonist 7,8-dihydroxyflavone (DHF) which produced the same MSK1-dependent increase in CREB S133 phosphorylation. The phosphorylation of CREB at S133 regulates its transcriptional activity (Alberini and Kandel, 2014) and could underlie the observation of over half of EE-induced transcription depending on MSK1 kinase activity (Figure 4.5). In support of this, chronic enhancement of CREB occludes the beneficial effect of environmental enrichment on spatial memory (Viosca et al., 2009), and increased CREB phosphorylation can be induced by environmental enrichment (Hu et al., 2013). This work therefore highlights a key role for MSK1 in regulating the beneficial effects of environmental enrichment.

Additionally, DHF has been investigated for use as a nootropic, and has been seen to improve deficits in spatial memory in an Alzheimer's disease model (Castello et al., 2014) and synaptic plasticity in a schizophrenia model (Yang et al., 2014b). DHF seen here to phosphorylate CREB in an MSK1-dependent manner (Figure 3.3), can penetrate the blood brain barrier unlike BDNF and makes an attractive pharmacological intervention in cognitive disorders implicating BDNF dysregulation (Liu et al., 2016). Indeed, oral administration of DHF

for 4 months (at 5 mg/kg/day) has been seen to be well tolerated and prevented synaptic loss and behavioural deficits, and promoted dendritic branching and synaptic plasticity in a mouse model of Alzheimer's disease (Zhang et al., 2014). However as can be seen from BDNF expression levels observed in Figure 4.8 C, BDNF levels are not necessarily chronically upregulated by EE, and may return to baseline after EE has induced sufficient changes in hippocampal structure and connectivity. Additionally, EE-induced changes in *in vivo* synaptic transmission have been observed to decay after longer exposure to EE (Irvine et al., 2006). This highlights the necessity in mapping the temporal course of beneficial changes in BDNF before applying "enviromimetics" ("therapeutics that mimic or enhance the beneficial effects of environmental stimulation" (McOmish and Hannan, 2007)) such as DHF, which mimics the effect of BDNF/TrkB signalling, and has seen success in targeting various neurological pathologies including Parkinson's disease, Huntington's Disease and Alzheimer's disease (Castello et al., 2014, Liu et al., 2016). BDNF is an unsuitable candidate as an enviromimetic, due to its poor absorption by the body and its inability to penetrate the blood-brain barrier, issues DHF does not experience (Liu et al., 2016). Of interest for future experimentation would therefore be the chronic administration of DHF orally in WT mice, for a similar period to EE timeframes, to establish the degree with which transcriptomic changes overlap with those of EE. This would establish a role for DHF as an enviromimetic and could highlight a beneficial role for DHF in cases of recovery from neurological insult or in situations where environmental stimulation is lacking.

7.3 MSK1 kinase activity induced by chronic EE regulates structural changes to the hippocampal extracellular environment, the expression of IEGs and appears to be homeostatically regulated.

The observation of functional enrichment for extracellular matrix remodelling, primary cilia regulation and vasculature development among the gene expression changes regulated by MSK1 following EE led to the conclusion that after 3 months of environmental enrichment, structural remodelling of the hippocampus had occurred. This remodelling could underpin environmental enrichment -induced changes within the brain, and could be the result of new pathways, neurons and connections being formed within the hippocampus after

environmental enrichment that could explain EE-mediated improvements. Indeed, the downregulation of IEGs, usually activated following periods of neuronal plasticity (Guzowski et al., 2001, Minatohara et al., 2015) could be important in preserving network level improvements in connectivity brought about by long-lasting environmental enrichment.

In section 4.3.4 the idea of homeostatic regulation after 3 months of EE of the IEGs Egr1 and Arc/Arg3.1 (MSK1 kinase function-dependent) and MSK1 itself (MSK1-kinase function-independent) was discussed. A recent study from the Frengueilli lab has confirmed that the RNA expression data presented here is carried over to the protein level for both Egr1 and Arc/Arg3.1 (Privitera et al., 2020), where the same significant differences have been observed in contemporaneous tissue. This lends more substance to the conclusions made here, such as the idea that, by keeping expression levels low following environmental enrichment, without affecting the normal transcription of synaptic plasticity genes, neurons can be "primed" to respond to novel stimuli by allowing subsequent stimulus-dependent upregulation of IEG expression to have a much larger fold-change effect on IEG signalling. In the perspective of the recent findings of the Frenguelli lab, that MSK1 kinase activity is necessary for an EE-induced increase the dynamic range of SC/CA1 synapse plasticity (Privitera et al., 2020) this downregulation of IEG signalling in the absence of stimulation may allow for greater relative induction of IEGS in response to stimulation. With Egr1 known to be induced during L-LTP induction (Chen et al., 2017) perhaps this greater dynamic range of transcriptional induction regulated by MSK1 underlies the facilitation of LTP observed.

Following 3 months of EE, WT mice, but not MSK1 KD mice display improvements in a reversal-learning task (Privitera et al., 2020), a spatial memory task that is thought to test cognitive flexibility and which induces the upregulation of Arc/Arg3.1 in the hippocampus (Guzowski et al., 2001). The activity-dependent release of BDNF within the hippocampus plays an essential role in the formation of memory during behavioural trials (Sakata et al., 2013). Disruption of BDNF impairs reversal-learning during MWM trials, despite mice displaying normal spatial memory and impairs L-LTP but not E-LTP (Sakata et al., 2013). BDNF-induced Arc/Arg3.1 expression is mediated by MSK1 via phosphorylation of histone H3 (Hunter et al., 2017), and regulation of Arc/Arg3.1 expression by MSK1 has also been observed during homeostatic synaptic scaling (Corrêa et al., 2012). Using an Arc/Arg3.1 mutant, in which

Arc/Arg3.1 was resistant to degradation, and which could acquire spatial memory normally, Wall et al. (2018) showed that abnormal persistant Arc/Arg3.1 expression following a reversal learning task impaired performance and cognitive flexibility. These mice additionally demonstrate an abnormally reduced threshold for LTD induction (Wall et al., 2018), which could underlie these behavioural deficits. This indicates that the correct temporal regulation of Arc/Arg3.1 expression dynamics following reversal learning is important for cognitive flexibility and for new memory formation to displace prior learning which conflicts with new information. There could therefore be a deficit in Arc/Arg3.1 regulation following 3 months of EE in MSK1 KD mice compared to WT mice that results in the lack of EE-mediated LTD enhancement, and consequently impairs reversal learning performance within MSK1 KD mice following EE.

This could be tested either by measuring total levels of Arc/Arg3.1 and Egr1 protein and RNA expression in both WT and MSK1 KD mice housed in SH and EE immediately following a hippocampus-dependent behavioural assay such as contextual fear conditioning or spatial memory-dependent reversal-learning and comparing to the baseline levels obtained here. Alternatively, by utilising the TRAP-seq method employed by Chen et al. (2017), levels of IEG RNA expression can be quantified before and after LTP and LTD induction, in order to determine if differences in Egr1 and Arc/Arg3.1 expression correspond to the different levels of synaptic plasticity enhancement observed in Privitera et al. (2020).

7.4 Environmental enrichment could promote an MSK1-independent form of metaplastcity at SC/CA1 synapses, which may facilitate LTP and explain recently observed MSK1-dependent enhancement of LTP following EE.

The kinase inactivation of MSK1 has previously displayed no effect on several forms of spatial memory nor TBS and HFS LTP induction and LTD, indicating mice are still capable of forming new memories and that plasticity can still occur in these mice (Daumas et al., 2017). The effect of 3 months of EE on MSK1-mediated synaptic plasticity was not directly addressed within this thesis, instead relying on researchers within the Frenguelli lab performing concomitant experiments testing the effects of 3 months of EE on synaptic plasticity and

cognition (Privitera et al., 2020). Recently, using WT and MSK1 KD mice exposed to EE for 3 months, the Frenguelli lab have demonstrated that EE facilitates both LTP and LTD within WT mice, but not MSK1 KD (Privitera et al., 2020). Whilst MSK1 KD mice can induce these forms of Hebbian plasticity, consistent with prior work in Daumas et al. 2017, they do not benefit from the EE-induced enhancement to LTP nor LTD (Privitera et al., 2020). EE therefore expands the dynamic range of synaptic modulation in WT mice, a benefit that is dependent on the kinase activity of MSK1.

What underlies this mechanism is likely a mixture of different MSK1-dependent effects. One possibility is that the MSK1-dependent transcriptomic changes identified in Chapter 4 underlie this enhanced synaptic plasticity. In Section 4.3.3, DEGs identified as changing expression in both WT and MSK1 KD mice following 3 months of EE were associated with “vasculature development”, “blood vessel development” and “cellular response to growth factor” (Figure 4.7 B). However, DEGs identified as changing expression in only WT mice and therefore affected by MSK1 kinase inactivation, displayed functional enrichment for “extracellular matrix organisation”, “extracellular structure organisation”, “Microtubule bundle formation”, “cilium organisation” and “clilium assembly” (Figure 4.7 C). As discussed on page 111, correct regulation of extracellular matrix organisation is necessary for the extracellular remodelling associated with angiogenesis and cell migration to occur properly (Neve et al., 2014). The primary cilium plays a role in integration of adult-born neurons (neurogenesis) and regulating dendrite complexity (Kumamoto et al., 2012, Lepanto et al., 2016). Perhaps the dysregulation of genes associated with regulating the extracellular matrix and primary cilium in MSK1 KD mice after EE underpins the lack of EE-mediated benefits they experience compared to WT mice.

Another possibility is that LTP is enhanced through additional signalling as a result of the EE-dependent regulation of CP-AMPARs. Discussed in Section 1.2.3 (pgs. 26 – 30), CP-AMPARs have emerged as an important source of postsynaptic plasticity during LTP induction, where their transient insertion has been seen to be important for L-LTP formation (Park et al., 2018, Plant et al., 2006, Park et al., 2016) especially at silent synapses (Morita et al., 2014). CP-AMPARs are homomeric or heteromeric assemblies of the GluA1, GluA3 and GluA4 subunits of the AMPAR, lacking the GluA2 subunit that blocks Ca^{2+} influx through GluA2-

containing AMPARs (Sommer et al., 1991, Cull-Candy et al., 2006, Chater and Goda, 2014). Within this thesis, expression of GluA2 was seen to be significantly reduced in both WT and MSK1 KD mice following 3 months of EE with no equivalent reduction in GluA1 expression (Figure 4.8 B + D). These mice also experienced enhancements to the dynamic range of synaptic plasticity changes (enchanced LTP and LTD) (Privitera et al., 2020). The enhancement in LTP following 3 months of EE could therefore be mediated by an increase in CP-AMPAR expression, in this regard EE could function as a metaplasticity event, by regulating the proportion of CP-AMPARs available within the intracellular AMPAR pool and therefore priming synapses for LTP induction.

However, as highlighted in section 5.3.1, acute periods of 1 wk and 5 wks EE induces an MSK1-independent decrease in postsynaptic CP-AMPAR expression at SC/CA1 synapses (Figures 5.5 A and B). This indicates that even early periods of EE can affect CP-AMPAR expression, and also that the decrease in GluA2 but not GluA1 expression observed following 3 months of EE may not be reflected in basal postsynaptic CP-AMPAR expression, but instead could constitute a change in the intracellular AMPAR pool subunit composition. If 3 months of EE leads to a reduction in GluA2 expression with no stoichiometric decrease in GluA1 expression, this could indicate that more AMPARs lack the GluA2 subunit, and are therefore Ca2+-permeable. Since 1 wk and 5 wks of EE lead to a decrease in CP-AMPAR expression under unpotentiated conditions at SC/CA1 synapses, perhaps after LTP induction, an increased proportion of CP-AMPARs are inserted into the postsynaptic membrane, leading to increased Ca^{2+} influx on top of NMDARs, resulting in stronger Ca^{2+}-dependent signalling following LTP induction? Ca^{2+} influx via NMDARs is thought to underlie LTP, initially via activation of CaMKIIa (Sweatt, 2016), but also via activation of other calcium-sensitive proteins, PKA, MAPK pathway. NMDA independent LTP can occur during pharmacological block of NMDARs in GluA2-lacking mice (Jia et al., 1996) and without inhibition of NMDARs, CP-AMPARs and NMDARs have been seen to co-operate to enhance LTP induction (Jia et al., 1996). EE has been seen to facilitate L-LTP induction, converting E-LTP to L-LTP in response to the same stimulus in a PKA-dependent manner (Duffy et al., 2001).

The increased intracellular Ca^{2+} influx through the presence of CP-AMPARs following EE may then recruit MSK1-dependent pathways during LTP induction: Intracellular Ca^{2+} influx

during LTP induction results in PKA activation via Ca^{2+} activation of adenyl cyclase. PKA can phosphorylate Erk1/2 (Costes et al., 2006) which induces MSK1 activation (Simon et al., 2004). Ca^{2+} influx can also activate Ras and thus the MAPK pathway (Waltereit and Weller, 2003). In addition, during contextual fear conditioning, co-activation of PKA, MAPK, MSK1 and CREB is observed in response to Ca(2+)-stimulated adenylyl cyclase activity (Sindreu et al., 2007). In this way, perhaps MSK1 KD mice receive the same extra Ca^{2+} influx during LTP induction after EE, but perhaps cannot convert this into additional transcription that could underlie the increased facilitation of LTP seen in WT mice. Lending support to this argument, significant functional enrichment of DEGs identified as changing expression following 3 months of EE in both WT and MSK1 KD mice were associated with "positive regulation of the MAPK cascade", and 2 of the most significant DEGS identified between WTEE and KDEE mice were Spry4 and Rarres2. Downregulation of the MAPK inhibitor Spry4, and upregulation of the MAPK activator Rarres2 in WTEE compared to KDEE mice may contribute to enhanced MAPK pathway activity in WT mice following 3 months of EE that MSK1 KD mice do not experience. This idea of previous experience modulating the synaptic response to new stimuli is termed "synaptic metaplasticity" (Sweatt, 2016), and is summarised in Figure 7.1 below.

- Increased CP-AMPAR proportion in pool of intracellular AMPARs following 3mths EE at non-potentiated state.
- Transient insertion occurs immediately after LTP induction.

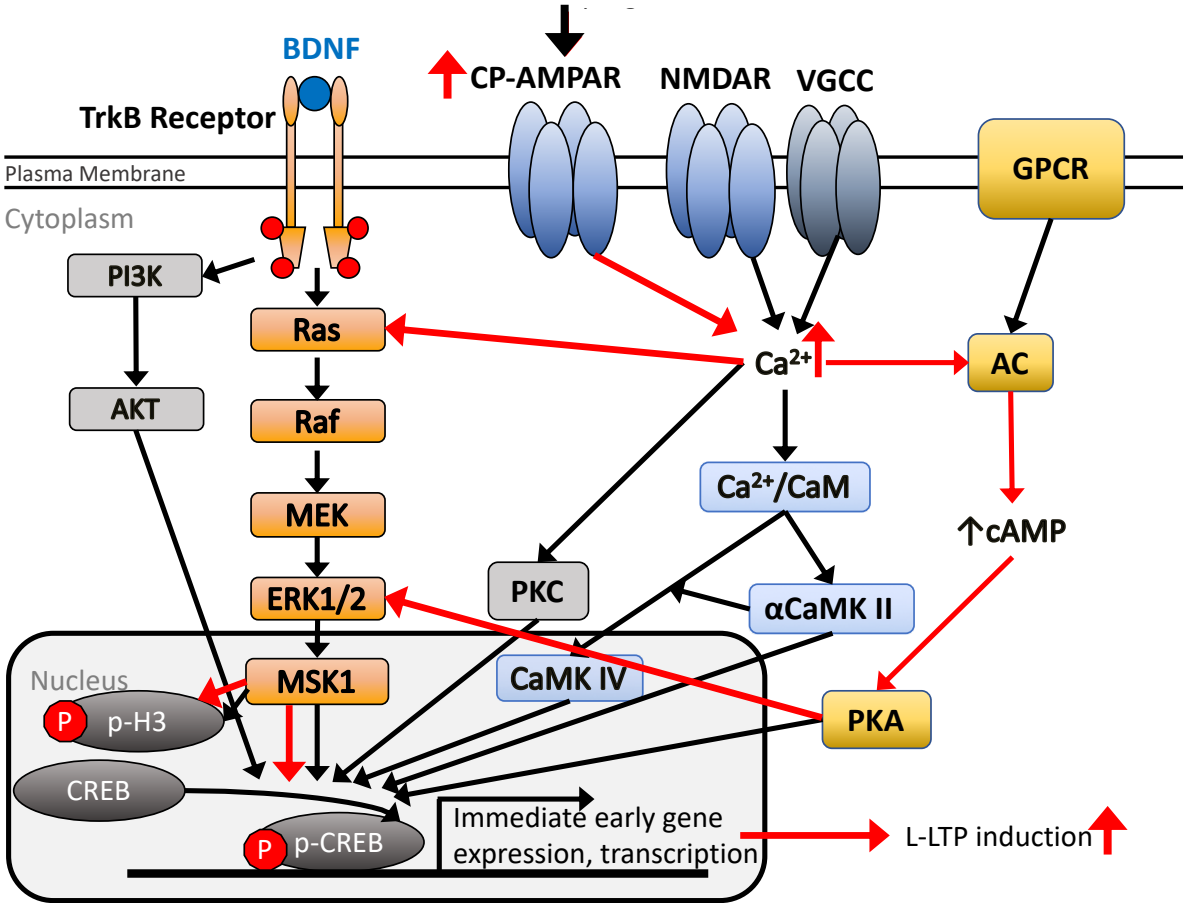

Figure 7.1. Proposed signalling pathway underlying enhancement of LTP following EE-induced metaplastic increase in transient CP-AMPAR expression at the postsynapse.

7.5 Overall summary

In summary, the results presented in this thesis add to a growing body of evidence that the kinase activity of MSK1 regulates the hippocampal response to environmental enrichment, at least in part through activation of CREB- and histone H3-mediated transcription, including key IEGs Egr1 and Arc/Arg3.1. This appears to be regulated in a homeostatic manner, restructuring the hippocampal environment to build a better brain through the activity-dependent regulation of gene transcription by MSK1 and may involve the dendritic restructuring of CA1 cells, transient modulation of glutamatergic transmission at SC/CA1 synapses. Additionally, a novel role for MSK1 in mediating the preference for social novelty has been presented, which could perhaps relate to a wider role for MSK1 in mediating

novelty motivation in general. This work helps characterise the relatively unknown mechanisms of EE-induced benefit to the brain, and may be useful for the successful targeting of future pharmacotherapies relying on enviromimetics.

Bibliography

ABRAHAM, W. C., LOGAN, B., GREENWOOD, J. M. & DRAGUNOW, M. 2002. Induction and experience-dependent consolidation of stable long-term potentiation lasting months in the hippocampus. *J Neurosci,* 22**,** 9626-34.

ACSÁDY, L., KAMONDI, A., SÍK, A., FREUND, T. & BUZSÁKI, G. 1998. GABAergic Cells Are the Major Postsynaptic Targets of Mossy Fibers in the Rat Hippocampus. *The Journal of Neuroscience,* 18**,** 3386.

ALBERINI, C. M. & KANDEL, E. R. 2014. The regulation of transcription in memory consolidation. *Cold Spring Harbor perspectives in biology,* 7**,** a021741-a021741.

ALDER, J., THAKKER-VARIA, S., BANGASSER, D. A., KUROIWA, M., PLUMMER, M. R., SHORS, T. J. & BLACK, I. B. 2003. Brain-derived neurotrophic factor-induced gene expression reveals novel actions of VGF in hippocampal synaptic plasticity. *J Neurosci,* 23**,** 10800-8.

ALEXA, A., RAHNENFÜHRER, J. & LENGAUER, T. 2006. Improved scoring of functional groups from gene expression data by decorrelating GO graph structure. *Bioinformatics,* 22**,** 1600-1607.

ALONSO, M., MEDINA, J. H. & POZZO-MILLER, L. 2004. ERK1/2 activation is necessary for BDNF to increase dendritic spine density in hippocampal CA1 pyramidal neurons. *Learn Mem,* 11**,** 172-8.

ALSINA, F. C., IRALA, D., FONTANET, P. A., HITA, F. J., LEDDA, F. & PARATCHA, G. 2012. Sprouty4 Is an Endogenous Negative Modulator of TrkA Signaling and Neuronal Differentiation Induced by NGF. *PLOS ONE,* 7**,** e32087.

ANDERS, S., PYL, P. T. & HUBER, W. 2015. HTSeq--a Python framework to work with high-throughput sequencing data. *Bioinformatics,* 31**,** 166-9.

ANDERSEN, P., MORRIS, R., AMARAL, D. G., BLISS, T. & O' KEEFE, J. 2009. *The Hippocampus Book*, Oxford University Press.

ANDREWS 2010. FastQC: a quality control tool for high throughput sequence data. *v0.11.3.* Available online at: http://www.bioinformatics.babraham.ac.uk/projects/fastqc.

ARAQUE, A., PARPURA, V., SANZGIRI, R. P. & HAYDON, P. G. 1999. Tripartite synapses: glia, the unacknowledged partner. *Trends Neurosci,* 22**,** 208-15.

ARGUELLO, A. A., YE, X., BOZDAGI, O., POLLONINI, G., TRONEL, S., BAMBAH-MUKKU, D., HUNTLEY, G. W., PLATANO, D. & ALBERINI, C. M. 2013. CCAAT enhancer binding protein delta plays an essential role in memory consolidation and reconsolidation. *J Neurosci,* 33**,** 3646-58.

ARIKKATH, J. & REICHARDT, L. F. 2008. Cadherins and catenins at synapses: roles in synaptogenesis and synaptic plasticity. *Trends in neurosciences,* 31**,** 487-494.

ARTHUR, J. S. C. 2008. MSK activation and physiological roles. *Frontiers in bioscience : a journal and virtual library* [Online], 13. [Accessed 2008].

ARTHUR, S. J., FONG, A. L., DWYER, J. M., DAVARE, M., REESE, E., OBRIETAN, K. & IMPEY, S. 2004. Mitogen- and Stress-Activated Protein Kinase 1 Mediates cAMP Response Element-Binding Protein Phosphorylation and Activation by Neurotrophins. *The Journal of Neuroscience,* 24**,** 4324.

ARTOLA, A., VON FRIJTAG, J. C., FERMONT, P. C., GISPEN, W. H., SCHRAMA, L. H., KAMAL, A. & SPRUIJT, B. M. 2006. Long-lasting modulation of the induction of LTD and LTP in

rat hippocampal CA1 by behavioural stress and environmental enrichment. *Eur J Neurosci,* 23**,** 261-72.
AU - DENNINGER, J. K., AU - SMITH, B. M. & AU - KIRBY, E. D. 2018. Novel Object Recognition and Object Location Behavioral Testing in Mice on a Budget. *JoVE***,** e58593.
AZEVEDO, F. A., CARVALHO, L. R., GRINBERG, L. T., FARFEL, J. M., FERRETTI, R. E., LEITE, R. E., JACOB FILHO, W., LENT, R. & HERCULANO-HOUZEL, S. 2009. Equal numbers of neuronal and nonneuronal cells make the human brain an isometrically scaled-up primate brain. *J Comp Neurol,* 513**,** 532-41.
BALLARD, I. C., WAGNER, A. D. & MCCLURE, S. M. 2019. Hippocampal pattern separation supports reinforcement learning. *Nature Communications,* 10**,** 1073.
BALSCHUN, D., WOLFER, D. P., GASS, P., MANTAMADIOTIS, T., WELZL, H., SCHÜTZ, G., FREY, J. U. & LIPP, H.-P. 2003. Does cAMP response element-binding protein have a pivotal role in hippocampal synaptic plasticity and hippocampus-dependent memory? *The Journal of neuroscience : the official journal of the Society for Neuroscience,* 23**,** 6304-6314.
BAMBAH-MUKKU, D., TRAVAGLIA, A., CHEN, D. Y., POLLONINI, G. & ALBERINI, C. M. 2014. A Positive Autoregulatory BDNF Feedback Loop via C/EBPβ Mediates Hippocampal Memory Consolidation. *The Journal of Neuroscience,* 34**,** 12547.
BAPTISTA, P. & ANDRADE, J. P. 2018. Adult Hippocampal Neurogenesis: Regulation and Possible Functional and Clinical Correlates. *Frontiers in Neuroanatomy,* 12**,** 44.
BARCO, A., ALARCON, J. M. & KANDEL, E. R. 2002. Expression of constitutively active CREB protein facilitates the late phase of long-term potentiation by enhancing synaptic capture. *Cell,* 108**,** 689-703.
BARCO, A., JANCIC, D. & KANDEL, E. R. 2008. CREB-Dependent Transcription and Synaptic Plasticity. *In:* DUDEK, S. M. (ed.) *Transcriptional Regulation by Neuronal Activity: To the Nucleus and Back.* Boston, MA: Springer US.
BARCO, A. & MARIE, H. 2011. Genetic approaches to investigate the role of CREB in neuronal plasticity and memory. *Mol Neurobiol,* 44**,** 330-49.
BARKER, G. R. I. & WARBURTON, E. C. 2011. When Is the Hippocampus Involved in Recognition Memory? *The Journal of Neuroscience,* 31**,** 10721.
BARROS, C. S., FRANCO, S. J. & MÜLLER, U. 2011. Extracellular matrix: functions in the nervous system. *Cold Spring Harbor perspectives in biology,* 3**,** a005108-a005108.
BASHIR, Z. I., ALFORD, S., DAVIES, S. N., RANDALL, A. D. & COLLINGRIDGE, G. L. 1991. Long-term potentiation of NMDA receptor-mediated synaptic transmission in the hippocampus. *Nature,* 349**,** 156-8.
BASHIR, Z. I., BORTOLOTTO, Z. A., DAVIES, C. H., BERRETTA, N., IRVING, A. J., SEAL, A. J., HENLEY, J. M., JANE, D. E., WATKINS, J. C. & COLLINGRIDGE, G. L. 1993. Induction of LTP in the hippocampus needs synaptic activation of glutamate metabotropic receptors. *Nature,* 363**,** 347-350.
BASTRIKOVA, N., GARDNER, G. A., REECE, J. M., JEROMIN, A. & DUDEK, S. M. 2008. Synapse elimination accompanies functional plasticity in hippocampal neurons. *Proceedings of the National Academy of Sciences of the United States of America,* 105**,** 3123-3127.
BASU, J. & SIEGELBAUM, S. A. 2015. The Corticohippocampal Circuit, Synaptic Plasticity, and Memory. *Cold Spring Harbor Perspectives in Biology,* 7.

BEAUQUIS, J., ROIG, P., DE NICOLA, A. F. & SARAVIA, F. 2010. Short-Term Environmental Enrichment Enhances Adult Neurogenesis, Vascular Network and Dendritic Complexity in the Hippocampus of Type 1 Diabetic Mice. *PLOS ONE,* 5**,** e13993.

BEER, Z., VAVRA, P., ATUCHA, E., RENTZING, K., HEINZE, H.-J. & SAUVAGE, M. M. 2018. The memory for time and space differentially engages the proximal and distal parts of the hippocampal subfields CA1 and CA3. *PLOS Biology,* 16**,** e2006100.

BICKS, L. K., KOIKE, H., AKBARIAN, S. & MORISHITA, H. 2015. Prefrontal Cortex and Social Cognition in Mouse and Man. *Frontiers in Psychology,* 6.

BILIMORIA, P. M. & STEVENS, B. 2015. Microglia function during brain development: New insights from animal models. *Brain Res,* 1617**,** 7-17.

BIRCH, A. M. & KELLY, Á. M. 2019. Lifelong environmental enrichment in the absence of exercise protects the brain from age-related cognitive decline. *Neuropharmacology,* 145**,** 59-74.

BITO, H., DEISSEROTH, K. & TSIEN, R. W. 1996. CREB Phosphorylation and Dephosphorylation: A Ca2+- and Stimulus Duration–Dependent Switch for Hippocampal Gene Expression. *Cell,* 87**,** 1203-1214.

BLENDY, J. A., KAESTNER, K. H., SCHMID, W., GASS, P. & SCHUTZ, G. 1996. Targeting of the CREB gene leads to up-regulation of a novel CREB mRNA isoform. *The EMBO journal,* 15**,** 1098-1106.

BLISS, T. V. & COLLINGRIDGE, G. L. 1993. A synaptic model of memory: long-term potentiation in the hippocampus. *Nature,* 361**,** 31-9.

BLISS, T. V. & GARDNER-MEDWIN, A. R. 1973. Long-lasting potentiation of synaptic transmission in the dentate area of the unanaestetized rabbit following stimulation of the perforant path. *J Physiol,* 232**,** 357-74.

BLISS, T. V. & LOMO, T. 1973. Long-lasting potentiation of synaptic transmission in the dentate area of the anaesthetized rabbit following stimulation of the perforant path. *J Physiol,* 232**,** 331-56.

BLISS, T. V. P., COLLINGRIDGE, G. L., MORRIS, R. G. M. & REYMANN, K. G. 2018. Long-term potentiation in the hippocampus: discovery, mechanisms and function. *Neuroforum.*

BOLTON, M. M., PITTMAN, A. J. & LO, D. C. 2000. Brain-derived neurotrophic factor differentially regulates excitatory and inhibitory synaptic transmission in hippocampal cultures. *J Neurosci,* 20**,** 3221-32.

BOURTCHULADZE, R., FRENGUELLI B FAU - BLENDY, J., BLENDY J FAU - CIOFFI, D., CIOFFI D FAU - SCHUTZ, G., SCHUTZ G FAU - SILVA, A. J. & SILVA, A. J. 1994. Deficient long-term memory in mice with a targeted mutation of the cAMP-responsive element-binding protein. *Cell.*

BOWIE, D. & MAYER, M. L. 1995. Inward rectification of both AMPA and kainate subtype glutamate receptors generated by polyamine-mediated ion channel block. *Neuron,* 15**,** 453-462.

BRIAND, L. A., LEE, B. G., LELAY, J., KAESTNER, K. H. & BLENDY, J. A. 2015. Serine 133 phosphorylation is not required for hippocampal CREB-mediated transcription and behavior. *Learn Mem,* 22**,** 109-15.

BRUN, V. H., OTNASS, M. K., MOLDEN, S., STEFFENACH, H. A., WITTER, M. P., MOSER, M. B. & MOSER, E. I. 2002. Place cells and place recognition maintained by direct entorhinal-hippocampal circuitry. *Science,* 296**,** 2243-6.

BUSCHLER, A. & MANAHAN-VAUGHAN, D. 2012. Brief environmental enrichment elicits metaplasticity of hippocampal synaptic potentiation in vivo. *Frontiers in Behavioral Neuroscience,* 6.

BUTLER, C. W., KEISER, A. A., KWAPIS, J. L., BERCHTOLD, N. C., WALL, V. L., WOOD, M. A. & COTMAN, C. W. 2019. Exercise opens a temporal window for enhanced cognitive improvement from subsequent physical activity. *Learning & Memory,* 26**,** 485-492.

BYE, C. M. & MCDONALD, R. J. 2019. A Specific Role of Hippocampal NMDA Receptors and Arc Protein in Rapid Encoding of Novel Environmental Representations and a More General Long-Term Consolidation Function. *Frontiers in Behavioral Neuroscience,* 13**,** 8.

CALZÀ, L., GIARDINO, L., GIULIANI, A., ALOE, L. & LEVI-MONTALCINI, R. 2001. Nerve growth factor control of neuronal expression of angiogenetic and vasoactive factors. *Proceedings of the National Academy of Sciences,* 98**,** 4160.

CANTO, C. B., WOUTERLOOD, F. G. & WITTER, M. P. 2008. What does the anatomical organization of the entorhinal cortex tell us? *Neural plasticity,* 2008**,** 381243-381243.

CARDOSO, A. M., MANFREDI, L. H., ZANINI, D., BAGATINI, M. D., GUTIERRES, J. M., CARVALHO, F., TREMBLAY, A., BELLO-KLEIN, A., RUBIN, M. A., MORSCH, V. M., SEVIGNY, J. & SCHETINGER, M. R. C. 2019. Physical exercise prevents memory impairment in an animal model of hypertension through modulation of CD39 and CD73 activities and A2A receptor expression. *J Hypertens,* 37**,** 135-143.

CARLSON, M. 2018. *Mus musculus* ontology org.Mm.eg.db (v3.6.0).

CARUANA, D. A., ALEXANDER, G. M. & DUDEK, S. M. 2012. New insights into the regulation of synaptic plasticity from an unexpected place: hippocampal area CA2. *Learn Mem,* 19**,** 391-400.

CASTELLO, N. A., NGUYEN, M. H., TRAN, J. D., CHENG, D., GREEN, K. N. & LAFERLA, F. M. 2014. 7,8-Dihydroxyflavone, a Small Molecule TrkB Agonist, Improves Spatial Memory and Increases Thin Spine Density in a Mouse Model of Alzheimer Disease-Like Neuronal Loss. *PLoS ONE,* 9**,** e91453.

CHANG, M. C., PARK, J. M., PELKEY, K. A., GRABENSTATTER, H. L., XU, D., LINDEN, D. J., SUTULA, T. P., MCBAIN, C. J. & WORLEY, P. F. 2010. Narp regulates homeostatic scaling of excitatory synapses on parvalbumin-expressing interneurons. *Nature neuroscience,* 13**,** 1090-1097.

CHATER, THOMAS E. & GODA, Y. 2013. CA3 Mossy Fiber Connections: Giant Synapses that Gain Control. *Neuron,* 77**,** 4-6.

CHATER, T. E. & GODA, Y. 2014. The role of AMPA receptors in postsynaptic mechanisms of synaptic plasticity. *Frontiers in cellular neuroscience,* 8**,** 401-401.

CHEN, P. B., KAWAGUCHI, R., BLUM, C., ACHIRO, J. M., COPPOLA, G., O'DELL, T. J. & MARTIN, K. C. 2017. Mapping Gene Expression in Excitatory Neurons during Hippocampal Late-Phase Long-Term Potentiation.

CHEN, X., NELSON, C. D., LI, X., WINTERS, C. A., AZZAM, R., SOUSA, A. A., LEAPMAN, R. D., GAINER, H., SHENG, M. & REESE, T. S. 2011. PSD-95 is required to sustain the molecular organization of the postsynaptic density. *J Neurosci,* 31**,** 6329-38.

CHOWDHURY, S., SHEPHERD, J. D., OKUNO, H., LYFORD, G., PETRALIA, R. S., PLATH, N., KUHL, D., HUGANIR, R. L. & WORLEY, P. F. 2006. Arc/Arg3.1 interacts with the endocytic machinery to regulate AMPA receptor trafficking. *Neuron,* 52**,** 445-59.

CHRIVIA, J. C., KWOK, R. P., LAMB, N., HAGIWARA, M., MONTMINY, M. R. & GOODMAN, R. H. 1993. Phosphorylated CREB binds specifically to the nuclear protein CBP. *Nature,* 365**,** 855-9.

CHWANG, W. B., ARTHUR, J. S., SCHUMACHER, A. & SWEATT, J. D. 2007. The Nuclear Kinase Mitogen- and Stress-Activated Protein Kinase 1 Regulates Hippocampal Chromatin Remodeling in Memory Formation. *The Journal of Neuroscience,* 27**,** 12732-12742.

CHWANG, W. B., O'RIORDAN, K. J., LEVENSON, J. M. & SWEATT, J. D. 2006. ERK/MAPK regulates hippocampal histone phosphorylation following contextual fear conditioning. *Learn Mem,* 13**,** 322-8.

CITRI, A. & MALENKA, R. C. 2008. Synaptic Plasticity: Multiple Forms, Functions, and Mechanisms. *Neuropsychopharmacology,* 33**,** 18-41.

CLARK, K. A. & COLLINGRIDGE, G. L. 1995. Synaptic potentiation of dual-component excitatory postsynaptic currents in the rat hippocampus. *J Physiol,* 482 (Pt 1)**,** 39-52.

COHEN, J. 1988. *Statistical Power Analysis for the Behavioral Sciences.,* New York, Routledge.

COHEN, S. J. & STACKMAN, R. W., JR. 2015. Assessing rodent hippocampal involvement in the novel object recognition task. A review. *Behavioural brain research,* 285**,** 105-117.

COLLINGRIDGE, G. L., KEHL, S. J. & MCLENNAN, H. 1983. Excitatory amino acids in synaptic transmission in the Schaffer collateral-commissural pathway of the rat hippocampus. *J Physiol,* 334**,** 33-46.

COLLINGRIDGE, G. L., PEINEAU, S., HOWLAND, J. G. & WANG, Y. T. 2010. Long-term depression in the CNS. *Nat Rev Neurosci,* 11**,** 459-73.

CONKRIGHT, M. D., CANETTIERI, G., SCREATON, R., GUZMAN, E., MIRAGLIA, L., HOGENESCH, J. B. & MONTMINY, M. 2003. TORCs: transducers of regulated CREB activity. *Mol Cell,* 12**,** 413-23.

CONNER, J. M., FRANKS, K. M., TITTERNESS, A. K., RUSSELL, K., MERRILL, D. A., CHRISTIE, B. R., SEJNOWSKI, T. J. & TUSZYNSKI, M. H. 2009. NGF is essential for hippocampal plasticity and learning. *The Journal of neuroscience : the official journal of the Society for Neuroscience,* 29**,** 10883-10889.

COOKE, S. F., WU, J., PLATTNER, F., ERRINGTON, M., ROWAN, M., PETERS, M., HIRANO, A., BRADSHAW, K. D., ANWYL, R., BLISS, T. V. P. & GIESE, K. P. 2006. Autophosphorylation of alphaCaMKII is not a general requirement for NMDA receptor-dependent LTP in the adult mouse. *The Journal of physiology,* 574**,** 805-818.

CORE-TEAM, R. 2018. R: A language and environment for statistical computing. R Foundation for Statistical Computing. *v3.5.0*.

CORRÊA, S. A. L., HUNTER, C. J., PALYGIN, O., WAUTERS, S. C., MARTIN, K. J., MCKENZIE, C., MCKELVEY, K., MORRIS, R. G. M., PANKRATOV, Y., ARTHUR, J. S. C. & FRENGUELLI, B. G. 2012. MSK1 Regulates Homeostatic and Experience-Dependent Synaptic Plasticity. *The Journal of Neuroscience,* 32**,** 13039-13051.

COSTES, S., BROCA, C., BERTRAND, G., LAJOIX, A. D., BATAILLE, D., BOCKAERT, J. & DALLE, S. 2006. ERK1/2 control phosphorylation and protein level of cAMP-responsive element-binding protein: a key role in glucose-mediated pancreatic beta-cell survival. *Diabetes,* 55**,** 2220-30.

COWANSAGE, K. K., LEDOUX, J. E. & MONFILS, M. H. 2010. Brain-derived neurotrophic factor: a dynamic gatekeeper of neural plasticity. *Curr Mol Pharmacol,* 3**,** 12-29.

CRAWLEY, J. N. 2004. Designing mouse behavioral tasks relevant to autistic-like behaviors. *Ment Retard Dev Disabil Res Rev,* 10**,** 248-58.
CREER, D. J., ROMBERG, C., SAKSIDA, L. M., VAN PRAAG, H. & BUSSEY, T. J. 2010. Running enhances spatial pattern separation in mice. *Proc Natl Acad Sci U S A,* 107**,** 2367-72.
CROSIO, C., HEITZ, E., ALLIS, C. D., BORRELLI, E. & SASSONE-CORSI, P. 2003. Chromatin remodeling and neuronal response: multiple signaling pathways induce specific histone H3 modifications and early gene expression in hippocampal neurons. *J Cell Sci,* 116**,** 4905-14.
CULL-CANDY, S., KELLY, L. & FARRANT, M. 2006. Regulation of Ca2+-permeable AMPA receptors: synaptic plasticity and beyond. *Curr Opin Neurobiol,* 16**,** 288-97.
D'AMATO, F. R., ZANETTINI, C., SGOBIO, C., SARLI, C., CARONE, V., MOLES, A. & AMMASSARI-TEULE, M. 2011. Intensification of maternal care by double-mothering boosts cognitive function and hippocampal morphology in the adult offspring. *Hippocampus,* 21**,** 298-308.
DANI, J. W., CHERNJAVSKY, A. & SMITH, S. J. 1992. Neuronal activity triggers calcium waves in hippocampal astrocyte networks. *Neuron,* 8**,** 429-40.
DANZER, S. C., CROOKS, K. R. C., LO, D. C. & MCNAMARA, J. O. 2002. Increased Expression of Brain-Derived Neurotrophic Factor Induces Formation of Basal Dendrites and Axonal Branching in Dentate Granule Cells in Hippocampal Explant Cultures. *The Journal of Neuroscience,* 22**,** 9754.
DAUMAS, S., HUNTER, C. J., MISTRY, R. B., MORÈ, L., PRIVITERA, L., COOPER, D. D., REYSKENS, K. M., FLYNN, H. T., MORRIS, R. G. M., ARTHUR, J. S. C. & FRENGUELLI, B. G. 2017. The Kinase Function of MSK1 Regulates BDNF Signaling to CREB and Basal Synaptic Transmission, But Is Not Required for Hippocampal Long-Term Potentiation or Spatial Memory. *eNeuro,* 4**,** ENEURO.0212-16.2017.
DAYER, A. G., FORD, A. A., CLEAVER, K. M., YASSAEE, M. & CAMERON, H. A. 2003. Short-term and long-term survival of new neurons in the rat dentate gyrus. *The Journal of Comparative Neurology,* 460**,** 563-572.
DE BAAIJ, J. H. F., KOMPATSCHER, A., VIERING, D. H. H. M., BOS, C., BINDELS, R. J. M. & HOENDEROP, J. G. J. 2016. P2X6 Knockout Mice Exhibit Normal Electrolyte Homeostasis. *PLOS ONE,* 11**,** e0156803.
DE CARVALHO, C. R., PANDOLFO, P., PAMPLONA, F. A. & TAKAHASHI, R. N. 2010. Environmental enrichment reduces the impact of novelty and motivational properties of ethanol in spontaneously hypertensive rats. *Behavioural Brain Research,* 208**,** 231-236.
DE LA TREMBLAYE, P. B., CHENG, J. P., BONDI, C. O. & KLINE, A. E. 2019. Environmental enrichment, alone or in combination with various pharmacotherapies, confers marked benefits after traumatic brain injury. *Neuropharmacology,* 145**,** 13-24.
DEISSEROTH, K., BITO, H. & TSIEN, R. W. 1996. Signaling from synapse to nucleus: postsynaptic CREB phosphorylation during multiple forms of hippocampal synaptic plasticity. *Neuron,* 16**,** 89-101.
DI GIOVANNA, A. P., TIBO, A., SILVESTRI, L., MÜLLENBROICH, M. C., COSTANTINI, I., ALLEGRA MASCARO, A. L., SACCONI, L., FRASCONI, P. & PAVONE, F. S. 2018. Whole-Brain Vasculature Reconstruction at the Single Capillary Level. *Scientific Reports,* 8**,** 12573.
DOBIN, A., DAVIS, C. A., SCHLESINGER, F., DRENKOW, J., ZALESKI, C., JHA, S., BATUT, P., CHAISSON, M. & GINGERAS, T. R. 2013. STAR: ultrafast universal RNA-seq aligner. *Bioinformatics,* 29**,** 15-21.

DONALDSON, Z. R. & YOUNG, L. J. 2008. Oxytocin, vasopressin, and the neurogenetics of sociality. *Science,* 322**,** 900-4.
DUCLOT, F. & KABBAJ, M. 2017. The Role of Early Growth Response 1 (EGR1) in Brain Plasticity and Neuropsychiatric Disorders. *Front Behav Neurosci,* 11**,** 35.
DUDEK, S. M., ALEXANDER, G. M. & FARRIS, S. 2016. Rediscovering area CA2: unique properties and functions. *Nat Rev Neurosci,* 17**,** 89-102.
DUFFY, S. N., CRADDOCK KJ FAU - CRADDOCK, K. J., ABEL T FAU - ABEL, T. & NGUYEN PV FAU - NGUYEN, P. V. 2001. Environmental Enrichment Modifies the PKA-Dependence of Hippocampal LTP and Improves Hippocampus-Dependent Memory.
DUPRET, D., REVEST, J. M., KOEHL, M., ICHAS, F., DE GIORGI, F., COSTET, P., ABROUS, D. N. & PIAZZA, P. V. 2008. Spatial relational memory requires hippocampal adult neurogenesis. *PLoS One,* 3**,** e1959.
ECHEGOYEN, J., NEU, A., GRABER, K. D. & SOLTESZ, I. 2007. Homeostatic Plasticity Studied Using In Vivo Hippocampal Activity-Blockade: Synaptic Scaling, Intrinsic Plasticity and Age-Dependence. *PLOS ONE,* 2**,** e700.
ECKERT, M. J. & ABRAHAM, W. C. 2013. Effects of environmental enrichment exposure on synaptic transmission and plasticity in the hippocampus.
ECKERT, M. J., BILKEY, D. K. & ABRAHAM, W. C. 2010. Altered plasticity in hippocampal CA1, but not dentate gyrus, following long-term environmental enrichment. *J Neurophysiol,* 103**,** 3320-9.
EICHENBAUM, H. 2017. The role of the hippocampus in navigation is memory. *J Neurophysiol,* 117**,** 1785-1796.
EKSTROM, A. D., MELTZER, J., MCNAUGHTON, B. L. & BARNES, C. A. 2001. NMDA receptor antagonism blocks experience-dependent expansion of hippocampal "place fields". *Neuron,* 31**,** 631-8.
ERNST, P., WANG, J., HUANG, M., GOODMAN, R. H. & KORSMEYER, S. J. 2001. MLL and CREB bind cooperatively to the nuclear coactivator CREB-binding protein. *Mol Cell Biol,* 21**,** 2249-58.
EROGLU, C. & BARRES, B. A. 2010. Regulation of synaptic connectivity by glia. *Nature,* 468**,** 223-231.
EVANS, P. R., GERBER, K. J., DAMMER, E. B., DUONG, D. M., GOSWAMI, D., LUSTBERG, D. J., ZOU, J., YANG, J. J., DUDEK, S. M., GRIFFIN, P. R., SEYFRIED, N. T. & HEPLER, J. R. 2018. Interactome Analysis Reveals Regulator of G Protein Signaling 14 (RGS14) is a Novel Calcium/Calmodulin (Ca2+/CaM) and CaM Kinase II (CaMKII) Binding Partner. *Journal of Proteome Research,* 17**,** 1700-1711.
EVANS, P. R., LEE, S. E., SMITH, Y. & HEPLER, J. R. 2014. Postnatal developmental expression of regulator of G protein signaling 14 (RGS14) in the mouse brain. *J Comp Neurol,* 522**,** 186-203.
FABCZAK, H. & OSINKA, A. 2019. Role of the Novel Hsp90 Co-Chaperones in Dynein Arms' Preassembly. *International journal of molecular sciences,* 20**,** 6174.
FAHERTY, C. J., KERLEY D FAU - SMEYNE, R. J. & SMEYNE, R. J. 2003. A Golgi-Cox morphological analysis of neuronal changes induced by environmental enrichment.
FALKENBERG, T., MOHAMMED, A. K., HENRIKSSON, B., PERSSON, H., WINBLAD, B. & LINDEFORS, N. 1992. Increased expression of brain-derived neurotrophic factor mRNA in rat hippocampus is associated with improved spatial memory and enriched environment. *Neuroscience Letters,* 138**,** 153-156.

FAWCETT, J. W., OOHASHI, T. & PIZZORUSSO, T. 2019. The roles of perineuronal nets and the perinodal extracellular matrix in neuronal function. *Nature Reviews Neuroscience,* 20**,** 451-465.

FIGUROV, A., POZZO-MILLER, L. D., OLAFSSON, P., WANG, T. & LU, B. 1996. Regulation of synaptic responses to high-frequency stimulation and LTP by neurotrophins in the hippocampus. *Nature,* 381**,** 706-709.

FINKBEINER, S., TAVAZOIE, S. F., MALORATSKY, A., JACOBS, K. M., HARRIS, K. M. & GREENBERG, M. E. 1997. CREB: A Major Mediator of Neuronal Neurotrophin Responses. *Neuron,* 19**,** 1031-1047.

FONSECA, R., NAGERL, U. V. & BONHOEFFER, T. 2006. Neuronal activity determines the protein synthesis dependence of long-term potentiation. *Nat Neurosci,* 9**,** 478-80.

FRANK, L. M., STANLEY, G. B. & BROWN, E. N. 2004. Hippocampal plasticity across multiple days of exposure to novel environments. *The Journal of neuroscience : the official journal of the Society for Neuroscience,* 24**,** 7681-7689.

FRENGUELLI, B. G. & CORREA, S. A. 2012. Regulation and Role of MSK in the Mammalian Brain. *In:* SIMON, A. C. (ed.) *MSKs.* Austin, Texas: Landes Bioscience.

FREY, U., FREY, S., SCHOLLMEIER, F. & KRUG, M. 1996. Influence of actinomycin D, a RNA synthesis inhibitor, on long-term potentiation in rat hippocampal neurons in vivo and in vitro. *The Journal of Physiology,* 490**,** 703-711.

FRICK, K. M., BAXTER, M. G., MARKOWSKA, A. L., OLTON, D. S. & PRICE, D. L. 1995. Age-related spatial reference and working memory deficits assessed in the water maze. *Neurobiol Aging,* 16**,** 149-60.

FRICK, K. M., STEARNS, N. A., PAN, J.-Y. & BERGER-SWEENEY, J. 2003. Effects of Environmental Enrichment on Spatial Memory and Neurochemistry in Middle-Aged Mice. *Learning & Memory,* 10**,** 187-198.

FRICK, K. M., STILLNER, E. T. & BERGER-SWEENEY, J. 2000. Mice are not little rats: species differences in a one-day water maze task. *Neuroreport,* 11**,** 3461-5.

FYHN, M., MOLDEN, S., WITTER, M. P., MOSER, E. I. & MOSER, M. B. 2004. Spatial representation in the entorhinal cortex. *Science,* 305**,** 1258-64.

GAGE, F. H. 2002. Neurogenesis in the adult brain. *J Neurosci.* United States.

GALLO, F. T., KATCHE, C., MORICI, J. F., MEDINA, J. H. & WEISSTAUB, N. V. 2018. Immediate Early Genes, Memory and Psychiatric Disorders: Focus on c-Fos, Egr1 and Arc. *Frontiers in Behavioral Neuroscience,* 12.

GÄRTNER, A. & STAIGER, V. 2002. Neurotrophin secretion from hippocampal neurons evoked by long-term-potentiation-inducing electrical stimulation patterns. *Proceedings of the National Academy of Sciences of the United States of America,* 99**,** 6386-6391.

GASS, P., WOLFER, D. P., BALSCHUN, D., RUDOLPH, D., FREY, U., LIPP, H. P. & SCHÜTZ, G. 1998. Deficits in memory tasks of mice with CREB mutations depend on gene dosage. *Learning & memory (Cold Spring Harbor, N.Y.),* 5**,** 274-288.

GIESE, K. P., FEDOROV, N. B., FILIPKOWSKI, R. K. & SILVA, A. J. 1998. Autophosphorylation at Thr286 of the alpha calcium-calmodulin kinase II in LTP and learning. *Science,* 279**,** 870-3.

GILBERT, P. E., KESNER, R. P. & LEE, I. 2001. Dissociating hippocampal subregions: double dissociation between dentate gyrus and CA1. *Hippocampus,* 11**,** 626-36.

GINTY, D. D., BONNI A FAU - GREENBERG, M. E. & GREENBERG, M. E. 1994. Nerve growth factor activates a Ras-dependent protein kinase that stimulates c-fos transcription via phosphorylation of CREB.

GOBBO, O. L. & O'MARA, S. M. 2004. Impact of enriched-environment housing on brain-derived neurotrophic factor and on cognitive performance after a transient global ischemia. *Behav Brain Res,* 152**,** 231-41.

GODOY, L. D., ROSSIGNOLI, M. T., DELFINO-PEREIRA, P., GARCIA-CAIRASCO, N. & DE LIMA UMEOKA, E. H. 2018. A Comprehensive Overview on Stress Neurobiology: Basic Concepts and Clinical Implications. *Frontiers in Behavioral Neuroscience,* 12**,** 127.

GONZALES, R. B., DELEON GALVAN, C. J., RANGEL, Y. M. & CLAIBORNE, B. J. 2001. Distribution of thorny excrescences on CA3 pyramidal neurons in the rat hippocampus. *J Comp Neurol,* 430**,** 357-68.

GONZALEZ, G. A. & MONTMINY, M. R. 1989. Cyclic AMP stimulates somatostatin gene transcription by phosphorylation of CREB at serine 133. *Cell,* 59**,** 675-80.

GORALSKI, K. B., MCCARTHY, T. C., HANNIMAN, E. A., ZABEL, B. A., BUTCHER, E. C., PARLEE, S. D., MURUGANANDAN, S. & SINAL, C. J. 2007. Chemerin, a Novel Adipokine That Regulates Adipogenesis and Adipocyte Metabolism. *Journal of Biological Chemistry,* 282**,** 28175-28188.

GOTTMANN, K., MITTMANN, T. & LESSMANN, V. 2009. BDNF signaling in the formation, maturation and plasticity of glutamatergic and GABAergic synapses. *Exp Brain Res,* 199**,** 203-34.

GOUVEIA, K. & HURST, J. L. 2017. Optimising reliability of mouse performance in behavioural testing: the major role of non-aversive handling. *Scientific Reports,* 7**,** 44999.

GOWER, A. J. & LAMBERTY, Y. 1993. The aged mouse as a model of cognitive decline with special emphasis on studies in NMRI mice. *Behav Brain Res,* 57**,** 163-73.

GRAY, E. E., FINK, A. E., SARINANA, J., VISSEL, B. & O'DELL, T. J. 2007. Long-term potentiation in the hippocampal CA1 region does not require insertion and activation of GluR2-lacking AMPA receptors. *J Neurophysiol,* 98**,** 2488-92.

GREGER, I. H., KHATRI, L., KONG, X. & ZIFF, E. B. 2003. AMPA receptor tetramerization is mediated by Q/R editing. *Neuron,* 40**,** 763-74.

GRÉGOIRE, C.-A., BONENFANT, D., LE NGUYEN, A., AUMONT, A. & FERNANDES, K. J. L. 2014. Untangling the influences of voluntary running, environmental complexity, social housing and stress on adult hippocampal neurogenesis. *PloS one,* 9**,** e86237-e86237.

GUBERT, C. & HANNAN, A. J. 2019. Environmental enrichment as an experience-dependent modulator of social plasticity and cognition. *Brain Res*.

GUEMEZ-GAMBOA, A., COUFAL, N. G. & GLEESON, J. G. 2014. Primary cilia in the developing and mature brain. *Neuron,* 82**,** 511-521.

GUTIÈRREZ-MECINAS, M., TROLLOPE, A. F., COLLINS, A., MORFETT, H., HESKETH, S. A., KERSANTÉ, F. & REUL, J. M. H. M. 2011. Long-lasting behavioral responses to stress involve a direct interaction of glucocorticoid receptors with ERK1/2–MSK1–Elk-1 signaling. *Proceedings of the National Academy of Sciences,* 108**,** 13806-13811.

GUZOWSKI, J. F., LYFORD, G. L., STEVENSON, G. D., HOUSTON, F. P., MCGAUGH, J. L., WORLEY, P. F. & BARNES, C. A. 2000. Inhibition of Activity-Dependent Arc Protein Expression in the Rat Hippocampus Impairs the Maintenance of Long-Term Potentiation and the Consolidation of Long-Term Memory. *The Journal of Neuroscience,* 20**,** 3993-4001.

GUZOWSKI, J. F. & MCGAUGH, J. L. 1997. Antisense oligodeoxynucleotide-mediated disruption of hippocampal cAMP response element binding protein levels impairs consolidation of memory for water maze training. *Proc Natl Acad Sci U S A,* 94**,** 2693-8.

GUZOWSKI, J. F., SETLOW, B., WAGNER, E. K. & MCGAUGH, J. L. 2001. Experience-dependent gene expression in the rat hippocampus after spatial learning: a comparison of the immediate-early genes Arc, c-fos, and zif268. *J Neurosci,* 21**,** 5089-98.

HAETTIG, J., STEFANKO, D. P., MULTANI, M. L., FIGUEROA, D. X., MCQUOWN, S. C. & WOOD, M. A. 2011. HDAC inhibition modulates hippocampus-dependent long-term memory for object location in a CBP-dependent manner. *Learn Mem,* 18**,** 71-9.

HAFTING, T., FYHN, M., MOLDEN, S., MOSER, M. B. & MOSER, E. I. 2005. Microstructure of a spatial map in the entorhinal cortex. *Nature,* 436**,** 801-6.

HALL, J., THOMAS, K. L. & EVERITT, B. J. 2000. Rapid and selective induction of BDNF expression in the hippocampus during contextual learning. *Nat Neurosci,* 3**,** 533-5.

HANSEN-ALGENSTAEDT, N., ALGENSTAEDT, P., SCHAEFER, C., HAMANN, A., WOLFRAM, L., CINGÖZ, G., KILIC, N., SCHWARZLOH, B., SCHROEDER, M., JOSCHECK, C., WIESNER, L., RÜTHER, W. & ERGÜN, S. 2006. Neural driven angiogenesis by overexpression of nerve growth factor. *Histochemistry and Cell Biology,* 125**,** 637-649.

HARATI, H., MAJCHRZAK, M., COSQUER, B., GALANI, R., KELCHE, C., CASSEL, J. C. & BARBELIVIEN, A. 2011. Attention and memory in aged rats: Impact of lifelong environmental enrichment. *Neurobiol Aging,* 32**,** 718-36.

HAUG, H. 1986. History of neuromorphometry. *Journal of Neuroscience Methods,* 18**,** 1-17.

HAUSOTT, B., VALLANT, N., SCHLICK, B., AUER, M., NIMMERVOLL, B., OBERMAIR, G. J., SCHWARZER, C., DAI, F., BRAND-SABERI, B. & KLIMASCHEWSKI, L. 2012. Sprouty2 and -4 regulate axon outgrowth by hippocampal neurons. *Hippocampus,* 22**,** 434-41.

HEBB, D. 1949. *The organisation of behaviour,* McGill University, New York JOHN WILEY and SONS.

HELFER, G. & WU, Q.-F. 2018. Chemerin: a multifaceted adipokine involved in metabolic disorders. *The Journal of endocrinology,* 238**,** R79-R94.

HENDERSHOTT, T. R., CRONIN, M. E., LANGELLA, S., MCGUINNESS, P. S. & BASU, A. C. 2016. Effects of environmental enrichment on anxiety-like behavior, sociability, sensory gating, and spatial learning in male and female C57BL/6J mice. *Behav Brain Res,* 314**,** 215-25.

HENLEY, J. M. & WILKINSON, K. A. 2013. AMPA receptor trafficking and the mechanisms underlying synaptic plasticity and cognitive aging. *Dialogues in Clinical Neuroscience,* 15**,** 11-27.

HENLEY, J. M. & WILKINSON, K. A. 2016. Synaptic AMPA receptor composition in development, plasticity and disease. *Nat Rev Neurosci,* 17**,** 337-50.

HERCULANO-HOUZEL, S. 2012. The remarkable, yet not extraordinary, human brain as a scaled-up primate brain and its associated cost. *Proceedings of the National Academy of Sciences of the United States of America,* 109 Suppl 1**,** 10661-10668.

HERNANDEZ, P. J. & ABEL, T. 2008. The role of protein synthesis in memory consolidation: Progress amid decades of debate. *Neurobiology of learning and memory,* 89**,** 293-311.

HEROLD, S., JAGASIA, R., MERZ, K., WASSMER, K. & LIE, D. C. 2011. CREB signalling regulates early survival, neuronal gene expression and morphological development in adult subventricular zone neurogenesis. *Mol Cell Neurosci,* 46**,** 79-88.

HILL, A. S., SAHAY, A. & HEN, R. 2015. Increasing Adult Hippocampal Neurogenesis is Sufficient to Reduce Anxiety and Depression-Like Behaviors. *Neuropsychopharmacology,* 40**,** 2368-2378.

HITTI, F. L. & SIEGELBAUM, S. A. 2014. The hippocampal CA2 region is essential for social memory. *Nature,* 508**,** 88-92.

HONG, S., BEJA-GLASSER, V. F., NFONOYIM, B. M., FROUIN, A., LI, S., RAMAKRISHNAN, S., MERRY, K. M., SHI, Q., ROSENTHAL, A., BARRES, B. A., LEMERE, C. A., SELKOE, D. J. & STEVENS, B. 2016. Complement and microglia mediate early synapse loss in Alzheimer mouse models. *Science (New York, N.Y.),* 352**,** 712-716.

HU, Y.-S., LONG, N., PIGINO, G., BRADY, S. T. & LAZAROV, O. 2013. Molecular mechanisms of environmental enrichment: impairments in Akt/GSK3β, neurotrophin-3 and CREB signaling. *PloS one,* 8**,** e64460-e64460.

HUANG, F. L., HUANG, K.-P., WU, J. & BOUCHERON, C. 2006. Environmental enrichment enhances neurogranin expression and hippocampal learning and memory but fails to rescue the impairments of neurogranin null mutant mice. *The Journal of neuroscience : the official journal of the Society for Neuroscience,* 26**,** 6230-6237.

HUANG, Y. Y., NGUYEN, P. V., ABEL, T. & KANDEL, E. R. 1996. Long-lasting forms of synaptic potentiation in the mammalian hippocampus. *Learning & Memory,* 3**,** 74-85.

HUERTA, P. T., SUN, L. D., WILSON, M. A. & TONEGAWA, S. 2000. Formation of temporal memory requires NMDA receptors within CA1 pyramidal neurons. *Neuron,* 25**,** 473-80.

HUMMLER, E., COLE, T. J., BLENDY, J. A., GANSS, R., AGUZZI, A., SCHMID, W., BEERMANN, F. & SCHUTZ, G. 1994. Targeted mutation of the CREB gene: compensation within the CREB/ATF family of transcription factors. *Proc Natl Acad Sci U S A,* 91**,** 5647-51.

HUNTER, C. J., REMENYI, J., CORREA, S. A., PRIVITERA, L., REYSKENS, K., MARTIN, K. J., TOTH, R., FRENGUELLI, B. G. & ARTHUR, J. S. C. 2017. MSK1 regulates transcriptional induction of Arc/Arg3.1 in response to neurotrophins. *FEBS Open Bio,* 7**,** 821-834.

HUTTENRAUCH, M., SALINAS, G. & WIRTHS, O. 2016. Effects of Long-Term Environmental Enrichment on Anxiety, Memory, Hippocampal Plasticity and Overall Brain Gene Expression in C57BL6 Mice. *Front Mol Neurosci,* 9**,** 62.

INTLEKOFER, K. A., BERCHTOLD, N. C., MALVAEZ, M., CARLOS, A. J., MCQUOWN, S. C., CUNNINGHAM, M. J., WOOD, M. A. & COTMAN, C. W. 2013. Exercise and sodium butyrate transform a subthreshold learning event into long-term memory via a brain-derived neurotrophic factor-dependent mechanism. *Neuropsychopharmacology : official publication of the American College of Neuropsychopharmacology,* 38**,** 2027-2034.

IRVINE, G. I., LOGAN, B., ECKERT, M. & ABRAHAM, W. C. 2006. Enriched environment exposure regulates excitability, synaptic transmission, and LTP in the dentate gyrus of freely moving rats. *Hippocampus,* 16**,** 149-60.

ISA, T., IINO, M., ITAZAWA, S. & OZAWA, S. 1995. Spermine mediates inward rectification of Ca(2+)-permeable AMPA receptor channels. *Neuroreport,* 6**,** 2045-8.

ISAAC, J. T., NICOLL, R. A. & MALENKA, R. C. 1995. Evidence for silent synapses: implications for the expression of LTP. *Neuron,* 15**,** 427-34.

ISAAC, J. T. R., ASHBY, M. C. & MCBAIN, C. J. 2007. The Role of the GluR2 Subunit in AMPA Receptor Function and Synaptic Plasticity. *Neuron,* 54**,** 859-871.
ISHIZUKA, N., COWAN, W. M. & AMARAL, D. G. 1995. A quantitative analysis of the dendritic organization of pyramidal cells in the rat hippocampus. *J Comp Neurol,* 362**,** 17-45.
JACK, C. R., JR., PETERSEN, R. C., XU, Y. C., O'BRIEN, P. C., SMITH, G. E., IVNIK, R. J., BOEVE, B. F., WARING, S. C., TANGALOS, E. G. & KOKMEN, E. 1999. Prediction of AD with MRI-based hippocampal volume in mild cognitive impairment. *Neurology,* 52**,** 1397-1403.
JACKMAN, S. L. & REGEHR, W. G. 2017. The Mechanisms and Functions of Synaptic Facilitation. *Neuron,* 94**,** 447-464.
JÄKEL, S. & DIMOU, L. 2017. Glial Cells and Their Function in the Adult Brain: A Journey through the History of Their Ablation. *Frontiers in cellular neuroscience,* 11**,** 24-24.
JAKOVCEVSKI, M., RUAN, H., SHEN, E. Y., DINCER, A., JAVIDFAR, B., MA, Q., PETER, C. J., CHEUNG, I., MITCHELL, A. C., JIANG, Y., LIN, C. L., POTHULA, V., STEWART, A. F., ERNST, P., YAO, W. D. & AKBARIAN, S. 2015. Neuronal Kmt2a/Mll1 histone methyltransferase is essential for prefrontal synaptic plasticity and working memory. *J Neurosci,* 35**,** 5097-108.
JANG, S. W., LIU X FAU - YEPES, M., YEPES M FAU - SHEPHERD, K. R., SHEPHERD KR FAU - MILLER, G. W., MILLER GW FAU - LIU, Y., LIU Y FAU - WILSON, W. D., WILSON WD FAU - XIAO, G., XIAO G FAU - BLANCHI, B., BLANCHI B FAU - SUN, Y. E., SUN YE FAU - YE, K. & YE, K. 2010. A selective TrkB agonist with potent neurotrophic activities by 7,8-dihydroxyflavone.
JI, J. & MAREN, S. 2008. Differential roles for hippocampal areas CA1 and CA3 in the contextual encoding and retrieval of extinguished fear. *Learning & Memory,* 15**,** 244-251.
JI, K., AKGUL, G., WOLLMUTH, L. P. & TSIRKA, S. E. 2013. Microglia actively regulate the number of functional synapses. *PloS one,* 8**,** e56293-e56293.
JI, Y., LU, Y., YANG, F., SHEN, W., TANG, T. T.-T., FENG, L., DUAN, S. & LU, B. 2010. Acute and gradual increases in BDNF concentration elicit distinct signaling and functions in neurons. *Nature neuroscience,* 13**,** 302-309.
JIA, Z., AGOPYAN, N., MIU, P., XIONG, Z., HENDERSON, J., GERLAI, R., TAVERNA, F. A., VELUMIAN, A., MACDONALD, J., CARLEN, P., ABRAMOW-NEWERLY, W. & RODER, J. 1996. Enhanced LTP in mice deficient in the AMPA receptor GluR2. *Neuron,* 17**,** 945-56.
JOHANNESSEN, M., DELGHANDI, M. P. & MOENS, U. 2004. What turns CREB on? *Cell Signal,* 16**,** 1211-27.
JOHNSON, J. W. & ASCHER, P. 1990. Voltage-dependent block by intracellular Mg2+ of N-methyl-D-aspartate-activated channels. *Biophysical journal,* 57**,** 1085-1090.
JONAS, P., RACCA, C., SAKMANN, B., SEEBURG, P. H. & MONYER, H. 1994. Differences in Ca2+ permeability of AMPA-type glutamate receptor channels in neocortical neurons caused by differential GluR-B subunit expression. *Neuron,* 12**,** 1281-9.
KACZMAREK-HÁJEK, K., LÖRINCZI, E., HAUSMANN, R. & NICKE, A. 2012. Molecular and functional properties of P2X receptors--recent progress and persisting challenges. *Purinergic signalling,* 8**,** 375-417.
KAIDANOVICH-BEILIN, O., LIPINA, T., VUKOBRADOVIC, I., RODER, J. & WOODGETT, J. R. 2011. Assessment of social interaction behaviors. *J Vis Exp*.
KAJIWARA, R., WOUTERLOOD, F. G., SAH, A., BOEKEL, A. J., BAKS-TE BULTE, L. T. & WITTER, M. P. 2008. Convergence of entorhinal and CA3 inputs onto pyramidal neurons and

interneurons in hippocampal area CA1--an anatomical study in the rat. *Hippocampus,* 18**,** 266-80.
KANDEL, E. R. 2012. The molecular biology of memory: cAMP, PKA, CRE, CREB-1, CREB-2, and CPEB. *Molecular Brain,* 5**,** 1-12.
KANG, H. & SCHUMAN, E. M. 1995. Long-lasting neurotrophin-induced enhancement of synaptic transmission in the adult hippocampus. *Science,* 267**,** 1658-62.
KANG, H., WELCHER, A. A., SHELTON, D. & SCHUMAN, E. M. 1997. Neurotrophins and time: different roles for TrkB signaling in hippocampal long-term potentiation. *Neuron,* 19**,** 653-64.
KARELINA, K., HANSEN, K. F., CHOI, Y.-S., DEVRIES, A. C., ARTHUR, J. S. C. & OBRIETAN, K. 2012. MSK1 regulates environmental enrichment-induced hippocampal plasticity and cognitive enhancement. *Learning & Memory,* 19**,** 550-560.
KEE, B. L., ARIAS, J. & MONTMINY, M. R. 1996. Adaptor-mediated Recruitment of RNA Polymerase II to a Signal-dependent Activator. *Journal of Biological Chemistry,* 271**,** 2373-2375.
KELLER, D., ERO, C. & MARKRAM, H. 2018. Cell Densities in the Mouse Brain: A Systematic Review. *Front Neuroanat,* 12**,** 83.
KELLY, Á. & HANNAN, A. J. 2019. Therapeutic impacts of environmental enrichment: Neurobiological mechanisms informing molecular targets for enviromimetics. *Neuropharmacology,* 145**,** 1-2.
KEMPERMANN, G. 2019. Environmental enrichment, new neurons and the neurobiology of individuality. *Nature Reviews Neuroscience,* 20**,** 235-245.
KENNARD, J. & WOODRUFF-PAK, D. 2011. Age Sensitivity of Behavioral Tests and Brain Substrates of Normal Aging in Mice. *Frontiers in Aging Neuroscience,* 3**,** 9.
KENTROS, C., HARGREAVES, E., HAWKINS, R. D., KANDEL, E. R., SHAPIRO, M. & MULLER, R. V. 1998. Abolition of long-term stability of new hippocampal place cell maps by NMDA receptor blockade. *Science,* 280**,** 2121-6.
KERIMOGLU, C., SAKIB, M. S., JAIN, G., BENITO, E., BURKHARDT, S., CAPECE, V., KAURANI, L., HALDER, R., AGÍS-BALBOA, R. C., STILLING, R., URBANKE, H., KRANZ, A., STEWART, A. F. & FISCHER, A. 2017. KMT2A and KMT2B Mediate Memory Function by Affecting Distinct Genomic Regions. *Cell Reports,* 20**,** 538-548.
KESNER, R. P. 2007. A behavioral analysis of dentate gyrus function. *Prog Brain Res,* 163**,** 567-76.
KESSLAK, J. P., SO, V., CHOI, J., COTMAN, C. W. & GOMEZ-PINILLA, F. 1998. Learning upregulates brain-derived neurotrophic factor messenger ribonucleic acid: a mechanism to facilitate encoding and circuit maintenance? *Behav Neurosci,* 112**,** 1012-9.
KIDA, S. 2012. A Functional Role for CREB as a Positive Regulator of Memory Formation and LTP. *Exp Neurobiol,* 21**,** 136-140.
KIDA, S., JOSSELYN SA FAU - PENA DE ORTIZ, S., PENA DE ORTIZ S FAU - KOGAN, J. H., KOGAN JH FAU - CHEVERE, I., CHEVERE I FAU - MASUSHIGE, S., MASUSHIGE S FAU - SILVA, A. J. & SILVA, A. J. 2002. CREB required for the stability of new and reactivated fear memories. *Nat, Neurosci*.
KIM, J. & TSIEN, R. W. 2008. Synapse-specific adaptations to inactivity in hippocampal circuits achieve homeostatic gain control while dampening network reverberation. *Neuron,* 58**,** 925-37.

KIMELBERG, H. K. 2010. Functions of mature mammalian astrocytes: a current view. *Neuroscientist,* 16**,** 79-106.
KOH, S., CHUNG, H., XIA, H., MAHADEVIA, A. & SONG, Y. 2005. Environmental enrichment reverses the impaired exploratory behavior and altered gene expression induced by early-life seizures. *J Child Neurol,* 20**,** 796-802.
KOHARA, K., KITAMURA, A., MORISHIMA, M. & TSUMOTO, T. 2001. Activity-dependent transfer of brain-derived neurotrophic factor to postsynaptic neurons. *Science,* 291**,** 2419-23.
KONDO, M. 2017. Molecular mechanisms of experience-dependent structural and functional plasticity in the brain. *Anat Sci Int,* 92**,** 1-17.
KORZUS, E., ROSENFELD, M. G. & MAYFORD, M. 2004. CBP Histone Acetyltransferase Activity Is a Critical Component of Memory Consolidation. *Neuron,* 42**,** 961-972.
KOWIAŃSKI, P., LIETZAU, G., CZUBA, E., WAŚKOW, M., STELIGA, A. & MORYŚ, J. 2018. BDNF: A Key Factor with Multipotent Impact on Brain Signaling and Synaptic Plasticity. *Cellular and Molecular Neurobiology,* 38**,** 579-593.
KUMAMOTO, N., GU, Y., WANG, J., JANOSCHKA, S., TAKEMARU, K., LEVINE, J. & GE, S. 2012. A role for primary cilia in glutamatergic synaptic integration of adult-born neurons. *Nat Neurosci,* 15**,** 399-405, s1.
KUMAR, S. S., BACCI, A., KHARAZIA, V. & HUGUENARD, J. R. 2002. A developmental switch of AMPA receptor subunits in neocortical pyramidal neurons. *J Neurosci,* 22**,** 3005-15.
LALO, U., BOGDANOV, A., MOSS, G. W. J., FRENGUELLI, B. G. & PANKRATOV, Y. 2018. Role for Astroglia-Derived BDNF and MSK1 in Homeostatic Synaptic Plasticity. *Neuroglia,* 1.
LARSON, J. & MUNKÁCSY, E. 2015. Theta-burst LTP. *Brain research,* 1621**,** 38-50.
LARSON, J., WONG, D. & LYNCH, G. 1986. Patterned stimulation at the theta frequency is optimal for the induction of hippocampal long-term potentiation. *Brain Res,* 368**,** 347-50.
LAUTERBORN, J. C., JAFARI, M., BABAYAN, A. H. & GALL, C. M. 2013. Environmental Enrichment Reveals Effects of Genotype on Hippocampal Spine Morphologies in the Mouse Model of Fragile X Syndrome. *Cerebral Cortex,* 25**,** 516-527.
LEE, KEA J., QUEENAN, BRIDGET N., ROZEBOOM, AARON M., BELLMORE, R., LIM, SEUNG T., VICINI, S. & PAK, DANIEL T. S. 2013. Mossy Fiber-CA3 Synapses Mediate Homeostatic Plasticity in Mature Hippocampal Neurons. *Neuron,* 77**,** 99-114.
LEE, S. E., SIMONS, S. B., HELDT, S. A., ZHAO, M., SCHROEDER, J. P., VELLANO, C. P., COWAN, D. P., RAMINENI, S., YATES, C. K., FENG, Y., SMITH, Y., SWEATT, J. D., WEINSHENKER, D., RESSLER, K. J., DUDEK, S. M. & HEPLER, J. R. 2010. RGS14 is a natural suppressor of both synaptic plasticity in CA2 neurons and hippocampal-based learning and memory. *Proc Natl Acad Sci U S A,* 107**,** 16994-8.
LEHMANN, M. L., BRACHMAN, R. A., MARTINOWICH, K., SCHLOESSER, R. J. & HERKENHAM, M. 2013. Glucocorticoids orchestrate divergent effects on mood through adult neurogenesis. *The Journal of neuroscience : the official journal of the Society for Neuroscience,* 33**,** 2961-2972.
LEIN, E. S., HAWRYLYCZ, M. J., AO, N., AYRES, M., BENSINGER, A., BERNARD, A., BOE, A. F., BOGUSKI, M. S., BROCKWAY, K. S., BYRNES, E. J., CHEN, L., CHEN, L., CHEN, T.-M., CHI CHIN, M., CHONG, J., CROOK, B. E., CZAPLINSKA, A., DANG, C. N., DATTA, S., DEE, N. R., DESAKI, A. L., DESTA, T., DIEP, E., DOLBEARE, T. A., DONELAN, M. J., DONG, H.-W., DOUGHERTY, J. G., DUNCAN, B. J., EBBERT, A. J., EICHELE, G., ESTIN, L. K., FABER, C.,

FACER, B. A., FIELDS, R., FISCHER, S. R., FLISS, T. P., FRENSLEY, C., GATES, S. N., GLATTFELDER, K. J., HALVERSON, K. R., HART, M. R., HOHMANN, J. G., HOWELL, M. P., JEUNG, D. P., JOHNSON, R. A., KARR, P. T., KAWAL, R., KIDNEY, J. M., KNAPIK, R. H., KUAN, C. L., LAKE, J. H., LARAMEE, A. R., LARSEN, K. D., LAU, C., LEMON, T. A., LIANG, A. J., LIU, Y., LUONG, L. T., MICHAELS, J., MORGAN, J. J., MORGAN, R. J., MORTRUD, M. T., MOSQUEDA, N. F., NG, L. L., NG, R., ORTA, G. J., OVERLY, C. C., PAK, T. H., PARRY, S. E., PATHAK, S. D., PEARSON, O. C., PUCHALSKI, R. B., RILEY, Z. L., ROCKETT, H. R., ROWLAND, S. A., ROYALL, J. J., RUIZ, M. J., SARNO, N. R., SCHAFFNIT, K., SHAPOVALOVA, N. V., SIVISAY, T., SLAUGHTERBECK, C. R., SMITH, S. C., SMITH, K. A., SMITH, B. I., SODT, A. J., STEWART, N. N., STUMPF, K.-R., SUNKIN, S. M., SUTRAM, M., TAM, A., TEEMER, C. D., THALLER, C., THOMPSON, C. L., VARNAM, L. R., VISEL, A., WHITLOCK, R. M., WOHNOUTKA, P. E., WOLKEY, C. K., WONG, V. Y., et al. 2007. Genome-wide atlas of gene expression in the adult mouse brain. *Nature,* 445**,** 168-176.

LEPANTO, P., BADANO, J. L. & ZOLESSI, F. R. 2016. Neuron's little helper: The role of primary cilia in neurogenesis. *Neurogenesis (Austin),* 3**,** e1253363.

LEVENSON, J. M. & SWEATT, J. D. 2005. Epigenetic mechanisms in memory formation. *Nat Rev Neurosci,* 6**,** 108-18.

LI, Y., KRUPA, B., KANG, J.-S., BOLSHAKOV, V. Y. & LIU, G. 2009. Glycine site of NMDA receptor serves as a spatiotemporal detector of synaptic activity patterns. *Journal of neurophysiology,* 102**,** 578-589.

LI, Y., SACCHI, S., POLLEGIONI, L., BASU, A. C., COYLE, J. T. & BOLSHAKOV, V. Y. 2013. Identity of endogenous NMDAR glycine site agonist in amygdala is determined by synaptic activity level. *Nature communications,* 4**,** 1760-1760.

LIAO, D., HESSLER, N. A. & MALINOW, R. 1995. Activation of postsynaptically silent synapses during pairing-induced LTP in CA1 region of hippocampal slice. *Nature,* 375**,** 400-4.

LIN, P. Y., KAVALALI, E. T. & MONTEGGIA, L. M. 2018. Genetic Dissection of Presynaptic and Postsynaptic BDNF-TrkB Signaling in Synaptic Efficacy of CA3-CA1 Synapses. *Cell Rep,* 24**,** 1550-1561.

LISMAN, J., COOPER, K., SEHGAL, M. & SILVA, A. J. 2018. Memory formation depends on both synapse-specific modifications of synaptic strength and cell-specific increases in excitability. *Nature Neuroscience,* 21**,** 309-314.

LIU, C., CHAN, C. B. & YE, K. 2016. 7,8-dihydroxyflavone, a small molecular TrkB agonist, is useful for treating various BDNF-implicated human disorders. *Translational Neurodegeneration,* 5**,** 2.

LIU, P. Z. & NUSSLOCK, R. 2018. Exercise-Mediated Neurogenesis in the Hippocampus via BDNF. *Front Neurosci,* 12**,** 52.

LLORENS-MARTIN, M., JURADO-ARJONA, J., AVILA, J. & HERNANDEZ, F. 2015. Novel connection between newborn granule neurons and the hippocampal CA2 field. *Exp Neurol,* 263**,** 285-92.

LONZE, B. E. & GINTY, D. D. 2002. Function and Regulation of CREB Family Transcription Factors in the Nervous System. *Neuron,* 35**,** 605-623.

LOPEZ-ATALAYA, J. P., CICCARELLI, A., VIOSCA, J., VALOR, L. M., JIMENEZ-MINCHAN, M., CANALS, S., GIUSTETTO, M. & BARCO, A. 2011. CBP is required for environmental enrichment-induced neurogenesis and cognitive enhancement. *Embo j,* 30**,** 4287-98.

LORENTE DE NÓ, R. 1934. Studies on the structure of the cerebral cortex. II. Continuation of the study of the ammonic system. *Journal für Psychologie und Neurologie,* 46**,** 113-177.

LOVE, M. I., HUBER, W. & ANDERS, S. 2014. Moderated estimation of fold change and dispersion for RNA-seq data with DESeq2. *Genome Biol,* 15**,** 550.

LU, Y., CHRISTIAN, K. & LU, B. 2008. BDNF: a key regulator for protein synthesis-dependent LTP and long-term memory? *Neurobiology of learning and memory,* 89**,** 312-323.

LUJAN, R., NUSSER, Z., ROBERTS, J. D., SHIGEMOTO, R. & SOMOGYI, P. 1996. Perisynaptic location of metabotropic glutamate receptors mGluR1 and mGluR5 on dendrites and dendritic spines in the rat hippocampus. *Eur J Neurosci,* 8**,** 1488-500.

LUTTER, R. & RAVANETTI, L. 2019. Cadherin-related family member 3 (CDHR3) drives differentiation of ciliated bronchial epithelial cells and facilitates rhinovirus C infection, although with a little help. *Journal of Allergy and Clinical Immunology,* 144**,** 926-927.

LYNCH, G., KRAMAR, E. A. & GALL, C. M. 2015. Protein synthesis and consolidation of memory-related synaptic changes. *Brain Res,* 1621**,** 62-72.

LYNCH, G., LARSON, J., KELSO, S., BARRIONUEVO, G. & SCHOTTLER, F. 1983. Intracellular injections of EGTA block induction of hippocampal long-term potentiation. *Nature,* 305**,** 719-721.

MA, H., GROTH, R. D., COHEN, S. M., EMERY, J. F., LI, B., HOEDT, E., ZHANG, G., NEUBERT, T. A. & TSIEN, R. W. 2014. gammaCaMKII shuttles Ca(2)(+)/CaM to the nucleus to trigger CREB phosphorylation and gene expression. *Cell,* 159**,** 281-94.

MACDONALD, C. J., LEPAGE, K. Q., EDEN, U. T. & EICHENBAUM, H. 2011. Hippocampal "time cells" bridge the gap in memory for discontiguous events. *Neuron,* 71**,** 737-749.

MAINEN, Z. F., JIA, Z., RODER, J. & MALINOW, R. 1998. Use-dependent AMPA receptor block in mice lacking GluR2 suggests postsynaptic site for LTP expression. *Nat Neurosci,* 1**,** 579-86.

MALIK, R. & CHATTARJI, S. 2012. Enhanced intrinsic excitability and EPSP-spike coupling accompany enriched environment-induced facilitation of LTP in hippocampal CA1 pyramidal neurons.

MANKIN, E. A., DIEHL, G. W., SPARKS, F. T., LEUTGEB, S. & LEUTGEB, J. K. 2015. Hippocampal CA2 activity patterns change over time to a larger extent than between spatial contexts. *Neuron,* 85**,** 190-201.

MARX, M., GUNTER RH FAU - HUCKO, W., HUCKO W FAU - RADNIKOW, G., RADNIKOW G FAU - FELDMEYER, D. & FELDMEYER, D. 2012. Improved biocytin labeling and neuronal 3D reconstruction. *Nat. Protocols*.

MATSUDA, N., LU, H., FUKATA, Y., NORITAKE, J., GAO, H., MUKHERJEE, S., NEMOTO, T., FUKATA, M. & POO, M.-M. 2009. Differential Activity-Dependent Secretion of Brain-Derived Neurotrophic Factor from Axon and Dendrite. *The Journal of Neuroscience,* 29**,** 14185.

MAYER, M. L. & WESTBROOK, G. L. 1987. Permeation and block of N-methyl-D-aspartic acid receptor channels by divalent cations in mouse cultured central neurones. *The Journal of physiology,* 394**,** 501-527.

MAYR, B. M., CANETTIERI, G. & MONTMINY, M. R. 2001. Distinct effects of cAMP and mitogenic signals on CREB-binding protein recruitment impart specificity to target gene activation via CREB. *Proc Natl Acad Sci U S A,* 98**,** 10936-41.

MCDONALD, M. W., HAYWARD, K. S., ROSBERGEN, I. C. M., JEFFERS, M. S. & CORBETT, D. 2018. Is Environmental Enrichment Ready for Clinical Application in Human Post-stroke Rehabilitation? *Frontiers in Behavioral Neuroscience,* 12**,** 135.

MCEWEN, B., TANAPAT, P. & WEILAND, N. 1999. Inhibition of Dendritic Spine Induction on Hippocampal CA1 Pyramidal Neurons by a Nonsteroidal Estrogen Antagonist in Female Rats 1. *Endocrinology,* 140**,** 1044-7.

MCEWEN, B. S. & AKIL, H. 2020. Revisiting the Stress Concept: Implications for Affective Disorders. *The Journal of Neuroscience,* 40**,** 12.

MCHUGH, T. J., BLUM, K. I., TSIEN, J. Z., TONEGAWA, S. & WILSON, M. A. 1996. Impaired Hippocampal Representation of Space in CA1-Specific NMDAR1 Knockout Mice. *Cell,* 87**,** 1339-1349.

MCHUGH, T. J. & TONEGAWA, S. 2009. CA3 NMDA receptors are required for the rapid formation of a salient contextual representation. *Hippocampus,* 19**,** 1153-1158.

MCOMISH, C. E. & HANNAN, A. J. 2007. Enviromimetics: exploring gene environment interactions to identify therapeutic targets for brain disorders. *Expert Opinion on Therapeutic Targets,* 11**,** 899-913.

MCPHERSON, C. S. & LAWRENCE, A. J. 2007. The nuclear transcription factor CREB: involvement in addiction, deletion models and looking forward. *Current neuropharmacology,* 5**,** 202-212.

MCQUAID, R. J., DUNN, R., JACOBSON-PICK, S., ANISMAN, H. & AUDET, M.-C. 2018. Post-weaning Environmental Enrichment in Male CD-1 Mice: Impact on Social Behaviors, Corticosterone Levels and Prefrontal Cytokine Expression in Adulthood. *Frontiers in behavioral neuroscience,* 12**,** 145-145.

MEANS, A. R. 2000. Regulatory Cascades Involving Calmodulin-Dependent Protein Kinases. *Molecular Endocrinology,* 14**,** 4-13.

MERZ, K., HEROLD, S. & LIE, D. C. 2011. CREB in adult neurogenesis--master and partner in the development of adult-born neurons? *Eur J Neurosci,* 33**,** 1078-86.

MESA-GRESA, P., PÉREZ-MARTINEZ, A. & REDOLAT, R. 2013. Environmental Enrichment Improves Novel Object Recognition and Enhances Agonistic Behavior in Male Mice. *Aggressive Behavior,* 39**,** 269-279.

MESSAOUDI, E., KANHEMA, T., SOULÉ, J., TIRON, A., DAGYTE, G., DA SILVA, B. & BRAMHAM, C. R. 2007. Sustained Arc/Arg3.1 Synthesis Controls Long-Term Potentiation Consolidation through Regulation of Local Actin Polymerization in the Dentate Gyrus In Vivo. *The Journal of Neuroscience,* 27**,** 10445.

MINATOHARA, K., AKIYOSHI, M. & OKUNO, H. 2015. Role of Immediate-Early Genes in Synaptic Plasticity and Neuronal Ensembles Underlying the Memory Trace. *Front Mol Neurosci,* 8**,** 78.

MINICHIELLO, L. 2009. TrkB signalling pathways in LTP and learning. *Nat Rev Neurosci,* 10**,** 850-60.

MINICHIELLO, L., KORTE M FAU - WOLFER, D., WOLFER D FAU - KUHN, R., KUHN R FAU - UNSICKER, K., UNSICKER K FAU - CESTARI, V., CESTARI V FAU - ROSSI-ARNAUD, C., ROSSI-ARNAUD C FAU - LIPP, H. P., LIPP HP FAU - BONHOEFFER, T., BONHOEFFER T FAU - KLEIN, R. & KLEIN, R. 1999. Essential role for TrkB receptors in hippocampus-mediated learning.

MOCKETT, B. G., GUÉVREMONT, D., ELDER, M. K., PARFITT, K. D., PEPPERCORN, K., MORRISSEY, J., SINGH, A., HINTZ, T. J., KOCHEN, L., TOM DIECK, S., SCHUMAN, E., TATE, W. P., WILLIAMS, J. M. & ABRAHAM, W. C. 2019. Glutamate receptor

trafficking and protein synthesis mediate the facilitation of ltp by secreted amyloid precursor protein-alpha. *The Journal of Neuroscience*, 1826-18.
MORA, F., SEGOVIA, G. & DEL ARCO, A. 2007. Aging, plasticity and environmental enrichment: Structural changes and neurotransmitter dynamics in several areas of the brain. *Brain Research Reviews,* 55, 78-88.
MORENO-JIMENEZ, E. P., FLOR-GARCIA, M., TERREROS-RONCAL, J., RABANO, A., CAFINI, F., PALLAS-BAZARRA, N., AVILA, J. & LLORENS-MARTIN, M. 2019. Adult hippocampal neurogenesis is abundant in neurologically healthy subjects and drops sharply in patients with Alzheimer's disease. *Nat Med,* 25, 554-560.
MORITA, D., RAH, J. C. & ISAAC, J. T. 2014. Incorporation of inwardly rectifying AMPA receptors at silent synapses during hippocampal long-term potentiation. *Philos Trans R Soc Lond B Biol Sci,* 369, 20130156.
MORRIS, R. G. 2006. Elements of a neurobiological theory of hippocampal function: the role of synaptic plasticity, synaptic tagging and schemas. *Eur J Neurosci,* 23, 2829-46.
MORRIS, R. G., ANDERSON, E., LYNCH, G. S. & BAUDRY, M. 1986. Selective impairment of learning and blockade of long-term potentiation by an N-methyl-D-aspartate receptor antagonist, AP5. *Nature,* 319, 774-6.
MORRIS, R. G. M., GARRUD, P., RAWLINS, J. N. P. & O'KEEFE, J. 1982. Place navigation impaired in rats with hippocampal lesions. *Nature,* 297, 681-683.
MOSER, K. V., REINDL, M., BLASIG, I. & HUMPEL, C. 2004. Brain capillary endothelial cells proliferate in response to NGF, express NGF receptors and secrete NGF after inflammation. *Brain Research,* 1017, 53-60.
MOSER, M. B., ROWLAND, D. C. & MOSER, E. I. 2015. Place cells, grid cells, and memory. *Cold Spring Harb Perspect Biol,* 7, a021808.
MOWLA, S. J., FARHADI, H. F., PAREEK, S., ATWAL, J. K., MORRIS, S. J., SEIDAH, N. G. & MURPHY, R. A. 2001. Biosynthesis and Post-translational Processing of the Precursor to Brain-derived Neurotrophic Factor. *Journal of Biological Chemistry,* 276, 12660-12666.
MOY, S. S., NADLER, J. J., PEREZ, A., BARBARO, R. P., JOHNS, J. M., MAGNUSON, T. R., PIVEN, J. & CRAWLEY, J. N. 2004. Sociability and preference for social novelty in five inbred strains: an approach to assess autistic-like behavior in mice. *Genes Brain Behav,* 3, 287-302.
MURÍNOVÁ, J., HLAVÁČOVÁ, N., CHMELOVÁ, M. & RIEČANSKÝ, I. 2017. The Evidence for Altered BDNF Expression in the Brain of Rats Reared or Housed in Social Isolation: A Systematic Review. *Frontiers in behavioral neuroscience,* 11, 101-101.
NAKA, F., NARITA, N., OKADO, N. & NARITA, M. 2005. Modification of AMPA receptor properties following environmental enrichment. *Brain Dev,* 27, 275-8.
NAKAZAWA, K., MCHUGH, T. J., WILSON, M. A. & TONEGAWA, S. 2004. NMDA receptors, place cells and hippocampal spatial memory. *Nature Reviews Neuroscience,* 5, 361-372.
NAKAZAWA, K., QUIRK, M. C., CHITWOOD, R. A., WATANABE, M., YECKEL, M. F., SUN, L. D., KATO, A., CARR, C. A., JOHNSTON, D., WILSON, M. A. & TONEGAWA, S. 2002. Requirement for hippocampal CA3 NMDA receptors in associative memory recall. *Science,* 297, 211-8.
NAKAZAWA, K., SUN, L. D., QUIRK, M. C., RONDI-REIG, L., WILSON, M. A. & TONEGAWA, S. 2003. Hippocampal CA3 NMDA receptors are crucial for memory acquisition of one-time experience. *Neuron,* 38, 305-15.

NAQVI, S., MARTIN, KIRSTY J. & ARTHUR, J. SIMON C. 2014. CREB phosphorylation at Ser133regulates transcription via distinct mechanisms downstream of cAMP and MAPK signalling. *Biochemical Journal,* 458**,** 469.

NAU, R., RIBES, S., DJUKIC, M. & EIFFERT, H. 2014. Strategies to increase the activity of microglia as efficient protectors of the brain against infections. *Front Cell Neurosci,* 8**,** 138.

NAVE, K.-A. 2010. Myelination and support of axonal integrity by glia. *Nature,* 468**,** 244-252.

NEVE, A., CANTATORE, F. P., MARUOTTI, N., CORRADO, A. & RIBATTI, D. 2014. Extracellular matrix modulates angiogenesis in physiological and pathological conditions. *BioMed research international,* 2014**,** 756078-756078.

NEVES, G., COOKE, S. F. & BLISS, T. V. P. 2008. Synaptic plasticity, memory and the hippocampus: a neural network approach to causality. *Nat Rev Neurosci,* 9**,** 65-75.

NGUYEN, P. V., ABEL, T. & KANDEL, E. R. 1994. Requirement of a critical period of transcription for induction of a late phase of LTP. *Science,* 265**,** 1104-7.

NICHOLLS, R. E., ALARCON, J. M., MALLERET, G., CARROLL, R. C., GRODY, M., VRONSKAYA, S. & KANDEL, E. R. 2008. Transgenic Mice Lacking NMDAR-Dependent LTD Exhibit Deficits in Behavioral Flexibility. *Neuron,* 58**,** 104-117.

NICOLL, R. A. 2017. A Brief History of Long-Term Potentiation. *Neuron,* 93**,** 281-290.

NITHIANANTHARAJAH, J. & HANNAN, A. J. 2006. Enriched environments, experience-dependent plasticity and disorders of the nervous system. *Nature Reviews Neuroscience,* 7**,** 697-709.

NITHIANANTHARAJAH, J., LEVIS, H. & MURPHY, M. 2004. Environmental enrichment results in cortical and subcortical changes in levels of synaptophysin and PSD-95 proteins. *Neurobiol Learn Mem,* 81**,** 200-10.

NOVKOVIC, T., MITTMANN, T. & MANAHAN-VAUGHAN, D. 2015. BDNF contributes to the facilitation of hippocampal synaptic plasticity and learning enabled by environmental enrichment. *Hippocampus,* 25**,** 1-15.

O'BRIEN, R. J., KAMBOJ, S., EHLERS, M. D., ROSEN, K. R., FISCHBACH, G. D. & HUGANIR, R. L. 1998. Activity-dependent modulation of synaptic AMPA receptor accumulation. *Neuron,* 21**,** 1067-78.

O'KEEFE, J. & DOSTROVSKY, J. 1971. The hippocampus as a spatial map. Preliminary evidence from unit activity in the freely-moving rat. *Brain Res,* 34**,** 171-5.

O'KEEFE, J. & NADEL, L. 1978. *The Hippocampus as a Cognitive Map,* Oxford, The Clarendon Press.

O'SHEA, A., COHEN, R. A., PORGES, E. C., NISSIM, N. R. & WOODS, A. J. 2016. Cognitive Aging and the Hippocampus in Older Adults. *Frontiers in aging neuroscience,* 8**,** 298-298.

OHLINE, S. M. & ABRAHAM, W. C. 2019. Environmental enrichment effects on synaptic and cellular physiology of hippocampal neurons. *Neuropharmacology,* 145**,** 3-12.

OKUNO, H., AKASHI, K., ISHII, Y., YAGISHITA-KYO, N., SUZUKI, K., NONAKA, M., KAWASHIMA, T., FUJII, H., TAKEMOTO-KIMURA, S., ABE, M., NATSUME, R., CHOWDHURY, S., SAKIMURA, K., WORLEY, P. F. & BITO, H. 2012. Inverse synaptic tagging of inactive synapses via dynamic interaction of Arc/Arg3.1 with CaMKIIβ. *Cell,* 149**,** 886-898.

ORTEGA-MARTÍNEZ, S. 2015. A new perspective on the role of the CREB family of transcription factors in memory consolidation via adult hippocampal neurogenesis. *Frontiers in Molecular Neuroscience,* 8.

OSTROWSKI, L. E., YIN, W., ROGERS, T. D., BUSALACCHI, K. B., CHUA, M., O'NEAL, W. K. & GRUBB, B. R. 2010. Conditional deletion of dnaic1 in a murine model of primary ciliary dyskinesia causes chronic rhinosinusitis. *Am J Respir Cell Mol Biol,* 43**,** 55-63.

OTSU, N. 1975. A threshold selection method from gray-level histograms. *Automatica,* 11**,** 23-27.

PAGANI, J. H., ZHAO, M., CUI, Z., AVRAM, S. K., CARUANA, D. A., DUDEK, S. M. & YOUNG, W. S. 2015. Role of the vasopressin 1b receptor in rodent aggressive behavior and synaptic plasticity in hippocampal area CA2. *Mol Psychiatry,* 20**,** 490-9.

PALMER, T. D., TAKAHASHI, J. & GAGE, F. H. 1997. The adult rat hippocampus contains primordial neural stem cells. *Mol Cell Neurosci,* 8**,** 389-404.

PANJA, D. & BRAMHAM, C. R. 2014. BDNF mechanisms in late LTP formation: A synthesis and breakdown. *Neuropharmacology,* 76**,** 664-676.

PAOLICELLI, R. C. & FERRETTI, M. T. 2017. Function and Dysfunction of Microglia during Brain Development: Consequences for Synapses and Neural Circuits. *Frontiers in synaptic neuroscience,* 9**,** 9-9.

PARK, P., KANG, H., SANDERSON, T. M., BORTOLOTTO, Z. A., GEORGIOU, J., ZHUO, M., KAANG, B.-K. & COLLINGRIDGE, G. L. 2018. The Role of Calcium-Permeable AMPARs in Long-Term Potentiation at Principal Neurons in the Rodent Hippocampus. *Frontiers in Synaptic Neuroscience,* 10**,** 42.

PARK, P., SANDERSON, T. M., AMICI, M., CHOI, S.-L., BORTOLOTTO, Z. A., ZHUO, M., KAANG, B.-K. & COLLINGRIDGE, G. L. 2016. Calcium-Permeable AMPA Receptors Mediate the Induction of the Protein Kinase A-Dependent Component of Long-Term Potentiation in the Hippocampus. *The Journal of neuroscience : the official journal of the Society for Neuroscience,* 36**,** 622-631.

PARK, S., PARK, J. M., KIM, S., KIM, J.-A., SHEPHERD, J. D., SMITH-HICKS, C. L., CHOWDHURY, S., KAUFMANN, W., KUHL, D., RYAZANOV, A. G., HUGANIR, R. L., LINDEN, D. J. & WORLEY, P. F. 2008. Elongation factor 2 and fragile X mental retardation protein control the dynamic translation of Arc/Arg3.1 essential for mGluR-LTD. *Neuron,* 59**,** 70-83.

PARKHURST, C. N., YANG, G., NINAN, I., SAVAS, J. N., YATES, J. R., 3RD, LAFAILLE, J. J., HEMPSTEAD, B. L., LITTMAN, D. R. & GAN, W.-B. 2013. Microglia promote learning-dependent synapse formation through brain-derived neurotrophic factor. *Cell,* 155**,** 1596-1609.

PARSLEY, S. L., PILGRAM, S. M., SOTO, F., GIESE, K. P. & EDWARDS, F. A. 2007. Enriching the environment of alphaCaMKIIT286A mutant mice reveals that LTD occurs in memory processing but must be subsequently reversed by LTP. *Learn Mem,* 14**,** 75-83.

PATTERSON, S. L., GROVER, L. M., SCHWARTZKROIN, P. A. & BOTHWELL, M. 1992. Neurotrophin expression in rat hippocampal slices: a stimulus paradigm inducing LTP in CA1 evokes increases in BDNF and NT-3 mRNAs. *Neuron,* 9**,** 1081-8.

PEARSON, B. L., DEFENSOR, E. B., BLANCHARD, D. C. & BLANCHARD, R. J. 2010. C57BL/6J mice fail to exhibit preference for social novelty in the three-chamber apparatus. *Behavioural brain research,* 213**,** 189-194.

PELLEGRINI-GIAMPIETRO, D. E. 2003. An activity-dependent spermine-mediated mechanism that modulates glutamate transmission. *Trends Neurosci,* 26**,** 9-11.

PICKARD, L., NOEL, J., HENLEY, J. M., COLLINGRIDGE, G. L. & MOLNAR, E. 2000. Developmental changes in synaptic AMPA and NMDA receptor distribution and

AMPA receptor subunit composition in living hippocampal neurons. *J Neurosci,* 20**,** 7922-31.

PITTENGER, C., HUANG YY FAU - PALETZKI, R. F., PALETZKI RF FAU - BOURTCHOULADZE, R., BOURTCHOULADZE R FAU - SCANLIN, H., SCANLIN H FAU - VRONSKAYA, S., VRONSKAYA S FAU - KANDEL, E. R. & KANDEL, E. R. 2002. Reversible inhibition of CREB/ATF transcription factors in region CA1 of the dorsal hippocampus disrupts hippocampus-dependent spatial memory.

PLACE, R., LYKKEN, C., BEER, Z., SUH, J., MCHUGH, T. J., TONEGAWA, S., EICHENBAUM, H. & SAUVAGE, M. M. 2012. NMDA signaling in CA1 mediates selectively the spatial component of episodic memory. *Learn Mem,* 19**,** 164-9.

PLANT, K., PELKEY, K. A., BORTOLOTTO, Z. A., MORITA, D., TERASHIMA, A., MCBAIN, C. J., COLLINGRIDGE, G. L. & ISAAC, J. T. 2006. Transient incorporation of native GluR2-lacking AMPA receptors during hippocampal long-term potentiation. *Nat Neurosci,* 9**,** 602-4.

PLATH, N., OHANA, O., DAMMERMANN, B., ERRINGTON, M. L., SCHMITZ, D., GROSS, C., MAO, X., ENGELSBERG, A., MAHLKE, C., WELZL, H., KOBALZ, U., STAWRAKAKIS, A., FERNANDEZ, E., WALTEREIT, R., BICK-SANDER, A., THERSTAPPEN, E., COOKE, SAM F., BLANQUET, V., WURST, W., SALMEN, B., BÖSL, MICHAEL R., LIPP, H.-P., GRANT, SETH G. N., BLISS, T. V. P., WOLFER, D. P. & KUHL, D. 2006. Arc/Arg3.1 Is Essential for the Consolidation of Synaptic Plasticity and Memories. *Neuron,* 52**,** 437-444.

POSER, S. & STORM, D. R. 2001. Role of Ca2+-stimulated adenylyl cyclases in LTP and memory formation. *Int J Dev Neurosci,* 19**,** 387-94.

POZO, K. & GODA, Y. 2010. Unraveling Mechanisms of Homeostatic Synaptic Plasticity. *Neuron,* 66**,** 337-351.

PRIVITERA, L., MORÈ, L., COOPER, D. D., RICHARDSON, P., TSOGKA, M., HEBENSTREIT, D., ARTHUR, J. S. C. & FRENGUELLI, B. G. 2020. Experience recruits MSK1 to expand the dynamic range of synapses and enhance cognition. *The Journal of Neuroscience***,** JN-RM-2765-19.

QUATTROMANI, M. J., PRUVOST, M., GUERREIRO, C., BACKLUND, F., ENGLUND, E., ASPBERG, A., JAWORSKI, T., HAKON, J., RUSCHER, K., KACZMAREK, L., VIVIEN, D. & WIELOCH, T. 2018. Extracellular Matrix Modulation Is Driven by Experience-Dependent Plasticity During Stroke Recovery. *Molecular Neurobiology,* 55**,** 2196-2213.

RAE, M., ZANOS, P., GEORGIOU, P., CHIVERS, P., BAILEY, A. & CAMARINI, R. 2018. Environmental enrichment enhances conditioned place preference to ethanol via an oxytocinergic-dependent mechanism in male mice. *Neuropharmacology,* 138**,** 267-274.

RAMPON, C., JIANG, C. H., DONG, H., TANG, Y. P., LOCKHART, D. J., SCHULTZ, P. G., TSIEN, J. Z. & HU, Y. 2000a. Effects of environmental enrichment on gene expression in the brain. *Proceedings of the National Academy of Sciences of the United States of America,* 97**,** 12880-12884.

RAMPON, C., TANG, Y. P., GOODHOUSE, J., SHIMIZU, E., KYIN, M. & TSIEN, J. Z. 2000b. Enrichment induces structural changes and recovery from nonspatial memory deficits in CA1 NMDAR1-knockout mice. *Nat Neurosci,* 3**,** 238-44.

REDOLAT, R. & MESA-GRESA, P. 2012. Potential benefits and limitations of enriched environments and cognitive activity on age-related behavioural decline. *Curr Top Behav Neurosci,* 10**,** 293-316.

REINER, A. & LEVITZ, J. 2018. Glutamatergic Signaling in the Central Nervous System: Ionotropic and Metabotropic Receptors in Concert. *Neuron,* 98**,** 1080-1098.
REYSKENS, K. M. S. E. & ARTHUR, J. S. C. 2016. Emerging Roles of the Mitogen and Stress Activated Kinases MSK1 and MSK2. *Frontiers in Cell and Developmental Biology,* 4.
RHEE, S., KIRSCHEN, G. W., GU, Y. & GE, S. 2016. Depletion of primary cilia from mature dentate granule cells impairs hippocampus-dependent contextual memory. *Sci Rep,* 6**,** 34370.
ROBINSON, J. T., THORVALDSDOTTIR, H., WINCKLER, W., GUTTMAN, M., LANDER, E. S., GETZ, G. & MESIROV, J. P. 2011. Integrative genomics viewer. *Nat Biotechnol.* United States.
ROSENBERG, D., ARTOUL, S., SEGAL, A. C., KOLODNEY, G., RADZISHEVSKY, I., DIKOPOLTSEV, E., FOLTYN, V. N., INOUE, R., MORI, H., BILLARD, J.-M. & WOLOSKER, H. 2013. Neuronal Serine and Glycine Release Via the Asc-1 Transporter Regulates NMDA Receptor-Dependent Synaptic Activity. *The Journal of Neuroscience,* 33**,** 3533.
ROZOV, A., SPRENGEL, R. & SEEBURG, P. 2012. GluA2-lacking AMPA receptors in hippocampal CA1 cell synapses: evidence from gene-targeted mice. *Frontiers in Molecular Neuroscience,* 5**,** 22.
RUTHERFORD, L. C., NELSON, S. B. & TURRIGIANO, G. G. 1998. BDNF has opposite effects on the quantal amplitude of pyramidal neuron and interneuron excitatory synapses. *Neuron,* 21**,** 521-30.
SAJIKUMAR, S., NAVAKKODE, S. & FREY, J. U. 2008. Distinct single but not necessarily repeated tetanization is required to induce hippocampal late-LTP in the rat CA1. *Learn Mem,* 15**,** 46-9.
SAKAMOTO, K., KARELINA, K. & OBRIETAN, K. 2011. CREB: a multifaceted regulator of neuronal plasticity and protection. *J Neurochem,* 116**,** 1-9.
SAKATA, K., MARTINOWICH, K., WOO, N. H., SCHLOESSER, R. J., JIMENEZ, D. V., JI, Y., SHEN, L. & LU, B. 2013. Role of activity-dependent BDNF expression in hippocampal–prefrontal cortical regulation of behavioral perseverance. *Proceedings of the National Academy of Sciences,* 110**,** 15103-15108.
SALE, A., BERARDI, N. & MAFFEI, L. 2014. Environment and brain plasticity: towards an endogenous pharmacotherapy. *Physiol Rev,* 94**,** 189-234.
SAMPEDRO-PIQUERO, P. & BEGEGA, A. 2017. Environmental Enrichment as a Positive Behavioral Intervention Across the Lifespan. *Current neuropharmacology,* 15**,** 459-470.
SAWAMOTO, A., OKUYAMA, S., YAMAMOTO, K., AMAKURA, Y., YOSHIMURA, M., NAKAJIMA, M. & FURUKAWA, Y. 2016. 3,5,6,7,8,3',4'-Heptamethoxyflavone, a Citrus Flavonoid, Ameliorates Corticosterone-Induced Depression-like Behavior and Restores Brain-Derived Neurotrophic Factor Expression, Neurogenesis, and Neuroplasticity in the Hippocampus. *Molecules,* 21**,** 541.
SCHARFMAN, H., GOODMAN, J., MACLEOD, A., PHANI, S., ANTONELLI, C. & CROLL, S. 2005. Increased neurogenesis and the ectopic granule cells after intrahippocampal BDNF infusion in adult rats. *Exp Neurol,* 192**,** 348-56.
SCHILDT, S., ENDRES, T., LESSMANN, V. & EDELMANN, E. 2013. Acute and chronic interference with BDNF/TrkB-signaling impair LTP selectively at mossy fiber synapses in the CA3 region of mouse hippocampus. *Neuropharmacology,* 71**,** 247-54.
SCHOENFELD, T. J. & CAMERON, H. A. 2015. Adult neurogenesis and mental illness. *Neuropsychopharmacology,* 40**,** 113-28.

SCOVILLE, W. B. & MILNER, B. 1957. Loss of recent memory after bilateral hippocampal lesions. *Journal of neurology, neurosurgery, and psychiatry,* 20**,** 11-21.
SEESE, R. R., WANG, K., YAO, Y. Q., LYNCH, G. & GALL, C. M. 2014. Spaced training rescues memory and ERK1/2 signaling in fragile X syndrome model mice. *Proceedings of the National Academy of Sciences,* 111**,** 16907.
SHAYWITZ, A. J. & GREENBERG, M. E. 1999. CREB: A Stimulus-Induced Transcription Factor Activated by A Diverse Array of Extracellular Signals. *Annual Review of Biochemistry,* 68**,** 821-861.
SHENG, M. & GREENBERG, M. E. 1990. The regulation and function of c-fos and other immediate early genes in the nervous system. *Neuron,* 4**,** 477-85.
SHENG, M., MCFADDEN, G. & GREENBERG, M. E. 1990. Membrane depolarization and calcium induce c-fos transcription via phosphorylation of transcription factor CREB. *Neuron,* 4**,** 571-82.
SHENG, M., THOMPSON, M. A. & GREENBERG, M. E. 1991. CREB: a Ca(2+)-regulated transcription factor phosphorylated by calmodulin-dependent kinases. *Science,* 252**,** 1427-30.
SHEPHERD, J. D., RUMBAUGH, G., WU, J., CHOWDHURY, S., PLATH, N., KUHL, D., HUGANIR, R. L. & WORLEY, P. F. 2006. Arc/Arg3.1 mediates homeostatic synaptic scaling of AMPA receptors. *Neuron,* 52**,** 475-84.
SHI, F., LIU, B., ZHOU, Y., YU, C. & JIANG, T. 2009. Hippocampal volume and asymmetry in mild cognitive impairment and Alzheimer's disease: Meta-analyses of MRI studies. *Hippocampus,* 19**,** 1055-64.
SHINOHARA, Y., HOSOYA, A., YAHAGI, K., FERECSKO, A. S., YAGUCHI, K., SIK, A., ITAKURA, M., TAKAHASHI, M. & HIRASE, H. 2012. Hippocampal CA3 and CA2 have distinct bilateral innervation patterns to CA1 in rodents. *Eur J Neurosci,* 35**,** 702-10.
SHOLL, D. A. 1953. Dendritic organization in the neurons of the visual and motor cortices of the cat. *J Anat,* 87**,** 387-406.
SILVA, A. J., KOGAN, J. H., FRANKLAND, P. W. & KIDA, S. 1998. CREB and memory. *Annu Rev Neurosci,* 21**,** 127-48.
SIMON, J., ARTHUR, C., FONG, A. L., DWYER, J. M., DAVARE, M., REESE, E., OBRIETAN, K. & IMPEY, S. 2004. Mitogen- and Stress-Activated Protein Kinase 1 Mediates cAMP Response Element-Binding Protein Phosphorylation and Activation by Neurotrophins. *The Journal of Neuroscience,* 24**,** 4324-4332.
SIMONS, M. & NAVE, K.-A. 2015. Oligodendrocytes: Myelination and Axonal Support. *Cold Spring Harbor perspectives in biology,* 8**,** a020479-a020479.
SINDREU, C. B., SCHEINER, Z. S. & STORM, D. R. 2007. Ca2+ -stimulated adenylyl cyclases regulate ERK-dependent activation of MSK1 during fear conditioning. *Neuron,* 53**,** 79-89.
SMITH, B. M., YAO, X., CHEN, K. S. & KIRBY, E. D. 2018. A Larger Social Network Enhances Novel Object Location Memory and Reduces Hippocampal Microgliosis in Aged Mice. *Frontiers in aging neuroscience,* 10**,** 142-142.
SMITH, M. A., ELLIS-DAVIES, G. C. R. & MAGEE, J. C. 2003. Mechanism of the distance-dependent scaling of Schaffer collateral synapses in rat CA1 pyramidal neurons. *The Journal of physiology,* 548**,** 245-258.
SOARES, C., LEE, K. F. H. & BEIQUE, J. C. 2017. Metaplasticity at CA1 Synapses by Homeostatic Control of Presynaptic Release Dynamics. *Cell Rep,* 21**,** 1293-1303.

SOLOAGA, A., THOMSON, S., WIGGIN, G. R., RAMPERSAUD, N., DYSON, M. H., HAZZALIN, C. A., MAHADEVAN, L. C. & ARTHUR, J. S. 2003. MSK2 and MSK1 mediate the mitogen- and stress-induced phosphorylation of histone H3 and HMG-14. *Embo j,* 22**,** 2788-97.

SOMMER, B., KOHLER M FAU - SPRENGEL, R., SPRENGEL R FAU - SEEBURG, P. H. & SEEBURG, P. H. 1991. RNA editing in brain controls a determinant of ion flow in glutamate-gated channels.

SONG, I. & DITYATEV, A. 2018. Crosstalk between glia, extracellular matrix and neurons. *Brain Research Bulletin,* 136**,** 101-108.

SOTELO, C. 2003. Viewing the brain through the master hand of Ramon y Cajal. *Nature Reviews Neuroscience,* 4**,** 71.

SPANGENBERG, E. M. F. & WICHMAN, A. 2018. Methods for Investigating the Motivation of Mice to Explore and Access Food Rewards. *Journal of the American Association for Laboratory Animal Science : JAALAS,* 57**,** 244-252.

SPEISMAN, R. B., KUMAR, A., RANI, A., PASTORIZA, J. M., SEVERANCE, J. E., FOSTER, T. C. & ORMEROD, B. K. 2013. Environmental enrichment restores neurogenesis and rapid acquisition in aged rats. *Neurobiol Aging,* 34**,** 263-74.

SQUINTO, S. P., STITT, T. N., ALDRICH, T. H., DAVIS, S., BIANCO, S. M., RADZIEJEWSKI, C., GLASS, D. J., MASIAKOWSKI, P., FURTH, M. E., VALENZUELA, D. M. & ET AL. 1991. trkB encodes a functional receptor for brain-derived neurotrophic factor and neurotrophin-3 but not nerve growth factor. *Cell,* 65**,** 885-93.

SQUIRE, L. R. 2009. The Legacy of Patient H.M. for Neuroscience. *Neuron,* 61**,** 6-9.

SQUIRE, L. R., GENZEL, L., WIXTED, J. T. & MORRIS, R. G. 2015. Memory consolidation. *Cold Spring Harb Perspect Biol,* 7**,** a021766.

STAUBLI, U. & LYNCH, G. 1987. Stable hippocampal long-term potentiation elicited by 'theta' pattern stimulation. *Brain Res,* 435**,** 227-34.

STEIN, L. R., O'DELL, K. A., FUNATSU, M., ZORUMSKI, C. F. & IZUMI, Y. 2016. Short-term environmental enrichment enhances synaptic plasticity in hippocampal slices from aged rats. *Neuroscience,* 329**,** 294-305.

STERN, Y. 2012. Cognitive reserve in ageing and Alzheimer's disease. *The Lancet. Neurology,* 11**,** 1006-1012.

STEVENSON, E. L. & CALDWELL, H. K. 2014. Lesions to the CA2 region of the hippocampus impair social memory in mice. *Eur J Neurosci,* 40**,** 3294-301.

STEWARD, O., FARRIS, S., PIRBHOY, P. S., DARNELL, J. & DRIESCHE, S. J. 2014. Localization and local translation of Arc/Arg3.1 mRNA at synapses: some observations and paradoxes. *Front Mol Neurosci,* 7**,** 101.

STEWARD, O., WALLACE, C. S., LYFORD, G. L. & WORLEY, P. F. 1998. Synaptic Activation Causes the mRNA for the IEG Arc to Localize Selectively near Activated Postsynaptic Sites on Dendrites. *Neuron,* 21**,** 741-751.

SUZUKI, A., FUKUSHIMA, H., MUKAWA, T., TOYODA, H., WU, L. J., ZHAO, M. G., XU, H., SHANG, Y., ENDOH, K., IWAMOTO, T., MAMIYA, N., OKANO, E., HASEGAWA, S., MERCALDO, V., ZHANG, Y., MAEDA, R., OHTA, M., JOSSELYN, S. A., ZHUO, M. & KIDA, S. 2011. Upregulation of CREB-mediated transcription enhances both short- and long-term memory. *J Neurosci,* 31**,** 8786-802.

SWANSON, G. T., KAMBOJ, S. K. & CULL-CANDY, S. G. 1997. Single-channel properties of recombinant AMPA receptors depend on RNA editing, splice variation, and subunit composition. *J Neurosci,* 17**,** 58-69.

SWEATT, J. D. 2016. Neural plasticity and behavior – sixty years of conceptual advances. *Journal of Neurochemistry,* 139**,** 179-199.
TAKEUCHI, T., DUSZKIEWICZ AJ FAU - MORRIS, R. G. M. & MORRIS, R. G. 2014. The synaptic plasticity and memory hypothesis: encoding, storage and persistence.
TANG, Y. P., WANG, H., FENG, R., KYIN, M. & TSIEN, J. Z. 2001. Differential effects of enrichment on learning and memory function in NR2B transgenic mice. *Neuropharmacology,* 41**,** 779-90.
TANIGUCHI, K., SASAKI, K.-I., WATARI, K., YASUKAWA, H., IMAIZUMI, T., AYADA, T., OKAMOTO, F., ISHIZAKI, T., KATO, R., KOHNO, R.-I., KIMURA, H., SATO, Y., ONO, M., YONEMITSU, Y. & YOSHIMURA, A. 2009. Suppression of Sproutys Has a Therapeutic Effect for a Mouse Model of Ischemia by Enhancing Angiogenesis. *PLOS ONE,* 4**,** e5467.
TAO, X., FINKBEINER, S., ARNOLD, D. B., SHAYWITZ, A. J. & GREENBERG, M. E. 1998. Ca2+ influx regulates BDNF transcription by a CREB family transcription factor-dependent mechanism. *Neuron,* 20**,** 709-26.
TAVARES, RITA M., MENDELSOHN, A., GROSSMAN, Y., WILLIAMS, CHRISTIAN H., SHAPIRO, M., TROPE, Y. & SCHILLER, D. 2015. A Map for Social Navigation in the Human Brain. *Neuron,* 87**,** 231-243.
THONGRONG, S., HAUSOTT, B., MARVALDI, L., AGOSTINHO, A. S., ZANGRANDI, L., BURTSCHER, J., FOGLI, B., SCHWARZER, C. & KLIMASCHEWSKI, L. 2016. Sprouty2 and -4 hypomorphism promotes neuronal survival and astrocytosis in a mouse model of kainic acid induced neuronal damage. *Hippocampus,* 26**,** 658-67.
THOW, M. E., SUMMERS, M. J., SAUNDERS, N. L., SUMMERS, J. J., RITCHIE, K. & VICKERS, J. C. 2017. Further education improves cognitive reserve and triggers improvement in selective cognitive functions in older adults: The Tasmanian Healthy Brain Project. *Alzheimer's & dementia (Amsterdam, Netherlands),* 10**,** 22-30.
TORRES, L., DANVER, J., JI, K., MIYAUCHI, J. T., CHEN, D., ANDERSON, M. E., WEST, B. L., ROBINSON, J. K. & TSIRKA, S. E. 2016. Dynamic microglial modulation of spatial learning and social behavior. *Brain, behavior, and immunity,* 55**,** 6-16.
TSIEN, J. Z., HUERTA, P. T. & TONEGAWA, S. 1996. The Essential Role of Hippocampal CA1 NMDA Receptor–Dependent Synaptic Plasticity in Spatial Memory. *Cell,* 87**,** 1327-1338.
TULLAI, J. W., SCHAFFER, M. E., MULLENBROCK, S., SHOLDER, G., KASIF, S. & COOPER, G. M. 2007. Immediate-early and delayed primary response genes are distinct in function and genomic architecture. *The Journal of biological chemistry,* 282**,** 23981-23995.
TURRIGIANO, G. 2012. Homeostatic Synaptic Plasticity: Local and Global Mechanisms for Stabilizing Neuronal Function. *Cold Spring Harbor Perspectives in Biology,* 4**,** a005736.
TURRIGIANO, G. G. 2008. The self-tuning neuron: synaptic scaling of excitatory synapses. *Cell,* 135**,** 422-35.
TURRIGIANO, G. G., LESLIE, K. R., DESAI, N. S., RUTHERFORD, L. C. & NELSON, S. B. 1998. Activity-dependent scaling of quantal amplitude in neocortical neurons. *Nature,* 391**,** 892-6.
TURRIGIANO, G. G. & NELSON, S. B. 2000. Hebb and homeostasis in neuronal plasticity. *Curr Opin Neurobiol,* 10**,** 358-64.
TZAKIS, N. & HOLAHAN, M. R. 2019. Social Memory and the Role of the Hippocampal CA2 Region. *Frontiers in Behavioral Neuroscience,* 13.

VAN PRAAG, H., KEMPERMANN, G. & GAGE, F. H. 1999. Running increases cell proliferation and neurogenesis in the adult mouse dentate gyrus. *Nature Neuroscience,* 2**,** 266-270.
VAN PRAAG, H., KEMPERMANN, G. & GAGE, F. H. 2000. Neural consequences of enviromental enrichment. *Nature Reviews Neuroscience,* 1**,** 191-198.
VIAENE, A. N., PETROF, I. & SHERMAN, S. M. 2013. Activation requirements for metabotropic glutamate receptors. *Neuroscience Letters,* 541**,** 67-72.
VILLANUEVA ESPINO, L. A., SILVA GÓMEZ, A. B. & BRAVO DURÁN, D. A. 2020. Cognitive training increases dendritic arborization in the dorsal hippocampal CA1 and CA3 neurons of female and male Long–Evans rats. *Synapse,* 74**,** e22140.
VILLERS, A., GODAUX, E. & RIS, L. 2012. Long-lasting LTP requires neither repeated trains for its induction nor protein synthesis for its development. *PLoS One,* 7**,** e40823.
VIOSCA, J., MALLERET, G., BOURTCHOULADZE, R., BENITO-GARAGORRI, E., VRONSKAVA, S., R KANDEL, E. & BARCO, A. 2009. Chronic enhancement of CREB activity in the hippocampus interferes with the retrieval of spatial information. *Learning & memory (Cold Spring Harbor, N.Y.),* 16**,** 198-209.
VITUREIRA, N. & GODA, Y. 2013. Cell biology in neuroscience: The interplay between Hebbian and homeostatic synaptic plasticity. *The Journal of cell biology,* 203**,** 175-86.
VOGEL-CIERNIA, A. & WOOD, M. A. 2014. Examining object location and object recognition memory in mice. *Curr Protoc Neurosci,* 69**,** 8.31.1-17.
VOGT, M. A., INTA, D., LUONI, A., ELKIN, H., PFEIFFER, N., RIVA, M. A. & GASS, P. 2014. Inducible forebrain-specific ablation of the transcription factor Creb during adulthood induces anxiety but no spatial/contextual learning deficits. *Frontiers in behavioral neuroscience,* 8**,** 407-407.
VON BARTHELD, C. S., BAHNEY, J. & HERCULANO-HOUZEL, S. 2016. The search for true numbers of neurons and glial cells in the human brain: A review of 150 years of cell counting. *J Comp Neurol,* 524**,** 3865-3895.
WALL, M. J., COLLINS, D. R., CHERY, S. L., ALLEN, Z. D., PASTUZYN, E. D., GEORGE, A. J., NIKOLOVA, V. D., MOY, S. S., PHILPOT, B. D., SHEPHERD, J. D., MÜLLER, J., EHLERS, M. D., MABB, A. M. & CORRÊA, S. A. L. 2018. The Temporal Dynamics of Arc Expression Regulate Cognitive Flexibility. *Neuron,* 98**,** 1124-1132.e7.
WALTEREIT, R. & WELLER, M. 2003. Signaling from cAMP/PKA to MAPK and synaptic plasticity. *Mol Neurobiol,* 27**,** 99-106.
WANG, X., LOU, N., XU, Q., TIAN, G. F., PENG, W. G., HAN, X., KANG, J., TAKANO, T. & NEDERGAARD, M. 2006. Astrocytic Ca2+ signaling evoked by sensory stimulation in vivo. *Nat Neurosci,* 9**,** 816-23.
WHITEHEAD, G., JO, J., HOGG, E. L., PIERS, T., KIM, D. H., SEATON, G., SEOK, H., BRU-MERCIER, G., SON, G. H., REGAN, P., HILDEBRANDT, L., WAITE, E., KIM, B. C., KERRIGAN, T. L., KIM, K., WHITCOMB, D. J., COLLINGRIDGE, G. L., LIGHTMAN, S. L. & CHO, K. 2013. Acute stress causes rapid synaptic insertion of Ca2+ -permeable AMPA receptors to facilitate long-term potentiation in the hippocampus. *Brain,* 136**,** 3753-65.
WHITLOCK, J. R., HEYNEN, A. J., SHULER, M. G. & BEAR, M. F. 2006. Learning induces long-term potentiation in the hippocampus. *Science,* 313**,** 1093-7.
WIEGERT, J. S. & OERTNER, T. G. 2013. Long-term depression triggers the selective elimination of weakly integrated synapses. *Proceedings of the National Academy of Sciences,* 110**,** E4510.

WIERSMA, M., BUSSIERE, M., HALSALL, J. A., TURAN, N., SLANY, R., TURNER, B. M. & NIGHTINGALE, K. P. 2016. Protein kinase Msk1 physically and functionally interacts with the KMT2A/MLL1 methyltransferase complex and contributes to the regulation of multiple target genes. *Epigenetics & Chromatin,* 9**,** 52.

WIGGIN, G. R., SOLOAGA, A., FOSTER, J. M., MURRAY-TAIT, V., COHEN, P. & ARTHUR, J. S. 2002. MSK1 and MSK2 are required for the mitogen- and stress-induced phosphorylation of CREB and ATF1 in fibroblasts. *Mol Cell Biol,* 22**,** 2871-81.

WINGATE, A. D., MARTIN, K. J., HUNTER, C., CARR, J. M., CLACHER, C. & ARTHUR, J. S. C. 2009. Generation of a conditional CREB Ser133Ala knockin mouse. *genesis,* 47**,** 688-696.

WU, Y., DISSING-OLESEN, L., MACVICAR, B. A. & STEVENS, B. 2015. Microglia: Dynamic Mediators of Synapse Development and Plasticity. *Trends in immunology,* 36**,** 605-613.

YAMADA, K. & NABESHIMA, T. 2003. Brain-derived neurotrophic factor/TrkB signaling in memory processes. *J Pharmacol Sci,* 91**,** 267-70.

YAMAMOTO, K. K., GONZALEZ, G. A., BIGGS, W. H., 3RD & MONTMINY, M. R. 1988. Phosphorylation-induced binding and transcriptional efficacy of nuclear factor CREB. *Nature,* 334**,** 494-8.

YANG, J., HARTE-HARGROVE, L. C., SIAO, C. J., MARINIC, T., CLARKE, R., MA, Q., JING, D., LAFRANCOIS, J. J., BATH, K. G., MARK, W., BALLON, D., LEE, F. S., SCHARFMAN, H. E. & HEMPSTEAD, B. L. 2014a. proBDNF negatively regulates neuronal remodeling, synaptic transmission, and synaptic plasticity in hippocampus. *Cell Rep,* 7**,** 796-806.

YANG, Y.-J., LI, Y.-K., WANG, W., WAN, J.-G., YU, B., WANG, M.-Z. & HU, B. 2014b. Small-molecule TrkB agonist 7,8-dihydroxyflavone reverses cognitive and synaptic plasticity deficits in a rat model of schizophrenia. *Pharmacology Biochemistry and Behavior,* 122**,** 30-36.

YASSA, M. A. & STARK, C. E. 2011. Pattern separation in the hippocampus. *Trends Neurosci,* 34**,** 515-25.

YIN, J. C. P., DEL VECCHIO, M., ZHOU, H. & TULLY, T. 1995. CREB as a Memory Modulator: induced expression of a dCREB2 activator isoform enhances long-term memory in drosophila. *Cell,* 81**,** 107-115.

YOSHII, A. & CONSTANTINE-PATON, M. 2014. Postsynaptic localization of PSD-95 is regulated by all three pathways downstream of TrkB signaling. *Frontiers in Synaptic Neuroscience,* 6**,** 6.

ZHANG, L. & HERNANDEZ, V. S. 2013. Synaptic innervation to rat hippocampus by vasopressin-immuno-positive fibres from the hypothalamic supraoptic and paraventricular nuclei. *Neuroscience,* 228**,** 139-62.

ZHANG, Z., LIU, X., SCHROEDER, J. P., CHAN, C.-B., SONG, M., YU, S. P., WEINSHENKER, D. & YE, K. 2014. 7,8-dihydroxyflavone prevents synaptic loss and memory deficits in a mouse model of Alzheimer's disease. *Neuropsychopharmacology : official publication of the American College of Neuropsychopharmacology,* 39**,** 638-650.

Appendix

Appendix Tables

		Aligned Reads		Discarded Reads		questionable - only polyA transcrip		QC	
Sample	**Reads**	**No. Aligned**	**% Aligned**	**Too many**	**Too short**	**Total trancripts >5 reads**	**Transcripts >5 reads/total**	**QC Fail?**	**Reason for removal**
Sample_1	37300930	33779256	90.56%	5.98%	3.37%	18883	38.10%	N	N/A
Sample_2	60872481	55368413	90.96%	5.43%	3.51%	-	-	N	Poor Intra-group correlation
Sample_3	68112714	63243581	92.85%	4.68%	2.36%	20452	41.26%	N	N/A
Sample_4	68708016	63584918	92.54%	5.03%	2.31%	20679	41.72%	N	N/A
Sample_5	23604176	21672446	91.82%	5.32%	2.74%	17943	36.20%	N	N/A
Sample_6	44747092	41767971	93.34%	4.10%	2.45%	19435	39.21%	N	N/A
Sample_7	16485055	15129511	91.78%	5.18%	2.94%	16828	33.95%	N	N/A
Sample_8	39806341	36135727	90.78%	4.32%	4.79%	19315	38.97%	N	N/A
Sample_9	11577051	10584291	91.42%	4.51%	3.96%	-	-	N	Poor Intra-group correlation
Sample_10	37601463	34910332	92.84%	4.86%	2.18%	18974	38.28%	N	N/A
Sample_11	29332842	27212145	92.77%	4.18%	2.94%	18308	36.94%	N	N/A
Sample_12	30636000	28221471	92.12%	4.78%	2.94%	-	-	N	Poor Intra-group correlation
Sample_13	52147252	48160623	92.36%	4.62%	2.90%	19979	40.31%	N	N/A
Sample_14	40972630	37553681	91.66%	6.42%	1.81%	19054	38.44%	N	N/A
Sample_15	37569198	35008929	93.19%	4.49%	2.21%	18767	37.86%	N	N/A
Sample_16	37002058	34430087	93.05%	4.34%	2.50%	19280	38.90%	N	N/A
Sample_17	30436947	28356787	93.17%	4.26%	2.48%	18812	37.95%	N	N/A
Sample_31B	38844976	36175720	93.13%	4.26%	2.48%	-	-	N	Poor Intra-group correlation
Sample_32A	41381932	38509329	93.06%	4.21%	2.61%	19378	39.09%	N	N/A
Sample_33A	57355419	53409931	93.12%	4.44%	2.32%	20347	41.05%	N	N/A
Sample_33B	*53128554*	*40661002*	*76.53%*	*6.65%*	*#####*	-	-	*Y*	*Mitochondrial RNA Contamination and poor intra-group correlation*
Sample_34B	*22090372*	*37345*	*0.17%*	*0.02%*	*#####*	-	-	*Y*	*rRNA contamination and low quality reads trimmed left reads too short for accurate unique alignment.*
Sample_35A	75444925	69720060	92.41%	4.55%	2.90%	-	-	N	Poor Intra-group correlation
Sample_36A	38731265	35438393	91.50%	4.55%	3.84%	18949	38.23%	N	N/A
Average	41757762	38562436	92.29%	0.048	0.028	19140.176	0.386		
SEM	3502053	3242282	0.18%	0.13%	0.15%	22928.20%	0.46%		
Total number of transcripts assayed:			49568	This includes non-coding RNA transcripts that would not be sampled in a polyA selected RNAseq assay. Only polyA transcripts assayed, so true					

Appendix Table i) RNAseq sample read quality summary and alignment statistics. Samples removed due to QC fails and poor intra-group correlation are indictaed.

sampleName	fileName	condition	genotype	housing
1	Sample_1.txt	KDSH	mut	house1
3	Sample_3.txt	KDSH	mut	house1
4	Sample_4.txt	KDSH	mut	house1
5	Sample_5.txt	KDSH	mut	house1
6	Sample_6.txt	KDSH	mut	house1
7	Sample_7.txt	KDEE	mut	house2
8	Sample_8.txt	KDEE	mut	house2
32A	Sample_32A.txt	KDEE	mut	house2
36A	Sample_36A.txt	KDEE	mut	house2
10	Sample_10.txt	WTSH	WT	house1
11	Sample_11.txt	WTSH	WT	house1
13	Sample_13.txt	WTSH	WT	house1
14	Sample_14.txt	WTSH	WT	house1
15	Sample_15.txt	WTSH	WT	house1
16	Sample_16.txt	WTEE	WT	house2
17	Sample_17.txt	WTEE	WT	house2
33A	Sample_33A.txt	WTEE	WT	house2

Appendix Table ii) Sample table used with DESeq2 including condition details.

Number of DEGs Adj. p.value<0.05	KDSH	KDEE	WTSH	WTEE
Kinase-dead standard-housed (**KDSH**)	x	**256**	**3**	N/A
Kinase-dead environmentally enriched (**KDEE**)	x	x	N/A	**11**
Wildtype standard-housed (**WTSH**)	x	x	x	**475**
Wildtype environmentally enriched (**WTEE**)	x	x	x	x

Appendix Table iii) Differentially-expressed gene summary table. Number of genes found to be differentially expressed for each condition between conditions compared.

WTEEvsKDEE	baseMean	log2FoldChange	lfcMLE	lfcSE	stat	pvalue	padj	ensembl	RefSeq	entrez
Dnaic2	117.581	0.614	0.965	0.109	5.607	2.06E-08	0.000358	ENSMUSG00000034706	NM_001034878	432611
Hist1h1c	671.166	0.584	0.978	0.111	5.262	1.42E-07	0.001237	ENSMUSG00000036181	NM_015786	50708
Cdhr3	123.360	0.511	0.934	0.112	4.556	5.21E-06	0.020609	ENSMUSG00000035860	NM_001024478	68764
Rarres2	108.718	0.504	0.861	0.111	4.529	5.92E-06	0.020609	ENSMUSG00000009281	NM_001347167	71660
Egr1	5476.114	-0.459	-0.676	0.105	-4.372	1.23E-05	0.030602	ENSMUSG00000038418	NM_007913	13653
Gm28578	34.352	0.474	1.152	0.111	4.262	2.03E-05	0.039225	NA	XR_386755	102639970
Vwa5b1	206.459	0.473	0.785	0.111	4.266	1.99E-05	0.039225	ENSMUSG00000028753	NM_029401	75718
Gm11992	63.534	0.457	0.766	0.111	4.106	4.03E-05	0.048739	ENSMUSG00000040978	NM_001037928	626870
P2rx6	238.816	0.414	0.568	0.101	4.114	3.88E-05	0.048739	ENSMUSG00000022758	NM_001159561	18440
Pih1d2	69.074	0.467	0.877	0.113	4.136	3.53E-05	0.048739	ENSMUSG00000000167	NM_028300	72614
Spry4	516.625	-0.414	-0.573	0.100	-4.133	3.58E-05	0.048739	ENSMUSG00000024427	NM_011898	24066

Appendix Table iv) List of differentially expressed genes found between conditions WTEE and KDEE.

WTSHvsKDSH	baseMean	log2FoldChai	lfcMLE	lfcSE	stat	pvalue	padj	ensembl	RefSeq	entrez
Rpl22l1	555.664	-0.461	-0.602	0.096	-4.806	1.54E-06	0.027123	ENSMUSG00000039221	NM_001347226	68028
Rpl39	1670.564	-0.434	-0.542	0.090	-4.800	1.58E-06	0.027123	ENSMUSG00000079641	NM_026055	67248
Gm44164	68.822	0.491	1.389	0.108	4.558	5.16E-06	0.044229	NA	NA	NA

Appendix Table v) List of differentially expressed genes found between conditions WTSH and KDSH.

WTEEvsWTSH	baseMean	log2FoldChar	lfcMLE	lfcSE	stat	pvalue	padj	ensembl	RefSeq	entrez
Krt8	75.437	1.471	2.909	0.113	13.023	9.08E-39	1.99E-34	ENSMUSG00000049382	NM_031170	16691
Sema3b	229.559	1.392	2.842	0.113	12.362	4.19E-35	4.59E-31	ENSMUSG00000057969	NM_001042779	20347
Slc16a8	88.463	1.320	3.022	0.112	11.808	3.57E-32	2.61E-28	ENSMUSG00000032988	NM_020516	57274
Gm44250	207.929	1.302	2.528	0.113	11.555	6.95E-31	3.05E-27	NA	NA	NA
Rdh5	181.945	1.299	2.810	0.112	11.569	5.90E-31	3.05E-27	ENSMUSG00000025350	NM_001358527	19682
Oca2	58.110	1.057	3.973	0.102	10.409	2.25E-25	8.24E-22	ENSMUSG00000030450	NM_021879	18431
Dab2	439.269	1.013	1.397	0.101	10.055	8.71E-24	2.73E-20	ENSMUSG00000022150	NM_001008702	13132
Mdfic	178.725	1.129	2.218	0.113	10.021	1.23E-23	3.38E-20	ENSMUSG00000041390	NM_175088	16543
Slc13a4	582.884	1.095	2.539	0.111	9.858	6.34E-23	1.55E-19	ENSMUSG00000029843	NM_172892	243755
Slc37a2	200.659	1.076	1.784	0.111	9.729	2.26E-22	4.97E-19	ENSMUSG00000032122	NM_001145960	56857
Slc4a2	1464.395	1.006	1.454	0.104	9.661	4.39E-22	8.76E-19	ENSMUSG00000028962	NM_001253892	20535
Col17a1	35.252	0.944	3.571	0.100	9.474	2.70E-21	4.55E-18	ENSMUSG00000025064	NM_001290825	12821
Tuba1c	94.880	1.035	2.692	0.109	9.482	2.50E-21	4.55E-18	ENSMUSG00000043091	NM_009448	22146
Cab39l	1254.415	0.976	1.389	0.103	9.452	3.32E-21	5.20E-18	ENSMUSG00000021981	NM_001360591	69008
Perp	156.592	1.051	1.802	0.111	9.430	4.08E-21	5.97E-18	ENSMUSG00000019851	NM_022032	64058
Wfikkn2	112.790	1.056	2.240	0.112	9.404	5.25E-21	7.20E-18	ENSMUSG00000044177	NM_181819	278507
Slc31a1	875.078	0.937	1.299	0.101	9.260	2.04E-20	2.63E-17	ENSMUSG00000066150	NM_175090	20529
Crhr2	108.619	1.011	1.622	0.110	9.206	3.40E-20	4.14E-17	ENSMUSG00000003476	NM_001288618	12922
Pon3	118.599	1.018	2.450	0.111	9.188	3.99E-20	4.61E-17	ENSMUSG00000029759	NM_173006	269823
Col4a4	89.384	1.027	2.323	0.112	9.183	4.21E-20	4.62E-17	ENSMUSG00000067158	NM_007735	12829
Col8a2	344.931	0.959	2.924	0.105	9.142	6.10E-20	6.37E-17	ENSMUSG00000056174	NM_199473	329941
Drc7	423.200	0.956	2.767	0.106	9.019	1.90E-19	1.89E-16	ENSMUSG00000031786	NM_001042715	330830
Large2	27.114	0.896	3.547	0.100	8.960	3.24E-19	3.09E-16	ENSMUSG00000040434	NM_001166633	228366
Cdkn1c	98.173	1.002	2.210	0.112	8.943	3.79E-19	3.46E-16	ENSMUSG00000037664	NM_001161624	12577
Ppp1r3b	75.293	1.004	2.131	0.113	8.925	4.46E-19	3.92E-16	ENSMUSG00000046794	NM_177741	244416
Bmp6	323.017	0.968	1.524	0.109	8.905	5.34E-19	4.50E-16	ENSMUSG00000039004	NM_007556	12161
Ace	1219.013	0.911	2.865	0.104	8.768	1.82E-18	1.48E-15	ENSMUSG00000020681	NM_001281819	11421
Tmprss11a	26.416	0.827	4.208	0.094	8.760	1.95E-18	1.52E-15	ENSMUSG00000072845	NM_001033233	194597
Nid2	241.314	0.965	1.637	0.111	8.685	3.77E-18	2.85E-15	ENSMUSG00000021806	NM_008695	18074
Ccdc108	410.574	0.805	1.033	0.093	8.632	6.03E-18	4.41E-15	NA	NA	NA
Aox1	343.085	0.763	0.950	0.089	8.536	1.39E-17	9.85E-15	ENSMUSG00000063558	NM_009676	11761
Epn3	238.829	0.885	2.803	0.104	8.515	1.67E-17	1.15E-14	ENSMUSG00000010080	NM_001361558	71889
Pcolce	344.499	0.935	2.220	0.111	8.447	2.99E-17	1.99E-14	ENSMUSG00000029718	NM_008788	18542
Serpinb1b	43.580	0.887	2.681	0.105	8.424	3.63E-17	2.34E-14	ENSMUSG00000051029	NM_173052	282663
Sulf1	817.121	0.896	2.542	0.106	8.416	3.90E-17	2.44E-14	ENSMUSG00000016918	NM_001198565	240725
Acaa2	659.270	0.711	0.857	0.085	8.381	5.23E-17	3.18E-14	ENSMUSG00000036880	NM_177470	52538
Slc38a3	2451.107	0.631	0.729	0.076	8.305	9.96E-17	5.90E-14	ENSMUSG00000010064	NM_001199217	76257
Cd59a	180.998	0.927	1.766	0.113	8.233	1.82E-16	1.03E-13	ENSMUSG00000032679	NM_001111060	12509
Fxyd1	797.001	0.729	0.905	0.089	8.236	1.78E-16	1.03E-13	ENSMUSG00000036570	NM_019503	56188
Rbp1	376.294	0.896	1.437	0.109	8.194	2.52E-16	1.38E-13	ENSMUSG00000046402	NM_011254	19659
Col8a1	281.989	0.732	3.926	0.090	8.174	2.98E-16	1.59E-13	ENSMUSG00000068196	NM_007739	12837
Igf2	2948.532	0.891	2.261	0.109	8.150	3.63E-16	1.89E-13	ENSMUSG00000048583	NM_001122736	16002
Ephx1	788.842	0.765	0.992	0.094	8.102	5.39E-16	2.75E-13	ENSMUSG00000038776	NM_001312918	13849
Tmem98	423.445	0.755	0.971	0.094	8.060	7.66E-16	3.82E-13	ENSMUSG00000035413	NM_029537	103743
Calml4	154.697	0.815	2.864	0.101	8.037	9.18E-16	4.47E-13	ENSMUSG00000032246	NM_001102468	75600
Elovl7	769.509	0.834	1.207	0.104	8.022	1.04E-15	4.95E-13	ENSMUSG00000021696	NM_029001	74559
Acacb	291.254	0.854	1.285	0.107	8.010	1.14E-15	5.34E-13	ENSMUSG00000042010	NM_133904	100705
Itpripl1	93.921	0.902	1.728	0.113	7.997	1.28E-15	5.84E-13	ENSMUSG00000074825	NM_001163527	73338
Cox8b	24.017	0.732	3.849	0.092	7.947	1.91E-15	8.53E-13	ENSMUSG00000025488	NM_007751	12869
Col4a3	55.257	0.784	2.900	0.099	7.934	2.12E-15	9.30E-13	ENSMUSG00000079465	NM_007734	12828
Vamp8	251.389	0.842	1.257	0.106	7.932	2.16E-15	9.30E-13	ENSMUSG00000050732	NM_016794	22320
Il17re	25.377	0.834	2.602	0.105	7.921	2.35E-15	9.91E-13	ENSMUSG00000043088	NM_001034029	57890
Tbc1d2	215.296	0.856	1.332	0.108	7.911	2.56E-15	1.06E-12	ENSMUSG00000039813	NM_198664	381605
Cndp1	32.332	0.854	2.297	0.108	7.871	3.52E-15	1.43E-12	ENSMUSG00000056162	NM_177450	338403
Mycbpap	120.898	0.886	1.664	0.113	7.869	3.58E-15	1.43E-12	ENSMUSG00000039110	NM_170671	104601
Fap	64.169	0.794	2.874	0.101	7.827	4.98E-15	1.95E-12	ENSMUSG00000000392	NM_007986	14089
Lbp	396.510	0.839	2.327	0.107	7.814	5.53E-15	2.13E-12	ENSMUSG00000016024	NM_008489	16803
Ucp2	711.441	0.863	1.440	0.111	7.808	5.81E-15	2.20E-12	ENSMUSG00000033685	NM_011671	22228
Igfbp2	1260.259	0.844	2.249	0.108	7.796	6.40E-15	2.38E-12	ENSMUSG00000039323	NM_001310659	16008
Efemp2	330.716	0.714	0.912	0.093	7.698	1.38E-14	5.06E-12	ENSMUSG00000024909	NM_001164352	58859
Slc16a12	93.242	0.863	1.549	0.112	7.694	1.43E-14	5.13E-12	ENSMUSG00000009378	NM_172838	240638
Tcea3	29.604	0.812	2.502	0.106	7.673	1.68E-14	5.93E-12	ENSMUSG00000001604	NM_011542	21401
Cgnl1	870.494	0.860	1.682	0.113	7.641	2.15E-14	7.48E-12	ENSMUSG00000032232	NM_001304362	68178
Rd3	45.288	0.836	2.102	0.109	7.639	2.19E-14	7.49E-12	ENSMUSG00000049353	NM_001177900	74023
E230013L22Rik	10.981	0.607	4.875	0.080	7.631	2.33E-14	7.86E-12	ENSMUSG00000096957	NR_126558	102132
Prlr	759.006	0.713	3.262	0.094	7.626	2.41E-14	8.02E-12	ENSMUSG00000005268	NM_001253781	19116
Hist1h1c	671.166	0.834	1.349	0.109	7.619	2.56E-14	8.37E-12	ENSMUSG00000036181	NM_015786	50708
Zfp185	190.395	0.853	1.687	0.113	7.574	3.62E-14	1.17E-11	ENSMUSG00000031351	NM_001109043	22673
Glb1l2	56.302	0.851	1.755	0.113	7.551	4.31E-14	1.37E-11	ENSMUSG00000036395	NM_001310768	244757
Gm45396	184.371	0.816	1.277	0.108	7.522	5.38E-14	1.68E-11	NA	NA	NA
Ctnnal1	745.912	0.657	0.808	0.088	7.494	6.67E-14	2.06E-11	ENSMUSG00000038816	NM_018761	54366
Nqo1	136.599	0.832	1.406	0.111	7.491	6.83E-14	2.08E-11	ENSMUSG00000003849	NM_008706	18104
Pcolce2	230.890	0.841	1.548	0.112	7.488	7.00E-14	2.10E-11	ENSMUSG00000015354	NM_029620	76477
Hfe	205.365	0.731	0.973	0.098	7.481	7.39E-14	2.19E-11	ENSMUSG00000006611	NM_001347493	15216
Slc16a9	93.220	0.839	1.810	0.112	7.477	7.62E-14	2.23E-11	ENSMUSG00000037762	NM_025807	66859
Cdr2	380.481	0.831	1.426	0.111	7.468	8.13E-14	2.35E-11	ENSMUSG00000030878	NM_001354986	12585
Cox6b2	84.392	0.823	1.364	0.111	7.443	9.88E-14	2.81E-11	ENSMUSG00000051811	NM_001289848	333182
Mpp7	145.959	0.813	1.328	0.110	7.385	1.53E-13	4.29E-11	ENSMUSG00000057440	NM_001081287	75739
Rab11fip1	128.761	0.796	1.229	0.108	7.364	1.78E-13	4.94E-11	ENSMUSG00000031488	NM_001080813	75767
Vwa5b1	206.459	0.804	1.292	0.109	7.350	1.98E-13	5.43E-11	ENSMUSG00000028753	NM_029401	75718
Bmp7	318.333	0.768	1.126	0.105	7.317	2.54E-13	6.87E-11	ENSMUSG00000008999	NM_007557	12162
Fam161a	162.500	0.778	1.170	0.107	7.300	2.88E-13	7.71E-11	ENSMUSG00000049811	NM_028672	73873
Npc2	1653.025	0.455	0.499	0.063	7.262	3.80E-13	1.01E-10	ENSMUSG00000021242	NM_023409	67963
Gstm2	60.499	0.814	1.765	0.112	7.253	4.08E-13	1.07E-10	ENSMUSG00000040562	NM_008183	14863
Spint2	709.127	0.784	1.231	0.108	7.242	4.42E-13	1.14E-10	ENSMUSG00000074227	NM_001082548	20733
Baiap2l1	68.018	0.732	2.520	0.102	7.215	5.41E-13	1.36E-10	ENSMUSG00000038859	NM_025833	66898
Iqub	108.074	0.808	1.431	0.112	7.215	5.39E-13	1.36E-10	ENSMUSG00000046192	NM_172535	214704
Cpq	371.383	0.698	0.920	0.097	7.206	5.77E-13	1.44E-10	ENSMUSG00000039007	NM_018755	54381
Slc2a12	365.550	0.712	2.589	0.100	7.130	1.00E-12	2.47E-10	ENSMUSG00000037490	NM_178934	353169
Enpp2	26671.269	0.651	3.073	0.091	7.125	1.04E-12	2.54E-10	ENSMUSG00000022425	NM_001136077	18606
Kl	2389.264	0.669	2.882	0.094	7.103	1.22E-12	2.94E-10	ENSMUSG00000058488	NM_013823	16591
Defb11	19.644	0.536	5.362	0.076	7.087	1.38E-12	3.28E-10	ENSMUSG00000045337	NM_139221	246081
Tcn2	765.977	0.763	1.182	0.108	7.084	1.40E-12	3.30E-10	ENSMUSG00000020432	NM_001130458	21452
Fhad1	254.951	0.732	1.048	0.103	7.081	1.43E-12	3.34E-10	ENSMUSG00000051435	NM_028429	329977
Msx1	334.223	0.777	1.900	0.110	7.059	1.68E-12	3.87E-10	ENSMUSG00000048450	NM_010835	17701
Eps8l2	112.209	0.792	1.736	0.112	7.055	1.72E-12	3.93E-10	ENSMUSG00000025504	NM_133191	98845
Sult1c2	13.822	0.538	4.840	0.077	6.998	2.60E-12	5.87E-10	ENSMUSG00000023122	NM_026935	69083
H2-Eb1	49.829	0.770	1.780	0.111	6.909	4.89E-12	1.09E-09	ENSMUSG00000060586	NM_010382	14969
Col9a3	914.223	0.730	2.122	0.106	6.893	5.47E-12	1.21E-09	ENSMUSG00000027570	NM_009936	12841
Cd82	689.634	0.612	0.761	0.089	6.855	7.13E-12	1.56E-09	ENSMUSG00000027215	NM_001136055	12521
Stra6	530.589	0.698	0.981	0.102	6.847	7.52E-12	1.63E-09	ENSMUSG00000032327	NM_001162475	20897
Frem1	315.198	0.754	1.801	0.111	6.817	9.27E-12	1.99E-09	ENSMUSG00000059049	NM_001198811	329872
Rsph1	181.479	0.715	1.059	0.105	6.787	1.15E-11	2.44E-09	ENSMUSG00000024033	NM_025290	22092
Gprc5c	165.947	0.719	1.083	0.106	6.756	1.41E-11	2.98E-09	ENSMUSG00000051043	NM_001110337	70355
Arsg	933.760	0.573	0.694	0.085	6.752	1.46E-11	3.06E-09	ENSMUSG00000020604	NM_001166177	74008
Scara5	46.130	0.645	2.677	0.096	6.722	1.79E-11	3.71E-09	ENSMUSG00000022032	NM_001168318	71145
Krt18	131.178	0.563	3.409	0.084	6.717	1.86E-11	3.81E-09	ENSMUSG00000023043	NM_010664	16668
Spag16	82.547	0.750	1.624	0.112	6.687	2.28E-11	4.64E-09	ENSMUSG00000053153	NM_001271533	66722
Pla2g5	73.668	0.570	3.520	0.085	6.681	2.37E-11	4.77E-09	ENSMUSG00000041193	NM_001122954	18784
Trpv4	240.084	0.592	3.081	0.089	6.661	2.72E-11	5.43E-09	ENSMUSG00000014158	NM_022017	63873
Tmem27	12.398	0.495	4.520	0.075	6.637	3.20E-11	6.32E-09	ENSMUSG00000015401	NM_001313719	57394
Cldn1	228.120	0.744	1.449	0.113	6.611	3.82E-11	7.48E-09	ENSMUSG00000022512	NM_016674	12737
Llgl2	64.737	0.736	1.606	0.112	6.557	5.49E-11	1.07E-08	ENSMUSG00000020782	NM_001252532	217325
Wdr63	70.732	0.722	1.750	0.110	6.546	5.91E-11	1.14E-08	ENSMUSG00000043020	NM_172864	242253
Zscan10	7.679	0.488	3.767	0.075	6.528	6.65E-11	1.27E-08	ENSMUSG00000023902	NM_001033425	332221
Abca4	421.496	0.544	3.189	0.084	6.480	9.16E-11	1.73E-08	ENSMUSG00000028125	NM_007378	11304
Tgfbi	147.577	0.679	0.998	0.105	6.469	9.85E-11	1.85E-08	ENSMUSG00000035493	NM_009369	21810
Arhgef5	114.600	0.716	1.255	0.112	6.409	1.47E-10	2.73E-08	ENSMUSG00000033542	NM_133674	54324
Cd74	95.784	0.708	1.730	0.111	6.402	1.54E-10	2.83E-08	ENSMUSG00000024610	NM_001042605	16149

WTEEvsWTSH	baseMean	log2FoldChar	lfcMLE	lfcSE	stat	pvalue	padj	ensembl	RefSeq	entrez
Car14	306.094	0.685	1.047	0.107	6.394	1.61E-10	2.93E-08	ENSMUSG00000038526	NM_001355750	23831
Tmem184a	19.988	0.577	2.858	0.090	6.394	1.62E-10	2.93E-08	ENSMUSG00000036687	NM_001161548	231832
Hemk1	549.991	0.546	0.664	0.086	6.384	1.73E-10	3.10E-08	ENSMUSG00000032579	NM_133984	69536
1500015O10Rik	509.574	0.494	3.756	0.078	6.374	1.84E-10	3.28E-08	ENSMUSG00000026051	NM_024283	78896
Slc39a4	75.745	0.680	1.878	0.107	6.346	2.20E-10	3.90E-08	ENSMUSG00000063354	NM_028064	72027
Prelp	1234.510	0.637	0.880	0.100	6.344	2.23E-10	3.92E-08	ENSMUSG00000041577	NM_054077	116847
Lama5	643.356	0.678	1.043	0.107	6.327	2.51E-10	4.27E-08	ENSMUSG00000015647	NM_001081171	16776
Olfr1507	14.279	0.538	3.055	0.085	6.326	2.51E-10	4.27E-08	ENSMUSG00000059887	NM_001170918	57269
Prr32	84.015	0.458	4.282	0.072	6.327	2.50E-10	4.27E-08	ENSMUSG00000037086	NM_026841	68800
Vat1l	1396.026	0.707	1.578	0.112	6.328	2.49E-10	4.27E-08	ENSMUSG00000046844	NM_173016	270097
Lepr	137.994	0.644	2.168	0.102	6.317	2.67E-10	4.50E-08	ENSMUSG00000057722	NM_001122899	16847
Hspb8	513.837	0.592	0.761	0.094	6.308	2.82E-10	4.72E-08	ENSMUSG00000041548	NM_030704	80888
Antxr1	630.953	0.602	0.793	0.096	6.295	3.08E-10	5.11E-08	ENSMUSG00000033420	NM_054041	69538
Stk39	2127.397	0.519	0.620	0.082	6.288	3.22E-10	5.31E-08	ENSMUSG00000027030	NM_016866	53416
Klhdc7a	829.047	0.567	0.708	0.090	6.284	3.30E-10	5.40E-08	ENSMUSG00000078234	NM_173427	242721
Cpt1a	1096.502	0.563	0.708	0.090	6.256	3.95E-10	6.42E-08	ENSMUSG00000024900	NM_013495	12894
Sowahc	509.370	0.673	1.040	0.108	6.247	4.17E-10	6.73E-08	ENSMUSG00000098188	NM_172939	268301
Frrs1	87.285	0.704	1.355	0.113	6.242	4.32E-10	6.87E-08	ENSMUSG00000033386	NM_001113478	20321
Mlf1	58.568	0.678	1.813	0.109	6.242	4.32E-10	6.87E-08	ENSMUSG00000048416	NM_001039543	17349
Crb2	295.293	0.667	1.025	0.107	6.221	4.94E-10	7.79E-08	ENSMUSG00000035403	NM_001163566	241324
Steap2	598.562	0.683	1.678	0.110	6.199	5.69E-10	8.91E-08	ENSMUSG00000015653	NM_001103156	74051
Lrrc23	154.561	0.680	1.108	0.110	6.189	6.06E-10	9.43E-08	ENSMUSG00000030125	NM_001302555	16977
Tc2n	23.814	0.566	2.685	0.092	6.183	6.30E-10	9.73E-08	ENSMUSG00000021187	NM_001082976	74413
Ctsd	4640.837	0.485	0.565	0.079	6.178	6.48E-10	9.94E-08	ENSMUSG00000007891	NM_009983	13033
Tbc1d9	3791.156	0.527	0.643	0.085	6.172	6.76E-10	1.03E-07	ENSMUSG00000031709	NM_001111304	71310
Cfap126	87.647	0.691	1.239	0.112	6.164	7.11E-10	1.08E-07	ENSMUSG00000026649	NM_001081275	75472
Arhgap28	36.335	0.617	2.149	0.100	6.152	7.63E-10	1.15E-07	ENSMUSG00000024043	NM_001347410	268970
Ezr	2320.611	0.575	0.745	0.094	6.121	9.32E-10	1.39E-07	ENSMUSG00000052397	NM_009510	22350
Inmt	32.454	0.621	2.156	0.102	6.111	9.90E-10	1.47E-07	ENSMUSG00000003477	NM_009349	21743
Slc6a20a	339.619	0.677	1.148	0.111	6.106	1.02E-09	1.51E-07	ENSMUSG00000036814	NM_139142	102680
Col18a1	236.575	0.686	1.280	0.112	6.104	1.03E-09	1.51E-07	ENSMUSG00000001435	NM_001109991	12822
Gm26684	13.453	0.562	2.659	0.092	6.103	1.04E-09	1.51E-07	NA	XR_001781621	102638507
B4galt1	269.636	0.571	0.735	0.094	6.101	1.05E-09	1.52E-07	ENSMUSG00000028413	NM_022305	14595
Myo5c	150.880	0.679	1.163	0.111	6.099	1.07E-09	1.53E-07	ENSMUSG00000033590	NM_001081322	208943
Acad8	990.478	0.548	0.686	0.090	6.089	1.13E-09	1.60E-07	ENSMUSG00000031969	NM_025862	66948
Dnaic2	117.581	0.653	1.006	0.107	6.087	1.15E-09	1.60E-07	ENSMUSG00000034706	NM_001034878	432611
Fzd4	536.373	0.662	1.053	0.109	6.087	1.15E-09	1.60E-07	ENSMUSG00000049791	NM_008055	14366
Pifo	37.820	0.665	1.722	0.109	6.089	1.14E-09	1.60E-07	ENSMUSG00000010136	NM_001200028	100503311
Tor3a	276.940	0.551	0.695	0.091	6.081	1.19E-09	1.66E-07	ENSMUSG00000060519	NM_023141	30935
Rilp	53.646	0.673	1.635	0.111	6.077	1.22E-09	1.69E-07	ENSMUSG00000038195	NM_001029938	280408
Htr2c	1804.500	0.628	0.915	0.104	6.039	1.55E-09	2.13E-07	ENSMUSG00000041380	NM_008312	15560
A2m	239.804	0.648	1.784	0.107	6.036	1.58E-09	2.16E-07	ENSMUSG00000030111	NM_175628	232345
Gpx8	131.298	0.664	1.643	0.110	6.032	1.62E-09	2.19E-07	ENSMUSG00000021760	NM_027127	69590
Fam189a2	388.929	0.470	0.546	0.078	6.023	1.72E-09	2.31E-07	ENSMUSG00000071604	NM_001114174	381217
Sod3	456.344	0.605	0.839	0.101	6.012	1.83E-09	2.44E-07	ENSMUSG00000072941	NM_011435	20657
Sostdc1	343.841	0.488	3.071	0.081	6.010	1.86E-09	2.47E-07	ENSMUSG00000036169	NM_025312	66042
Otx2os1	12.777	0.478	3.583	0.080	6.008	1.88E-09	2.48E-07	ENSMUSG00000098682	NR_029384	606497
Galm	118.684	0.663	1.119	0.111	5.977	2.27E-09	2.97E-07	ENSMUSG00000035473	NM_176963	319625
Tcaf2	38.076	0.630	1.897	0.105	5.975	2.30E-09	2.99E-07	ENSMUSG00000029851	NM_146174	232748
Cutal	16.256	0.589	2.165	0.099	5.960	2.52E-09	3.25E-07	ENSMUSG00000026870	NM_001308024	77996
Kcnj13	102.390	0.402	4.349	0.068	5.950	2.68E-09	3.42E-07	ENSMUSG00000079436	NM_001110227	100040591
Otx2	218.038	0.438	3.774	0.074	5.950	2.68E-09	3.42E-07	ENSMUSG00000021848	NM_001286481	18424
Tmem86a	407.548	0.530	0.658	0.089	5.918	3.25E-09	4.12E-07	ENSMUSG00000010307	NM_026436	67893
Abhd2	3923.077	0.525	0.654	0.089	5.906	3.51E-09	4.42E-07	ENSMUSG00000039202	NM_018811	54608
Folr1	406.250	0.420	3.910	0.071	5.899	3.66E-09	4.59E-07	ENSMUSG00000001827	NM_001252552	14275
Fam47e	23.554	0.611	1.877	0.104	5.891	3.83E-09	4.77E-07	ENSMUSG00000057068	NM_001033478	384198
Bsg	10938.613	0.461	0.538	0.078	5.884	4.00E-09	4.90E-07	ENSMUSG00000023175	NM_001077184	12215
Sh3d19	1070.171	0.567	0.751	0.096	5.885	3.97E-09	4.90E-07	ENSMUSG00000028082	NM_001082414	27059
Slc22a8	492.124	0.549	0.708	0.093	5.884	4.00E-09	4.90E-07	ENSMUSG00000063796	NM_001164634	19879
Xirp1	10.626	0.485	2.937	0.083	5.861	4.61E-09	5.61E-07	ENSMUSG00000079243	NM_001081339	22437
Paqr5	101.144	0.659	1.245	0.113	5.849	4.94E-09	5.98E-07	ENSMUSG00000032278	NM_028748	74090
2410004P03Rik	136.478	0.607	0.881	0.104	5.827	5.65E-09	6.81E-07	ENSMUSG00000071398	NM_001201332	73667
Fkbp9	1328.248	0.381	0.422	0.066	5.810	6.24E-09	7.48E-07	ENSMUSG00000029781	NM_012056	27055
Cldn2	298.567	0.417	4.090	0.072	5.809	6.29E-09	7.49E-07	ENSMUSG00000047230	NM_016675	12738
4833427G06Rik	22.956	0.621	1.743	0.107	5.799	6.65E-09	7.89E-07	ENSMUSG00000032057	NM_177702	235345
Rbm47	86.837	0.465	3.176	0.080	5.793	6.92E-09	8.16E-07	ENSMUSG00000070780	NM_001127382	245945
Mxra8	214.242	0.617	0.941	0.107	5.780	7.46E-09	8.70E-07	ENSMUSG00000029070	NM_024263	74761
Myof	258.163	0.640	1.083	0.111	5.781	7.43E-09	8.70E-07	ENSMUSG00000048612	NM_001099634	226101
Sema3f	201.098	0.640	1.090	0.111	5.768	8.04E-09	9.33E-07	ENSMUSG00000034684	NM_001311151	20350
Agtrap	365.353	0.501	0.616	0.087	5.759	8.46E-09	9.76E-07	ENSMUSG00000029007	NM_001301281	11610
Acss3	60.377	0.635	1.570	0.110	5.757	8.55E-09	9.82E-07	ENSMUSG00000035948	NM_001142804	380660
4930511M06Rik	15.083	0.511	2.739	0.089	5.753	8.78E-09	9.88E-07	ENSMUSG00000086607	NR_015494	75084
Cd63	1520.352	0.471	0.558	0.082	5.754	8.70E-09	9.88E-07	ENSMUSG00000025351	NM_001042580	12512
Ltbp3	1149.699	0.572	0.787	0.099	5.755	8.68E-09	9.88E-07	ENSMUSG00000024940	NM_008520	16998
Mgp	334.737	0.645	1.185	0.112	5.753	8.74E-09	9.88E-07	ENSMUSG00000030218	NM_008597	17313
Gm853	6.777	0.388	3.874	0.068	5.720	1.06E-08	1.19E-06	ENSMUSG00000023120	NM_001034872	332942
Slc28a3	25.836	0.499	2.633	0.087	5.710	1.13E-08	1.25E-06	ENSMUSG00000021553	NM_022317	114304
Ccdc114	187.529	0.581	0.815	0.102	5.709	1.14E-08	1.25E-06	ENSMUSG00000040189	NM_001033243	211535
Gm28729	40.098	0.633	1.475	0.111	5.698	1.22E-08	1.33E-06	ENSMUSG00000099564	XM_006511607	102635744
Hbb-bs	771.503	0.619	0.985	0.109	5.690	1.27E-08	1.38E-06	ENSMUSG00000052305	NM_001201391	100503605
Rrh	17.429	0.535	2.282	0.094	5.690	1.27E-08	1.38E-06	ENSMUSG00000028012	NM_009102	20132
F11r	268.290	0.587	0.839	0.103	5.678	1.36E-08	1.47E-06	ENSMUSG00000038235	NM_172647	16456
Jhy	26.109	0.621	1.572	0.110	5.674	1.40E-08	1.50E-06	ENSMUSG00000032023	NM_001081121	70989
Piezo1	244.670	0.628	1.057	0.111	5.674	1.40E-08	1.50E-06	ENSMUSG00000014444	NM_001037298	234839
Mitf	304.206	0.563	0.770	0.099	5.661	1.51E-08	1.61E-06	ENSMUSG00000035158	NM_001113198	17342
Tor4a	133.608	0.596	0.873	0.105	5.657	1.54E-08	1.62E-06	ENSMUSG00000059555	NM_146115	227612
Creb3l1	163.894	0.573	0.802	0.101	5.655	1.56E-08	1.64E-06	ENSMUSG00000027230	NM_011957	26427
Prrg4	53.884	0.637	1.276	0.113	5.650	1.60E-08	1.66E-06	ENSMUSG00000027171	NM_178695	228413
Slco1c1	1730.317	0.552	0.738	0.098	5.650	1.60E-08	1.66E-06	ENSMUSG00000030235	NM_001177772	58807
Trip10	203.743	0.528	0.677	0.094	5.645	1.65E-08	1.70E-06	ENSMUSG00000019487	NM_001242389	106628
Foxj1	459.962	0.566	0.788	0.101	5.634	1.76E-08	1.81E-06	ENSMUSG00000034227	NM_008240	15223
Col1a2	439.292	0.621	1.038	0.110	5.631	1.79E-08	1.83E-06	ENSMUSG00000029661	NM_007743	12843
Trpm3	2956.294	0.631	1.354	0.112	5.622	1.89E-08	1.91E-06	ENSMUSG00000052387	NM_001035239	226025
D630024D03Rik	18.175	0.472	2.937	0.084	5.619	1.92E-08	1.93E-06	ENSMUSG00000085772	NR_102310	414116
Ackr4	16.172	0.555	2.018	0.099	5.597	2.18E-08	2.18E-06	ENSMUSG00000079355	NM_145700	252837
Gm11744	90.246	0.630	1.252	0.113	5.587	2.31E-08	2.30E-06	NA	NA	NA
Angptl2	179.391	0.554	2.033	0.100	5.571	2.54E-08	2.52E-06	ENSMUSG00000004105	NM_011923	26360
Klhdc8b	653.674	0.425	0.491	0.076	5.566	2.61E-08	2.57E-06	ENSMUSG00000032609	NM_001359428	78267
Dnali1	117.461	0.589	0.881	0.106	5.563	2.65E-08	2.60E-06	ENSMUSG00000042707	NM_175223	75563
Crtap	192.782	0.525	0.678	0.094	5.557	2.74E-08	2.68E-06	ENSMUSG00000032431	NM_019922	56693
Dlec1	164.322	0.574	0.815	0.103	5.556	2.75E-08	2.68E-06	ENSMUSG00000038060	NM_177117	320256
Pltp	1544.501	0.476	0.582	0.086	5.551	2.85E-08	2.76E-06	ENSMUSG00000017754	NM_011125	18830
Lgals3bp	630.262	0.596	0.917	0.108	5.541	3.00E-08	2.90E-06	ENSMUSG00000033880	NM_011150	19039
Fam46c	130.890	0.619	1.183	0.113	5.502	3.75E-08	3.57E-06	ENSMUSG00000044468	NM_001142952	74645
Hspb6	117.709	0.603	0.984	0.110	5.491	3.99E-08	3.76E-06	ENSMUSG00000036854	NM_001012401	243912
Phldb2	269.306	0.566	0.804	0.103	5.492	3.96E-08	3.76E-06	ENSMUSG00000033149	NM_001252442	208177
Tekt1	112.253	0.609	1.031	0.111	5.491	3.99E-08	3.76E-06	ENSMUSG00000020799	NM_001282006	21689
Cfap43	203.487	0.534	0.720	0.098	5.477	4.33E-08	4.06E-06	ENSMUSG00000044948	NM_027559	100048534
Sfrp5	36.610	0.495	2.266	0.091	5.464	4.66E-08	4.35E-06	ENSMUSG00000018822	NM_018780	54612
Cpt2	208.838	0.590	0.925	0.108	5.461	4.74E-08	4.40E-06	ENSMUSG00000028607	NM_009949	12896
Tjp3	73.047	0.570	1.752	0.105	5.451	5.01E-08	4.63E-06	ENSMUSG00000034917	NM_001282095	27375
Sep-10	191.035	0.567	0.825	0.104	5.435	5.48E-08	5.05E-06	ENSMUSG00000019917	NM_001024910	103080
Naga	628.844	0.381	0.429	0.070	5.428	5.70E-08	5.23E-06	ENSMUSG00000022453	NM_001355546	17939
Six3os1	43.480	0.567	1.707	0.104	5.427	5.73E-08	5.23E-06	ENSMUSG00000093460	NR_015385	100043902
Car12	1793.787	0.608	1.190	0.113	5.403	6.57E-08	5.98E-06	ENSMUSG00000032373	NM_001306148	76459
Slc7a10	899.769	0.466	0.570	0.086	5.401	6.61E-08	5.99E-06	ENSMUSG00000030495	NM_017394	53896
Myo7a	967.199	0.490	0.620	0.091	5.399	6.70E-08	6.04E-06	ENSMUSG00000030761	NM_001256081	17921
Ccdc113	65.382	0.608	1.177	0.113	5.396	6.82E-08	6.13E-06	ENSMUSG00000036598	NM_172914	244608
Scube3	270.121	0.602	1.084	0.112	5.384	7.30E-08	6.53E-06	ENSMUSG00000038677	NM_001004366	268935

WTEEvsWTSH	baseMean	log2FoldChar	lfcMLE	lfcSE	stat	pvalue	padj	ensembl	RefSeq	entrez
Emb	772.327	0.549	0.771	0.102	5.381	7.43E-08	6.62E-06	ENSMUSG00000021728	NM_010330	13723
Tns1	1749.212	0.471	0.581	0.088	5.371	7.81E-08	6.94E-06	ENSMUSG00000055322	NM_001289895	21961
Plscr2	53.061	0.606	1.211	0.113	5.371	7.85E-08	6.94E-06	ENSMUSG00000032372	NM_001195084	18828
Slc16a6	376.632	0.520	0.693	0.097	5.365	8.10E-08	7.14E-06	ENSMUSG00000041920	NM_001029842	104681
St6galnac2	203.547	0.571	1.664	0.106	5.363	8.20E-08	7.20E-06	ENSMUSG00000057286	NM_009180	20446
Dnajb13	37.933	0.582	1.538	0.109	5.358	8.43E-08	7.36E-06	ENSMUSG00000030708	NM_153527	69387
Dnah11	141.399	0.592	0.989	0.111	5.355	8.54E-08	7.41E-06	ENSMUSG00000018581	NM_010060	13411
Hmgcs2	251.470	0.544	0.765	0.102	5.355	8.55E-08	7.41E-06	ENSMUSG00000027875	NM_008256	15360
Rs1	20.572	0.524	2.003	0.098	5.336	9.52E-08	8.22E-06	ENSMUSG00000031293	NM_011302	20147
Sntb1	162.505	0.589	0.982	0.110	5.333	9.67E-08	8.31E-06	ENSMUSG00000060429	NM_016667	20649
Ccdc170	72.665	0.599	1.136	0.113	5.317	1.06E-07	9.01E-06	ENSMUSG00000019767	NM_001195672	100504234
Sfrp1	204.738	0.598	1.258	0.112	5.317	1.06E-07	9.01E-06	ENSMUSG00000031548	NM_013834	20377
Iqgap1	963.114	0.414	0.483	0.078	5.307	1.12E-07	9.49E-06	ENSMUSG00000030536	NM_016721	29875
Agbl2	80.804	0.597	1.111	0.112	5.304	1.13E-07	9.60E-06	ENSMUSG00000040812	NM_001356533	271813
Gm29538	8.280	0.394	2.838	0.074	5.301	1.15E-07	9.70E-06	NA	XR_387233	102636980
Tmem237	762.404	0.450	0.545	0.085	5.295	1.19E-07	1.00E-05	ENSMUSG00000038079	NM_001033449	381259
Pdpn	285.366	0.448	0.544	0.085	5.278	1.31E-07	1.09E-05	ENSMUSG00000028583	NM_001290822	14726
Slc1a5	75.536	0.587	1.014	0.111	5.262	1.42E-07	1.19E-05	ENSMUSG00000001918	NM_009201	20514
Lyz2	242.067	0.540	0.759	0.103	5.260	1.44E-07	1.20E-05	ENSMUSG00000069516	NM_017372	17105
Kif9	245.194	0.517	0.703	0.099	5.235	1.65E-07	1.36E-05	ENSMUSG00000032489	NM_001163569	16578
Tuft1	141.002	0.569	0.897	0.109	5.218	1.81E-07	1.49E-05	ENSMUSG00000005968	NM_001293728	22156
Catip	101.288	0.559	0.859	0.107	5.215	1.84E-07	1.50E-05	ENSMUSG00000073650	NM_001033345	241112
Ppfibp2	438.500	0.484	0.618	0.093	5.206	1.93E-07	1.57E-05	ENSMUSG00000036528	NM_001163557	19024
BC021767	9.980	0.445	2.360	0.086	5.197	2.02E-07	1.64E-05	NA	NR_033629	545551
Thbs1	120.007	0.584	1.206	0.113	5.186	2.14E-07	1.73E-05	ENSMUSG00000040152	NM_001313914	21825
Aph1c	393.719	0.423	0.501	0.082	5.175	2.27E-07	1.82E-05	ENSMUSG00000053040	NM_026674	68318
Lpin3	44.036	0.567	1.453	0.110	5.174	2.29E-07	1.82E-05	ENSMUSG00000027412	NM_001199118	64899
Tinagl1	200.895	0.582	1.090	0.112	5.174	2.30E-07	1.82E-05	ENSMUSG00000028776	NM_001168333	94242
Cfap44	426.808	0.509	0.695	0.099	5.166	2.39E-07	1.89E-05	ENSMUSG00000071550	NM_001033247	212517
Slc12a4	699.689	0.529	0.754	0.102	5.164	2.42E-07	1.91E-05	ENSMUSG00000017765	NM_001253804	20498
Prkcq	435.807	0.502	0.677	0.097	5.158	2.49E-07	1.96E-05	ENSMUSG00000026778	NM_008859	18761
Ttc25	80.386	0.565	0.911	0.110	5.155	2.53E-07	1.98E-05	ENSMUSG00000006784	NM_028918	74407
Bcam	453.042	0.485	0.629	0.094	5.151	2.59E-07	2.02E-05	ENSMUSG00000002980	NM_020486	57278
Esrrb	73.760	0.579	1.115	0.113	5.141	2.74E-07	2.12E-05	ENSMUSG00000021255	NM_001159500	26380
Islr	486.237	0.562	0.911	0.109	5.140	2.74E-07	2.12E-05	ENSMUSG00000037206	NM_001195431	26968
Aldh2	2919.237	0.441	0.541	0.086	5.109	3.23E-07	2.47E-05	ENSMUSG00000029455	NM_001308450	11669
H2-Aa	45.885	0.539	1.628	0.106	5.100	3.40E-07	2.59E-05	ENSMUSG00000036594	NM_010378	14960
Plcd1	384.260	0.463	0.591	0.091	5.072	3.94E-07	2.99E-05	ENSMUSG00000010660	NM_001293648	18799
Mrc2	263.876	0.544	0.832	0.107	5.069	4.00E-07	3.02E-05	ENSMUSG00000020695	NM_008626	17534
Slc19a1	519.772	0.430	0.524	0.085	5.056	4.29E-07	3.23E-05	ENSMUSG00000001436	NM_001199271	20509
Lgals1	319.880	0.489	0.648	0.097	5.044	4.56E-07	3.43E-05	ENSMUSG00000068220	NM_008495	16852
Slc26a7	38.484	0.485	1.927	0.096	5.034	4.81E-07	3.60E-05	ENSMUSG00000040569	NM_145947	208890
Dock6	852.519	0.469	0.608	0.093	5.019	5.20E-07	3.88E-05	ENSMUSG00000032198	NM_177030	319899
Glb1l	303.230	0.458	0.579	0.091	5.015	5.31E-07	3.95E-05	ENSMUSG00000026200	NM_029010	74577
Ttll6	45.073	0.563	1.186	0.113	4.999	5.76E-07	4.27E-05	ENSMUSG00000038756	NM_172799	237930
Pafah2	288.014	0.456	0.578	0.091	4.992	5.98E-07	4.42E-05	ENSMUSG00000037366	NM_001285872	100163
Dmrt3	30.546	0.545	1.417	0.109	4.991	6.02E-07	4.42E-05	ENSMUSG00000042372	NM_177360	240590
Sgk3	421.760	0.485	0.648	0.097	4.991	6.02E-07	4.42E-05	ENSMUSG00000025915	NM_001037759	170755
Acox2	20.737	0.459	2.035	0.092	4.988	6.09E-07	4.45E-05	ENSMUSG00000021751	NM_001161667	93732
Plin3	545.311	0.469	0.607	0.094	4.984	6.24E-07	4.55E-05	ENSMUSG00000024197	NM_025836	66905
Spata6	149.165	0.516	0.745	0.104	4.971	6.68E-07	4.80E-05	ENSMUSG00000034401	NM_001357231	67946
BC067074	160.607	0.513	1.632	0.104	4.947	7.55E-07	5.41E-05	ENSMUSG00000021763	XR_001781056	408066
Tgfbr3	588.978	0.502	0.704	0.102	4.931	8.18E-07	5.83E-05	ENSMUSG00000029287	NM_011578	21814
Neurod1	494.338	-0.439	-0.555	0.089	-4.924	8.49E-07	6.03E-05	ENSMUSG00000034701	NM_010894	18012
Mmp2	116.305	0.532	0.834	0.108	4.902	9.47E-07	6.70E-05	ENSMUSG00000031740	NM_008610	17390
Il17rc	132.608	0.525	0.804	0.107	4.898	9.67E-07	6.82E-05	ENSMUSG00000030281	NM_134159	171095
Slc25a13	84.522	0.545	0.946	0.111	4.888	1.02E-06	7.13E-05	ENSMUSG00000015112	NM_001177572	50799
Lum	131.901	0.535	0.869	0.110	4.882	1.05E-06	7.35E-05	ENSMUSG00000036446	NM_008524	17022
Fbln5	141.399	0.535	0.867	0.110	4.879	1.07E-06	7.44E-05	ENSMUSG00000021186	NM_001361987	23876
Hbb-bt	152.800	0.548	1.147	0.112	4.876	1.08E-06	7.51E-05	ENSMUSG00000073940	NM_008220	101488143
Nxn	353.018	0.494	0.698	0.102	4.859	1.18E-06	8.12E-05	ENSMUSG00000020844	NM_008750	18230
Hspg2	591.547	0.532	0.882	0.110	4.832	1.35E-06	9.20E-05	ENSMUSG00000028763	NM_008305	15530
Serping1	224.913	0.528	0.860	0.109	4.832	1.35E-06	9.20E-05	ENSMUSG00000023224	NM_009776	12258
Col4a5	202.536	0.538	0.940	0.111	4.829	1.38E-06	9.34E-05	ENSMUSG00000031274	NM_001163155	12830
Csrp2	136.075	0.541	1.019	0.112	4.812	1.49E-06	1.01E-04	ENSMUSG00000020186	NM_007792	13008
Cyb561	1971.444	0.390	0.459	0.082	4.781	1.75E-06	1.16E-04	ENSMUSG00000019590	NM_001356374	13056
Rom1	136.027	0.491	0.701	0.103	4.770	1.84E-06	1.23E-04	ENSMUSG00000071648	NM_009073	19881
Ogn	245.219	0.536	1.022	0.113	4.765	1.89E-06	1.25E-04	ENSMUSG00000021390	NM_008760	18295
Bdh2	60.038	0.532	1.201	0.112	4.756	1.97E-06	1.30E-04	ENSMUSG00000028167	NM_001172055	69772
Hyal3	16.334	0.483	1.666	0.102	4.722	2.33E-06	1.53E-04	ENSMUSG00000036091	NM_178020	109685
Aldh3b1	172.009	0.478	0.673	0.101	4.714	2.42E-06	1.58E-04	ENSMUSG00000024885	NM_026316	67689
Cfap206	81.364	0.531	1.052	0.113	4.715	2.42E-06	1.58E-04	ENSMUSG00000028294	NM_001347062	69329
Hba-a2	239.270	0.525	0.916	0.111	4.710	2.48E-06	1.61E-04	ENSMUSG00000069917	NM_001083955	110257
Dpp7	759.368	0.405	0.491	0.086	4.708	2.50E-06	1.62E-04	ENSMUSG00000026958	NM_031843	83768
Hist1h2bc	820.877	0.440	0.570	0.094	4.684	2.82E-06	1.82E-04	ENSMUSG00000018102	NM_001290380	68024
Ifi27	1065.867	0.476	0.663	0.102	4.680	2.87E-06	1.85E-04	ENSMUSG00000064215	NM_026790	52668
RP24-298N7.11	17.350	0.466	1.717	0.100	4.677	2.91E-06	1.87E-04	NA	NA	NA
Robo3	1160.606	0.508	0.809	0.109	4.678	2.90E-06	1.87E-04	ENSMUSG00000032128	NM_001164767	19649
Emilin1	98.989	0.515	0.855	0.110	4.669	3.02E-06	1.93E-04	ENSMUSG00000029163	NM_133918	100952
Cast	242.505	0.485	0.696	0.104	4.665	3.09E-06	1.97E-04	ENSMUSG00000021585	NM_001301153	12380
Gm16150	12.952	0.427	1.924	0.092	4.654	3.25E-06	2.07E-04	NA	XR_001778890	102638318
Chia1	57.128	0.524	1.058	0.113	4.647	3.37E-06	2.13E-04	ENSMUSG00000062778	NM_023186	81600
Sgms2	188.634	0.492	1.467	0.106	4.647	3.37E-06	2.13E-04	ENSMUSG00000050931	NM_028943	74442
Nek5	54.792	0.465	1.637	0.100	4.643	3.43E-06	2.16E-04	ENSMUSG00000037738	NM_001347318	330721
Fbn1	572.343	0.423	0.545	0.091	4.635	3.57E-06	2.24E-04	ENSMUSG00000027204	NM_007993	14118
Cfap70	88.849	0.494	0.756	0.107	4.614	3.95E-06	2.46E-04	ENSMUSG00000039543	NM_001163638	76670
Slc16a4	204.177	0.454	0.610	0.099	4.610	4.03E-06	2.50E-04	ENSMUSG00000027896	NM_001310705	229699
Dnaaf3	40.435	0.516	1.146	0.112	4.601	4.20E-06	2.59E-04	ENSMUSG00000055809	NM_001033548	436022
Nudt7	126.867	0.507	0.840	0.110	4.593	4.36E-06	2.68E-04	ENSMUSG00000031767	NM_001290180	67528
Loxl4	14.761	0.397	2.097	0.087	4.588	4.47E-06	2.74E-04	ENSMUSG00000025185	NM_001164311	67573
Nek11	50.757	0.517	0.985	0.113	4.584	4.56E-06	2.79E-04	ENSMUSG00000035032	NM_172461	208583
BC034090	346.315	0.399	0.495	0.087	4.569	4.91E-06	2.98E-04	ENSMUSG00000033722	XM_006530030	207792
Tspo	113.188	0.514	1.009	0.113	4.565	5.00E-06	3.03E-04	ENSMUSG00000041736	NM_009775	12257
Adh1	15.370	0.428	1.827	0.094	4.564	5.02E-06	3.04E-04	ENSMUSG00000074207	NM_007409	11522
Gas2l2	51.873	0.506	1.208	0.111	4.561	5.10E-06	3.07E-04	ENSMUSG00000020686	NM_001013759	237891
Ttc21a	159.644	0.510	0.951	0.112	4.545	5.50E-06	3.29E-04	ENSMUSG00000032514	NM_028735	74052
Aass	176.278	0.493	0.782	0.109	4.538	5.67E-06	3.38E-04	ENSMUSG00000029695	NM_013930	30956
Arhgef16	24.992	0.475	1.473	0.105	4.536	5.73E-06	3.41E-04	ENSMUSG00000029032	NM_001112744	230972
Col3a1	89.181	0.509	1.005	0.113	4.517	6.28E-06	3.71E-04	ENSMUSG00000026043	NM_009930	12825
Cpn1	17.381	0.462	1.496	0.102	4.515	6.34E-06	3.73E-04	ENSMUSG00000025196	NM_030703	93721
Ripk4	28.293	0.484	1.409	0.107	4.506	6.60E-06	3.87E-04	ENSMUSG00000005251	NM_023663	72388
Pcp4l1	1708.601	0.422	0.550	0.094	4.503	6.71E-06	3.92E-04	ENSMUSG00000038370	NM_025557	66425
Rsph4a	235.196	0.453	0.634	0.101	4.495	6.94E-06	4.04E-04	ENSMUSG00000039552	NM_001162957	212892
Gstt2	50.369	0.504	1.121	0.112	4.494	6.99E-06	4.06E-04	ENSMUSG00000033318	NM_010361	14872
Wdr78	468.331	0.420	0.538	0.094	4.487	7.22E-06	4.18E-04	ENSMUSG00000035126	NM_146254	242584
Bst2	103.498	0.496	1.190	0.111	4.471	7.79E-06	4.48E-04	ENSMUSG00000046718	NM_198095	69550
Col1a1	330.978	0.494	0.843	0.111	4.467	7.94E-06	4.55E-04	ENSMUSG00000001506	NM_007742	12842
Tep1	226.564	0.431	0.568	0.096	4.467	7.94E-06	4.55E-04	ENSMUSG00000006281	NM_009351	21745
Nt5dc1	99.239	0.495	0.841	0.111	4.462	8.13E-06	4.64E-04	ENSMUSG00000039480	NM_001347463	319638
Loxl2	23.678	0.452	1.581	0.101	4.456	8.35E-06	4.73E-04	ENSMUSG00000034205	NM_033325	94352
Serinc2	307.146	0.481	0.754	0.108	4.447	8.71E-06	4.92E-04	ENSMUSG00000023232	NM_001253386	230779
Cep41	207.419	0.434	0.584	0.098	4.443	8.86E-06	4.98E-04	ENSMUSG00000029790	NM_031998	83922
Cdc14b	356.020	0.448	0.614	0.101	4.429	9.45E-06	5.29E-04	ENSMUSG00000033102	NM_001122989	218294
Phactr2	1370.574	0.423	0.565	0.096	4.391	1.13E-05	6.26E-04	ENSMUSG00000062866	NM_001033257	215789
Dnah6	278.746	0.484	1.191	0.110	4.385	1.16E-05	6.39E-04	ENSMUSG00000052861	NM_001164669	330355
Spata18	63.032	0.484	1.172	0.111	4.376	1.21E-05	6.61E-04	ENSMUSG00000029155	NM_178387	73472
Rsph9	419.186	0.433	0.591	0.099	4.364	1.28E-05	6.98E-04	ENSMUSG00000023966	NM_029338	75564
Ubxn10	123.852	0.483	0.818	0.111	4.359	1.30E-05	7.10E-04	ENSMUSG00000043621	NM_001285928	212190
Slc22a18	15.422	0.426	1.600	0.098	4.355	1.33E-05	7.22E-04	ENSMUSG00000000154	NM_001042760	18400

WTEEvsWTSH	baseMean	log2FoldChar	lfcMLE	lfcSE	stat	pvalue	padj	ensembl	RefSeq	entrez
Slc29a4	1320.065	0.489	0.947	0.112	4.348	1.37E-05	7.44E-04	ENSMUSG00000050822	NM_146257	243328
Cgn	256.932	0.446	0.635	0.103	4.340	1.42E-05	7.67E-04	ENSMUSG00000068876	NM_001037711	70737
Spag8	67.881	0.483	0.835	0.111	4.336	1.45E-05	7.79E-04	ENSMUSG00000066196	NM_001007463	433700
Neat1	3434.586	0.440	0.617	0.102	4.325	1.52E-05	8.15E-04	ENSMUSG00000092274	NR_003513	66961
Crb3	53.250	0.470	1.248	0.109	4.324	1.54E-05	8.19E-04	ENSMUSG00000044279	NM_001347408	224912
Fbxo36	73.115	0.487	0.941	0.113	4.320	1.56E-05	8.30E-04	ENSMUSG00000073633	NM_025386	66153
Capn6	84.004	0.474	1.204	0.110	4.319	1.57E-05	8.32E-04	ENSMUSG00000067276	NM_007603	12338
Cped1	107.623	0.484	0.906	0.112	4.306	1.66E-05	8.76E-04	ENSMUSG00000062980	NM_001081351	214642
Trp73	174.356	0.470	0.767	0.109	4.307	1.66E-05	8.76E-04	ENSMUSG00000029026	NM_001126330	22062
Plekhg2	196.679	0.383	0.478	0.089	4.298	1.73E-05	9.07E-04	ENSMUSG00000037552	NM_001083912	101497
Cfh	768.619	0.418	0.559	0.097	4.288	1.80E-05	9.44E-04	ENSMUSG00000026365	NM_009888	12628
Cp	454.912	0.433	0.607	0.101	4.271	1.95E-05	1.02E-03	ENSMUSG00000003617	NM_001042611	12870
Sdc1	26.830	0.457	1.304	0.107	4.268	1.98E-05	1.03E-03	ENSMUSG00000020592	NM_011519	20969
Coch	251.360	0.480	0.985	0.113	4.263	2.01E-05	1.04E-03	ENSMUSG00000020953	NM_001198835	12810
Ptgds	11381.668	0.468	1.169	0.110	4.254	2.10E-05	1.09E-03	ENSMUSG00000015090	NM_008963	19215
Atp10d	120.238	0.446	0.657	0.106	4.220	2.44E-05	1.26E-03	ENSMUSG00000046808	NM_153389	231287
Txnip	524.172	0.429	0.605	0.102	4.202	2.65E-05	1.35E-03	ENSMUSG00000038393	NM_001009935	56338
Ngfr	96.833	0.472	0.984	0.113	4.196	2.71E-05	1.38E-03	ENSMUSG00000000120	NM_033217	18053
Ubxn11	454.377	0.431	0.618	0.103	4.194	2.74E-05	1.38E-03	ENSMUSG00000012126	NM_026257	67586
Ttc39a	78.119	0.470	0.992	0.112	4.182	2.90E-05	1.46E-03	ENSMUSG00000028555	NM_001145948	230603
Aebp1	633.806	0.422	0.602	0.101	4.165	3.11E-05	1.56E-03	ENSMUSG00000020473	NM_001291857	11568
Wnk4	214.115	0.429	0.623	0.103	4.165	3.11E-05	1.56E-03	ENSMUSG00000035112	NM_175638	69847
Col13a1	44.192	0.457	1.172	0.110	4.161	3.17E-05	1.59E-03	ENSMUSG00000058806	NM_001304757	12817
Colec12	252.331	0.462	0.796	0.111	4.160	3.18E-05	1.59E-03	ENSMUSG00000036103	NM_130449	140792
Loxl1	144.988	0.467	0.875	0.112	4.158	3.21E-05	1.60E-03	ENSMUSG00000032334	NM_010729	16949
Pdgfd	157.065	0.461	0.790	0.111	4.142	3.44E-05	1.71E-03	ENSMUSG00000032006	NM_001357397	71785
Hist1h1e	29.223	0.394	1.568	0.095	4.131	3.61E-05	1.78E-03	ENSMUSG00000051627	NM_015787	50709
Bmp4	53.215	0.456	1.124	0.110	4.129	3.65E-05	1.79E-03	ENSMUSG00000021835	NM_001316360	12159
Batf3	21.527	0.434	1.338	0.105	4.125	3.71E-05	1.82E-03	ENSMUSG00000026630	NM_030060	381319
Atp7a	280.622	0.462	0.847	0.112	4.122	3.76E-05	1.84E-03	ENSMUSG00000033792	NM_001109757	11977
Maats1	83.865	0.453	0.739	0.110	4.119	3.81E-05	1.86E-03	ENSMUSG00000022805	NM_001081025	320214
Fmod	314.540	0.426	1.354	0.104	4.102	4.10E-05	1.98E-03	ENSMUSG00000041559	NM_021355	14264
Rnaset2a	96.075	0.459	0.824	0.112	4.099	4.15E-05	2.00E-03	ENSMUSG00000095687	NM_001083938	100037283
Bcar3	347.176	0.389	0.509	0.095	4.085	4.40E-05	2.12E-03	ENSMUSG00000028121	NM_001355264	29815
Prdm16	706.912	0.394	0.532	0.097	4.073	4.63E-05	2.22E-03	ENSMUSG00000039410	NM_001177995	70673
Ctsc	361.513	0.402	0.547	0.099	4.072	4.67E-05	2.24E-03	ENSMUSG00000030560	NM_001311790	13032
Patj	216.710	0.434	0.668	0.107	4.064	4.83E-05	2.30E-03	ENSMUSG00000061859	NM_001005784	12695
Sdpr	284.398	0.400	0.534	0.099	4.052	5.08E-05	2.41E-03	NA	NA	NA
Vcam1	857.373	0.408	0.560	0.101	4.053	5.06E-05	2.41E-03	ENSMUSG00000027962	NM_011693	22329
Igfbp7	412.695	0.422	0.620	0.104	4.047	5.18E-05	2.44E-03	ENSMUSG00000036256	NM_001159518	29817
Ggh	355.522	0.418	0.601	0.103	4.045	5.24E-05	2.46E-03	ENSMUSG00000073987	NM_010281	14590
Gulp1	123.799	0.454	0.917	0.113	4.035	5.47E-05	2.56E-03	ENSMUSG00000056870	NM_027506	70676
Igf2os	15.268	0.400	1.405	0.099	4.035	5.47E-05	2.56E-03	ENSMUSG00000086266	NR_002855	111975
Map3k15	91.524	0.453	0.838	0.112	4.032	5.53E-05	2.58E-03	ENSMUSG00000031303	NM_001163085	270672
Mvd	561.210	0.395	0.534	0.098	4.031	5.56E-05	2.59E-03	ENSMUSG00000006517	NM_138656	192156
Slc6a13	302.954	0.442	1.123	0.110	4.023	5.74E-05	2.67E-03	ENSMUSG00000030108	NM_144512	14412
Tmc6	238.289	0.399	0.547	0.099	4.022	5.76E-05	2.67E-03	ENSMUSG00000025572	NM_145439	217353
Cd55	193.061	0.425	0.638	0.106	4.003	6.25E-05	2.89E-03	ENSMUSG00000026399	NM_010016	13136
Lgals3	38.293	0.432	1.185	0.108	4.000	6.34E-05	2.93E-03	ENSMUSG00000050335	NM_001145953	16854
Clic3	59.722	0.443	1.070	0.111	3.995	6.46E-05	2.97E-03	ENSMUSG00000015093	NM_027085	69454
Cish	68.186	0.444	1.024	0.112	3.978	6.94E-05	3.16E-03	ENSMUSG00000032578	NM_001317354	12700
Nek8	123.927	0.423	0.638	0.107	3.972	7.12E-05	3.23E-03	ENSMUSG00000017405	NM_080849	140859
Hey2	130.941	0.445	0.808	0.112	3.970	7.18E-05	3.25E-03	ENSMUSG00000019789	NM_013904	15214
Cox7a1	32.049	0.423	1.237	0.107	3.963	7.41E-05	3.32E-03	ENSMUSG00000074218	NM_009944	12865
Itga10	119.723	0.439	0.726	0.111	3.963	7.41E-05	3.32E-03	ENSMUSG00000090210	NM_001081053	213119
Cyp1b1	138.908	0.446	0.919	0.113	3.959	7.53E-05	3.37E-03	ENSMUSG00000024087	NM_009994	13078
Etnk2	84.649	0.441	1.022	0.112	3.958	7.57E-05	3.38E-03	ENSMUSG00000070644	NM_175443	214253
Trappc6a	161.476	0.404	0.572	0.103	3.941	8.10E-05	3.61E-03	ENSMUSG00000002043	NM_001331181	67091
H2-Ab1	33.726	0.406	1.300	0.104	3.908	9.30E-05	4.09E-03	ENSMUSG00000073421	NM_207105	14961
Col4a6	56.147	0.434	1.026	0.111	3.905	9.41E-05	4.12E-03	ENSMUSG00000031273	NM_053185	94216
Ccdc60	50.526	0.439	0.938	0.112	3.902	9.53E-05	4.16E-03	ENSMUSG00000043913	NM_001360004	269693
Gm11992	63.534	0.425	0.696	0.109	3.886	1.02E-04	4.41E-03	ENSMUSG00000040978	NM_001037928	626870
Gjb2	230.479	0.437	0.924	0.112	3.885	1.02E-04	4.43E-03	ENSMUSG00000046352	NM_008125	14619
Cfap52	100.723	0.436	0.897	0.113	3.872	1.08E-04	4.64E-03	ENSMUSG00000020904	NM_027963	71860
Hist1h2be	186.963	0.427	0.715	0.111	3.865	1.11E-04	4.76E-03	ENSMUSG00000047246	NM_001177653	319179
Ptgis	55.409	0.435	0.916	0.113	3.864	1.11E-04	4.76E-03	ENSMUSG00000017969	NM_008968	19223
Ttc12	99.912	0.420	0.666	0.109	3.854	1.16E-04	4.93E-03	ENSMUSG00000040219	NM_172770	235330
Ccdc141	595.410	0.402	0.589	0.105	3.849	1.18E-04	4.97E-03	ENSMUSG00000044033	NM_001025576	545428
Fbln1	462.808	0.401	0.589	0.104	3.849	1.19E-04	4.97E-03	ENSMUSG00000006369	NM_001347088	14114
Cmtm8	39.517	0.429	0.975	0.112	3.832	1.27E-04	5.25E-03	ENSMUSG00000041012	NM_027294	70031
Mvp	329.927	0.392	0.560	0.102	3.830	1.28E-04	5.28E-03	ENSMUSG00000030681	NM_080638	78388
Cdc42bpg	354.001	0.400	0.592	0.105	3.825	1.31E-04	5.38E-03	ENSMUSG00000024769	NM_001033342	240505
Ccdc187	252.451	0.416	0.680	0.109	3.824	1.31E-04	5.39E-03	ENSMUSG00000048038	NM_177841	329366
Slc12a2	3269.324	0.380	0.521	0.100	3.822	1.33E-04	5.44E-03	ENSMUSG00000024597	NM_009194	20496
Col20a1	312.518	0.423	0.729	0.111	3.808	1.40E-04	5.71E-03	ENSMUSG00000016356	NM_028518	73368
Smim5	48.272	0.410	1.139	0.108	3.800	1.44E-04	5.85E-03	ENSMUSG00000048442	NM_183259	66528
Strip2	1249.850	0.398	0.593	0.105	3.789	1.51E-04	6.09E-03	ENSMUSG00000039629	NM_001037740	320609
Cfap69	587.889	0.380	0.527	0.100	3.788	1.52E-04	6.09E-03	ENSMUSG00000040473	NM_172447	207686
Pih1d2	69.074	0.422	0.766	0.112	3.768	1.65E-04	6.56E-03	ENSMUSG00000000167	NM_028300	72614
Capsl	84.735	0.423	0.915	0.112	3.765	1.67E-04	6.62E-03	ENSMUSG00000039676	NM_029341	75568
Nt5e	132.734	0.387	0.546	0.103	3.761	1.69E-04	6.71E-03	ENSMUSG00000032420	NM_011851	23959
Aldh1a2	189.240	0.392	1.206	0.105	3.731	1.90E-04	7.41E-03	ENSMUSG00000013584	NM_009022	19378
Ctf1	52.471	0.420	0.802	0.113	3.728	1.93E-04	7.49E-03	ENSMUSG00000042340	NM_001301282	13019
Edn3	161.324	0.412	0.710	0.111	3.718	2.01E-04	7.74E-03	ENSMUSG00000027524	NM_007903	13616
Efhc1	65.538	0.418	0.908	0.112	3.718	2.01E-04	7.74E-03	ENSMUSG00000041809	NM_027974	71877
Trim21	85.491	0.417	0.774	0.112	3.710	2.08E-04	7.95E-03	ENSMUSG00000030966	NM_001082552	20821
Dynlrb2	46.515	0.410	1.008	0.111	3.709	2.08E-04	7.96E-03	ENSMUSG00000034467	NM_029297	75465
Hmgb2	146.660	0.414	0.746	0.112	3.698	2.17E-04	8.23E-03	ENSMUSG00000054717	NM_008252	97165
Tmco4	114.291	0.402	0.650	0.109	3.688	2.26E-04	8.50E-03	ENSMUSG00000041143	NM_001305423	77056
Tram2	71.403	0.415	0.794	0.113	3.688	2.26E-04	8.50E-03	ENSMUSG00000041779	NM_177409	170829
Loxl3	169.959	0.382	0.559	0.104	3.667	2.46E-04	9.13E-03	ENSMUSG00000000693	NM_013586	16950
Car13	35.129	0.395	1.104	0.108	3.664	2.49E-04	9.22E-03	ENSMUSG00000027555	NM_024495	71934
Erich2	31.509	0.405	0.972	0.111	3.648	2.64E-04	9.72E-03	ENSMUSG00000075302	NM_025744	66748
Gm20632	72.693	0.408	0.869	0.112	3.631	2.82E-04	1.02E-02	NA	NA	NA
Plekha4	63.534	0.407	0.909	0.112	3.631	2.82E-04	1.02E-02	ENSMUSG00000040428	NM_148927	69217
Gnmt	30.041	0.392	1.059	0.109	3.610	3.07E-04	1.10E-02	ENSMUSG00000002769	NM_010321	14711
Cfap61	98.563	0.406	0.805	0.113	3.601	3.16E-04	1.13E-02	ENSMUSG00000037143	NM_175280	78774
Slc12a7	234.642	0.402	0.726	0.112	3.600	3.18E-04	1.13E-02	ENSMUSG00000017756	NM_001360694	20499
Saxo2	123.708	0.403	0.728	0.112	3.598	3.20E-04	1.14E-02	ENSMUSG00000038570	NM_177894	330577
Aim1	59.228	0.405	0.795	0.113	3.596	3.24E-04	1.14E-02	NA	NA	NA
Tax1bp3	110.920	0.398	0.679	0.111	3.587	3.35E-04	1.18E-02	ENSMUSG00000040158	NM_029564	76281
1700040L02Rik	47.457	0.401	0.850	0.113	3.564	3.65E-04	1.27E-02	NA	NA	NA
Ramp3	117.916	0.388	0.608	0.109	3.547	3.90E-04	1.34E-02	ENSMUSG00000041046	NM_019511	56089
Angpt2	40.298	0.387	1.019	0.109	3.545	3.93E-04	1.35E-02	ENSMUSG00000031465	NM_007426	11601
Pqlc3	93.657	0.386	0.617	0.109	3.540	4.00E-04	1.37E-02	ENSMUSG00000045679	NM_001161111	217430
Angptl4	77.066	0.395	0.870	0.112	3.525	4.23E-04	1.43E-02	ENSMUSG00000002289	NM_020581	57875
Parp3	103.225	0.390	0.666	0.111	3.510	4.49E-04	1.50E-02	ENSMUSG00000023249	NM_001311150	235587
Espl1	69.956	0.395	0.742	0.112	3.508	4.51E-04	1.50E-02	ENSMUSG00000058290	NM_001014976	105988
A730056A06Rik	62.374	-0.394	-0.814	0.112	-3.506	4.56E-04	1.51E-02	ENSMUSG00000097756	NR_040324	319783
Mrc1	130.973	0.387	0.647	0.110	3.504	4.58E-04	1.51E-02	ENSMUSG00000026712	NM_008625	17533
Nkx2-2	90.907	-0.383	-0.587	0.109	-3.497	4.71E-04	1.55E-02	ENSMUSG00000027434	NM_001077632	18088
Syne3	100.985	0.392	0.856	0.112	3.490	4.84E-04	1.58E-02	ENSMUSG00000054150	NM_001042699	212073
Mansc4	33.964	0.381	0.947	0.110	3.450	5.61E-04	1.79E-02	ENSMUSG00000072662	NM_001034903	545893
Ppp1r1b	1339.195	0.387	0.744	0.112	3.447	5.67E-04	1.80E-02	ENSMUSG00000061718	NM_001313970	19049
Lrriq1	113.756	0.385	0.712	0.112	3.438	5.86E-04	1.85E-02	ENSMUSG00000019892	NM_001163559	74978
Fgl2	71.794	0.386	0.810	0.113	3.434	5.95E-04	1.87E-02	ENSMUSG00000039899	NM_008013	14190
Tmem220	44.220	0.381	0.904	0.111	3.422	6.23E-04	1.94E-02	ENSMUSG00000050270	NM_001291042	338369
Rubcnl	46.997	0.382	0.725	0.113	3.397	6.81E-04	2.06E-02	ENSMUSG00000034959	NM_198642	271221

Appendix Table vi) List of differentially expressed genes found between conditions WTSH and WTEE.

KDEEvsKDSH	baseMean	log2FoldChar	lfcMLE	lfcSE	stat	pvalue	padj	ensembl	RefSeq	entrez
Krt8	75.437	1.175	2.379	0.113	10.409	2.26E-25	2.55E-21	ENSMUSG00000049382	NM_031170	16691
Sema3b	229.559	1.178	2.385	0.113	10.430	1.81E-25	2.55E-21	ENSMUSG00000057969	NM_001042779	20347
Gm44250	207.929	1.095	2.071	0.113	9.723	2.41E-22	1.51E-18	NA	NA	NA
Slc16a8	88.463	1.094	2.491	0.113	9.712	2.67E-22	1.51E-18	ENSMUSG00000032988	NM_020516	57274
Rdh5	181.945	1.034	2.158	0.113	9.152	5.60E-20	2.53E-16	ENSMUSG00000025350	NM_001358527	19682
Cdkn1c	98.173	1.023	2.198	0.113	9.064	1.25E-19	4.72E-16	ENSMUSG00000037664	NM_001161624	12577
Wfikkn2	112.790	0.976	2.082	0.113	8.645	5.38E-18	1.73E-14	ENSMUSG00000044177	NM_181819	278507
Oca2	58.110	0.873	3.168	0.105	8.353	6.66E-17	1.88E-13	ENSMUSG00000030450	NM_021879	18431
Tmprss11a	26.416	0.804	4.027	0.098	8.228	1.91E-16	4.79E-13	ENSMUSG00000072845	NM_001033233	194597
Dab2	439.269	0.794	1.055	0.098	8.120	4.64E-16	1.05E-12	ENSMUSG00000022150	NM_001008702	13132
Bmp6	323.017	0.863	1.302	0.107	8.079	6.56E-16	1.35E-12	ENSMUSG00000039004	NM_007556	12161
Tuba1c	94.880	0.891	2.309	0.111	8.031	9.68E-16	1.82E-12	ENSMUSG00000043091	NM_009448	22146
Slc37a2	200.659	0.870	1.381	0.109	7.977	1.50E-15	2.61E-12	ENSMUSG00000032122	NM_001145960	56857
Slc13a4	582.884	0.893	2.028	0.112	7.937	2.07E-15	3.34E-12	ENSMUSG00000029843	NM_172892	243755
Slc4a2	1464.395	0.794	1.098	0.101	7.853	4.06E-15	6.12E-12	ENSMUSG00000028962	NM_001253892	20535
Slc31a1	875.078	0.757	1.007	0.098	7.734	1.05E-14	1.47E-11	ENSMUSG00000066150	NM_175090	20529
Col8a2	344.931	0.827	2.550	0.108	7.676	1.65E-14	2.09E-11	ENSMUSG00000056174	NM_199473	329941
Drc7	423.200	0.834	2.472	0.109	7.674	1.67E-14	2.09E-11	ENSMUSG00000031786	NM_001042715	330830
Pcolce	344.499	0.846	1.965	0.112	7.535	4.89E-14	5.82E-11	ENSMUSG00000029718	NM_008788	18542
Ace	1219.013	0.805	2.563	0.107	7.522	5.37E-14	6.07E-11	ENSMUSG00000020681	NM_001281819	11421
Mdfic	178.725	0.833	1.560	0.113	7.397	1.39E-13	1.49E-10	ENSMUSG00000041390	NM_175088	16543
Large2	27.114	0.751	2.836	0.103	7.301	2.86E-13	2.93E-10	ENSMUSG00000040434	NM_001166633	228366
Perp	156.592	0.802	1.331	0.110	7.261	3.85E-13	3.78E-10	ENSMUSG00000019851	NM_022032	64058
Sulf1	817.121	0.790	2.266	0.109	7.237	4.57E-13	4.30E-10	ENSMUSG00000016918	NM_001198565	240725
Cndp1	32.332	0.795	2.214	0.110	7.231	4.80E-13	4.33E-10	ENSMUSG00000056162	NM_177450	338403
Cldn1	228.120	0.804	1.483	0.113	7.149	8.76E-13	7.32E-10	ENSMUSG00000022512	NM_016674	12737
Nid2	241.314	0.786	1.281	0.110	7.153	8.52E-13	7.32E-10	ENSMUSG00000021806	NM_008695	18074
Cab39l	1254.415	0.708	0.965	0.100	7.076	1.49E-12	1.20E-09	ENSMUSG00000021981	NM_001360591	69008
Cox8b	24.017	0.675	3.394	0.096	7.065	1.61E-12	1.25E-09	ENSMUSG00000025488	NM_007751	12869
Mpp7	145.959	0.759	1.177	0.108	7.013	2.33E-12	1.76E-09	ENSMUSG00000057440	NM_001081287	75739
Col17a1	35.252	0.710	2.866	0.102	6.937	4.00E-12	2.91E-09	ENSMUSG00000025064	NM_001290825	12821
Slc16a12	93.242	0.771	1.329	0.111	6.920	4.53E-12	3.19E-09	ENSMUSG00000009378	NM_172838	240638
Prlr	759.006	0.673	3.109	0.098	6.906	4.99E-12	3.41E-09	ENSMUSG00000005268	NM_001253781	19116
Pon3	118.599	0.771	1.766	0.112	6.869	6.46E-12	4.29E-09	ENSMUSG00000029759	NM_173006	269823
Cgnl1	870.494	0.769	1.435	0.113	6.834	8.26E-12	5.33E-09	ENSMUSG00000032232	NM_001304362	68178
Lbp	396.510	0.748	2.027	0.110	6.809	9.83E-12	6.16E-09	ENSMUSG00000016024	NM_008489	16803
Col4a4	89.384	0.766	1.666	0.113	6.793	1.10E-11	6.68E-09	ENSMUSG00000067158	NM_007735	12829
Bmp7	318.333	0.684	0.960	0.102	6.678	2.43E-11	1.44E-08	ENSMUSG00000008999	NM_007557	12162
Calml4	154.697	0.696	2.372	0.105	6.659	2.76E-11	1.56E-08	ENSMUSG00000032246	NM_001102468	75600
Col8a1	281.989	0.623	3.490	0.094	6.659	2.76E-11	1.56E-08	ENSMUSG00000068196	NM_007739	12837
Tbc1d2	215.296	0.705	1.045	0.106	6.646	3.01E-11	1.66E-08	ENSMUSG00000039813	NM_198664	381605
Itpripl1	93.921	0.732	1.372	0.113	6.498	8.16E-11	4.39E-08	ENSMUSG00000074825	NM_001163527	73338
Igf2	2948.532	0.721	1.775	0.111	6.472	9.70E-11	5.09E-08	ENSMUSG00000048583	NM_001122736	16002
Ucp2	711.441	0.704	1.117	0.109	6.463	1.03E-10	5.26E-08	ENSMUSG00000033685	NM_011671	22228
Ppp1r3b	75.293	0.729	1.492	0.113	6.457	1.07E-10	5.36E-08	ENSMUSG00000046794	NM_177741	244416
Crhr2	108.619	0.697	1.103	0.109	6.418	1.38E-10	6.76E-08	ENSMUSG00000003476	NM_001288618	12922
Slc2a12	365.550	0.657	2.345	0.103	6.360	2.02E-10	9.71E-08	ENSMUSG00000037490	NM_178934	353169
Eps8l2	112.209	0.714	1.435	0.113	6.320	2.62E-10	1.23E-07	ENSMUSG00000025504	NM_133191	98845
Trpv4	240.084	0.579	3.151	0.093	6.230	4.67E-10	2.15E-07	ENSMUSG00000014158	NM_022017	63873
Scara5	46.130	0.611	2.574	0.099	6.152	7.64E-10	3.45E-07	ENSMUSG00000022032	NM_001168318	71145
Acaa2	659.270	0.496	0.583	0.081	6.129	8.85E-10	3.92E-07	ENSMUSG00000036880	NM_177470	52538
Epn3	238.829	0.650	2.023	0.107	6.081	1.19E-09	5.19E-07	ENSMUSG00000010080	NM_001361558	71889
Frem1	315.198	0.676	1.553	0.112	6.027	1.67E-09	7.12E-07	ENSMUSG00000059049	NM_001198811	329872
Igfbp2	1260.259	0.665	1.721	0.111	6.013	1.82E-09	7.62E-07	ENSMUSG00000039323	NM_001310659	16008
Thbs1	120.007	0.678	1.345	0.113	6.005	1.91E-09	7.84E-07	ENSMUSG00000040152	NM_001313914	21825
Olfr1507	14.279	0.524	4.026	0.088	5.950	2.69E-09	1.08E-06	ENSMUSG00000059887	NM_001170918	57269
Msx1	334.223	0.659	1.581	0.112	5.890	3.87E-09	1.53E-06	ENSMUSG00000048450	NM_010835	17701
Kl	2389.264	0.576	2.550	0.098	5.871	4.33E-09	1.68E-06	ENSMUSG00000058488	NM_013823	16591
Shroom3	196.151	0.588	0.805	0.100	5.861	4.61E-09	1.76E-06	ENSMUSG00000029381	NM_001077595	27428
Col4a3	55.257	0.596	2.400	0.102	5.852	4.85E-09	1.83E-06	ENSMUSG00000079465	NM_007734	12828
Col1a2	439.292	0.634	0.999	0.109	5.833	5.46E-09	2.01E-06	ENSMUSG00000029661	NM_007743	12843
Foxj1	459.962	0.569	0.753	0.098	5.831	5.52E-09	2.01E-06	ENSMUSG00000034227	NM_008240	15223
Rab11fip1	128.761	0.618	0.917	0.106	5.821	5.86E-09	2.10E-06	ENSMUSG00000031488	NM_001080813	75767
Llgl2	64.737	0.653	1.386	0.113	5.789	7.07E-09	2.50E-06	ENSMUSG00000020782	NM_001252532	217325
Col9a3	914.223	0.627	1.794	0.109	5.766	8.11E-09	2.82E-06	ENSMUSG00000027570	NM_009936	12841
Lama5	643.356	0.600	0.872	0.105	5.720	1.07E-08	3.65E-06	ENSMUSG00000015647	NM_001081171	16776
Rbp1	376.294	0.614	0.937	0.107	5.716	1.09E-08	3.68E-06	ENSMUSG00000046402	NM_011254	19659
Tmem184a	19.988	0.533	2.864	0.093	5.702	1.19E-08	3.93E-06	ENSMUSG00000036687	NM_001161548	231832
Cdr2	380.481	0.626	1.020	0.110	5.689	1.28E-08	4.17E-06	ENSMUSG00000030878	NM_001354986	12585
Defb11	19.644	0.451	5.134	0.079	5.687	1.29E-08	4.17E-06	ENSMUSG00000045337	NM_139221	246081
Slc16a9	93.220	0.641	1.334	0.113	5.681	1.34E-08	4.25E-06	ENSMUSG00000037762	NM_025807	66859
Enpp2	26671.269	0.542	2.674	0.095	5.678	1.37E-08	4.28E-06	ENSMUSG00000022425	NM_001136077	18606
Sowahc	509.370	0.598	0.879	0.105	5.671	1.42E-08	4.39E-06	ENSMUSG00000098188	NM_172939	268301
Serinc2	307.146	0.599	0.889	0.106	5.646	1.64E-08	5.01E-06	ENSMUSG00000023232	NM_001253386	230779
Zfp185	190.395	0.636	1.211	0.113	5.640	1.70E-08	5.11E-06	ENSMUSG00000031351	NM_001109043	22673
Otx2os1	12.777	0.468	3.831	0.083	5.636	1.74E-08	5.18E-06	ENSMUSG00000098682	NR_029384	606497
Gm26684	13.453	0.533	2.669	0.095	5.616	1.95E-08	5.72E-06	NA	XR_001781621	102638507
Elovl7	769.509	0.567	0.781	0.101	5.608	2.05E-08	5.94E-06	ENSMUSG00000021696	NM_029001	74559
Rd3	45.288	0.610	1.624	0.111	5.519	3.40E-08	9.72E-06	ENSMUSG00000049353	NM_001177900	74023
Tns1	1749.212	0.461	0.549	0.083	5.516	3.47E-08	9.79E-06	ENSMUSG00000055322	NM_001289895	21961
Tc2n	23.814	0.523	2.554	0.095	5.510	3.59E-08	1.00E-05	ENSMUSG00000021187	NM_001082976	74413
Arhgef5	114.600	0.608	1.005	0.111	5.503	3.73E-08	1.01E-05	ENSMUSG00000033542	NM_133674	54324
Hspg2	591.547	0.597	0.928	0.108	5.504	3.71E-08	1.01E-05	ENSMUSG00000028763	NM_008305	15530
Iqub	108.074	0.612	1.041	0.111	5.501	3.77E-08	1.01E-05	ENSMUSG00000046192	NM_172535	214704
A2m	239.804	0.604	1.645	0.110	5.499	3.82E-08	1.01E-05	ENSMUSG00000030111	NM_175628	232345
Cpq	371.383	0.512	0.654	0.093	5.491	4.00E-08	1.05E-05	ENSMUSG00000039007	NM_018755	54381
Lepr	137.994	0.577	1.897	0.105	5.488	4.08E-08	1.06E-05	ENSMUSG00000057722	NM_001122899	16847
Ackr4	16.172	0.555	2.267	0.101	5.484	4.17E-08	1.07E-05	ENSMUSG00000079355	NM_145700	252837
Sult1c2	13.822	0.440	4.406	0.080	5.472	4.45E-08	1.13E-05	ENSMUSG00000023122	NM_026935	69083
Crb2	295.293	0.575	0.838	0.105	5.465	4.63E-08	1.16E-05	ENSMUSG00000035403	NM_001163566	241324
Glb1l2	56.302	0.617	1.257	0.113	5.461	4.72E-08	1.17E-05	ENSMUSG00000036395	NM_001310768	244757
Ccdc108	410.574	0.488	0.606	0.090	5.425	5.79E-08	1.42E-05	NA	NA	NA
Mycbpap	120.898	0.608	1.092	0.112	5.422	5.89E-08	1.43E-05	ENSMUSG00000039110	NM_170671	104601
Il17re	25.377	0.577	1.752	0.107	5.386	7.22E-08	1.73E-05	ENSMUSG00000043088	NM_001034029	57890
Abhd2	3923.077	0.454	0.545	0.085	5.358	8.44E-08	2.01E-05	ENSMUSG00000039202	NM_018811	54608
Tcn2	765.977	0.564	0.827	0.105	5.352	8.72E-08	2.05E-05	ENSMUSG00000020432	NM_001130458	21452
Krt18	131.178	0.469	3.123	0.088	5.334	9.63E-08	2.24E-05	ENSMUSG00000023043	NM_010664	16668
Fap	64.169	0.557	1.844	0.105	5.326	1.01E-07	2.29E-05	ENSMUSG00000000392	NM_007986	14089
Tgfbi	147.577	0.549	0.775	0.103	5.327	1.00E-07	2.29E-05	ENSMUSG00000035493	NM_009369	21810
Acacb	291.254	0.555	0.798	0.104	5.320	1.04E-07	2.34E-05	ENSMUSG00000042010	NM_133904	100705
Car14	306.094	0.557	0.811	0.105	5.313	1.08E-07	2.41E-05	ENSMUSG00000038526	NM_001355750	23831
Esrrb	73.760	0.593	1.100	0.113	5.266	1.39E-07	3.08E-05	ENSMUSG00000021255	NM_001159500	26380
Sod3	456.344	0.512	0.678	0.098	5.248	1.54E-07	3.37E-05	ENSMUSG00000072941	NM_011435	20657
Frrs1	87.285	0.588	1.068	0.112	5.231	1.69E-07	3.67E-05	ENSMUSG00000033386	NM_001113478	20321
Rbm47	86.837	0.441	3.216	0.084	5.229	1.71E-07	3.67E-05	ENSMUSG00000070780	NM_001127382	245945
Col18a1	236.575	0.584	1.034	0.112	5.220	1.79E-07	3.81E-05	ENSMUSG00000001435	NM_001109991	12822
Baiap2l1	68.018	0.545	1.835	0.104	5.216	1.83E-07	3.83E-05	ENSMUSG00000038859	NM_025833	66898
Cox6b2	84.392	0.567	0.891	0.109	5.216	1.82E-07	3.83E-05	ENSMUSG00000051811	NM_001289848	333182
Angptl2	179.391	0.537	1.884	0.103	5.211	1.88E-07	3.89E-05	ENSMUSG00000004105	NM_011923	26360
B4galt1	269.636	0.471	0.586	0.090	5.206	1.93E-07	3.95E-05	ENSMUSG00000028413	NM_022305	14595
Tmem98	423.445	0.469	0.584	0.090	5.202	1.97E-07	4.01E-05	ENSMUSG00000035413	NM_029537	103743
Vamp8	251.389	0.537	0.766	0.104	5.183	2.18E-07	4.39E-05	ENSMUSG00000050732	NM_016794	22320
1500015O10Rik	509.574	0.424	3.688	0.082	5.181	2.21E-07	4.42E-05	ENSMUSG00000026051	NM_024283	78896
Hfe	205.365	0.491	0.633	0.095	5.178	2.24E-07	4.44E-05	ENSMUSG00000006611	NM_001347493	15216
Abca4	421.496	0.456	3.027	0.088	5.169	2.35E-07	4.60E-05	ENSMUSG00000028125	NM_007378	11304
Ephx1	788.842	0.468	0.584	0.091	5.158	2.49E-07	4.81E-05	ENSMUSG00000038776	NM_001312918	13849
Six3os1	43.480	0.545	1.846	0.106	5.119	3.07E-07	5.82E-05	ENSMUSG00000093460	NR_015385	100043902
Tjp3	73.047	0.547	1.661	0.107	5.112	3.19E-07	6.01E-05	ENSMUSG00000034917	NM_001282095	27375

KDEEvsKDSH	baseMean	log2FoldChar	lfcMLE	lfcSE	stat	pvalue	padj	ensembl	RefSeq	entrez
Fzd4	536.373	0.540	0.813	0.107	5.059	4.20E-07	7.85E-05	ENSMUSG00000049791	NM_008055	14366
Cldn2	298.567	0.383	4.193	0.076	5.044	4.55E-07	8.35E-05	ENSMUSG00000047230	NM_016675	12738
Slc39a4	75.745	0.551	1.557	0.109	5.046	4.51E-07	8.35E-05	ENSMUSG00000063354	NM_028064	72027
Mrc2	263.876	0.529	0.771	0.105	5.036	4.77E-07	8.61E-05	ENSMUSG00000020695	NM_008626	17534
Slc28a3	25.836	0.457	2.628	0.091	5.037	4.74E-07	8.61E-05	ENSMUSG00000021553	NM_022317	114304
Serpinb1b	43.580	0.540	1.639	0.107	5.027	4.99E-07	8.93E-05	ENSMUSG00000051029	NM_173052	282663
Ctnnal1	745.912	0.419	0.500	0.084	4.998	5.79E-07	1.03E-04	ENSMUSG00000038816	NM_018761	54366
Trp73	174.356	0.536	0.821	0.108	4.975	6.53E-07	1.15E-04	ENSMUSG00000029026	NM_001126330	22062
Tbc1d9	3791.156	0.398	0.468	0.081	4.911	9.06E-07	1.59E-04	ENSMUSG00000031709	NM_001111304	71310
Cd59a	180.998	0.550	0.996	0.112	4.895	9.83E-07	1.69E-04	ENSMUSG00000032679	NM_001111060	12509
Tekt1	112.253	0.537	0.866	0.110	4.895	9.83E-07	1.69E-04	ENSMUSG00000020799	NM_001282006	21689
Galm	118.684	0.535	0.859	0.110	4.885	1.03E-06	1.76E-04	ENSMUSG00000035473	NM_176963	319625
Bcam	453.042	0.443	0.552	0.091	4.883	1.05E-06	1.78E-04	ENSMUSG00000002980	NM_020486	57278
Steap2	598.562	0.545	1.273	0.112	4.873	1.10E-06	1.85E-04	ENSMUSG00000015653	NM_001103156	74051
Sh3d19	1070.171	0.451	0.571	0.093	4.869	1.12E-06	1.87E-04	ENSMUSG00000028082	NM_001082414	27059
Pla2g5	73.668	0.432	2.433	0.089	4.836	1.32E-06	2.20E-04	ENSMUSG00000041193	NM_001122954	18784
Fhad1	254.951	0.487	0.667	0.101	4.828	1.38E-06	2.27E-04	ENSMUSG00000051435	NM_028429	329977
Trpm3	2956.294	0.544	1.101	0.113	4.819	1.45E-06	2.35E-04	ENSMUSG00000052387	NM_001035239	226025
Car13	35.129	0.523	1.386	0.110	4.766	1.88E-06	3.03E-04	ENSMUSG00000027555	NM_024495	71934
Acss3	60.377	0.532	1.249	0.112	4.764	1.90E-06	3.04E-04	ENSMUSG00000035948	NM_001142804	380660
Car12	1793.787	0.535	0.980	0.112	4.757	1.97E-06	3.13E-04	ENSMUSG00000032373	NM_001306148	76459
Sostdc1	343.841	0.406	2.946	0.085	4.751	2.03E-06	3.20E-04	ENSMUSG00000036169	NM_025312	66042
Pcolce2	230.890	0.531	0.926	0.112	4.748	2.05E-06	3.22E-04	ENSMUSG00000015354	NM_029620	76477
Sgms2	188.634	0.515	1.435	0.109	4.746	2.08E-06	3.23E-04	ENSMUSG00000050931	NM_028943	74442
Spint2	709.127	0.500	0.742	0.106	4.712	2.45E-06	3.74E-04	ENSMUSG00000074227	NM_001082548	20733
Tspo	113.188	0.531	0.977	0.113	4.713	2.44E-06	3.74E-04	ENSMUSG00000041736	NM_009775	12257
Hspb8	513.837	0.424	0.528	0.090	4.702	2.57E-06	3.87E-04	ENSMUSG00000041548	NM_030704	80888
Efemp2	330.716	0.420	0.519	0.089	4.694	2.68E-06	3.98E-04	ENSMUSG00000024909	NM_001164352	58859
Slc7a10	899.769	0.386	0.457	0.082	4.694	2.68E-06	3.98E-04	ENSMUSG00000030495	NM_017394	53896
Cdkn1a	232.164	0.526	0.929	0.112	4.689	2.75E-06	4.06E-04	ENSMUSG00000023067	NM_001111099	12575
Lgals3bp	630.262	0.491	0.718	0.105	4.671	2.99E-06	4.28E-04	ENSMUSG00000033880	NM_011150	19039
Plek2	17.027	0.392	2.646	0.084	4.668	3.04E-06	4.32E-04	ENSMUSG00000021118	NM_013738	27260
Fzd7	409.596	0.467	0.633	0.100	4.665	3.08E-06	4.35E-04	ENSMUSG00000041075	NM_008057	14369
F11r	268.290	0.466	0.639	0.101	4.636	3.55E-06	4.98E-04	ENSMUSG00000038235	NM_172647	16456
Ripk4	28.293	0.509	1.293	0.110	4.633	3.61E-06	5.03E-04	ENSMUSG00000005251	NM_023663	72388
Slc25a13	84.522	0.511	0.846	0.111	4.620	3.84E-06	5.29E-04	ENSMUSG00000015112	NM_001177572	50799
Vat1l	1396.026	0.519	1.090	0.113	4.604	4.15E-06	5.68E-04	ENSMUSG00000046844	NM_173016	270097
Fam47e	23.554	0.483	1.635	0.105	4.588	4.47E-06	6.06E-04	ENSMUSG00000057068	NM_001033478	384198
Sfrp5	36.610	0.431	2.329	0.094	4.588	4.49E-06	6.06E-04	ENSMUSG00000018822	NM_018780	54612
Rilp	53.646	0.510	1.169	0.112	4.549	5.38E-06	7.23E-04	ENSMUSG00000038195	NM_001029938	280408
Tinagl1	200.895	0.507	0.892	0.112	4.526	6.01E-06	8.03E-04	ENSMUSG00000028776	NM_001168333	94242
Emb	772.327	0.447	0.602	0.099	4.521	6.16E-06	8.19E-04	ENSMUSG00000021728	NM_010330	13723
4930511M06Rik	15.083	0.415	2.101	0.092	4.501	6.77E-06	8.93E-04	ENSMUSG00000086607	NR_015494	75084
Gm16551	27.090	-0.483	-1.544	0.107	-4.490	7.11E-06	9.33E-04	ENSMUSG00000066477	NR_045284	100503019
Gm28729	40.098	0.500	1.179	0.112	4.464	8.05E-06	1.05E-03	ENSMUSG00000099564	XM_006511607	102635744
Cdhr3	123.360	-0.489	-0.857	0.110	-4.462	8.11E-06	1.05E-03	ENSMUSG00000035860	NM_001024478	68764
Cldn3	22.863	0.452	1.781	0.102	4.442	8.93E-06	1.15E-03	ENSMUSG00000070473	NM_009902	12739
Cish	68.186	0.498	1.068	0.113	4.419	9.90E-06	1.26E-03	ENSMUSG00000032578	NM_001317354	12700
Tcaf2	38.076	0.475	1.406	0.108	4.414	1.01E-05	1.29E-03	ENSMUSG00000029851	NM_146174	232748
Gprc5c	165.947	0.460	0.663	0.105	4.405	1.06E-05	1.32E-03	ENSMUSG00000051043	NM_001110337	70355
Myo7a	967.199	0.382	0.463	0.087	4.396	1.10E-05	1.38E-03	ENSMUSG00000030761	NM_001256081	17921
Lrriq1	113.756	0.488	0.843	0.112	4.377	1.21E-05	1.47E-03	ENSMUSG00000019892	NM_001163559	74978
Frmpd2	95.356	-0.463	-0.728	0.106	-4.367	1.26E-05	1.53E-03	ENSMUSG00000108841	XM_017316244	268729
Col1a1	330.978	0.477	0.757	0.109	4.366	1.27E-05	1.53E-03	ENSMUSG00000001506	NM_007742	12842
Ezr	2320.611	0.391	0.484	0.090	4.348	1.37E-05	1.64E-03	ENSMUSG00000052397	NM_009510	22350
Serpinb1a	290.483	-0.432	-0.583	0.099	-4.344	1.40E-05	1.66E-03	ENSMUSG00000044734	NM_025429	66222
H2-Ab1	33.726	0.459	1.442	0.106	4.323	1.54E-05	1.80E-03	ENSMUSG00000073421	NM_207105	14961
Arhgap28	36.335	0.443	1.615	0.103	4.311	1.62E-05	1.86E-03	ENSMUSG00000024043	NM_001347410	268970
Ccdc170	72.665	0.484	0.878	0.112	4.312	1.62E-05	1.86E-03	ENSMUSG00000019767	NM_001195672	100504234
Mitf	304.206	0.416	0.544	0.097	4.309	1.64E-05	1.86E-03	ENSMUSG00000035158	NM_001113198	17342
Piezo1	244.670	0.471	0.748	0.109	4.310	1.63E-05	1.86E-03	ENSMUSG00000014444	NM_001037298	234839
Serpinh1	596.762	0.466	0.726	0.108	4.305	1.67E-05	1.89E-03	ENSMUSG00000070436	NM_001111043	12406
Atp7a	280.622	0.479	0.823	0.111	4.301	1.70E-05	1.91E-03	ENSMUSG00000033792	NM_001109757	11977
Acox2	20.737	0.408	1.962	0.095	4.298	1.72E-05	1.92E-03	ENSMUSG00000021751	NM_001161667	93732
Plscr2	53.061	0.484	0.909	0.113	4.295	1.74E-05	1.93E-03	ENSMUSG00000032372	NM_001195084	18828
Ltc4s	22.285	0.424	1.574	0.100	4.236	2.27E-05	2.46E-03	ENSMUSG00000020377	NM_001313968	17001
Tgfbr3	588.978	0.418	0.560	0.099	4.236	2.27E-05	2.46E-03	ENSMUSG00000029287	NM_011578	21814
BC067074	160.607	0.446	1.364	0.107	4.182	2.89E-05	3.03E-03	ENSMUSG00000021763	XR_001781056	408066
H2-Aa	45.885	0.453	1.285	0.108	4.185	2.85E-05	3.03E-03	ENSMUSG00000036594	NM_010378	14960
Gpr34	292.742	-0.411	-0.548	0.098	-4.182	2.89E-05	3.03E-03	ENSMUSG00000040229	NM_011823	23890
Rsph1	181.479	0.432	0.609	0.104	4.167	3.09E-05	3.22E-03	ENSMUSG00000024033	NM_025290	22092
Mmp2	116.305	0.443	0.664	0.107	4.154	3.27E-05	3.41E-03	ENSMUSG00000031740	NM_008610	17390
Tead2	71.727	0.467	0.861	0.112	4.150	3.32E-05	3.44E-03	ENSMUSG00000030796	NM_001285498	21677
Fam161a	162.500	0.434	0.624	0.105	4.145	3.40E-05	3.50E-03	ENSMUSG00000049811	NM_028672	73873
Plekhf1	87.635	0.447	1.228	0.108	4.137	3.51E-05	3.59E-03	ENSMUSG00000074170	NM_024413	72287
Myof	258.163	0.451	0.718	0.109	4.116	3.85E-05	3.92E-03	ENSMUSG00000048612	NM_001099634	226101
RP24-298N7.10	24.013	0.415	1.499	0.101	4.108	3.99E-05	4.02E-03	NA	NA	NA
Ccdc153	162.792	-0.418	-0.606	0.103	-4.058	4.95E-05	4.83E-03	ENSMUSG00000070306	NM_001081369	270150
Vwa5b1	206.459	0.437	0.669	0.108	4.052	5.09E-05	4.93E-03	ENSMUSG00000028753	NM_029401	75718
Nt5e	132.734	0.404	0.550	0.100	4.049	5.15E-05	4.97E-03	ENSMUSG00000032420	NM_011851	23959
Strip2	1249.850	0.413	0.576	0.102	4.041	5.32E-05	5.09E-03	ENSMUSG00000039629	NM_001037740	320609
Ltbp3	1149.699	0.387	0.502	0.096	4.028	5.63E-05	5.34E-03	ENSMUSG00000024940	NM_008520	16998
Hcar1	35.269	0.436	1.201	0.108	4.023	5.74E-05	5.42E-03	ENSMUSG00000049241	NM_175520	243270
Chdh	258.283	0.444	0.732	0.110	4.017	5.90E-05	5.55E-03	ENSMUSG00000015970	NM_001136240	218865
Fscn2	17.822	0.390	1.570	0.097	4.011	6.04E-05	5.66E-03	ENSMUSG00000025380	NM_172802	238021
Htr2c	1804.500	0.405	0.556	0.101	4.008	6.13E-05	5.68E-03	ENSMUSG00000041380	NM_008312	15560
Fbln1	462.808	0.406	0.559	0.101	4.003	6.25E-05	5.76E-03	ENSMUSG00000006369	NM_001347088	14114
Opalin	807.776	-0.385	-0.516	0.096	-3.999	6.35E-05	5.81E-03	ENSMUSG00000050121	NM_153520	226115
Fam46c	130.890	0.449	0.808	0.112	3.996	6.45E-05	5.87E-03	ENSMUSG00000044468	NM_001142952	74645
Sntb1	162.505	0.433	0.683	0.109	3.974	7.06E-05	6.41E-03	ENSMUSG00000060429	NM_016667	20649
Wdr63	70.732	0.443	1.075	0.112	3.971	7.16E-05	6.44E-03	ENSMUSG00000043020	NM_172864	242253
Prrg4	53.884	0.448	0.861	0.113	3.970	7.19E-05	6.45E-03	ENSMUSG00000027171	NM_178695	228413
Gm16314	47.764	0.444	0.789	0.112	3.962	7.42E-05	6.60E-03	NA	NA	NA
Rs1	20.572	0.399	1.504	0.101	3.956	7.64E-05	6.76E-03	ENSMUSG00000031293	NM_011302	20147
Gpx8	131.298	0.442	1.045	0.112	3.953	7.73E-05	6.82E-03	ENSMUSG00000021760	NM_027127	69590
St6galnac2	203.547	0.431	1.159	0.109	3.947	7.90E-05	6.94E-03	ENSMUSG00000057286	NM_009180	20446
Map3k15	91.524	0.435	0.756	0.112	3.887	1.01E-04	8.57E-03	ENSMUSG00000031303	NM_001163085	270672
Rbm20	126.148	0.397	0.552	0.102	3.886	1.02E-04	8.60E-03	ENSMUSG00000043639	NM_001170847	73713
Ston1	148.190	0.433	0.747	0.112	3.882	1.04E-04	8.71E-03	ENSMUSG00000033855	NM_029858	77057
Dnajb13	37.933	0.425	1.122	0.110	3.859	1.14E-04	9.48E-03	ENSMUSG00000030708	NM_153527	69387
Slc12a7	234.642	0.425	0.706	0.111	3.833	1.27E-04	1.05E-02	ENSMUSG00000017756	NM_001360694	20499
Pifo	37.820	0.423	1.070	0.111	3.828	1.29E-04	1.07E-02	ENSMUSG00000010136	NM_001200028	100503311
Scube3	270.121	0.424	0.714	0.111	3.819	1.34E-04	1.11E-02	ENSMUSG00000038677	NM_001004366	268935
1700007K13Rik	79.564	0.429	0.803	0.113	3.808	1.40E-04	1.15E-02	ENSMUSG00000026831	NM_027040	69327
4930556I23Rik	71.461	-0.424	-0.780	0.112	-3.783	1.55E-04	1.26E-02	NA	XR_373329	102637491
Slc6a20a	339.619	0.413	0.659	0.109	3.771	1.62E-04	1.31E-02	ENSMUSG00000036814	NM_139142	102680
Gm45396	184.371	0.400	0.599	0.106	3.761	1.69E-04	1.34E-02	NA	NA	NA
Lama1	120.686	0.403	0.612	0.107	3.755	1.74E-04	1.37E-02	ENSMUSG00000032796	NM_008480	16772
Alx4	53.032	0.400	1.187	0.107	3.740	1.84E-04	1.44E-02	ENSMUSG00000040310	NM_007442	11695
Dmrt3	30.546	0.413	1.049	0.111	3.741	1.83E-04	1.44E-02	ENSMUSG00000042372	NM_177360	240590
Col4a5	202.536	0.408	0.670	0.110	3.698	2.17E-04	1.64E-02	ENSMUSG00000031274	NM_001163155	12830
Erich5	59.166	-0.413	-0.912	0.112	-3.683	2.31E-04	1.72E-02	ENSMUSG00000044726	NM_173421	239368
Dnah11	141.399	0.402	0.638	0.109	3.679	2.34E-04	1.74E-02	ENSMUSG00000018581	NM_010060	13411
Gm11744	90.246	0.414	0.770	0.113	3.670	2.42E-04	1.79E-02	NA	NA	NA
Parp3	103.225	0.400	0.646	0.110	3.640	2.72E-04	1.95E-02	ENSMUSG00000023249	NM_001311150	235587
Ppp1r1b	1339.195	0.408	0.720	0.112	3.641	2.71E-04	1.95E-02	ENSMUSG00000061718	NM_001313970	19049
Mlf1	58.568	0.400	1.014	0.111	3.622	2.92E-04	2.07E-02	ENSMUSG00000048416	NM_001039543	17349
Mansc4	33.964	0.404	0.943	0.112	3.620	2.95E-04	2.07E-02	ENSMUSG00000072662	NM_001034903	545893

KDEEvsKDSH	baseMean	log2FoldChar	lfcMLE	lfcSE	stat	pvalue	padj	ensembl	RefSeq	entrez
B130034C11Rik	54.469	-0.407	-0.787	0.112	-3.620	2.94E-04	2.07E-02	ENSMUSG00000093606	NR_040375	414095
Alpl	287.055	0.397	0.646	0.110	3.614	3.02E-04	2.11E-02	ENSMUSG00000028766	NM_001287172	11647
Coch	251.360	0.404	0.776	0.113	3.580	3.44E-04	2.36E-02	ENSMUSG00000020953	NM_001198835	12810
Pdgfd	157.065	0.390	0.636	0.110	3.543	3.96E-04	2.62E-02	ENSMUSG00000032006	NM_001357397	71785
Fam46a	219.551	0.396	0.696	0.112	3.538	4.03E-04	2.64E-02	ENSMUSG00000032265	NM_001160378	212943
Fam89a	44.391	-0.398	-0.784	0.113	-3.539	4.02E-04	2.64E-02	ENSMUSG00000043068	NM_001081120	69627
Csrp2	136.075	0.392	0.694	0.112	3.502	4.62E-04	2.96E-02	ENSMUSG00000020186	NM_007792	13008
Angpt2	40.298	0.388	0.965	0.111	3.499	4.67E-04	2.98E-02	ENSMUSG00000031465	NM_007426	11601
Ogn	245.219	0.392	0.702	0.112	3.492	4.79E-04	3.03E-02	ENSMUSG00000021390	NM_008760	18295
Smad6	67.733	0.394	0.801	0.113	3.491	4.81E-04	3.03E-02	ENSMUSG00000036867	NM_008542	17130
Itga11	143.632	-0.385	-0.666	0.111	-3.474	5.12E-04	3.16E-02	ENSMUSG00000032243	NM_176922	319480
Myb	33.498	-0.388	-0.924	0.112	-3.474	5.12E-04	3.16E-02	ENSMUSG00000019982	NM_001198914	17863
Fcgr2b	116.188	0.389	0.706	0.112	3.463	5.35E-04	3.25E-02	ENSMUSG00000026656	NM_001077189	14130
Ccdc102a	60.925	0.388	0.818	0.113	3.441	5.80E-04	3.44E-02	ENSMUSG00000063605	NM_001033533	234582
Mb21d1	65.161	-0.382	-0.675	0.111	-3.441	5.79E-04	3.44E-02	ENSMUSG00000032344	NM_173386	214763
Sfrp1	204.738	0.388	0.766	0.113	3.434	5.94E-04	3.50E-02	ENSMUSG00000031548	NM_013834	20377
Ifitm1	36.212	0.385	0.868	0.112	3.429	6.06E-04	3.56E-02	ENSMUSG00000025491	NM_001112715	68713
Klf2	192.148	0.384	0.696	0.112	3.415	6.38E-04	3.67E-02	ENSMUSG00000055148	NM_008452	16598
Sptbn5	56.570	0.380	0.660	0.112	3.404	6.64E-04	3.78E-02	ENSMUSG00000074899	XM_006500537	640524
Stbd1	53.264	0.381	0.769	0.113	3.376	7.34E-04	4.02E-02	ENSMUSG00000047963	NM_175096	52331

Appendix Table vii) List of differentially expressed genes found between conditions KDEE and KDSH.

DEGs Common to both WT and KD animals after EE					
Krt8	Tmem98	Enpp2	Slc6a20a	Tjp3	Atp7a
Sema3b	Calml4	Kl	Col18a1	Six3os1	Map3k15
Slc16a8	Elovl7	Defb11	Gm26684	Car12	Cish
Gm44250	Acacb	Tcn2	B4galt1	Slc7a10	H2-Ab1
Rdh5	Itpripl1	Fhad1	Fzd4	Myo7a	Fbln1
Oca2	Cox8b	Msx1	Pifo	Scube3	Strip2
Dab2	Col4a3	Eps8l2	Rilp	Emb	Nt5e
Mdfic	Vamp8	Sult1c2	Htr2c	Tns1	Car13
Slc13a4	Il17re	Col9a3	A2m	Plscr2	Slc12a7
Slc37a2	Tbc1d2	Frem1	Gpx8	St6galnac2	Angpt2
Slc4a2	Cndp1	Rsph1	Sod3	Dnajb13	Parp3
Col17a1	Mycbpap	Gprc5c	Sostdc1	Dnah11	Mansc4
Tuba1c	Fap	Scara5	Otx2os1	Rs1	Ppp1r1b
Cab39l	Lbp	Krt18	Galm	Sntb1	Lrriq1
Perp	Ucp2	Pla2g5	Tcaf2	Ccdc170	
Wfikkn2	Igfbp2	Trpv4	Abhd2	Sfrp1	
Slc31a1	Efemp2	Cldn1	Fam47e	Thbs1	
Crhr2	Slc16a12	Llgl2	Sh3d19	Tinagl1	
Pon3	Cgnl1	Wdr63	Cldn2	Bcam	
Col4a4	Rd3	Abca4	Rbm47	Esrrb	
Col8a2	Prlr	Tgfbi	Myof	H2-Aa	
Drc7	Zfp185	Arhgef5	Acss3	Mrc2	
Large2	Glb1l2	Car14	4930511M06	Dmrt3	
Cdkn1c	Gm45396	Tmem184a	Ltbp3	Acox2	
Ppp1r3b	Ctnnal1	1500015O10	Slc28a3	BC067074	
Bmp6	Pcolce2	Slc39a4	Gm28729	Tgfbr3	
Ace	Hfe	Lama5	F11r	Mmp2	
Tmprss11a	Slc16a9	Olfr1507	Piezo1	Slc25a13	
Nid2	Cdr2	Vat1l	Mitf	Hspg2	
Ccdc108	Cox6b2	Lepr	Prrg4	Col4a5	
Epn3	Mpp7	Hspb8	Foxj1	Csrp2	
Pcolce	Rab11fip1	Sowahc	Col1a2	Ogn	
Serpinb1b	Vwa5b1	Frrs1	Trpm3	Sgms2	
Sulf1	Bmp7	Mlf1	Ackr4	Tspo	
Acaa2	Fam161a	Crb2	Gm11744	Ripk4	
Cd59a	Spint2	Steap2	Angptl2	Col1a1	
Rbp1	Baiap2l1	Tc2n	Lgals3bp	Serinc2	
Col8a1	Iqub	Tbc1d9	Fam46c	Trp73	
Igf2	Cpq	Arhgap28	Tekt1	Coch	
Ephx1	Slc2a12	Ezr	Sfrp5	Pdgfd	

Appendix Table viii) List of differentially expressed genes common to both genotypes following exposure to enrichment.

DEGs Unique to WT animals after EE						
Aox1	Xirp1	Lyz2	Ifi27	Cgn	Tmc6	Erich2
Slc38a3	Paqr5	Kif9	RP24-298N7.11	Spag8	Cd55	Gm20632
Fxyd1	2410004P03Rik	Tuft1	Robo3	Neat1	Lgals3	Plekha4
Tcea3	Fkbp9	Catip	Emilin1	Crb3	Clic3	Gnmt
E230013L22Rik	4833427G06Rik	Ppfibp2	Cast	Fbxo36	Nek8	Cfap61
Hist1h1c	Mxra8	BC021767	Gm16150	Capn6	Hey2	Saxo2
Nqo1	Sema3f	Aph1c	Chia1	Cped1	Cox7a1	Aim1
Npc2	Agtrap	Lpin3	Nek5	Plekhg2	Itga10	Tax1bp3
Gstm2	Cd63	Cfap44	Fbn1	Cfh	Cyp1b1	1700040L02Rik
H2-Eb1	Mgp	Slc12a4	Cfap70	Cp	Etnk2	Ramp3
Cd82	Gm853	Prkcq	Slc16a4	Sdc1	Trappc6a	Pqlc3
Stra6	Ccdc114	Ttc25	Dnaaf3	Ptgds	Col4a6	Angptl4
Arsg	Hbb-bs	Islr	Nudt7	Atp10d	Ccdc60	Espl1
Spag16	Rrh	Aldh2	Loxl4	Txnip	Gm11992	Mrc1
Tmem27	Jhy	Plcd1	Nek11	Ngfr	Gjb2	Syne3
Zscan10	Tor4a	Slc19a1	BC034090	Ubxn11	Cfap52	Fgl2
Cd74	Creb3l1	Lgals1	Adh1	Ttc39a	Hist1h2be	Tmem220
Hemk1	Slco1c1	Slc26a7	Gas2l2	Aebp1	Ptgis	Rubcnl
Prelp	Trip10	Dock6	Ttc21a	Wnk4	Ttc12	Neurod1
Prr32	D630024D03Rik	Glb1l	Aass	Col13a1	Ccdc141	A730056A06Rik
Antxr1	Klhdc8b	Ttll6	Arhgef16	Colec12	Cmtm8	Nkx2-2
Stk39	Dnali1	Pafah2	Col3a1	Loxl1	Mvp	
Klhdc7a	Crtap	Sgk3	Cpn1	Hist1h1e	Cdc42bpg	
Cpt1a	Dlec1	Plin3	Pcp4l1	Bmp4	Ccdc187	
Lrrc23	Pltp	Spata6	Rsph4a	Batf3	Slc12a2	
Ctsd	Hspb6	Il17rc	Gstt2	Maats1	Col20a1	
Cfap126	Phldb2	Lum	Wdr78	Fmod	Smim5	
Inmt	Cfap43	Fbln5	Bst2	Rnaset2a	Cfap69	
Myo5c	Cpt2	Hbb-bt	Tep1	Bcar3	Pih1d2	
Acad8	Sept10	Nxn	Nt5dc1	Prdm16	Capsl	
Dnaic2	Naga	Serping1	Loxl2	Ctsc	Aldh1a2	
Tor3a	Ccdc113	Cyb561	Cep41	Patj	Ctf1	
Fam189a2	Slc16a6	Rom1	Cdc14b	Sdpr	Edn3	
Cutal	Hmgcs2	Bdh2	Phactr2	Vcam1	Efhc1	
Kcnj13	Iqgap1	Hyal3	Dnah6	Igfbp7	Trim21	
Otx2	Agbl2	Aldh3b1	Spata18	Ggh	Dynlrb2	
Tmem86a	Gm29538	Cfap206	Rsph9	Gulp1	Hmgb2	
Folr1	Tmem237	Hba-a2	Ubxn10	Igf2os	Tmco4	
Bsg	Pdpn	Dpp7	Slc22a18	Mvd	Tram2	
Slc22a8	Slc1a5	Hist1h2bc	Slc29a4	Slc6a13	Loxl3	

Appendix Table ix) List of differentially expressed genes common unique only to WT genotype following exposure to enrichment.

DEGs Unique to MSK1 KD animals after EE				
Shroom3	Hcar1	Fam46a	Frmpd2	Myb
Cdkn1a	Chdh	Smad6	Serpinb1a	Mb21d1
Plek2	Fscn2	Fcgr2b	Gpr34	
Fzd7	Gm16314	Ccdc102a	Ccdc153	
Cldn3	Rbm20	Ifitm1	Opalin	
Serpinh1	Ston1	Klf2	4930556I23Rik	
Ltc4s	1700007K13Rik	Sptbn5	Erich5	
Tead2	Lama1	Stbd1	B130034C11Rik	
Plekhf1	Alx4	Gm16551	Fam89a	
RP24-298N7.10	Alpl	Cdhr3	Itga11	

Appendix Table x) List of genes differentially expressed in only MSK1 kinase-dead animals following exposure to enrichment.

	GO.ID	Term	Annotated	Significant	Expected	Rank in fish.class	fish.class	Benjamini.Fish.Class
1	GO:0007155	cell adhesion	1107	43	13.46	1	7.30E-12	9.26E-09
2	GO:0022610	biological adhesion	1117	43	13.59	2	9.80E-12	9.26E-09
3	GO:0043062	extracellular structure organization	244	17	2.97	3	7.70E-09	4.85E-06
4	GO:0030198	extracellular matrix organization	204	15	2.48	4	3.00E-08	1.42E-05
5	GO:0007167	enzyme linked receptor protein signaling pathway	789	29	9.6	5	9.90E-08	3.74E-05
6	GO:0042221	response to chemical	3132	69	38.09	6	1.60E-07	5.04E-05
7	GO:0072358	cardiovascular system development	673	25	8.19	7	6.80E-07	1.70E-04
8	GO:0090092	regulation of transmembrane receptor protein serine/threonine kinase signaling pathway	194	13	2.36	8	7.40E-07	1.70E-04
9	GO:0001568	blood vessel development	633	24	7.7	9	8.10E-07	1.70E-04
10	GO:0048646	anatomical structure formation involved in morphogenesis	991	31	12.05	10	1.20E-06	2.06E-04
11	GO:0071363	cellular response to growth factor stimulus	513	21	6.24	11	1.20E-06	2.06E-04
12	GO:0070848	response to growth factor	523	21	6.36	12	1.70E-06	2.43E-04
13	GO:0001944	vasculature development	661	24	8.04	13	1.70E-06	2.43E-04
14	GO:0009653	anatomical structure morphogenesis	2352	54	28.61	14	1.80E-06	2.43E-04
15	GO:0007178	transmembrane receptor protein serine/threonine kinase signaling pathway	289	15	3.52	15	2.60E-06	3.28E-04
16	GO:0090100	positive regulation of transmembrane receptor protein serine/threonine kinase signaling pathway	97	9	1.18	16	2.80E-06	3.31E-04
17	GO:0072359	circulatory system development	984	30	11.97	17	3.00E-06	3.34E-04
18	GO:0015893	drug transport	166	11	2.02	18	6.00E-06	6.12E-04
19	GO:0030155	regulation of cell adhesion	570	21	6.93	19	6.40E-06	6.12E-04
20	GO:0090287	regulation of cellular response to growth factor stimulus	236	13	2.87	20	6.50E-06	6.12E-04
21	GO:0007162	negative regulation of cell adhesion	237	13	2.88	21	6.80E-06	6.12E-04
22	GO:0009887	animal organ morphogenesis	872	27	10.61	22	7.50E-06	6.44E-04
23	GO:0030509	BMP signaling pathway	141	10	1.71	23	8.80E-06	7.09E-04
24	GO:0060349	bone morphogenesis	85	8	1.03	24	9.00E-06	7.09E-04
25	GO:0048513	animal organ development	2775	58	33.75	25	1.30E-05	9.10E-04
26	GO:0071772	response to BMP	148	10	1.8	26	1.30E-05	9.10E-04
27	GO:0071773	cellular response to BMP stimulus	148	10	1.8	27	1.30E-05	9.10E-04
28	GO:0034755	iron ion transmembrane transport	13	4	0.16	28	1.40E-05	9.12E-04
29	GO:0010033	response to organic substance	2324	51	28.27	29	1.40E-05	9.12E-04
30	GO:0006820	anion transport	464	18	5.64	30	1.50E-05	9.45E-04
31	GO:0035239	tube morphogenesis	804	25	9.78	31	1.60E-05	9.75E-04
32	GO:0035295	tube development	972	28	11.82	32	1.90E-05	1.11E-03
33	GO:0060669	embryonic placenta morphogenesis	28	5	0.34	33	2.00E-05	1.11E-03
34	GO:0051216	cartilage development	155	10	1.89	34	2.00E-05	1.11E-03
35	GO:0048705	skeletal system morphogenesis	196	11	2.38	35	2.90E-05	1.57E-03
36	GO:0010817	regulation of hormone levels	443	17	5.39	36	3.10E-05	1.58E-03
37	GO:0010812	negative regulation of cell-substrate adhesion	50	6	0.61	37	3.10E-05	1.58E-03
38	GO:0051179	localization	5086	89	61.86	38	3.50E-05	1.74E-03
39	GO:0003006	developmental process involved in reproduction	590	20	7.18	39	3.60E-05	1.74E-03
40	GO:0043506	regulation of JUN kinase activity	76	7	0.92	40	3.80E-05	1.80E-03
41	GO:0043408	regulation of MAPK cascade	646	21	7.86	41	4.20E-05	1.93E-03
42	GO:0071495	cellular response to endogenous stimulus	1017	28	12.37	42	4.30E-05	1.93E-03
43	GO:0001501	skeletal system development	411	16	5	43	4.40E-05	1.93E-03
44	GO:0070887	cellular response to chemical stimulus	2299	49	27.96	44	4.70E-05	2.02E-03
45	GO:0051674	localization of cell	1314	33	15.98	45	5.20E-05	2.13E-03
46	GO:0048870	cell motility	1314	33	15.98	46	5.20E-05	2.13E-03
47	GO:0000041	transition metal ion transport	80	7	0.97	47	5.30E-05	2.13E-03
48	GO:0031589	cell-substrate adhesion	289	13	3.52	48	5.50E-05	2.17E-03
49	GO:0032835	glomerulus development	56	6	0.68	49	5.90E-05	2.26E-03
50	GO:0090031	positive regulation of steroid hormone biosynthetic process	7	3	0.09	50	6.00E-05	2.26E-03
51	GO:0009719	response to endogenous stimulus	1151	30	14	51	6.10E-05	2.26E-03
52	GO:0050896	response to stimulus	6556	107	79.74	52	6.40E-05	2.28E-03

	GO.ID	Term	Annotated	Significant	Expected	Rank in fish.class	fish.class	Benjamini.Fish.Class
53	GO:0040011	locomotion	1508	36	18.34	53	6.40E-05	2.28E-03
54	GO:0061448	connective tissue development	216	11	2.63	54	6.90E-05	2.41E-03
55	GO:0071310	cellular response to organic substance	1885	42	22.93	55	7.00E-05	2.41E-03
56	GO:0030510	regulation of BMP signaling pathway	84	7	1.02	56	7.30E-05	2.46E-03
57	GO:0098656	anion transmembrane transport	182	10	2.21	57	7.90E-05	2.62E-03
58	GO:0015711	organic anion transport	344	14	4.18	58	8.40E-05	2.74E-03
59	GO:0001655	urogenital system development	302	13	3.67	59	8.60E-05	2.75E-03
60	GO:0015677	copper ion import	8	3	0.1	60	9.50E-05	2.99E-03
61	GO:0060429	epithelium development	959	26	11.66	61	1.10E-04	3.35E-03
62	GO:0042476	odontogenesis	90	7	1.09	62	1.10E-04	3.35E-03
63	GO:0043405	regulation of MAP kinase activity	271	12	3.3	63	1.20E-04	3.54E-03
64	GO:0009888	tissue development	1558	36	18.95	64	1.20E-04	3.54E-03
65	GO:0048514	blood vessel morphogenesis	547	18	6.65	65	1.30E-04	3.58E-03
66	GO:0032872	regulation of stress-activated MAPK cascade	194	10	2.36	66	1.30E-04	3.58E-03
67	GO:0048771	tissue remodeling	158	9	1.92	67	1.40E-04	3.58E-03
68	GO:0015718	monocarboxylic acid transport	124	8	1.51	68	1.40E-04	3.58E-03
69	GO:0016477	cell migration	1205	30	14.66	69	1.40E-04	3.58E-03
70	GO:0001525	angiogenesis	453	16	5.51	70	1.40E-04	3.58E-03
71	GO:0051270	regulation of cellular component movement	865	24	10.52	71	1.40E-04	3.58E-03
72	GO:0000165	MAPK cascade	704	21	8.56	72	1.40E-04	3.58E-03
73	GO:0070302	regulation of stress-activated protein kinase signaling cascade	195	10	2.37	73	1.40E-04	3.58E-03
74	GO:0032836	glomerular basement membrane development	9	3	0.11	74	1.40E-04	3.58E-03
75	GO:0001892	embryonic placenta development	95	7	1.16	75	1.60E-04	4.03E-03
76	GO:0007166	cell surface receptor signaling pathway	2089	44	25.41	76	1.70E-04	4.23E-03
77	GO:0023014	signal transduction by protein phosphorylation	718	21	8.73	77	1.80E-04	4.42E-03
78	GO:0042475	odontogenesis of dentin-containing tooth	69	6	0.84	78	1.90E-04	4.60E-03
79	GO:0038063	collagen-activated tyrosine kinase receptor signaling pathway	10	3	0.12	79	2.00E-04	4.73E-03
80	GO:0002921	negative regulation of humoral immune response	10	3	0.12	80	2.00E-04	4.73E-03
81	GO:0001822	kidney development	245	11	2.98	81	2.10E-04	4.90E-03
82	GO:0060343	trabecula formation	25	4	0.3	82	2.20E-04	5.07E-03
83	GO:0030850	prostate gland development	46	5	0.56	83	2.30E-04	5.24E-03
84	GO:2000145	regulation of cell motility	786	22	9.56	84	2.40E-04	5.34E-03
85	GO:0046942	carboxylic acid transport	249	11	3.03	85	2.40E-04	5.34E-03
86	GO:0015849	organic acid transport	250	11	3.04	86	2.50E-04	5.49E-03
87	GO:0048608	reproductive structure development	384	14	4.67	87	2.60E-04	5.65E-03
88	GO:0060346	bone trabecula formation	11	3	0.13	88	2.70E-04	5.80E-03
89	GO:0065008	regulation of biological quality	3225	60	39.23	89	2.80E-04	5.82E-03
90	GO:1901343	negative regulation of vasculature development	104	7	1.26	90	2.80E-04	5.82E-03
91	GO:0060348	bone development	174	9	2.12	91	2.80E-04	5.82E-03
92	GO:0061458	reproductive system development	387	14	4.71	92	2.90E-04	5.96E-03
93	GO:0006811	ion transport	1321	31	16.07	93	3.00E-04	6.10E-03
94	GO:0040012	regulation of locomotion	858	23	10.44	94	3.20E-04	6.43E-03
95	GO:0030334	regulation of cell migration	752	21	9.15	95	3.40E-04	6.48E-03
96	GO:0061971	replacement bone morphogenesis	50	5	0.61	96	3.40E-04	6.48E-03
97	GO:0060350	endochondral bone morphogenesis	50	5	0.61	97	3.40E-04	6.48E-03
98	GO:0060351	cartilage development involved in endochondral bone morphogenesis	28	4	0.34	98	3.50E-04	6.48E-03
99	GO:0046879	hormone secretion	303	12	3.69	99	3.50E-04	6.48E-03
100	GO:0046916	cellular transition metal ion homeostasis	77	6	0.94	100	3.50E-04	6.48E-03
101	GO:0055076	transition metal ion homeostasis	108	7	1.31	101	3.50E-04	6.48E-03
102	GO:0042325	regulation of phosphorylation	1333	31	16.21	102	3.50E-04	6.48E-03
103	GO:0038065	collagen-activated signaling pathway	12	3	0.15	103	3.60E-04	6.48E-03
104	GO:0043508	negative regulation of JUN kinase activity	12	3	0.15	104	3.60E-04	6.48E-03

	GO.ID	Term	Annotated	Significant	Expected	Rank in fish.class	fish.class	Benjamini.Fish.Class
105	GO:1902337	regulation of apoptotic process involved in morphogenesis	12	3	0.15	105	3.60E-04	6.48E-03
106	GO:0051403	stress-activated MAPK cascade	220	10	2.68	106	3.70E-04	6.54E-03
107	GO:0010717	regulation of epithelial to mesenchymal transition	78	6	0.95	107	3.70E-04	6.54E-03
108	GO:0061383	trabecula morphogenesis	51	5	0.62	108	3.80E-04	6.65E-03
109	GO:0060740	prostate gland epithelium morphogenesis	29	4	0.35	109	4.00E-04	6.82E-03
110	GO:0060512	prostate gland morphogenesis	29	4	0.35	110	4.00E-04	6.82E-03
111	GO:0044092	negative regulation of molecular function	876	23	10.65	111	4.20E-04	6.82E-03
112	GO:0009914	hormone transport	310	12	3.77	112	4.30E-04	6.82E-03
113	GO:0022414	reproductive process	1109	27	13.49	113	4.40E-04	6.82E-03
114	GO:2000040	regulation of planar cell polarity pathway involved in axis elongation	3	2	0.04	114	4.40E-04	6.82E-03
115	GO:2000041	negative regulation of planar cell polarity pathway involved in axis elongation	3	2	0.04	115	4.40E-04	6.82E-03
116	GO:2000860	positive regulation of aldosterone secretion	3	2	0.04	116	4.40E-04	6.82E-03
117	GO:2000857	positive regulation of mineralocorticoid secretion	3	2	0.04	117	4.40E-04	6.82E-03
118	GO:0015679	plasma membrane copper ion transport	3	2	0.04	118	4.40E-04	6.82E-03
119	GO:0032346	positive regulation of aldosterone metabolic process	3	2	0.04	119	4.40E-04	6.82E-03
120	GO:0032349	positive regulation of aldosterone biosynthetic process	3	2	0.04	120	4.40E-04	6.82E-03
121	GO:0072001	renal system development	267	11	3.25	121	4.40E-04	6.82E-03
122	GO:0000003	reproduction	1110	27	13.5	122	4.40E-04	6.82E-03
123	GO:2000095	regulation of Wnt signaling pathway, planar cell polarity pathway	13	3	0.16	123	4.60E-04	7.01E-03
124	GO:1904748	regulation of apoptotic process involved in development	13	3	0.16	124	4.60E-04	7.01E-03
125	GO:0060986	endocrine hormone secretion	54	5	0.66	125	4.90E-04	7.41E-03
126	GO:0055085	transmembrane transport	1120	27	13.62	126	5.10E-04	7.65E-03
127	GO:0006826	iron ion transport	31	4	0.38	127	5.20E-04	7.68E-03
128	GO:0048762	mesenchymal cell differentiation	189	9	2.3	128	5.20E-04	7.68E-03
129	GO:0032502	developmental process	5147	85	62.6	129	5.30E-04	7.77E-03
130	GO:0060389	pathway-restricted SMAD protein phosphorylation	55	5	0.67	130	5.40E-04	7.79E-03
131	GO:0048869	cellular developmental process	3665	65	44.58	131	5.40E-04	7.79E-03
132	GO:0043410	positive regulation of MAPK cascade	463	15	5.63	132	5.60E-04	7.96E-03
133	GO:0022603	regulation of anatomical structure morphogenesis	951	24	11.57	133	5.60E-04	7.96E-03
134	GO:0007601	visual perception	117	7	1.42	134	5.70E-04	8.02E-03
135	GO:0042327	positive regulation of phosphorylation	896	23	10.9	135	5.80E-04	8.02E-03
136	GO:0002577	regulation of antigen processing and presentation	14	3	0.17	136	5.80E-04	8.02E-03
137	GO:1903825	organic acid transmembrane transport	85	6	1.03	137	5.90E-04	8.02E-03
138	GO:0034446	substrate adhesion-dependent cell spreading	85	6	1.03	138	5.90E-04	8.02E-03
139	GO:1905039	carboxylic acid transmembrane transport	85	6	1.03	139	5.90E-04	8.02E-03
140	GO:0060485	mesenchyme development	234	10	2.85	140	6.00E-04	8.04E-03
141	GO:0007169	transmembrane receptor protein tyrosine kinase signaling pathway	517	16	6.29	141	6.00E-04	8.04E-03
142	GO:0050793	regulation of developmental process	2285	45	27.79	142	6.20E-04	8.25E-03
143	GO:0046328	regulation of JNK cascade	157	8	1.91	143	6.80E-04	8.99E-03
144	GO:0001837	epithelial to mesenchymal transition	121	7	1.47	144	7.00E-04	9.06E-03
145	GO:0050953	sensory perception of light stimulus	121	7	1.47	145	7.00E-04	9.06E-03
146	GO:0090288	negative regulation of cellular response to growth factor stimulus	121	7	1.47	146	7.00E-04	9.06E-03
147	GO:0050886	endocrine process	88	6	1.07	147	7.10E-04	9.07E-03
148	GO:0048856	anatomical structure development	4812	80	58.53	148	7.20E-04	9.07E-03
149	GO:0046886	positive regulation of hormone biosynthetic process	15	3	0.18	149	7.20E-04	9.07E-03
150	GO:0061430	bone trabecula morphogenesis	15	3	0.18	150	7.20E-04	9.07E-03
151	GO:0071702	organic substance transport	2235	44	27.18	151	7.30E-04	9.14E-03
152	GO:0030513	positive regulation of BMP signaling pathway	34	4	0.41	152	7.40E-04	9.20E-03

Appendix Table xi) List of GOTerms significantly enriched within differentially expressed genes common to both genotypes following exposure to enrichment.

	GO.ID	Term	Annotated	Significant	Expected	Rank in fish.class	fish.class	Benjamini.Fish.Class
1	GO:0043062	extracellular structure organization	244	18	3.56	1	1.90E-08	3.59E-05
2	GO:0030198	extracellular matrix organization	204	16	2.97	2	5.20E-08	4.79E-05
3	GO:0001578	microtubule bundle formation	90	11	1.31	3	7.60E-08	4.79E-05
4	GO:0044782	cilium organization	303	18	4.42	4	5.10E-07	2.41E-04
5	GO:0003341	cilium movement	70	9	1.02	5	7.70E-07	2.91E-04
6	GO:0018057	peptidyl-lysine oxidation	3	3	0.04	6	3.10E-06	8.37E-04
7	GO:0035082	axoneme assembly	62	8	0.9	7	3.10E-06	8.37E-04
8	GO:0060271	cilium assembly	282	16	4.11	8	4.00E-06	9.45E-04
9	GO:0006820	anion transport	464	20	6.76	9	1.60E-05	3.36E-03
10	GO:0030199	collagen fibril organization	45	6	0.66	10	4.60E-05	8.69E-03

xii) List of significantly enriched GOTerms within genes differentially expressed in only wildtype animals following exposure to enrichment.

Appended published research papers

1) The work titled: “The Kinase Function of MSK1 Regulates BDNF Signaling to CREB and Basal Synaptic Transmission, But Is Not Required for Hippocampal Long-Term Potentiation or Spatial Memory” by Daumas et al. (2017) is included below.

eNeuro

New Research

Cognition and Behavior

The Kinase Function of MSK1 Regulates BDNF Signaling to CREB and Basal Synaptic Transmission, But Is Not Required for Hippocampal Long-Term Potentiation or Spatial Memory

Stephanie Daumas,[1,×] Christopher J. Hunter,[2,×] Rajen B. Mistry,[3] Lorenzo Morè,[3,×] Lucia Privitera,[3,×] Daniel D. Cooper,[3] Kathleen M. Reyskens,[4] Harry T. Flynn,[3] Richard G. M. Morris,[1] J. Simon C. Arthur,[4] and Bruno G. Frenguelli[3]

DOI:http://dx.doi.org/10.1523/ENEURO.0212-16.2017

[1]Centre for Cognitive and Neural Systems, The University of Edinburgh, Edinburgh EH8 9JZ, United Kingdom, [2]MRC Protein Phosphorylation Unit, College of Life Sciences, The University of Dundee, Dundee DD1 5EH, United Kingdom, [3]School of Life Sciences, The University of Warwick, Coventry CV4 7AL, United Kingdom, [4]Division of Cell Signalling and Immunology, College of Life Sciences, The University of Dundee, Dundee DD1 5EH, United Kingdom

Abstract

The later stages of long-term potentiation (LTP) *in vitro* and spatial memory *in vivo* are believed to depend upon gene transcription. Accordingly, considerable attempts have been made to identify both the mechanisms by which transcription is regulated and indeed the gene products themselves. Previous studies have shown that deletion of one regulator of transcription, the mitogen- and stress-activated kinase 1 (MSK1), causes an impairment of spatial memory. Given the ability of MSK1 to regulate gene expression via the phosphorylation of cAMP response element binding protein (CREB) at serine 133 (S133), MSK1 is a plausible candidate as a prime regulator of transcription underpinning synaptic plasticity and learning and memory. Indeed, prior work has revealed the necessity for MSK1 in homeostatic and experience-dependent synaptic plasticity. However, using a knock-in kinase-dead mouse mutant of MSK1, the current study demonstrates that, while the kinase function of MSK1 is important in regulating the phosphorylation of CREB at S133 and basal synaptic transmission in hippocampal area CA1, it is not required for metabotropic glutamate receptor-dependent long-term depression (mGluR-LTD), two forms of LTP or several forms of spatial learning in the watermaze. These data indicate that other functions of MSK1, such as a structural role for the whole enzyme, may explain previous observations of a role for MSK1 in learning and memory.

Key words: BDNF; CREB; learning; LTP; memory; MSK1

Significance Statement

The nuclear kinase mitogen- and stress-activated kinase 1 (MSK1) has been identified as a possible link between cell-surface neurotransmitter receptors and the gene expression necessary for long-term memory: by coupling the activation of BDNF receptors to the regulation of transcription via the phosphorylation of cAMP response element binding protein (CREB), MSK1 unites a neurotrophin heavily implicated in synaptic plasticity with changes in gene expression. Using a kinase-dead MSK1 mouse mutant, we show that, while MSK1 is necessary for CREB phosphorylation and the regulation of basal synaptic transmission, it is not required for metabotropic glutamate receptor-dependent long-term depression (mGluR-LTD), long-term potentiation (LTP), or several forms of spatial reference memory (SRM). MSK1 may instead play a homeostatic role in the CNS that allows synapses to adapt to prevailing synaptic or sensory experience.

January/February 2017, 4(1) e0212-16.2017 1–16

Introduction

The intracellular mechanisms that link the activation of cell surface neurotransmitter receptors to the genomic changes promoting neuronal morphological and functional adaptations has been a topic of considerable interest. This interest has arisen from the potential to both identify signaling pathways responsible for these changes, and to use this knowledge to intervene pharmacologically in a host of developmental, neurological, and psychiatric conditions (Guzman-Karlsson et al., 2014; Lynch et al., 2014).

In this regard, the nuclear kinase mitogen- and stress-activated kinase (MSK) (Deak et al., 1998) is well placed to couple activity at the cell surface to changes in gene expression. Of the two isoforms of MSK (MSK1 and MSK2), MSK1 is most highly expressed in brain (Arthur et al., 2004) and is activated in response to neurotrophins, including brain-derived neurotrophic factor (BDNF) (Arthur, 2008; Frenguelli and Corrêa, 2012; Reyskens and Arthur, 2016). The stimulation of BDNF TrkB receptors results in the activation of a number of signaling pathways including the MAPK cascade, and in particular of ERK1/2 and p38 (Minichiello, 2009; Panja and Bramham, 2014). These enzymes translocate to the nucleus and are responsible for the direct activation of MSK1 via phosphorylation of key residues on the C-terminal kinase domain, which then phosphorylates residues on the N-terminal kinase domain (McCoy et al., 2005). Once activated, the N-terminal kinase domain of MSK1 phosphorylates cAMP response element binding protein (CREB) at serine 133 (S133) (Deak et al., 1998; Arthur, 2008; Frenguelli and Corrêa, 2012; Reyskens and Arthur, 2016). From observations in *Aplysia* (Dash et al., 1990), *Drosophila* (Yin et al., 1994), and mice (Bourtchuladze et al., 1994), CREB has emerged as an evolutionarily-conserved mechanism by which neurons convert activity into persistent modifications of synaptic function and the formation and stabilization of memories (Sakamoto et al., 2011; Kandel, 2012; Kida and Serita, 2014).

Accordingly, by linking BDNF to CREB-dependent gene transcription, MSK1 is positioned to respond to the many experiential and synaptic stimuli that provoke the release of BDNF and to convert these stimuli into long-term structural, functional, and cognitive adaptations. Indeed, prior work using MSK single or double knock-out mice has suggested that MSKs regulate neurogenesis (Choi et al., 2012; Karelina et al., 2012; Karelina et al., 2015) and BDNF-induced CREB phosphorylation (Arthur et al., 2004). These observations, as well as a role for MSK1 in posttranslational modifications of histones (Chwang et al., 2007; Chandramohan et al., 2008), and in the regulation of the plasticity-related protein Arc/Arg3.1 (Shepherd and Bear, 2011; Corrêa et al., 2012), may explain the reported deficits in MSK1 knock-out mice in spatial learning in the watermaze; fear conditioning (Chwang et al., 2007); the display of behavioral immobility in the forced swim test (Chandramohan et al., 2008); learning in the Barnes maze; and discrimination in novel object recognition (Karelina et al., 2012).

Although these knock-out studies suggest an important role of MSK1 in various aspects of learning and memory, this role may involve other aspects of MSK1 beyond its kinase function. For example, it has been reported that MSK1 forms a structural complex with ERK1/2 and the glucocorticoid receptor which is necessary for transcription of the immediate early genes c-Fos and Egr-1 (Gutierrez-Mecinas et al., 2011). Thus, the phenotype of knock-outs of MSK1 does not directly discriminate between structural and kinase roles for MSK1 in synaptic and cognitive function. In order to address this issue, an MSK1 mutant has been generated in which the kinase activity of MSK1 is selectively inactivated, but one in which protein levels of MSK1 remain close to wild-type levels (Corrêa et al., 2012). This kinase-dead mutation involves the knock-in substitution of an alanine for the aspartate at position 194 in the DFG motif of the N-terminal kinase domain of the endogenous MSK1 gene. Mutations in the DFG motif are commonly used to abolish the kinase activity of enzymes (Moran et al., 1988; Vijayan et al., 2015), and confirmation that this results in a kinase-dead version of MSK1 (MSK1 KD) was previously evidenced by the inability of MSK1 KD to phosphorylate peptide substrates, even when overexpressed in cell lines (Deak et al., 1998; McCoy et al., 2005; Corrêa et al., 2012).

Using this MSK1 KD mutant, we show that, while there is reduction in BDNF stimulation of CREB phosphorylation and a deficit in basal synaptic transmission in hippocampal area CA1, there is no change in paired-pulse facilitation, metabotropic glutamate receptor-dependent long-term depression (mGluR-LTD), or tetanus- or theta-burst-induced long-term potentiation (LTP). Moreover, we observe no overt deficits in various watermaze paradigms. These observations suggest that, under conditions of typical rearing of experimental rodents, the kinase activity of MSK1 is not necessary for several forms of synaptic plasticity and spatial learning, but may instead be

Received July 19, 2016; accepted January 9, 2017; First published February 09, 2017.

The authors declare no competing financial interests.

Author contributions: R.G.G.M., J.S.C.A., and B.G.F. designed research; S.D., C.J.H., R.B.M., L.M., L.P., D.D.C., K.R., and H.T.F. performed research; DDC contributed unpublished reagents/analytic tools; S.D., C.J.H., R.B.M., L.M., L.P., D.D.C., K.R., H.T.F., R.G.G.M., J.S.C.A., and B.G.F. analyzed data; S.D., L.M., L.P., R.G.G.M., J.S.C.A., and B.G.F. wrote the paper.

This research was supported by MRC (R.G.M.M., B.G.F., J.S.C.A.), BBSRC (B.G.F.), EU FP6 (Sirocco) (J.S.C.A.), ERC (R.G.M.M.), WPH Charitable Trust (B.G.F.), and a Wellcome Trust PhD Studentship (C.J.H.).

*S.D., C.J.H., R.B.M., L.M., and L.P. contributed equally to this work.

S. Daumas's present address: Neuroscience Paris Seine (NPS), Institut de Biologie Paris Seine (IBPS), Sorbonne Universités, UPMC UM CR18, INSERM U1130, CNRS UMR 8246, Paris 75005, France.

Acknowledgements: We thank Julia Carr for genotyping and the staff of the Biomedical Services Units of Dundee, Edinburgh and Warwick Universities for their excellent animal husbandry and colony management.

Correspondence should be addressed to Bruno G. Frenguelli at the above address, E-mail: b.g.frenguelli@warwick.ac.uk.

DOI:http://dx.doi.org/10.1523/ENEURO.0212-16.2017

required for homeostatic adaptation to prevailing synaptic activity.

Materials and Methods

Animals

A kinase-dead MSK1 mouse was generated by mutating Asp194 to Ala (D194A) in the DFG motif in the endogenous MSK1 gene (Corrêa et al., 2012). The knock-in was produced by TaconicArtemis GmbH using standard targeting methods in C57BL/6 ES cells. Routine genotyping was carried out by PCR using the primers 5'-CGGCC-ATGTGGTGCTGACAGC-3' and 5'-GGGTCAGAGGC-CTGCACTAGG-3', which gives 378- and 529-bp products for wild-type and targeted alleles, respectively. Western blottings of MSK1 protein (n = 4 per genotype) revealed that MSK1 was expressed in MSK1 KD mice at approximately 65% of the levels found in wild-type mice (data not shown).

Unless otherwise stated, all mice were kept in individually ventilated cages (Tecniplast Blue Line 1284L) with a sawdust substrate, paper shavings and at least one cardboard play tunnel with water and food provided *ad libitum*. Mice were kept in social groups where possible with a maximum of five mice per cage and maintained on a 12/12 h light/dark cycle with lights on at 7 A.M. The care and accommodation of all the animals held in the facility comply with the standards set out in relevant codes of practice for the housing and care of animals used for scientific purposes.

Extracellular recordings

Male C57BL/6 WT and MSK1 KD mice (two to five months old) were killed by cervical dislocation in accordance with appropriate animal welfare legislation. Sagittal brain slices (400 µm) were prepared, and extracellular recordings were made from stratum radiatum in area CA1 at 32-33°C from slices that were either submerged in aCSF or, in the case of the Actinomycin-D (Act-D) experiments, held at a humidified and oxygenated air/aCSF interface. A two-pathway stimulation protocol was adopted with each electrode placed either side of the recording electrode. Each pathway was stimulated in an alternating fashion with either 60 s (submerged slices) or 90 s (interface slices) between stimuli to a given pathway. A prolonged interval between stimuli avoids activity-dependent fatigue of LTP (Fonseca et al., 2006a; Villers et al., 2012). That the stimulated fiber pathways were convergent but independent was confirmed with a cross-pathway paired-pulse facilitation protocol (50-ms interpulse interval) that showed no facilitation across pathways.

Stimulus input/output curves were generated over a range of electrical stimuli from 10-300 µA (0.1 ms in duration) using a Digitimer DS3 constant current isolated stimulator. Paired-pulse facilitation was measured over a range of 50 to 350 ms interpulse interval.

LTP was induced using two protocols: a tetanus of 100 stimuli at 100 Hz, and a theta-burst stimulation (TBS) protocol at test intensity (1 mV fEPSP amplitude in submerged slices; 3 mV fEPSP amplitude in interface slices). Bursts consisted of four stimuli at 100 Hz. Each train was composed of 10 bursts separated by 200 ms. Trains were repeated three times with an interval of 20 s. That TBS resulted in transcription-dependent LTP was tested in two series of experiments (in interface chambers) using either 40 µM Act-D (in 0.08% DMSO) applied for the duration of the experiment (>30 min before TBS and at least 80 min after TBS), or 25 µM Act-D (0.05% DMSO) given 15 min before and until 15 min after TBS. An additional series of interleaved experiments were performed in DMSO, which was present throughout the experiments at the level (0.08%) found in the 40 µM Act-D experiments.

mGluR-LTD was induced in hippocampal slices via the application of the Group I (Gl) mGluR agonist DHPG (100 µM; 10 min) in the presence of both the $GABA_A$ receptor antagonist picrotoxin (50 µM) and the NMDA receptor glycine site antagonist L689,560 (5 µM).

Stimulation and recording parameters, as well as the analysis of evoked fEPSPs, were under the control of WinLTP data acquisition software. Experiments were interleaved and performed blind to the genotype of the mice, which was revealed only after the experiments had been analysed and confirmed with *post hoc* genotyping.

Immunohistochemistry for CREB phosphorylation at S133

After cutting, hippocampal slices (300 µm) were suspended on a mesh located within a 50 ml beaker (up to four slices/beaker) for 3 h in oxygenated circulating aCSF at 34°C. Slices were then either treated with 50 ng/ml recombinant human BDNF (Cell Guidance Systems; GFH1) or forskolin (50 µM; Sigma Aldrich; F6886) for 10 min or left untreated to serve as parallel time controls. Treated and untreated slices were rapidly immersed in 4 % paraformaldehyde in PBS, pH 7.4, and fixed overnight. The slices were washed three times in PBS and then incubated at room temperature in a solution containing both 10 % goat serum, to prevent nonspecific antibody binding, and 0.4 % Triton X-100 in PBS to permeabilize slices. After three washes in PBS the slices were incubated for 4 h at room temperature with a phospho-CREB primary antibody targeting S133 (rabbit mAb; Cell Signalling; #9198) diluted 1:400 in 10 % donor goat serum and 0.4 % Triton X-100 in PBS. The slices were then washed twice in PBS and incubated for 1.5 h at room temperature in Alexa Fluor 488 goat anti-rabbit antibody (Molecular Probes; #A-11008) diluted 1:800 in 10 % donor goat serum and 0.4 % Triton X-100 in PBS. The slices were then washed again in PBS three times. The slices were viewed, and images were acquired blind to the genotype using identical settings with Zeiss ZEN2 software on an LSM 880 laser confocal-scanning system coupled to a Zeiss inverted microscope. Images were taken using a 40 × oil immersion objective. Averages of four scans were collected for each image. The mean pixel intensity in the CA1 cell body region was determined using ImageJ 1.46r. The pixel intensity corresponding to individual CA1 neurons (identified by a threshold mask) was averaged on a per slice basis and comparisons were made between treated and untreated slices in terms of absolute fluorescence [arbitrary units (AU)], measured us-

ing identical acquisition parameters, and the % change in pixel intensity in BDNF- or forskolin-treated slices over the corresponding untreated controls was calculated. Immunofluorescence data was acquired from a total of 11 wild-type and 13 MSK1 KD mice from which between 1 and 5 slices each were used for the imaging studies for each experimental condition (control, BDNF, and forskolin). On average, approximately 70 neurons were analysed per slice across the various experimental conditions. The specificity of the phospho-CREB primary antibody was confirmed by testing the antibody in hippocampal slices prepared from a conditional CREB S133 mutant mouse in which S133 is mutated to alanine (CREB S133A; Wingate et al., 2009). No fluorescent signal was detected in CA1 pyramidal neurons (data not shown).

Behavior

Male MSK1 KD mice (n = 12) and control littermates (n = 12), aged 15 weeks at the start of the analysis, received daily handling during the last week of a quarantine period, and were subject to a total of five weeks of experimentation. During this period, they were group housed, had *ad libitum* access to food and water, and were maintained on a light/dark cycle of 14/10 h with lights on at 8 A.M. All mice were trained and tested "blind" for genotype.

The watermaze

The open-field watermaze is 2 m in diameter and was housed in a large laboratory room with prominent extramaze cues. The water was filled and drained daily, maintained at 25 ± 2°C, and made opaque by the addition of 500 ml of liquid latex. Each mouse was gently placed into the water facing the side walls at one of the four preplanned start positions (North, South, East, and West). If a mouse failed to reach the platform after 90 s (during training) or 60 s (probe tests) had elapsed, it was guided by hand to the escape platform. Once on the platform, each mouse was allowed to remain for 30 s. After 30 s, the mouse was taken away from the platform using a paint roller and put under a heat lamp until the next trial. The swimming path of the mice was tracked using the Actimetrics Watermaze software (Coulbourn Electronics).

Visible cue task in the watermaze

Curtains were drawn around the pool to exclude the extramaze cues. Escape from the water was via a single moveable platform of 20 cm in diameter located 1.5 cm beneath the water surface. The platform was made visible by placing upon it a red/black plastic ball (about 20 cm in height). Mice were tested in groups of no more than six. Each mouse was given 3 d of training (four trials/day; t = 90 s). Each cardinal point was used once as the starting position on each day. The intertrial interval was 10 min, and the platform location was changed across trials.

Spatial reference memory task

Curtains were absent for the rest of the spatial training, in order for mice to use extramaze cues to build up a spatial representation of the room. The escape platform, still beneath the water surface, was now uncued and remained at the same spatial location throughout the spatial reference memory (SRM) training, forcing the animals to use a spatial strategy to retrieve the platform location. The animals were subjected to 5 d of training with four trials/day, and an intertrial interval of 10 min. As in the cue task, mice were released from each cardinal point in a random order. Twenty-four hours after the last trial, a probe test (PT1) was conducted in which the platform was removed and the animal placed in the pool to swim for 60 s.

Serial spatial memory task

The animals were then subjected to serial spatial learning, a series of five spatial reference memory tasks trained to a criterion of performance as described by Chen et al. (2000) and Daumas et al. (2008). Each task constituted a separate spatial problem, with all five problems taking place in the same watermaze in the same experimental room (starting 24-48 h after SRM completion). The platform location was varied from placement on an inner "virtual" ring (1 m in diameter) or an outer ring (1.5 m in diameter). In this way, the location differed between problems but remained the same within each day of training and each spatial problem, until the chosen criterion was reached. The animals had a maximum of 32 trials to acquire a spatial problem task, but if they reached the criterion of an average escape latency of <20 s on three consecutive trials, the training for the given spatial problem was stopped. The training for the next spatial problem began 2 d later. There was a maximum of eight trials per day, with an intertrial interval of 10 min. If an animal did not reach the platform within 90 s, it was directed to the platform using a small paint roller and allowed to rest for 30 s.

In order to assess the strength of memory for each platform location, a probe test was conducted. To study short-term memory the probe test was given 10 min after reaching criterion on each of the five problems. To study long-term memory the probe test was given 24 h after reaching criterion. A 13 cm in diameter Atlantis platform was used to avoid extinction between probe tests. This platform, which was unavailable to the mice during the test, is software-driven to rise after the 60 s of the probe trial had elapsed. The animals had 30 additional seconds to find the platform and, if they did not, were guided to the platform with a paint roller and left there for 30 s.

Massed spatial watermaze task

A week after the end of the serial spatial task, mice were submitted to four consecutive sessions of four trials, with an intersession delay of 15 min, during which they were returned to their home cage. The Atlantis platform was submerged 0.5 cm beneath the surface of the water. Animals were introduced in the maze from different starting points and allowed to swim freely or until they reached the platform. Mice failing to find the platform within 90 s were gently guided to the platform and left on it for 30 s. The starting positions were determined in a pseudorandom order, and the sequence of starting locations was randomized such as each of them was used four times during the four training sessions.

Ten minutes, 24 h, and 7 d after the last training session mice were submitted to a probe test using the Atlantis platform, which rose after the 60 s of the probe trial had elapsed, after which mice were allowed to search for it for an additional 30 s.

Statistical analysis

Statistical analysis was performed using IBM SPSS Statistics 22 using the tests described in Table 1. Statistical significance was set at $p < 0.05$.

Results

MSK1 is required for BDNF-dependent phosphorylation of CREB S133

To confirm the kinase-dead nature of the mutation in the MSK1 gene in the MSK1 KD mutant mice, we conducted a series of experiments utilizing acutely-prepared hippocampal slices taken from wild-type and MSK1 KD mice of an age similar to those used for the electrophysiology and behavioral studies. Incubation of wild-type hippocampal slices with BDNF (50 ng/ml; 10 min) resulted in a significant increase in CA1 immunoreactivity for phosphorylated CREB at S133 (79.2 ± 5.1 AU; 21 slices from eight mice[a]) compared to parallel control, untreated slices from the same animal (59.3 ± 4.8 AU; 15 slices from eight mice; $p = 0.004$[a]; Fig. 1A, upper panels). There was little or no increase in CREB phosphorylation in slices taken from MSK1 KD mice (63.4 ± 4.7 vs 56.7 ± 3.4 AU in BDNF; both 20 slices from 10 mice; $p = 0.29$[a]; Fig. 1A, lower panels). There was no difference in basal pCREB fluorescence between the two genotypes ($p = 0.55$[a]). A comparison of the BDNF-induced change in immunofluorescence showed a significant BDNF-dependent increase in CREB phosphorylation in wild-type mice (139.5 ± 8.4%, n = 21 slices from eight mice[b]), but no overall change in pCREB immunoreactivity in the CA1 region of slices taken from MSK1 KD mice (95.3 ± 7.9%, n = 20 slices from 10 mice; $t_{39} = 3.83$; $p = 0.0004$[b]; Fig. 1B). That CREB could be phosphorylated in MSK1 KD mice was demonstrated by the incubation of slices from wild-type and MSK1 KD mice in the adenylate cyclase activator forskolin (50 μM; 10 min; data not shown). Basal phospho-CREB immunofluorescence was similar across both genotypes (66.2 ± 8.9 AU for wild-type; seven slices from five mice; vs 78.8 ± 7.8 AU for MSK1 KD slices; 15 slices from six mice; $p = 0.37$[c]) and rose to 100.5 ± 9.8 AU and 104.9 ± 8.2 AU after forskolin application in wild-type and MSK1 KD slices, respectively (n = 8 slices from five wild-type mice and 16 slices from six MSK1 KD mice; $p = 0.003$[c]). Expressed as a percentage, forskolin application increased phospho-CREB immunofluorescence to a similar extent in wild-type slices (148.1 ± 12.7%; n = 8 slices from five mice) and MSK1 KD slices (137.3 ± 9.0%; n = 16 slices from six mice).

The regulation of basal synaptic transmission, but not the probability of transmitter release, mGluR-LTD or LTP, is dependent upon the kinase activity of MSK1

To establish the role of MSK1 in synaptic function we performed electrophysiological experiments in area CA1 of hippocampal slices prepared from MSK1 KD and wild-type mice.

The construction of stimulus input/output curves (10-300 μA) revealed a mild reduction in excitatory synaptic transmission in the MSK1 KD mutants (n = 12 mice; 17 pathways) when compared to wild-type animals (n = 18 mice; 27 pathways). This was apparent when the fEPSP slope was compared to the presynaptic fiber volley (Fig. 2A), or when the slope of the fEPSP was plotted as a function of the stimulus strength (Fig. 2B): There was a main effect of genotype ($p = 0.032$[d]) and a significant interaction between genotype and stimulus intensity ($p = 0.0001$[d]) at the higher stimulus strengths (200-300 μA; $p = 0.048$, $p = 0.035$, and $p = 0.033$, respectively[e]). However, there was no appreciable difference in the size of the presynaptic fiber volley between mutant and wild-type mice $p = 0.23$[f]) nor was there a fiber volley genotype x stimulus intensity interaction ($p = 0.42$[g]; Fig. 2C). To rule out differences in GABAergic inhibition between mutant and wild-type animals, input/output curves were constructed from slices taken from a different set of animals in the presence of the $GABA_A$ receptor antagonist picrotoxin (50 μM; five pathways from four wild-type mice and seven pathways from five MSK1 KD mice). The deficit in synaptic transmission at higher stimulus strengths (200-300 μA) in slices from MSK1 KD mice persisted during antagonism of $GABA_A$ receptors ($p = 0.001$) at 200, 250, and 300 μA ($p = 0.048$, $p = 0.035$, and $p = 0.040$, respectively[h]; Fig. 2D).

To test whether this deficit in basal synaptic transmission had a presynaptic component, we measured the facilitation of synaptic transmission associated with delivering pairs of electrical stimuli at 50 to 350 ms intervals. Such paired-pulse facilitation is taken as an index of the initial probability of transmitter release. There was no difference in paired-pulse facilitation between mutant (22 pathways from 19 mice) and wild-type mice (21 pathways from 18 mice), with the paired-pulse facilitation profile over the 50 to 350 ms range essentially overlapping in the two genotypes (Fig. 3A). Thus, as far as can be determined with paired-pulse facilitation and the similar magnitudes of the presynaptic fiber volley, the deficit in basal synaptic transmission in the MSK1 KD mice is not presynaptic and instead appears likely to have a postsynaptic locus, potentially via a reduction in synaptic AMPA-type glutamate receptors.

To test whether this impairment in basal synaptic transmission reflected a LTD-type state, we examined the LTD induced by the activation of GI mGluRs. This form of LTD requires the induction of Arc/Arg3.1 (Waung et al., 2008), and a deficit in Arc/Arg3.1 regulation has been observed in MSK1 KD neurons in response to activity deprivation (Corrêa et al., 2012), which may explain the failure to induce bidirectional homeostatic plasticity in MSK1 KD mutant neurons. Accordingly, we applied the GI mGluR agonist DHPG (100 μM; 10 min) to hippocampal slices from both MSK1 KD mutant and wild-type slices and measured fEPSPs from area CA1. DHPG caused a ~40% inhibition of the fEPSP 60 min after the onset of DHPG

Table 1: Results statistics summary

ID	Measure	Distribution	Type of test	F or t; p value	DoF	95% CI WT Lower; Upper	95% CI KD Lower; Upper
a	BDNF/CREB phosphorylation	Normal	Two-way ANOVA Genotype x Treatment effect Simple Main Effects Control: WT vs. KD BDNF: WT vs. KD WT: Control vs. BDNF KD: Control vs. BDNF	**8.31; 0.005** 0.36; 0.55 **13.08; 0.001** **8.74; 0.004** 1.12; 0.29	1,72 1,33 1,39 1,34 1,38	Control: 49.05; 69.62 BDNF: 68.55; 89.88	Control: 53.60; 73.22 BDNF: 49.65; 63.81
b	BDNF/CREB phosphorylation increase %	Normal	Independent Samples T-test (2-tailed)	**3.83; 0.0004**	39	101.76; 188.51	51.78; 142.31
c	Forskolin/CREB phosphorylation	Normal	Two-way ANOVA Treatment effect Genotype effect Control: WT vs. KD Forskolin: WT vs. KD WT: Control vs. Forskolin KD: Control vs. Forskolin	 **10.25; 0.003** 0.82; 0.37 0.85; 0.36 0.11; 0.74 **4.91; 0.032** **5.86; 0.020**	 1,42 1,42 1,20 1,22 1,13 1,29	Control: 62.19; 87.44 Forskolin: 90.53; 116.33 67.52; 101.47 Control: 44.30; 88.07 Forskolin: 77.31; 123.72	 79.91; 104.65 Control: 62.02; 95.65 Forskolin: 87.50; 122.27
d	Input/Output fEPSP Overall	Normal	One-way RM-ANOVA Genotype effect	 **4.93; 0.032**	 1,42	 -1.45; -1.02	 -1.08; -0.75
e	Input/Output fEPSP Higher stimulus	Normal	One-way RM-ANOVA Genotype x Stimulus-intensity effect	**4.00; 0.0001**	7,294	NA	NA
	strengths		Simple Main Effects for 200; 250; 300 µA	**4.15; 0.048** **4.75; 0.035** **4.84; 0.033**	1,42 1,42 1,42	-2.39; -1.65 -3.07; -1.96 -3.43; -2.17	-1.80; -1.22 -2.07; -1.36 -1.08; -0.74
f	Input/Output Fiber volley	Normal	One-way RM-ANOVA Genotype effect	 1.51; 0.23	 1,42	 -0.35; -0.26	 -0.32; -0.22
g	Input/Output Fiber volley	Normal	One-way RM-ANOVA Genotype x Stimulus-intensity effect	1.01; 0.42	7,294	NA	NA
h	Input/Output fEPSP Higher stimulus strengths	Normal	One-way RM-ANOVA Genotype x Stimulus intensity effect Simple Main Effects for 200; 250; 300 µA	**4.32; 0.001** **5.09; 0.048** **5.92; 0.035** **5.55; 0.040**	7,70 1,10 1,10 1,10	NA -3.95; -2.14 -4.30; -2.09 -4.55; -1.92	NA -2.77; -1.26 -2.73; -1.34 -2.70; -1.39
i	LTD DHPG	Normal	One-way RM-ANOVA Genotype effect RM-ANOVA Genotype x minute effect	0.065; 0.81 0.94; 0.49	1,23 9,207	50.46; 74.69 NA	50.93; 70.24 NA
j	Tetanus and TBS-induced LTP	Normal	One-way RM-ANOVA Genotype effect, Tetanus Genotype effect, TBS	 0.41; 0.53 0.27; 0.61	 1,15 1,12	 103.48; 147.98 110.41; 165.52	 118.94; 147.56 115.84; 146.72
k	LTP Actinomycin-D	Normal	One-way RM-ANOVA Drug effect WT: DMSO vs. Act-25 WT: DMSO vs. Act-40 KD: DMSO vs. Act-25	 **33.33; 0.000** **28.46; 0.000** **28.46; 0.000** **10.61; 0.001**	 2,13 1,12 1,8 1,12	 DMSO: 124.50; 142.50 Act-D 25µM: 103.16; 112.18 Act-D 40µM: 98.13; 108.36	

(Continued)

Table 1: Continued

			KD: DMSO vs. Act-40	**10.61; 0.004**	1,8		
l	LTP Actinomycin-D	Normal	One-way RM-ANOVA Genotype effect	0.82; 0.46	1,13	101.49; 124.51	104.82; 122.46
m	Cued learning watermaze	Normal	One-way RM-ANOVA Day of training effect	**52.69; 0.0001**	2,44	day 1: 23.07; 36.76 day 3: 6.72; 12.12	
n	Cued learning watermaze	Normal	One-way RM-ANOVA Genotype effect	0.74; 0.40	1,22	11.16; 21.45	12.30; 27.47
o	Cued learning watermaze	Normal	One-way RM-ANOVA Genotype x Day effect	1.72; 0.19	2,44	NA	NA
p	Spaced trials task	Normal	One-way RM-ANOVA Day of training effect	**18.66; 0.0001**	4,92	day 1: 31.18; 46.61 day 5: 11.60; 18.70	
q	Spaced trials task	Normal	One-way RM-ANOVA Genotype effect	0.16; 0.69	1,23	19.53; 24.10	16.89; 24.97
r	Spaced trials task	Normal	One-way RM-ANOVA Genotype x Day effect	0.91; 0.46	4,92	NA	NA
s	Spaced trials task probe trial	Normal	One-sample Wilcoxon Signed Rank Test (WT and KD)	**NA; 0.002**	NA	36.74; 47.36	31.92; 43.49
t	Spaced trials task probe trial	Normal	Independent Samples T-test (2-tailed)	-1.20; 0.24	23	as above	as above
u	Serial spatial learning task	Normal	One-way RM-ANOVA Task order effect	**6.48; 0.0001**	4,88	Spatial problem 1: 6.12; 10.88 Spatial problem 5: 3.87; 5.71	
v	Serial spatial learning task	Normal	One-way RM-ANOVA Genotype effect	0.33; 0.57	1,22	4.85; 7.41	4.62; 6.78
w	Serial spatial learning task	Normal	One-way RM-ANOVA Genotype x Task effect	0.014; 0.91	4,88	NA	NA
x	Serial spatial learning task 10 min probe trial	Normal	One-sample Wilcoxon Signed Rank Test (WT and KD) Average for spatial pr. 1 to 5	**NA; 0.002**	NA	23.15; 29.26	18.37; 27.42
y	Serial spatial learning task 10 min probe trial	Normal	One-way RM-ANOVA Genotype effect	1.80; 0.19	1,22	as above	as above
z	Serial spatial learning task 10 min probe trial	Normal	One-way RM-ANOVA Genotype x Task effect	1.71; 0.16	4,88	NA	NA
aa	Serial spatial learning task 10 min probe trial	Normal	Independent Samples T-test (2-tailed) 1st spatial problem	1.925; 0.067	22	23.32; 43.94	15.48; 29.82
ab	Serial spatial learning task 24 hr probe trial	Normal	One-sample Wilcoxon Signed Rank Test (WT and KD)	**NA; 0.002**	NA	17.48; 23.93	18.23; 22.60
ac	Serial spatial learning task 24 hr probe trial	Normal	One-way RM-ANOVA Genotype effect	0.02; 0.88	1,22	as above	as above
ad	Serial spatial learning task 24 hr probe trial	Normal	One-way RM-ANOVA Genotype x Task effect	0.18; 0.95	4,88	NA	NA
ae	Massed training spatial learning	Normal	One-way RM-ANOVA Session effect	**3.33; 0.025**	3,66	session 1: 18.89; 27.56 session 4: 11.37; 20.80	
af	Massed training spatial learning	Normal	One-way RM-ANOVA Genotype effect	0.22; 0.64	1,22	13.19; 21.95	11.37; 26.53
ag	Massed training spatial learning	Normal	One-way RM-ANOVA Genotype x Session effect	0.76; 0.39	3,66	NA	NA
ah	Massed training spatial learning probe trial at 10 min	Normal	One-sample Wilcoxon Signed Rank Test: WT; KD;	**NA; 0.015** **NA; 0.005**	NA NA	26.82; 38.13	30.68; 41.66
ai	Massed training spatial learning probe trial at 10 min	Normal	One-way ANOVA Genotype effect	1.06; 0.31	1,22	as above	as above

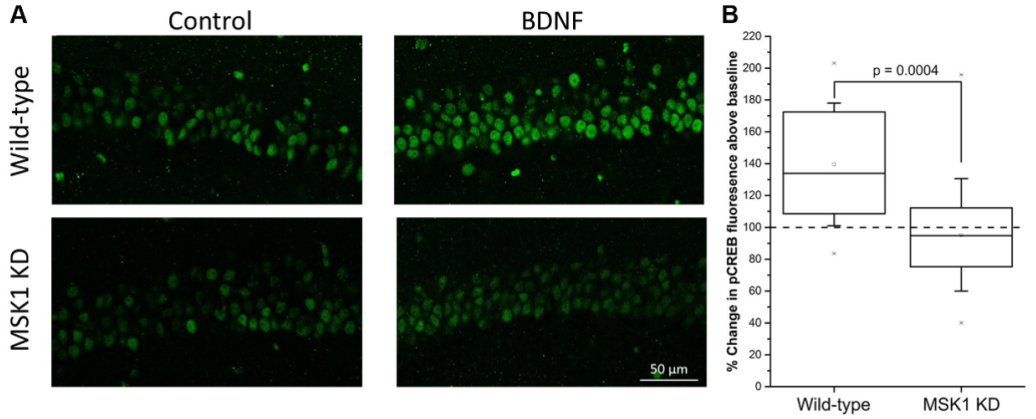

Figure 1. MSK1 is necessary for BDNF-dependent CREB phosphorylation in area CA1. ***A***, Treatment of wild-type hippocampal slices (upper panels) with BDNF (50 ng/ml; 10 min) resulted in a robust increase in CREB phosphorylation in CA1 neurons, compared to control untreated slices, as indicated by changes in immunofluorescence associated with a monoclonal antibody directed at the phosphorylation of CREB S133. In contrast, BDNF induced little or no effect on CREB phosphorylation in slices taken from MSK1 KD mice (lower panels). ***B***, Box and whisker plot showing mean (open square), median, 25 and 75 percentile (box), and ±1 standard deviation (whiskers) of data from 21 BDNF-treated slices from eight wild-type mice and 20 BDNF-treated slices from 10 MSK1 KD mice. The specificity of the antibody for the phosphorylation of CREB S133 in CA1 pyramidal neurons was confirmed using a mouse expressing a CREB S133-alanine point mutation (data not shown).

application that was no different between MSK1 KD and wild-type slices[i] (Fig. 3*B*).

To establish instead whether LTP, which also has a requirement for Arc/Arg3.1 (Plath et al., 2006), would be affected by the MSK1 KD mutation, we performed dual-pathway LTP experiments in both mutant and wild-type slices and used both tetanus and theta-burst stimulation (TBS) paradigms as they have been reported to recruit different intracellular signaling pathways. In particular, in contrast to single tetanus LTP, TBS is reported to recruit both ERK1/2- (Winder et al., 1999), and transcription-dependent LTP (Nguyen and Kandel, 1997) and where a deficit in slices from MSK1 KD mice might be expected to be observed.

Given the difference in basal synaptic transmission between the MSK1 KD and wild-type mice (Fig. 2), and to avoid bias associated with differential postsynaptic depolarization caused by LTP-inducing high-frequency stimulation, basal fEPSP amplitude was set to 1 mV across the two genotypes. This protocol has been adopted previously with mutant mice displaying impaired basal synaptic transmission (Patterson et al., 1996). It should be noted that while such stimulus matching is important in allowing comparisons regarding relative enhancements of synaptic transmission after high-frequency stimulation, it does so only at a fixed stimulus strength. Thus, in the absence of full input-output curves before and after LTP, it is conceivable that MSK1 KD mice would still display a deficit in basal synaptic transmission after LTP when compared to wild-type mice.

Both tetanus and TBS induced robust LTP which persisted for the duration of the experiment (180 min after high-frequency stimulation). There was no obvious difference between either the initial potentiation or the potentiation at 180 min between the two genotypes or stimulation protocols (Fig. 3*C*,*D*). For wild-type mice tetanus-induced LTP measured over the last 10 min of the experiment was 127.1 ± 9.9% (n = 9), whereas after TBS, it was 137.6 ± 10.9% (both relative to the preceding baseline; n = 7); and in the MSK1 KD mutants, the corresponding values were: tetanus-induced LTP at 132.6 ± 6.4 (n = 8) and theta-burst induced LTP at 130.9 ± 6.1% (n = 7). Neither tetanus- nor TBS-induced LTP differed significantly across the genotypes (p = 0.53 and p = 0.61[j], respectively). Accordingly, it would seem that the kinase activity of MSK1 is not required for LTP, at least over the time course (3 h) of the present experiments.

To confirm that the late LTP evoked required gene transcription, we performed a series of experiments using the transcription inhibitor Act-D during TBS-induced LTP (Nguyen and Kandel, 1997). In these experiments, slices were maintained in an interface chamber, in which a deficit in basal synaptic transmission was still observed in slices from MSK1 KD mice (data not shown). Due to the larger fEPSPs evoked from slices in interface chambers (Reid et al., 1988; Croning and Haddad, 1998; Bortolotto et al., 2011), basal fEPSP amplitudes in both genotypes were set at 3 mV.

When applied at 40 **µ**M for the duration of the experiment (n = 5; four wild-type and one MSK1 KD mice), Act-D resulted in a return of LTP to baseline values within 80 min after TBS compared to interleaved DMSO control experiments (n = 5; three wild-type and two MSK1 KD mice[k]) where the LTP was maintained at ~130% of control (Fig. 3*E*). However, a ~15% decrease in the control pathway was observed with this protocol that could

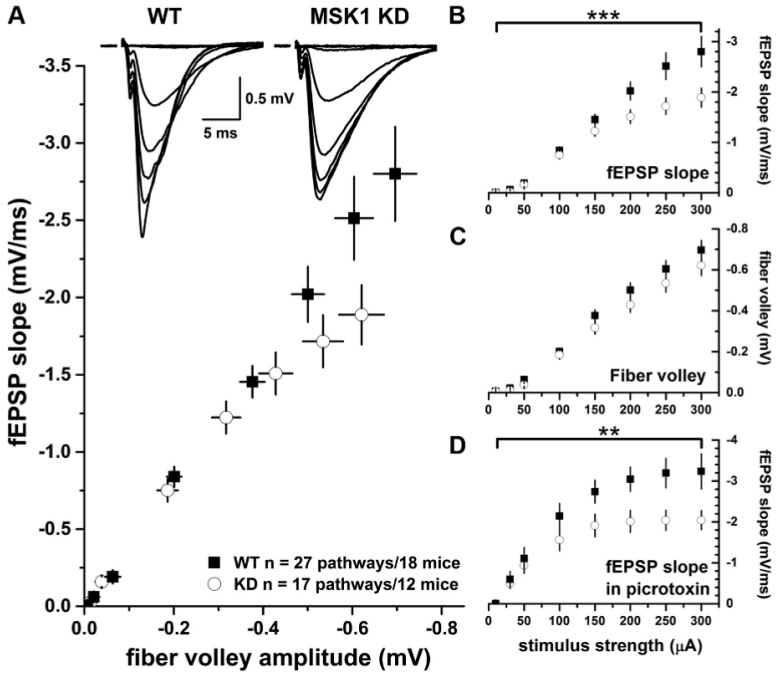

Figure 2. MSK1 KD mice display a deficit in basal synaptic transmission which is not due to increased GABAergic inhibition. Basal synaptic transmission was measured in the CA1 region of hippocampal slices from wild-type (black squares) or MSK1 KD (white circles) mice. ***A***, Plot of fibre volley amplitude versus fEPSP slope demonstrates that MSK1 KD mice show reduced synaptic transmission at higher stimulus strengths. Inset is representative fEPSPs at 10 to 300 **μ**A stimulus strengths for both genotypes (n = 27 pathways from 18 wild-type mice and 17 pathways from 12 MSK1 KD mice). This deficit is also observed when fEPSP slope is plotted against stimulus strength (***B***; ×××p = 0.0001; genotype x stimulus strength interaction). In contrast, a plot of fibre volley amplitude against stimulus strength (***C***) showed no significant difference between the genotypes. ***D***, The deficit in fEPSP was maintained when the experiments were repeated in the presence of 50 **μ**M of the $GABA_A$ receptor antagonist picrotoxin (n = 5 pathways from four wild-type mice and seven pathways from five MSK1 KD mice; ××p = 0. 001; genotype x stimulus strength interaction). Error bars represent SEM.

have accounted, at least in part, for the observed decrementing LTP. We therefore conducted an additional series of experiments where a lower concentration of Act-D (25 **μ**M; n = 9; three wild-type mice and four MSK1 KD mice; Fig. 3*E*) was applied for 15 min before and until 15 min after TBS. This lower concentration and shorter duration of Act-D had a similar inhibitory effect on TBS-induced LTP, with a return to baseline at approximately 80 min, but with less of an influence (<10%) on the control pathway, and which was similar to that recorded in the DMSO control experiments. Since the above experiments combined slices from both wild-type and MSK1 KD slices, and showed that the effects of 25 and 40 **μ**M Act-D on LTP were similar, we segregated the Act-D data on the basis of genotype (seven slices from seven wild-type mice and seven slices from five MSK1 KD mice). This analysis showed that TBS-induced LTP in both wild-type and MSK1 KD slices was equally sensitive to Act-D (Fig. 3*F*). These data confirm that LTP induced by TBS requires gene transcription for its maintenance[k,l] (Nguyen and Kandel, 1997) in both wild-type and MSK1 KD mice and further indicate that transcription regulated by MSK1 is not required.

The kinase activity of MSK1 is not required for spatial memory tasks in the watermaze

Given previous reports that MSK1 is required for a number of learning tasks (Chwang et al., 2007; Chandramohan et al., 2008; Karelina et al., 2012), we examined MSK1 KD mice in a variety of hippocampal-dependent watermaze training protocols (Figs. 4-6). In the cued version of the watermaze (Fig. 4*A*), mice of both genotypes improved their performance over the 3d of training with a decline in escape latency ($p < 0.0001$[m]); there was no significant effect due to the genotype ($p = 0.40$[n]), nor a significant interaction between genotype and day ($p = 0.19$[o]). These data indicate that the MSK1 KD mutant does not display gross motor or sensory deficits.

In the spaced trials hidden platform version of the watermaze (Fig. 4*B*), mice of both genotypes improved

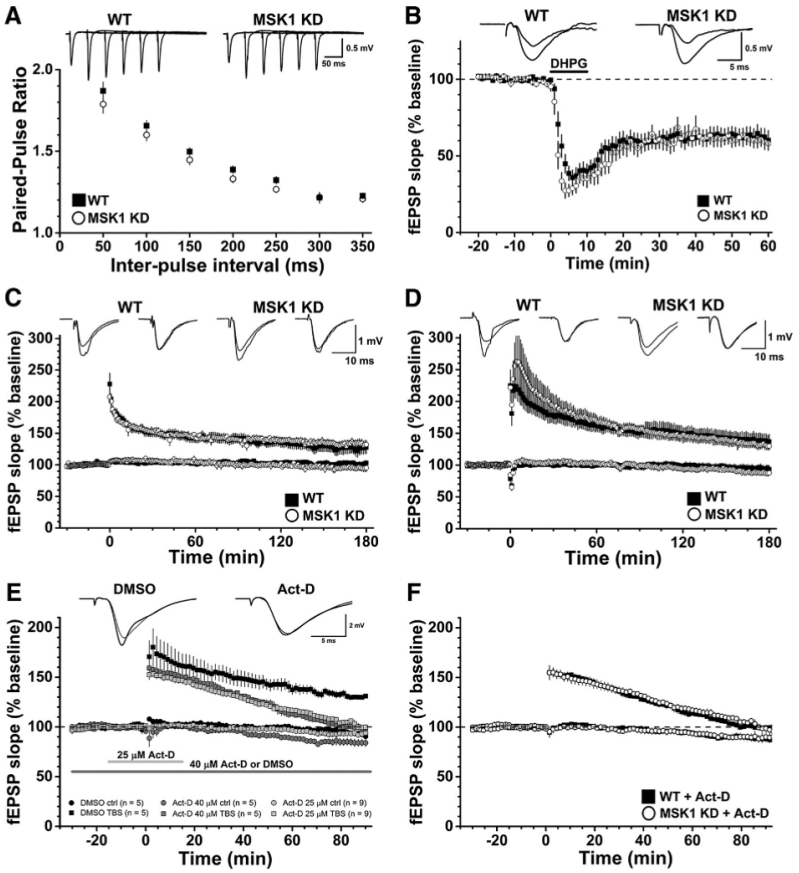

Figure 3. Electrophysiological characterization of MSK1 KD mice shows no deficit in paired-pulse facilitation, mGluR-LTD, or LTP. ***A***, Paired-pulse facilitation in area CA1 was measured in hippocampal slices prepared from adult wild-type (black squares; 21 pathways from 18 animals) or MSK1 KD (white circles, 22 pathways from 19 animals) mice. Representative families of paired fEPSPs taken over the 50 to 250 ms interstimulus interval range are shown in the upper panel, and quantification of the paired-pulse ratios in the lower panel. Data are expressed as mean and error bars (where visible) represent the SEM. ***B***, mGluR-LTD was induced in area CA1 of hippocampal slices from wild-type (black squares) and MSK1 KD (white circles) mice. The Gl mGluR agonist DHPG (100 **μ**M) was applied from time 0-10 min (as indicated by the black bar on the graph) in the presence of both picrotoxin (50 **μ**M) and the NMDA receptor glycine site antagonist L689,560 (5 **μ**M). Inset are representative fEPSPs taken 10 min before and 50 min after the end of DHPG application in wild-type and MSK1 KD slices (n = 15 and 10 slices from 11 wild-type and 8 MSK1 KD mice, respectively). Data are expressed as mean, and error bars represent the SEM. ***C***, ***D***, Tetanus- (***C***) and theta-burst stimulation-induced LTP (***D***) were measured in the area CA1 of hippocampal slices from adult mice. Inset are representative fEPSPs taken 10 min before and 120 min after induction of LTP (at time zero) in the stimulated (left) and control (right) pathways for each genotype. Data are expressed as mean, and error bars represent the SEM. For tetanus-induced LTP, data are taken from single slices from nine wild-type and eight MSK1 KD mice, while for theta-burst-induced LTP, individual slices from seven wild-type and seven MSK1 KD mice were used. ***E***, TBS-LTP is sensitive to the transcription inhibitor Act-D. Graphs show the effects of DMSO vehicle (0.08%) applied throughout the experiment (black squares and dark grey bar; n = 5; three wild-type and two MSK1 KD mice); 40 **μ**M Act-D applied for the duration of the experiment (dark grey squares and dark grey bar; n = 5; four wild-type and one MSK1 KD mice); and 25 **μ**M Act-D (0.05% DMSO) applied for 15 min before and after TBS (light grey squares and light grey bar; n = 9; three wild-type mice and six slices from four MSK1 KD mice). Both concentrations of Act-D affect LTP similarly, but the lower concentration and shorter duration of application of 25 **μ**M has less of an effect on the control pathway. Data are expressed as mean, and error bars represent the SEM. ***F***, The inhibitory effects of Act-D on late TBS-LTP are independent of genotype. Data are replotted from ***E*** but with respect to genotype instead of concentration: black squares, seven slices from seven wild-type mice; open circles, seven slices from five MSK1 KD mice. Data are expressed as mean, and error bars represent the SEM.

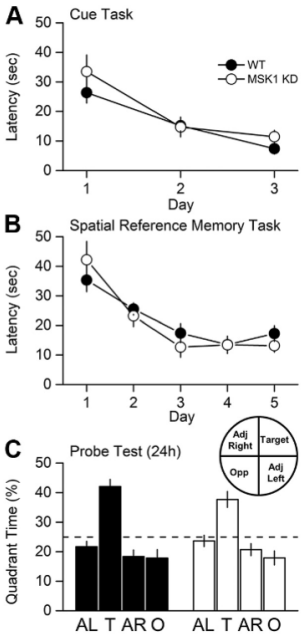

Figure 4. MSK1 KD mice display no deficit in the watermaze test for spatial reference memory. ***A***, The ability to locate a visible platform in a 2-m pool was assessed by a 3-d visual cue task as described in Daumas et al. (2008). Both wild-type (WT) and MSK1 KD mice improved their latency to the platform with time at an equivalent rate. ***B***, Spatial reference memory was assessed using a standard 5-d protocol (four spaced trials/day, 10-cm hidden platform, probe test after 24 h). No learning deficit was observed during training. ***C***, The retention "probe" test indicated good memory in both groups, revealed as greater time spent searching in the training quadrant. Broken line, chance level = 25 %.

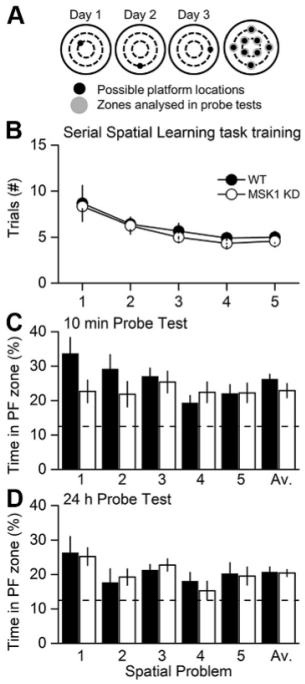

Figure 5. MSK1 KD mice display no deficit in the watermaze test for serial spatial learning. ***A***, A serial spatial learning task was used to assess memory flexibility as described in Daumas et al. (2008). In this task, the platform location changes between up to eight separate locations and between days, with each location trained until the animals reached a fixed criterion of performance (latency < 20 s over three trials). The measure of learning now is not latency, but the number of trials (#) required to reach criterion. ***B***, Both groups showed similar performance. After reaching criterion for each of five serial locations, memory was assessed at 10 min (***C***) and 24 h (***D***). The proportion of time spent in the relevant platform zone (extended to 20 cm in diameter) relative to the other seven possible platform locations was analysed (broken line, chance level = 12.5 %).

their performance over the 5 d of training ($p < 0.0001$[p]); there was no significant effect due to the genotype ($p = 0.69$[q]), nor a significant interaction between genotype and day ($p = 0.46$[r]). In a probe trial given 24 h later (Fig. 4*C*), both mutant and wild-type mice displayed selective searching in the training quadrant (42 and 38% for WT and MSK1 KD, respectively) compared to chance level (25 %; $p = 0.002$[s] for both) demonstrating memory retention in both genotypes. The time spent in the training quadrant did not differ between genotypes ($p = 0.24$[t]).

In a further iteration of the watermaze that maximizes the opportunity for interference, mice were subjected to a serial spatial learning task in which a new platform location was used across a series of sessions (Fig. 5*A*), and the number of trials required to identify the new location of the platform taken as a measure of learning. This test proved to be exceptionally sensitive in a study of age-related changes of performance in human mutant APP mice (Chen et al., 2000). As before, the wild-type and MSK1 mutant mice performed similarly in the acquisition phase (Fig. 5*B*): a repeated-measures (RM)-ANOVA showed that mice of both genotypes improved their performance in relation to the task order presentation ($p < 0.0001$[u]; i.e., the number of trials required for spatial problem 1 > spatial problem 2 and 3 > spatial problem 4 and 5). It also showed that there was no effect due to the genotype ($p = 0.57$[v]), nor any significant interaction between spatial problem and genotype ($p = 0.91$[w]).

In a probe test trial given 10 min after the last training session for each platform location (Fig. 5*C*), the performance of the mutant and wild-type was similar: the average performance was above the chance level (12.5 %; $p = 0.002$[x] for both WT and MSK1-KD). An RM-ANOVA showed that there was no effect due to genotype ($p = 0.19$[y]), nor any significant interaction between task and genotype ($p = 0.16$[z]). The apparent better performance

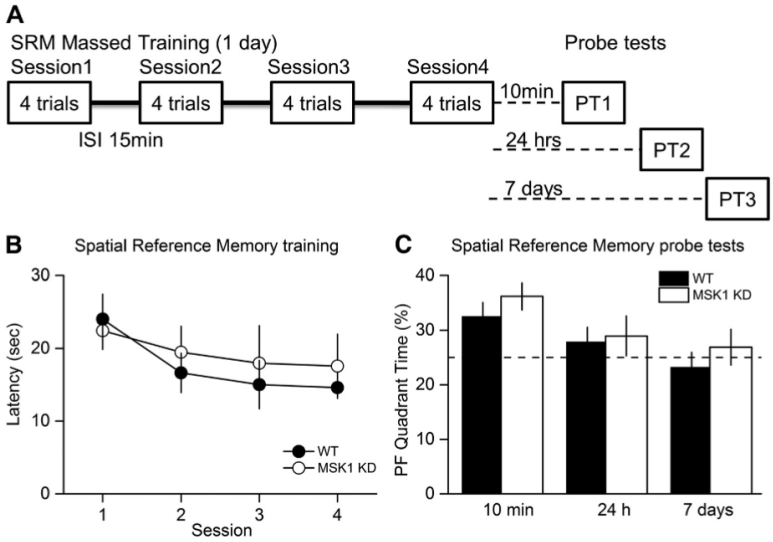

Figure 6. MSK1 KD mice display no deficit in the watermaze test for spatial reference memory with a massed training protocol. ***A***, In a massed training protocol (16 trials, in four trial blocks over 1 d), learning was comparable (***B***), and spatial memory assessed at 10 min, 24 h, and 7 d after training (***C***) showed the expected and more rapid forgetting over time with no group differences between WT and MSK1 KD mice.

by WT mice on the first spatial problem did not reach statistical significance ($p = 0.067^{(aa)}$).

Similarly, mutant and wild-type mice behaved no differently from each other in a probe test given 24 h after the training sessions (Fig. 5*D*): the average performance was above the chance level (12.5 %; $p = 0.002^{(ab)}$ for both WT and MSK1-KD). An RM-ANOVA showed that there was no effect due to genotype ($p = 0.88^{(ac)}$), nor any significant interaction between task and genotype ($p = 0.95^{(ad)}$).

Massed training tends to give rise to a weaker memory trace that fails to show lasting retention, a level of performance that may be more sensitive for revealing a subtle phenotype. To examine the decay of memory over time, both genotypes were therefore exposed to massed training in which four watermaze trials were given per session with a 15 min interval between the four sessions (Fig. 6*A*). Mice of both genotypes showed a steady decline in escape latency over the four sessions of training ($p = 0.025^{(ae)}$); there was no significant effect due to the genotype ($p = 0.64^{(af)}$), nor a significant interaction between genotype and day ($p = 0.39^{(ag)}$; Fig. 6*B*).

Mice were then tested for memory of the location of the platform 10 min, 24 h, and 7 d later (Fig. 6*C*). At the 10 min probe test only, mice of both genotypes spent more time in the platform quadrant than the chance level (25 %; $p = 0.015$ and $0.005^{(ah)}$ for WT and MSK1 KD, respectively), but the percentages did not differ between genotypes ($p = 0.31^{(ai)}$). Forgetting was observed in both groups over 24 h and 7 d.

These data indicate that, while there is a deficit in BDNF signalling to CREB and basal synaptic transmission in the MSK1 KD mouse, this does not translate into an impairment of mGluR-LTD, LTP or in long-term hippocampal-dependent spatial learning in the watermaze. Moreover, intact long-term learning and memory in the watermaze is consistent with intact LTP in the hippocampus in the mutant mice.

Discussion

Our main findings are that mice harboring a knock-in kinase-dead mutation of MSK1 display a deficit in BDNF-dependent phosphorylation of CREB and of basal synaptic transmission, but not of paired-pulse facilitation, mGluR-LTD or LTP induced by either tetanic or theta-burst stimulation. In addition, MSK1 mutant mice showed no impairment in various tests of spatial memory in the watermaze. These data suggest that the kinase activity of MSK1 is not directly required for several forms of synaptic plasticity or spatial learning and memory, at least under standard housing conditions. Instead, our observations of changes in basal synaptic transmission, and thus the long-term regulation of synaptic strength, support observations of a deficit in homeostatic and experience-dependent plasticity in MSK1 KD mutants (Corrêa et al., 2012).

MSK1 as a CREB S133 kinase

The immunofluorescence associated with the phosphorylation of CREB at S133 was similar under basal conditions between MSK1 KD and wild-type mice. This suggests that under normal circumstances the many CREB kinases, which include CaMKs, PKA, and RSKs

(Flavell and Greenberg, 2008; Sakamoto et al., 2011; Kida and Serita, 2014), ensure an appropriate level of CREB S133 phosphorylation and presumably the maintenance of CREB-dependent transcription. The wide variety of CREB S133 kinases and their recruitment in an activity-dependent manner also potentially explains the minimal synaptic and behavioral phenotype of the MSK1 KD mutant mouse. Thus, there may only be specific circumstances in which MSK1 is recruited as a CREB S133 kinase, for example, in response to environmental enrichment (Corrêa et al., 2012; Karelina et al., 2012) or, interestingly, to molecules such as BDNF (Arthur et al., 2004), which is believed to play an important role in mediating the beneficial effects of enrichment on neuronal structure, synaptic function, and cognition (Cowansage et al., 2010; Bekinschtein et al., 2011).

Accordingly, stimulation of hippocampal slices with BDNF resulted in an increase in phosphorylation of CREB S133 in CA1 neurons of wild-type mice but not in MSK1 KD mice. These observations confirm the long-held view of MSK1 as a CREB kinase (Deak et al., 1998; Reyskens and Arthur, 2016) and, in particular, the observations made in primary neuronal cell culture of MSK1 and MSK2 single and double knock-outs of the necessity for MSK1 in neurotrophin-mediated phosphorylation of CREB (Arthur et al., 2004). However, as others have shown, MSK1 is also downstream of other signalling cascades that culminate in CREB phosphorylation, including that of the cAMP/PKA pathway (Frödin et al., 1994; Delghandi et al., 2005). Although we observed no obvious deficit in forskolin-stimulated CREB phosphorylation in slices from MSK1 KD mice, which may reflect a dominant contribution of PKA under our experimental conditions, others have reported that the Ca^{2+}-stimulated adenylyl cyclase/PKA pathway recruits MSK1 in a subset of CA1 neurons in response to contextual fear conditioning (Sindreu et al., 2007). Since the number of CA1 neurons in our analysis of CREB phosphorylation were similar across genotypes and basal and stimulated conditions (~70 cells/slice), we do not see evidence of subsets of responding neurons. This may reflect the bath application of BDNF and forskolin, as opposed to the pathway specificity of a behavioral stimulus.

Role of MSK1 in synaptic transmission and plasticity

Despite there being a number of studies describing various roles for MSK1 in neuronal and cognitive function, there have been no reports to date of synaptic plasticity in MSK1 mutant mice. The observations we have made here suggest that the kinase activity of MSK1 is necessary to regulate basal synaptic transmission as MSK1 KD mice showed smaller CA1 fEPSPs in response to stimulation of the afferent Schaffer pathway, a phenotype they share with BDNF knock-out mice (Patterson et al., 1996). In the MSK1 KD mutants, this impairment was not due to reduced excitability or number of presynaptic fibres, since the amplitude of the presynaptic fibre volley was no different from wild-type animals. In addition, this deficit did not reflect either an increase in inhibitory GABAergic synaptic transmission, as the difference between mutant and wild-type slices persisted in the presence of a $GABA_A$ receptor antagonist, or reduced probability of transmitter release since the paired-pulse facilitation profile was no different between mutant and wild-type slices. Instead, one possibility is that this deficit reflects reduced numbers of postsynaptic AMPA receptors, which mediate the majority of excitatory synaptic transmission at these synapses. Indeed, in whole-cell recordings from MSK1 KD and wild-type neurons, a ~10-15 % reduction in the amplitude of miniature excitatory postsynaptic currents (mEPSCs) in hippocampal slices from animals of a similar age was observed (Corrêa et al., 2012). This observation is in contrast to the situation in cultured neurons prepared from neonatal animals where mEPSCs are larger in neurons prepared from MSK1 KD mice, likely due to the increased cell surface expression of GluA1 (but not GluA2) AMPA receptor subunits (Corrêa et al., 2012). This suggests either that the influence of MSK1 on synaptic strength may be developmentally regulated, or that homeostatic synaptic changes induced by the preparation of cultured neurons and acute brain slices do not occur in the MSK1 KD mutants.

The mechanism underlying the deficit in synaptic transmission is not clear but could potentially involve the reduced BDNF-dependent stimulation of CREB phosphorylation in hippocampal slices we observed. Such a deficit in the ERK signalling cascade could give rise to deficits in the induction of the immediate early gene Arc/Arg3.1 (Korb and Finkbeiner, 2011). Arc/Arg3.1 has been implicated in regulating synaptic strength via its association with the endocytotic proteins dynamin and endophilin (Chowdhury et al., 2006). Indeed, MSK1 KD mutants failed to downregulate Arc/Arg3.1 during prolonged (24 h) activity deprivation *in vitro*, and, likely as a consequence, the expected increase in mEPSC amplitude was not observed (Corrêa et al., 2012). Similarly, the larger spines reported in MSK1 KD neurons (Corrêa et al., 2012) has parallels with the increased number of larger spines in the Arc/Arg3.1 knock-out (Peebles et al., 2010). However, mGluR-LTD, which requires Arc/Arg3.1 for its induction (Waung et al., 2008), was not affected by the loss of MSK1 kinase activity suggesting that there are alternative means by which Arc/Arg3.1 can be regulated to support mGluR-LTD.

The LTP induction protocols used in this study evoked long-lasting (3 h) potentiation of synaptic transmission in slices from both wild-type and MSK1 KD mice. Such longevity has been previously reported for TBS-induced LTP (Nguyen and Kandel, 1997) but is not considered to be a feature of LTP induced by a single tetanus. However, it is clear from a number of studies that long-lasting LTP can be induced by a single tetanus (Bortolotto and Collingridge, 2000; Fonseca et al., 2004; Capron et al., 2006; Fonseca et al., 2006a; Fonseca et al., 2006b; Sajikumar et al., 2008; Villers et al., 2012), although there is debate as to whether or when this requires protein synthesis, as there is for TBS-induced LTP (Lynch et al., 2015). Such factors that may influence the persistence of LTP after a tetanus include the strength (Tsokas et al., 2005) or the frequency of basal synaptic transmission, with less fre-

quent stimulation, as seen in alternating two pathway experiments such as ours, prolonging the magnitude and duration of the tetanus-induced LTP (Fonseca et al., 2006a; Villers et al., 2012).

Given the persistence of the LTP seen in our experiments, the lack of effect of the MSK1 KD mutation is at first glance somewhat surprising given that: (1) MSK1 phosphorylates CREB; (2) CREB has been implicated in synaptic plasticity, albeit with some controversy (Sakamoto et al., 2011); (3) the original CREB knock-out mouse showed a deficit in LTP over a period of 90 min (Bourtchuladze et al., 1994); (4) the MAPK/ERK pathway may be recruited preferentially by TBS (Winder et al., 1999); and (5) the ensuing LTP is sensitive to inhibition of transcription (Nguyen and Kandel, 1997).

One potential, if unlikely, explanation is that the mutation of the MSK1 gene has allowed an additional form of LTP to be evoked, in response to both TBS and tetanic stimulation, that displays identical magnitude, kinetics, and duration (to 3 h) to that evoked in slices from wild-type mice. It is thus superficially indistinguishable, to the point that it too is dependent upon transcription, at least for TBS-induced LTP. This will remain a possibility until a full biophysical and pharmacological characterization of LTP in MSK1 KD slices is performed.

A more parsimonious interpretation of the lack of an effect of the MSK1 KD mutation on LTP may arise from the work using residue-specific mutations of the BDNF TrkB receptor: an LTP deficit, over a similar time course to the present experiments (3 h), was only observed in mice with a mutation in TrkB Y816, which signals to PLCγ, CaM kinase IV, and CREB, and not mutations in TrkB Y515, which signals via Shc and the MAPK cascade, downstream of which is MSK1 (Korte et al., 2000; Minichiello et al., 2002).

MSK1 and spatial learning

Previous reports have shown that MSK single or double knock-outs are impaired on the watermaze, fear conditioning, the Barnes maze, and in the display of behavioral immobility in the forced-swim test (Chwang et al., 2007; Chandramohan et al., 2008; Frenguelli and Corrêa, 2012; Karelina et al., 2012; Reyskens and Arthur, 2016). However, in our studies of MSK1 KD mice, we observed no deficit in various watermaze paradigms. This is consistent with the intact LTP we recorded but is at odds with previous work in other laboratories using MSK1 knock-outs. One potential explanation is that, especially in the context of the previous watermaze studies (Chwang et al., 2007), subtle differences in the way the test is conducted or the animals housed could influence the signalling pathways recruited. Indeed, other paradigms such as fear conditioning or forced swimming could recruit MSK1-dependent signalling pathways and underpin learning in those models.

An alternative explanation is that that MSK1 subserves two functions, one as a kinase and the other as a scaffolding partner in a signalling complex. The latter possibility has been made all the more likely by the observation that MSK1 forms a complex with the glucocorticoid receptor and ERK1/2 for optimal phosphorylation (serine 10) and acetylation (lysine 14; via Elk-1) of histone H3. This complex resulted in the induction of c-Fos and Egr-1 during a 15-min forced swim test (Gutierrez-Mecinas et al., 2011). Loss of the entire MSK1 protein in the knock-out may thus compromise this scaffolding role as well as the kinase pathway, and its effect may be more pronounced in tests associated with increased stress, for example, fear conditioning, forced swimming and the use of aversive motivation in the Barnes maze. Thus, whereas the MSK1 KO studies have to date been interpreted as relating to the loss of kinase activity, our use of the kinase-dead (KD) mutation raises questions about this interpretation.

Conclusions

Mice with an inactivating kinase-dead knock-in mutation in the N-terminal kinase domain MSK1 show normal mGluR-LTD, tetanus and theta-burst LTP, and were unaffected in spatial memory tasks in the watermaze. However, these mice display a deficit in basal synaptic transmission and in BDNF-mediated phosphorylation of CREB. These data suggest that MSK1 may be important in regulating long-term, adaptive neuronal properties, rather than the acute response to experience. This is consistent with previous observations that demonstrate the necessity for MSK1 in homeostatic synaptic scaling *in vitro* and environmental enrichment-induced synaptic plasticity *in vivo* (Corrêa et al., 2012).

References

Arthur JS (2008) MSK activation and physiological roles. Front Biosci 13:5866 –5879. Medline

Arthur JS, Fong AL, Dwyer JM, Davare M, Reese E, Obrietan K, Impey S (2004) Mitogen- and stress-activated protein kinase 1 mediates cAMP response element-binding protein phosphorylation and activation by neurotrophins. J Neurosci 24:4324 –4332.

Bekinschtein P, Oomen CA, Saksida LM, Bussey TJ (2011) Effects of environmental enrichment and voluntary exercise on neurogenesis, learning and memory, and pattern separation: BDNF as a critical variable? Semin Cell Dev Biol 22:536 –542. CrossRef

Bortolotto ZA, Amici M, Anderson WW, Isaac JT, Collingridge GL (2011) Synaptic plasticity in the hippocampal slice preparation. Curr Protoc Neurosci Chapter 6:Unit 6 13.

Bortolotto ZA, Collingridge GL (2000) A role for protein kinase C in a form of metaplasticity that regulates the induction of long-term potentiation at CA1 synapses of the adult rat hippocampus. Eur J Neurosci 12:4055–4062. Medline

Bourtchuladze R, Frenguelli BG, Blendy J, Cioffi D, Schutz G, Silva AJ (1994) Deficient long-term memory in mice with a targeted mutation of the cAMP-responsive element-binding protein. Cell 79:59 –68. Medline

Capron B, Sindic C, Godaux E, Ris L (2006) The characteristics of LTP induced in hippocampal slices are dependent on slice-recovery conditions. Learn Mem 13:271–277. CrossRef Medline

Chandramohan Y, Droste SK, Arthur JS, Reul JM (2008) The forced swimming-induced behavioural immobility response involves histone H3 phospho-acetylation and c-Fos induction in dentate gyrus granule neurons via activation of the N-methyl-D-aspartate/extracellular signal-regulated kinase/mitogen- and stress-activated kinase signalling pathway. Eur J Neurosci 27:2701–2713. CrossRef

Chen G, Chen KS, Knox J, Inglis J, Bernard A, Martin SJ, Justice A, McConlogue L, Games D, Freedman SB, Morris RG (2000) A learning deficit related to age and beta-amyloid plaques in a

mouse model of Alzheimer's disease. Nature 408:975–979. CrossRef Medline
Choi YS, Karelina K, zate-Correa D, Hoyt KR, Impey S, Simon AJ, Obrietan K (2012) Mitogen- and stress-activated kinases regulate progenitor cell proliferation and neuron development in the adult dentate gyrus. J Neurochem 123:676 –688. CrossRef
Chowdhury S, Shepherd JD, Okuno H, Lyford G, Petralia RS, Plath N, Kuhl D, Huganir RL, Worley PF (2006) Arc/Arg3.1 interacts with the endocytic machinery to regulate AMPA receptor trafficking. Neuron 52:445–459. CrossRef Medline
Chwang WB, Arthur JS, Schumacher A, Sweatt JD (2007) The nuclear kinase mitogen- and stress-activated protein kinase 1 regulates hippocampal chromatin remodeling in memory formation. J Neurosci 27:12732–12742. CrossRef
Corrêa SA, Hunter CJ, Palygin O, Wauters SC, Martin KJ, McKenzie C, McKelvey K, Morris RG, Pankratov Y, Arthur JS, Frenguelli BG (2012) MSK1 regulates homeostatic and experience-dependent synaptic plasticity. J Neurosci 32:13039 –13051.
Cowansage KK, Ledoux JE, Monfils MH (2010) Brain-derived neurotrophic factor: a dynamic gatekeeper of neural plasticity. Curr Mol Pharmacol 3:12–29. Medline
Croning MD, Haddad GG (1998) Comparison of brain slice chamber designs for investigations of oxygen deprivation *in vitro*. J Neurosci Methods 81:103–111. CrossRef
Dash PK, Hochner B, Kandel ER (1990) Injection of the cAMP-responsive element into the nucleus of Aplysia sensory neurons blocks long-term facilitation. Nature 345:718 –721. CrossRef Medline
Daumas S, Sandin J, Chen KS, Kobayashi D, Tulloch J, Martin SJ, Games D, Morris RG (2008) Faster forgetting contributes to impaired spatial memory in the PDAPP mouse: deficit in memory retrieval associated with increased sensitivity to interference? Learn Mem 15:625–32.
Deak M, Clifton AD, Lucocq LM, Alessi DR (1998) Mitogen- and stress-activated protein kinase-1 (MSK1) is directly activated by MAPK and SAPK2/p38, and may mediate activation of CREB. EMBO J 17:4426 –4441. CrossRef
Delghandi MP, Johannessen M, Moens U (2005) The cAMP signalling pathway activates CREB through PKA, p38 and MSK1 in NIH 3T3 cells. Cell Signal 17:1343–1351. CrossRef Medline
Flavell SW, Greenberg ME (2008) Signaling mechanisms linking neuronal activity to gene expression and plasticity of the nervous system. Annu Rev Neurosci 31:563–590. CrossRef Medline
Fonseca R, Nägerl UV, Bonhoeffer T (2006a) Neuronal activity determines the protein synthesis dependence of long-term potentiation. Nat Neurosci 9:478 –480. CrossRef Medline
Fonseca R, Nägerl UV, Morris RG, Bonhoeffer T (2004) Competing for memory: hippocampal LTP under regimes of reduced protein synthesis. Neuron 44:1011–1020. CrossRef Medline
Fonseca R, Vabulas RM, Hartl FU, Bonhoeffer T, Nagerl UV (2006b) A balance of protein synthesis and proteasome-dependent degradation determines the maintenance of LTP. Neuron 52:239–245.
Frenguelli BG, Corrêa SA (2012) Regulation and role of MSK in the mammalian brain. In: MSKs (Vermeulen L, Arthur JS, eds). Austin: Landes Bioscience.
Frödin M, Peraldi P, Van OE (1994) Cyclic AMP activates the mitogen-activated protein kinase cascade in PC12 cells. J Biol Chem 269:6207–6214. Medline
Gutierrez-Mecinas M, Trollope AF, Collins A, Morfett H, Hesketh SA, Kersante F, Reul JM (2011) Long-lasting behavioral responses to stress involve a direct interaction of glucocorticoid receptors with ERK1/2-MSK1-Elk-1 signaling. Proc Natl Acad Sci USA 108: 13806 –13811. CrossRef
Guzman-Karlsson MC, Meadows JP, Gavin CF, Hablitz JJ, Sweatt JD (2014) Transcriptional and epigenetic regulation of Hebbian and non-Hebbian plasticity. Neuropharmacology 80:3-17.
Kandel ER (2012) The molecular biology of memory: cAMP, PKA, CRE, CREB-1, CREB-2, and CPEB. Mol Brain 5:14. CrossRef Medline
Karelina K, Hansen KF, Choi YS, DeVries AC, Arthur JS, Obrietan K (2012) MSK1 regulates environmental enrichment-induced hippocampal plasticity and cognitive enhancement. Learn Mem 19: 550 –560. CrossRef
Karelina K, Liu Y, zate-Correa D, Wheaton KL, Hoyt KR, Arthur JS, Obrietan K (2015) Mitogen and stress-activated kinases 1/2 regulate ischemia-induced hippocampal progenitor cell proliferation and neurogenesis. Neuroscience 285:292–302. CrossRef
Kida S, Serita T (2014) Functional roles of CREB as a positive regulator in the formation and enhancement of memory. Brain Res Bull 105:17–24. CrossRef Medline
Korb E, Finkbeiner S (2011) Arc in synaptic plasticity: from gene to behavior. Trends Neurosci 34:591–598. CrossRef Medline
Korte M, Minichiello L, Klein R, Bonhoeffer T (2000) Shc-binding site in the TrkB receptor is not required for hippocampal long-term potentiation. Neuropharmacology 39:717–724. Medline
Lynch G, Cox CD, Gall CM (2014) Pharmacological enhancement of memory or cognition in normal subjects. Front Syst Neurosci 8:90 CrossRef Medline
Lynch G, Kramár EA, Gall CM (2015) Protein synthesis and consolidation of memory-related synaptic changes. Brain Res 1621:62–72. CrossRef Medline
McCoy CE, Campbell DG, Deak M, Bloomberg GB, Arthur JS (2005) MSK1 activity is controlled by multiple phosphorylation sites. Biochem.J 387:507–517. CrossRef Medline
Minichiello L (2009) TrkB signalling pathways in LTP and learning. Nat Rev Neurosci 10:850 –860. CrossRef Medline
Minichiello L, Calella AM, Medina DL, Bonhoeffer T, Klein R, Korte M (2002) Mechanism of TrkB-mediated hippocampal long-term potentiation. Neuron 36:121–137. Medline
Moran MF, Koch CA, Sadowski I, Pawson T (1988) Mutational analysis of a phosphotransfer motif essential for v-fps tyrosine kinase activity. Oncogene 3:665–672. Medline
Nguyen PV, Kandel ER (1997) Brief theta-burst stimulation induces a transcription-dependent late phase of LTP requiring cAMP in area CA1 of the mouse hippocampus. Learn Mem 4:230–243. CrossRef
Panja D, Bramham CR (2014) BDNF mechanisms in late LTP formation: a synthesis and breakdown. Neuropharmacology 76:664 –676.
Patterson SL, Abel T, Deuel TA, Martin KC, Rose JC, Kandel ER (1996) Recombinant BDNF rescues deficits in basal synaptic transmission and hippocampal LTP in BDNF knockout mice. Neuron 16:1137–1145. Medline
Peebles CL, Yoo J, Thwin MT, Palop JJ, Noebels JL, Finkbeiner S (2010) Arc regulates spine morphology and maintains network stability in vivo. Proc Natl Acad Sci USA 107:18173–18178. CrossRef Medline
Plath N, Ohana O, Dammermann B, Errington ML, Schmitz D, Gross C, Mao X, Engelsberg A, Mahlke C, Welzl H, Kobalz U, Stawrakakis A, Fernandez E, Waltereit R, Bick-Sander A, Therstappen E, Cooke SF, Blanquet V, Wurst W, Salmen B, et al. (2006) Arc/Arg3.1 is essential for the consolidation of synaptic plasticity and memories. Neuron 52:437–444. CrossRef
Reid KH, Edmonds HL, Schurr A, Tseng MT, West CA (1988) Pitfalls in the use of brain slices. Prog Neurobiol 31:1–18. Medline
Reyskens KM, Arthur JS (2016) Emerging Roles of the Mitogen and Stress Activated Kinases MSK1 and MSK2. Front Cell Dev Biol 4:56. CrossRef Medline
Sajikumar S, Navakkode S, Frey JU (2008) Distinct single but not necessarily repeated tetanization is required to induce hippocampal late-LTP in the rat CA1. Learn Mem 15:46 –49. CrossRef Medline
Sakamoto K, Karelina K, Obrietan K (2011) CREB: a multifaceted regulator of neuronal plasticity and protection. J Neurochem 116: 1–9. CrossRef Medline
Shepherd JD, Bear MF (2011) New views of Arc, a master regulator of synaptic plasticity. Nat Neurosci 14:279–284. CrossRef Medline
Sindreu CB, Scheiner ZS, Storm DR (2007) Ca2+ -stimulated adenylyl cyclases regulate ERK-dependent activation of MSK1 during fear conditioning. Neuron 53:79 –89. CrossRef Medline

Tsokas P, Grace EA, Chan P, Ma T, Sealfon SC, Iyengar R, Landau EM, Blitzer RD (2005) Local protein synthesis mediates a rapid increase in dendritic elongation factor 1A after induction of late long-term potentiation. J Neurosci 25:5833–5843. CrossRef

Vijayan RS, He P, Modi V, Duong-Ly KC, Ma H, Peterson JR, Dunbrack RL Jr, Levy RM (2015) Conformational analysis of the DFG-out kinase motif and biochemical profiling of structurally validated type II inhibitors. J Med Chem 58:466 –479. CrossRef

Villers A, Godaux E, Ris L (2012) Long-lasting LTP requires neither repeated trains for its induction nor protein synthesis for its development. PLoS One 7:e40823. CrossRef Medline

Waung MW, Pfeiffer BE, Nosyreva ED, Ronesi JA, Huber KM (2008) Rapid translation of Arc/Arg3.1 selectively mediates mGluR-dependent LTD through persistent increases in AMPAR endocytosis rate. Neuron 59:84 –97. CrossRef

Winder DG, Martin KC, Muzzio IA, Rohrer D, Chruscinski A, Kobilka B, Kandel ER (1999) ERK plays a regulatory role in induction of LTP by theta frequency stimulation and its modulation by beta-adrenergic receptors. Neuron 24:715–726. CrossRef

Wingate AD, Martin KJ, Hunter C, Carr JM, Clacher C, Arthur JS (2009) Generation of a conditional CREB Ser133Ala knockin mouse. Genesis 47:688 –696. CrossRef Medline

Yin JC, Wallach JS, Del VM, Wilder EL, Zhou H, Quinn WG, Tully T (1994) Induction of a dominant negative CREB transgene specifically blocks long-term memory in Drosophila. Cell 79:49 –58. CrossRef

2) The work entitled: “Experience recruits MSK1 to expand the dynamic range of synapses and enhance cognition” by Privitera et al. 2020 featuring the work from Chapter 4 of this thesis is currently available as an accepted manuscript currently undergoing final edits on the Journal of Neuroscience website at the following URL:
https://www.jneurosci.org/content/jneuro/early/2020/05/05/JNEUROSCI.2765-19.2020.full.pdf
Due to its current length (65 pages), due to its unedited form, it is not appended to this thesis.